



Payam Fayyaz



**Effects of salt stress on ecophysiological
and molecular characteristics of *Populus
euphratica* Oliv., *Populus x canescens*
(Aiton) Sm. and *Arabidopsis thaliana* L.**



 Cuvillier Verlag Göttingen

Effects of salt stress on ecophysiological and molecular
characteristics of *Populus euphratica* Oliv., *Populus x canescens*
(Aiton) Sm. and *Arabidopsis thaliana* L.

Dissertation

In Partial Fulfillment of the Requirements for the Degree Doctor of Philosophy
(PhD)
of Faculty of Forest Sciences and Forest Ecology
Georg-August-University Göttingen

Submitted by

Payam Fayyaz

Born in Lahijan, Iran

Göttingen, den 17. Dezember 2007

Bibliografische Information der Deutschen Nationalbibliothek

Die Deutsche Nationalbibliothek verzeichnet diese Publikation in der Deutschen Nationalbibliografie; detaillierte bibliografische Daten sind im Internet über <http://dnb.ddb.de> abrufbar.

1. Aufl. - Göttingen : Cuvillier, 2008

Zugl.: Göttingen, Univ., Diss., 2007

978-3-86727-536-1

D7

Referentin:	Frau Prof. Dr. Andrea Polle
Korreferent:	Herr Prof. Dr. Reiner Finkeldey
Tag der mündlichen Prüfung:	23. Januar 2008

© CUVILLIER VERLAG, Göttingen 2008

Nonnenstieg 8, 37075 Göttingen

Telefon: 0551-54724-0

Telefax: 0551-54724-21

www.cuvillier.de

Alle Rechte vorbehalten. Ohne ausdrückliche Genehmigung des Verlages ist es nicht gestattet, das Buch oder Teile daraus auf fotomechanischem Weg (Fotokopie, Mikrokopie) zu vervielfältigen.

1. Auflage, 2008

Gedruckt auf säurefreiem Papier

978-3-86727-536-1

Table of contents

List of abbreviations

List of companies

1	Introduction	1
1.1	Soil salinity	1
1.2	Water and salt uptake	2
1.3	Effects of salt stress in plants	3
1.4	Salt tolerance mechanisms	4
1.5	<i>P. euphratica</i> and response to salinity and osmotic stress	5
1.6	Lipocalins structure and function	7
1.7	Objectives	10
2	Materials and Methods	11
2.1	Plant materials and preparation	11
2.2	Experimental treatments	14
2.2.1	Salt shock of <i>P. euphratica</i> and <i>P. x canescens</i>	14
2.2.2	Short term salt adaptation of <i>P. euphratica</i> and <i>P. x canescens</i>	14
2.2.3	Long term salt adaptation of <i>P. euphratica</i>	15
2.2.4	Germination rate and root growth assays of <i>Arabidopsis thaliana</i>	16
2.3	Ecophysiological measurements	17
2.3.1	Analysis of plant performance	17
2.3.2	Membrane permeability	17
2.3.3	Leaf water potential	18
2.3.4	Pigment analysis	18
2.3.5	Gas exchange measurements	19

2.3.6	Analysis of chlorophyll fluorescence	19
2.3.7	Carbohydrate analysis	20
2.4	Molecular biology	21
2.4.1	RNA handling.....	21
2.4.1.1	RNA extraction.....	21
2.4.1.2	Evaluation of RNA concentration and purity	22
2.4.1.3	RNA gel electrophoresis	22
2.4.1.4	DNase treatment	23
2.4.1.5	Synthesis of first strand cDNA	24
2.4.2	DNA handling	24
2.4.2.1	Genomic DNA extraction from <i>Arabidopsis</i>	24
2.4.2.2	Primer design.....	25
2.4.2.3	Polymerase chain reaction (PCR).....	26
2.4.2.3.1	Standard PCR conditions.....	26
2.4.2.3.2	Quantitative real time PCR (qRT-PCR).....	26
2.4.2.4	DNA gel electrophoresis	29
2.4.2.5	Gel extraction	29
2.4.2.6	Sequencing	29
2.4.3	<i>Arabidopsis</i> Salk line T-DNA knock out mutants.....	30
2.4.3.1	Selection of <i>Arabidopsis</i> mutants having T-DNA insertion	30
2.4.3.2	PCR based screening for homozygous Salk lines	30
2.4.4	Vector transformation preparation	30
2.4.4.1	Preparation of electrocompetent <i>E. coli</i>	30
2.4.4.2	Preparation of electrocompetent <i>Agrobacterium</i>	31
2.4.4.3	Electroporation	32
2.4.5	PCR based gene isolation	33
2.4.6	Cloning genes of interest into pGEM T-vector	33
2.4.6.1	Ligation in pGEM-T Easy I vector.....	34
2.4.6.2	Blue-white screening	34
2.4.6.3	Glycerine stock preparation.....	35
2.4.7	Cloning genes of interest in to a plant cloning vector	35
2.4.7.1	Ligation of DNA fragment into plasmid	36

2.4.7.2	Plasmid extraction by Mini-Prep (<i>E. coli</i> and <i>Agrobacterium</i>).....	36
2.4.8	In silico analysis	37
2.4.9	Phylogenetic analysis	38
2.4.10	Protein sequence annotation.....	38
2.4.11	Promoter analysis	38
2.5	Statistical analyses	39
3	Results.....	40
3.1	Ecophysiological characteristics of <i>P. euphratica</i> and <i>P. x canescens</i> during salt adaptation.....	40
3.1.1	Effect of short term salt adaptation on plant performance	40
3.1.2	Performance of <i>P. euphratica</i> during long term salt adaptation	44
3.1.3	Carbohydrates in leaf exudates.....	48
3.1.4	Electrolyte conductivity as a measure for salt uptake and salt induced leaf injury	49
3.1.5	Leaf water potential under salt stress	53
3.1.6	Pigment analysis.....	54
3.1.7	Effect of salt adaptation on photosynthetic parameters of <i>P. x canescens</i> and <i>P. euphratica</i>	55
3.1.8	Influence of salinity on chlorophyll fluorescence	57
3.2	Selection of salt-related candidate genes.....	60
3.3	Identification and nomenclature of PeuTIL and PcaTIL (lipocalin like protein)	61
3.4	Characterization of putative temperature induced lipocalin like proteins PeuTIL and PcaTIL	61
3.4.1	Gene expression analysis.....	61
3.4.1.1	Expression changes induced by salt shock.....	61
3.4.1.2	Expression changes induced by salt adaptation	63
3.4.2	Gene isolation and sequencing	64
3.4.3	Gain of function of PeuTIL in <i>A. thaliana</i> and <i>P. x canescens</i>	65
3.4.4	In silico analysis of temperature induced lipocalin like proteins	65
3.4.4.1	Amino acid distribution histogram.....	66
3.4.5	Phylogenetic studies of plant lipocalins	69

3.4.6	Topology and GPI anchor signal prediction.....	71
3.4.7	Subcellular localization	71
3.4.8	Promoter analysis of lipocalin	74
3.4.9	Loss of function analysis.....	77
3.4.9.1	Characterisation of AthTIL knock out lines.....	77
3.4.9.2	Phenotypic analysis of AthTIL knock out lines	81
3.4.9.3	Performance of AthTIL knock out lines under stress.....	82
3.5	Characterization of salt induced serine rich proteins PeuSIS and PcaSIS ...	84
3.5.1	Identification and nomination of SIS	84
3.5.2	Expression analysis	84
3.5.2.1	Expression changes induced by salt shock.....	84
3.5.2.2	Expression changes induced by salt adaptation	85
3.5.3	Gene isolation and sequencing	86
3.5.4	In silico analysis of salt induced serine rich proteins.....	88
3.5.4.1	Amino acid distribution histogram	88
3.5.5	Phylogenetic studies of salt induced serine rich like proteins.....	91
3.5.6	Topology prediction	92
3.5.7	Subcellular localization	93
3.5.8	Investigating phosphorylation sites	93
3.5.9	Promoter analysis of salt induced serine rich protein.....	95
3.5.10	PatMatch analysis for identification of SIS protein	100
3.5.11	Loss of function analysis.....	100
3.5.11.1	Characterisation of AthSIS knock out lines	100
3.5.11.2	Phenotypic analysis of AthSIS knock out lines.....	102
3.5.11.3	Performance of AthSIS knock out lines under stress.....	103
4	Discussion	105
4.1	Ecophysiological characteristics of <i>P. euphratica</i> and <i>P. x canescens</i> during salt adaptation	105
4.1.1	Effect of salinity on plant performance and morphology.....	105
4.1.2	Salinity and osmotic adjustment.....	106
4.1.3	Electrolyte leakage and plasma membrane injury	107
4.1.4	Performance of photosynthesis in response to salinity	108

4.2	Molecular characteristics of temperature induced lipocalin like proteins...	109
4.3	Molecular characteristics of salt induced serine rich proteins	111
4.4	Outlook.....	113
5	Summary	114
6	References	117
7	Appendix	126
7.1	Half MS (Murashige and Skoog) medium for <i>Populus euphratica</i>	126
7.2	WPM medium for <i>Populus euphratica</i>	126
7.3	Nutrient solution for hydroculture modified according to Long Ashton	127
7.4	Propagation medium for <i>Populus x canescens</i>	127
7.5	Rooting medium for <i>Populus x canescens</i> and <i>Arabidopsis thaliana</i>	127
7.6	Rooting medium for <i>Arabidopsis thaliana</i> (produce less lateral root).....	128
7.7	Stock solutions for micro propagation and rooting mediums	128
7.7.1	Macronutrients-MS	128
7.7.2	Micronutrients-MS	128
7.7.3	Vitamins-MS	128
7.7.4	Glycine-MS	128
7.7.5	Inositol-MS	128
7.7.6	Fe-Solution-MS	129
7.7.7	Macronutrients-SH	129
7.7.8	Macronutrients-GD	129
7.7.9	Micronutrients-GD	129
7.8	Extraction buffer for RNA	129
7.9	SSTE buffer for RNA extraction.....	129
7.10	10x MOPS running buffer for RNA gel electrophoresis.....	130
7.11	RNA loading dye (2x).....	130
7.12	Lists of primers used	131
7.13	SOC medium (for <i>Ecoli</i> transformation).....	132
7.14	YEB medium for <i>Agrobacterium</i> transformation	132
7.15	LB medium for <i>Ecoli</i> cultures	132
7.16	Indicator agar plates for bleu white screening (for 200 ml medium).....	133
7.17	TBE buffer (10x).....	133

7.18	DNA loading dye (10x).....	133
7.19	λ Pst DNA ladder (0.2 μ g λ Pst/ μ l)	133
7.20	Extraction buffer for DNA extraction from <i>Arabidopsis</i>	133
7.21	10x TE buffer for DNA extraction from <i>Arabidopsis</i>	134
7.22	SOB medium for preparation of <i>E. coli</i> electrocompetent cells.....	134
7.23	GTE buffer for plasmid extraction (Mini-Prep)	134
7.24	SDS / NaOH solution for plasmid extraction (Mini-Prep)	134
7.25	TE buffer for solving DNA pellets.....	134
7.26	Potassium acetate (5M) for plasmid extraction (Mini-Prep).....	135
7.27	Amino acid abbreviations.....	135
7.28	Mean and SD of maximum electrolyte conductivity.....	136
7.29	Publication.....	136

List of abbreviations

aa	Amino acid
ABA	Abscic acid
abs	Absorption
Amp ^r	Ampicillin resistance
Aph (3') II	Aminoglycoside (kanamycin) phosphotransferase
ApR	Ampicillin resistance
<i>Ath</i>	<i>Arabidopsis thaliana</i>
BLAST	Basic Local Alignment Search Tool
Blc	Bacterial lipocalin or outer membrane lipoprotein
bp	Base pair
C	Control
<i>ca.</i>	Circa, approximately
CaMV	Cauliflower mosaic virus
Car	Carotenoid
CbR	Carbenicillin resistance
CCC	Cation-chloride-cotransporter
cDNA	Complementary DNA
CDS	Coding sequence
CF	Chlorophyll fluorescence
Chl	Chlorophyll
CHL	Chloroplastic lipocalin
CLC	Chloride channel
CTAB	Hexadecyltrimethylammonium bromide
C-terminus	Carboxyl-terminus
Da	Dalton
ddH ₂ O	Double distilled water
DEPC	Diethyl pyrocarbonate
DMSO	Dimethyl Sulfoxide
DNA	Desoxyribonucleic acid
DOF	DNA binding with one finger transcription factor
dsDNA	Double strand DNA
DW	Dry weight
<i>E. coli</i>	<i>Escherichia coli</i>
EC	Electrolyte conductivity
EDTA	Ethylenediamine tetraacetic acid
EST	Expressed sequence tag
<i>et al.</i>	Et alia (Latin)= and others
EtOH	Ethanol

EMBL	European Molecular Biology Laboratory
EtBr	Ethidium bromide
ETR	Electron transport rate
F	Base fluorescence
F ₀	Minimal fluorescence level (dark)
F' ₀	Minimal fluorescence level achieved by infra red light
FABP	Fatty acid-binding protein
FAE	Formaldehyde : Acetic acid : Ethanol
F _m	Maximal fluorescence level (darkness)
fmol	Femtomol, 10 ⁻¹⁵ mol
FW	Fresh weight
GA	Gibberellic acid
gDNA	Genomic DNA
Gent	Gentamycin
GFP	Green fluorescence protein
GPI	Glycosylphosphatidylinositol
h	Hour
HEPES	4-(2-hydroxyethyl)-1-piperazineethanesulfonic acid
I	Plasma membrane injury
JGI	Joint Genome Institute
JPTG	Isopropyl β-D-1-thiogalactopyranoside
KD	Kyte and Doolittle hydrophobicity scale
kDa	Kilodaltons
Km ^R	Kanamycin resistance
KR	Number of lysine and arginine
kV	Kilo voltage
<i>LacZ</i>	β-Galactosidase
LB	Left border
L1	Length of loop
LP	Left primer, 5' primer, forward primer
M	λPst DNA ladder
min	Minute
MOPS	3-[N-morpholino] propane sulfonic acid
MPa	Mega Pascal
MPI	Metalloprotease inhibitor
mRNA	Messenger RNA
MS	Murashige and Skoog
NAA	1-naphthaleneacetic acid (auxin family)
NASC	Nottingham <i>Arabidopsis</i> stock centre
NCBI	National Centre for Biotechnology Information
NJ	Neighbour joining
NPQ	Non Photochemical excitation quenching
N-terminus	Amino-terminus

OD	Optical density
ORF	Open reading frame
PAL	lyase phenylalanine ammonia
pAg4	Polyadenylation sequences from the gene 4 of the TL-DNA
PAnos	Polyadenylation sequences from the nopaline synthase gene
PAR	Photosynthetic active radiation
<i>Pca</i>	<i>Populus x canescens</i>
Pca	Pressure of CO ₂ in ambient air
Pci	Pressure of CO ₂ in leaf
PCR	Polymerase chain reaction
pDNA	Plasmid DNA
PEG	Polyethylene glycol
<i>Peu</i>	<i>Populus euphratica</i>
PI	Isoelectric point
Pg5	Promoter of T _L -DNA gene 5
PKC	Protein kinase C
Pnos	Popaline synthetase promoter
ppm	Parts per million
PQ	Plastoquinone
Ψ	Water potential
PSI	Photosystem I
PSII	Photosystem II
<i>Ptr</i>	<i>Populus trichocarpa</i>
PVP	polyvinyl pyrrolidone
qN	Non photochemical quenching
qP	Photochemical quenching
RB	Right border
REW	Relative extractable soil water
RH	Relative humidity
Rif	Rifamycin
rpm	Rotation per minute
RNA	Ribonucleic acid
RP	Right primer, 3' primer, backward primer
SAR	Sodium absorption ratio
SCR	Structurall conserved region
SD	Standard deviation
SDS	Sodium dodecyl sulphate
SIS	Salt induced serine riche
SSTE	Sodium chloride SDS Tris HCl EDTA
SURE	Sulfur responsive element
Ta	Annealing temperature
TAIR	The <i>Arabidopsis</i> Information Resource
Taq	<i>Thermus aquaticum</i>

TBE	Tris-Borate EDTA
T-DNA	Transfer DNA
TF	Transcription factor
TIL	Temperature induce lipocalin
TG	Trans gene
Tm	Melting temperature
Tris	Tris-(hydroxymethyl)-amino methane
U	Unit
UTR	Untranslated region
UV	Ultraviolet
VDE	Violaxanthin de-epoxidase
v/v	Volume/volume
WPM	Woody plant medium
WT	Wilde type
w/v	Weight/volume
X-Gal	5-bromo-4-chloro-3-indolyl- beta-D-galactopyranoside
ZEP	Zeaxanthin epoxidase

List of companies

Ambion	Austin	USA
Archut GmbH	Lauterbach	Germany
Beckman Fullerton	California	USA
Beckman instruments Inc.	Fullerton	USA
Becton, Dickson	Sparks	USA
Bioquell	Hants	England
Biorad Laboratories	California	USA
Biorad	Munich	Germany
Biozym GmbH	Hess. Oldendorf	Germany
Brand GmbH & Co.	Wertheim	Germany
Comfort	Eppendorf	Germany
Difco	Sparks	USA
Eppendorf	Hamburg	Germany
Eppendorf-Netheler-Hinz GmbH	Hamburg	Germany
Kimax	Naters	Germany
Konrad Benda	Wiesloch	Germany
MBI-Fermentas	St. Leon-Rot	Germany
Merck	Darmstadt	Germany
MWG-Biotech	Ebersberg	Germany
Nalgene	New York	USA
Qiagen	Hilden	Germany
Retsch	Haan	Germany
Roth	Karlsruhe	Germany
Sarstedt	Nümbrecht	Germany
Schott Duran	Württemberg	Germany
SEQLAB	Göttingen	Germany
Serva	Heidelberg	Germany
Siemens Electrogeräte GmbH	Neumünster	Germany
Sigma	Steinheim	Germany
Soil Moisture	Santa Barbara	USA
SPSS Inc.	Illinois	USA
Thermo Finnigan	San Jose	USA
UP Umweltanalytische Produkte GmbH	Landshut	Germany
Walz	Effeltrich	Germany
WTW Wissenschaftlich-Technische Werkstätten	Weilheim	Germany
ZIRBUS technology GmbH	Bad Grund	Germany

1

Introduction

1.1 Soil salinity

Soil salinity is a problem in many parts of the world, especially in arid and semi arid regions where soluble salts accumulate in the soil because precipitation is much lower than evaporation. It is estimated that over 30% of the land area of the world is affected by high salinity (Epstein and Rains, 1987; Landis, 1988). Soil salinity can occur naturally as primary salinity or as the result of human activities as secondary salinity. Examples of activities that cause secondary salinity are inappropriate irrigation regimes and dam building that affect on the hydro-geomorphy (Prathapar *et al.*, 2005). The salt content of the soil affects the vegetation and can easily be estimated by electrolyte conductivity. According to classification of "U.S. Salinity Laboratory Staff" (1969), salinity has been classified based on electrolyte conductivity and plants growth response (Table 1).

Table 1. Soil salinity rating based on soil extract electroconductivity and growth response of agricultural crops (U.S. Salinity Laboratory Staff, 1969)

EC (dS/m)	Soil salinity rating	Plant growth response
0 to 2	Non-saline	Salinity effects negligible
2 to 4	Weakly saline	Growth of very sensitive crops may be restricted
4 to 8	Moderately saline	Yield of many crops restricted
8 to 16	Strongly saline	Only in tolerant crops satisfactory yield
> 16	Very strongly saline	Only a few very tolerant crops grow satisfactorily

There are three groups of salt affected soils: saline soils, sodic soils and salt-sodic soils. Saline soils have high concentrations of all salts. In sodic soils just the amount of sodium is high, saline-sodic soils are containing high amounts of sodium salts mostly as NaCl. Salt affected soils have been classified by evaluating the pH, EC and SAR (James *et al.*, 1982) (Table 2).

Table 2. Classification of salt affected soils based on saturation extract analysis (adapted by James *et al.*, 1982).

Classification	Electrical conductivity (dS/m)	Soil pH	Sodium absorption ratio (SAR)
Saline	>4	<8.5	<13
Sodic	<4	>8.5	≥13
Saline-Sodic	>4	>8.5	≥13

* The SAR (sodium absorption ratio) is calculated as:

$$SAR = [Na^+] / \sqrt{[Ca^{2+} + Mg^{2+}]}$$

where the ion concentration is based on molarities.

1.2 Water and salt uptake

Nutrients enter the plants *via* roots by water inflow. Generally water moves from a high to low water potential (Ouyang, 2002). The hydraulic gradient between soil solution and xylem sap leads to water influx into the xylem from where it is transported to the leaves which have the lowest water potential.

By increasing salinity the amount of solute in the soil or growth medium will increase and cause water deficit because of a decrease in water potential in the growth medium. When excess Na⁺ and Cl⁻ have been taken up an ion-specific stress develops resulting from low K⁺/Na⁺ ratios. Persistent salinity raises the amount of Na⁺ and Cl⁻ in the plant to concentrations that inhibit plant growth (Yamaguchi and Blumwald, 2005). High salt concentrations (greater than 0.4 M NaCl) change the hydrophobic and electrostatic balance of protein molecules and inhibit proper activity of most enzymes (Wyn Jones and Pollard, 1983). However, toxic effects on cells occur at much lower concentrations (about 0.1 M) pointing to specific targets of salt toxicity (Serrano, 1996).

Plants can not prevent the passive influx of solutes into the cortex cells of root, but can reduce their entrance into the vascular system by devices like Casparian band, retention of salt in the vacuoles and active exclusion. Na^+ may interfere with sites involved in binding of cations such as K^+ , Ca^{2+} or Mg^{2+} (Wyn Jones and Pollard, 1983; Serrano, 1996). Na^+ can move passively through general cation channels into the cytoplasm (Blumwald, 2000; Mansour *et al.*, 2003). Export of Na^+ through Na^+/H^+ antiporters is also known (Hunte *et al.*, 2005). In plants, K^+ is the major cation to maintain cellular ion homeostasis by establishing an electrochemical concentration gradient across the plasma membrane. K^+ contributes in regulating hydraulic and osmotic pressure and balances the pH. Excess Na^+ disturbs these functions. Chloride (Cl^-) is also causing toxicity and osmotic stress in plants (Ruiz *et al.*, 1999), but is one of the main elements to control cell homeostasis and the regulation of cell volume specially by involving volume activated Cl^- channels like CLC-3 (Wang *et al.*, 2000). Cl^- may interfere with anionic sites involved in binding of RNA and anionic metabolites such as bicarbonates, carboxylates and sugar phosphates (ATP, ADP, NADH) (Wyn Jones and Pollard, 1983; Serrano, 1996). Active absorption of Cl^- is very important for normal plant development. By silencing cation-chloride-cotransporter (CCC) in *Arabidopsis*, elongation of inflorescence was severely reduced and leaves showed necrosis (Colmenero-Flores *et al.*, 2007).

1.3 Effects of salt stress in plants

In response to salinity, plants can be divided into halophytes and glycophytes. Halophytes accumulate a high amount of ions in their organisms while glycophytes exclude salt from their tissues. Halophytes have been classified as facultative and obligatory halophytes. Obligatory halophytes are not able to grow in non saline conditions whereas facultative halophytes prefer non saline environment but also can grow and survive in saline areas (Flowers, 1977). Plants differ in salt tolerance. For example, *Atriplex vesicaria* produced high yield in 700 mM NaCl (Black, 1960), while *Atriplex nummularia* died at 600 mM NaCl (Ashby and Beadle, 1957). *Salicornia europaea* plants remained alive in 1020 mM NaCl (Montfort and Brandup, 1927), while species of the halophyte alga *Dunaliella* even survived in 4 M NaCl (Johnson *et al.*, 1927).

Except a small group of obligatory halophytes, salt stress reduces plant growth and productivity (Ashraf and Orooj, 2006; Sudhir and Murthy, 2004). In most glycophytes,

increasing external NaCl concentrations increases the amount of Na⁺ and Cl⁻ in both shoot and roots, whereas K⁺ and Ca²⁺ decrease with the progressive rise in salinity (Ashraf and Orooj, 2006). Increasing solutes during salt stress and consequently decreasing water potential in the rhizosphere, decreases or even disrupts water uptake of plants in the early stages of salt stress causing water deficit in the plant. The capability of plants to adjust a proper gradient is different from species to species but generally plants respond to increasing salinity by stomatal closure that is induced by ABA signalling. This is followed by a decrease in evapotranspiration to prevent loss of turgor and recovery of osmotic homeostasis with the accumulation of inorganic ions, amino acids, sugars and other metabolites (Ashraf and Orooj, 2006; Katerji *et al.*, 2000). In sensitive species organic materials contribute more to osmotic adjustment than in tolerant species, where osmotic adjustment is due to Na⁺ and Cl⁻ accumulation (Meloni *et al.*, 2001). One of the common salt stress symptoms is reduction of photosynthesis and transpiration (Sudhir and Murthy, 2004). The chlorophyll content decreased in salt susceptible plants such as tomato, potato and pea, but chlorophyll content increased in salt tolerant plants such as mustard and wheat (Sudhir and Murthy, 2004; Venkatesan *et al.*, 2005). The content of carotenoids increased in rice plants under salt stress (Kulshreshta *et al.*, 1987) and decreased in black cumin (Hajar *et al.*, 1996). Photosystem II (PSII) is a pigment-protein complex in the thylakoid membrane mediating non-cyclic electron transport from water to first mobile electron carrier, namely plastoquinone (PQ). Maximum efficiency of photosystem II does not decrease in salt resistant plants and is reduced in salt sensitive species (Wang *et al.*, 2007).

1.4 Salt tolerance mechanisms

The mechanism of salt tolerance differs from species to species (Parida and Das, 2005). However, the sensitivity of cytosolic enzymes to salt is similar in both glycophytes and halophytes, indicating that the maintenance of a high cytosolic K⁺/Na⁺ ratio is a key requirement for plant growth in soils with a high concentration of salt (Glenn *et al.*, 1999). Maintenance of K⁺/Na⁺ and Ca²⁺/Na⁺ ratios is one of strategies of salt tolerance (Yeo, 1998). This is possible either by active exclusion of Na⁺ from the intracellular space and or by active absorption of K⁺ into the cytoplasm. Na⁺/H⁺ antiporters and K⁺/Cl⁻ cotransporters can help plant to maintain K⁺/Na⁺ homeostasis (Colmenero-Flores *et al.*, 2007).

Other salt tolerance mechanisms are accumulation of low-molecular-mass compounds like proline, glycine betaine, sugars (like glucose, fructose) and polyols (like mannitol, pinitol) in cytoplasm to establish osmotic homeostasis between vacuole and cytoplasm. This supports continued water influx by lowering the internal water potential (Parida *et al.*, 2004; Zhu, 2001).

Improving salt tolerance in plants is possible in different ways: direct selection of tolerant varieties of a species in saline environments or by mapping quantitative trait loci and subsequent use of selection markers or by generation of transgenic plants by introducing a novel gene or changing the expression level of an existing gene (Yamaguchi and Blumwald, 2005).

1.5 *P. euphratica* and response to salinity and osmotic stress

The genus *Populus* L. from Salicaceae is an important tree model system for the study of tree physiology and genetics and it is famous for its short rotation time and high productivity level (Ceulemans and Deraedt, 1999). Poplars are dioecious, wind pollinated, and are mostly distributed along river floodplains (Bradshaw *et al.*, 2000). *Populus x canescens* (Aiton) Sm., an endemic poplar species in Europe is natural hybrid between *Populus alba* and *Populus tremula* that can growth in slightly acidic to slightly alkaline soils and is known as salt sensitive species (Bolu and Polle, 2004). In contrast, *Populus euphratica* (Oliv.), an exotic poplar species in Europe, belongs to the Irano-Turanian and Saharo-Arabian bio- climatic zone (Gruenberg-Fertig, 1996). It is native to northwest China, middle and west Asia (Lledo *et al.*, 1995; Xu, 1988). It can growth in arid environments and it can tolerate a considerable amount of salt in soil but is susceptible to soil water deficit, late frost and pests (Bogeat-Triboulot *et al.*, 2007; Ottow *et al.*, 2005; Wan *et al.*, 2004).

Since both salinity and water deficit induce osmotic stress in plants, the response of *P. euphratica* to osmotic stress induced by withholding water has been analysed in an independent study as well (Bogeat-Triboulot *et al.*, 2007). In this study, anatomical, ecophysiological and molecular responses of *P. euphratica* to gradually developing water deficit were investigated (Bogeat-Triboulot *et al.*, 2007; see App. 7.29). The anatomical studies were contributed as part of this thesis (see App. 7.29) and revealed that water deficit decreased vessel and fibre lumen area and increased fiber cell wall thickness.

P. euphratica showed stomatal closure under water deficit and the compatible solutes (inositol, salicin, glucose, fructose, sucrose, and galactose) increased. Chlorophyll and carotenoid content per leaf area were not affected, but the chlorophyll a/b ratio increased under water deficit. Water deficit led to lipid peroxidation. At the molecular level lipocalins (see 1.6) were upregulated at strong water stress (Bogeat-Triboulot *et al.*, 2007).

These data underline that *P. euphratica* is very drought sensitive. Under field conditions, it was shown that the mortality of plantations in loamy and sandy sites at an early age is very high (Wang *et al.*, 1996; Khamzina *et al.*, 2006). *P. euphratica* is mostly distributed at springs, river banks and valleys, where it forms pre-dominant populations in regions with periodical waterlogging (Wang *et al.*, 1996; Khamzina *et al.*, 2006). It dislikes shade and is intolerant of root or branch competition (Huxley, 1992).

In native forests of *P. euphratica* the salt content in soil can be about 1%, but can reach up to 7% (Ma *et al.*, 1997). Under hydroponic conditions, 3-months-old saplings of *P. euphratica* could cope with up to 450 mM NaCl for one month and removal of the saline medium caused vigorous flushes. Increasing salinity to 600 mM caused mortality of *P. euphratica* (Gu *et al.*, 2004).

Initially, growth of *P. euphratica* increased after irrigating with 100 mM NaCl in soil but decreased later on (Ottow, 2004). When exposed to 150 mM NaCl in the nutrient solution, *P. euphratica* loses turgor pressure within 1h and regains it after one day. Shoot tip water potential dropped in first 30 min and recovered after 12h and decreased again after 2 days. Na⁺ and Cl⁻ accumulated in leaves and roots of salt treated *P. euphratica* with 150 mM NaCl for 9 weeks, K⁺ concentration did not change in leaves and roots but decreased in xylem sap, whereas the Ca²⁺ concentrations were decreased in roots and increased in the xylem sap. At the subcellular level, localization of sodium and chloride revealed that both elements were accumulated in the apoplastic space of leaves whereas the potassium concentration was reduced in leaf apoplast and vacuoles (Ottow *et al.*, 2005). Increasing either NaCl (0, 50, 150, 250 mM) or osmotic stress (0, 200, 300 and 400 mM mannitol) in *P. euphratica* caused accumulation of proline in both old and young leaves (Watanabe *et al.*, 2000). The chlorophyll content of *P. euphratica* supplemented with 150 mM NaCl did not change during short term exposure (Ottow, 2004). In a long term experiment, chlorophyll a was enhanced in both low and high salt stress (irrigating with 50 mM and 200 mM NaCl for 10 days) and the content of other pigments (chlorophyll b and carotenoids) was reduced (Ma

et al., 1997). Increasing salinity up to final concentrations of 200 mM NaCl over 16 days increased membrane permeability of a sensitive poplar species, *P. popularis* by 130%, but membrane permeability of *P. euphratica* did not change (Wang *et al.*, 2007).

Ma *et al.* (1997) showed that net photosynthesis of *P. euphratica* irrigated with high salt concentration (200 mM) declined but recovered after three weeks close to the control values. No difference in photosynthesis was observed under low salt concentrations (50 mM). Studies on four poplar species (*P. x euramericana*, *P. deltoides* x *P. alba*, *P. alba* and *P. euphratica*) in response to salinity revealed that *P. euphratica* retained the highest net photosynthesis rate in 137 mM NaCl among these species (Sixto *et al.*, 2005). By exposing *P. euphratica* to 50 mM NaCl, net photosynthesis rate and transpiration rate of one-year-old seedlings was reduced within 4 hours because of stomata closure and recovered after 24 hours (Wang *et al.*, 2007). Increasing salinity to 200 mM for 16 days did not change the photosynthesis rate and transpiration rate of *P. euphratica* significantly, whereas in the salt sensitive *P. popularis*, irrigation with 150 mM NaCl caused a severe drop of photosynthesis rate and transpiration after 4 days (Wang *et al.*, 2007).

Initially salinity (50 mM NaCl after one day in one year old plants) did not affect maximum photosystem II efficiency of both *P. euphratica* (salt resistant) and *P. popularis* (salt sensitive), but increasing NaCl stress to 200 mM for 12 days reduced maximum photosystem II efficiency *P. popularis* because of reduction in minimal fluorescence level (F_0) and increasing in maximal fluorescence level (F_m), but no change in *P. euphratica* was observed (Wang *et al.*, 2007).

There is some evidence that ABA signalling is involved in early response to dehydration. ABA is transported from the root and through the xylem sap to the leaves and causes stomatal closure before any water deficit in leaves take place (Chaves and Oliveira, 2004). According to Chen *et al.* (2001, 2002), the concentration of ABA in the xylem increased more rapidly in *P. euphratica* than in other more salt-sensitive poplar species. This compilation shows that *P. euphratica* is salt but not drought tolerant. The mechanisms leading to salt tolerance are not understood.

1.6 Lipocalins structure and function

There is some evidence that lipocalins may play an important role under environmental stress. This gene became up-regulated in both osmotic (Bogeat-Triboulot *et*

al., 2007) and salt (Brinker and Polle, 2005) stress in *P. euphratica*. The term lipocalin originated from “Lipo” which means lipid and “Calix” (Latin: *Calyc*, *Calyx*; Greek: *Kalyx*) which means cup-form, describing highly conserved structure and lipid-binding properties of members of this family. They belong to a large family of extracellular proteins which bind with hydrophobic molecules but their function (often putative) is very diverse and in many cases not yet known (Bishop *et al.*, 1995; Bishop, 2000; Flower *et al.*, 2000). Lipocalins are present in bacteria, protozoa, plants, arthropods, and cordates (Sánchez *et al.*, 2003). Ligand-binding properties of lipocalins have been summarized by Flower (1996). Three families of ligand binding proteins; ie., lipocalins, fatty acid-binding proteins (FABPs), avidins together with a group of metalloprotease inhibitors (MPis) and triabin, form the calycin superfamily (Flower *et al.*, 2000). In lipocalins three structurally conserved regions (SCRs) related to features of the β -barrel are conserved: SCR1 (strand A and 3_{10} -like helix preceding it; consensus GWxR), SCR2 (portions of strands F and G, and the loop linking them; consensus TDY), and SCR3 (portion of strand H, the beginning of the following helix and the loop in between; consensus R) (Figure 1). Lipocalins are involved in the regulation of cell homeostasis and the modulation of the immune system activation in mammals (Flower, 1996). The plasma membrane anchored lipocalins also seems to have an important role in membrane biogenesis and repair, and in adaptation of cells to high osmotic stress (Bishop, 2000). First plant lipocalins were identified from xanthophyll cycle enzymes such as violaxanthin de-epoxidase (VDE) and zeaxanthin epoxidase (ZEP) that catalyze the addition and removal of epoxide groups (cyclic ether with only three ring atom) in carotenoids of the xanthophyll cycle in plants (Bugos *et al.*, 1998). These two members of lipocalin in compare with “true plant lipocalins” (see follow) do not share all three SCRs motifs and other domains except lipocalin are also present in their structural features (Charron and Sarhan, 2006).

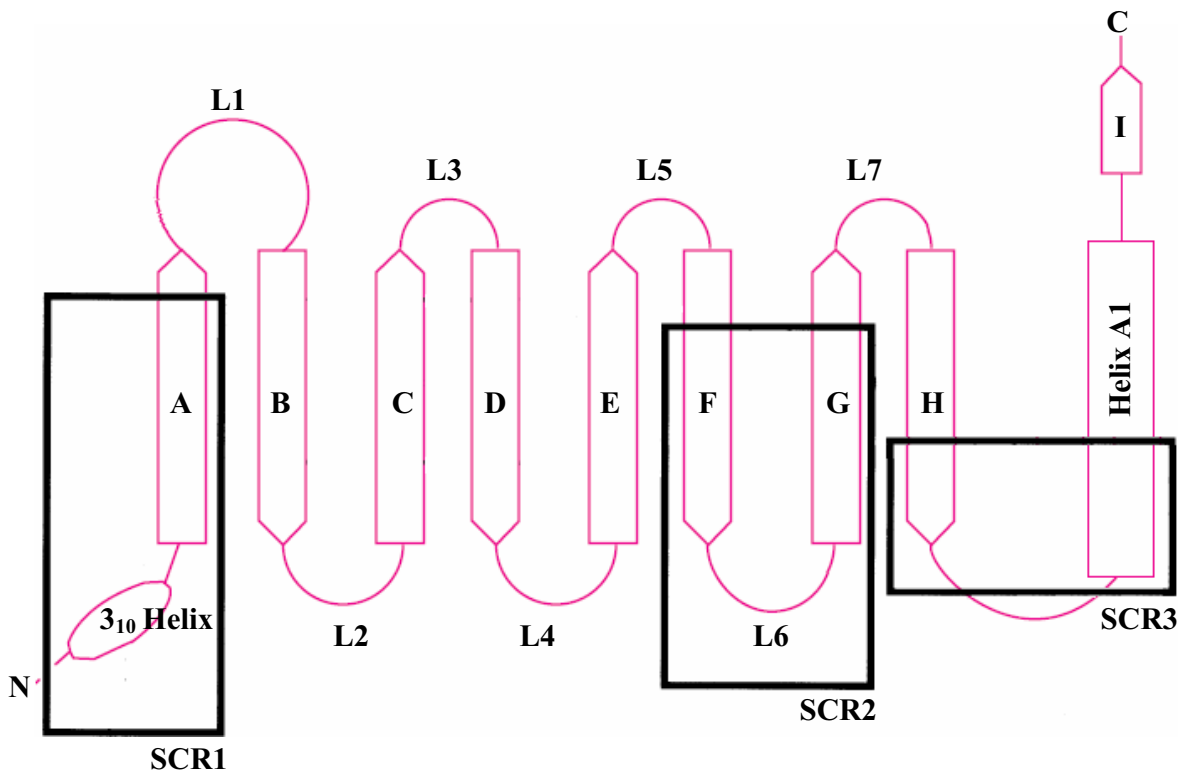


Figure 1. Scheme of lipocalin folding structure. Nine β -strands (labeled A to I) together with seven loops (labeled as L1 to L7) form a closed β -barrel and a 3_{10} helix closing this end. Three structurally conserved regions (SCRs) are marked as boxes. N and C are the amino and carboxy termini of the protein, respectively. Modified after Flower *et al.* (2000).

True plant lipocalins were first identified from an EST database of cold-acclimated wheat. Based on an integrated approach of data mining, expression studies, cellular localization, and phylogenetic analyses new plant lipocalin members were identified and classified in two groups: temperature induced lipocalins (TILs) and chloroplast lipocalins (CHLs) (Charron *et al.*, 2005). Considering the plant lipocalin properties, tissue specificity, response to temperature stress, and their association with chloroplasts and plasma membranes of green leaves, a protective function of the photosynthetic system against temperature stress has been hypothesized (Charron *et al.*, 2005). Sequence analysis revealed that plant lipocalins share significant homology with three evolutionary related lipocalins, the mammalian apolipoprotein D, the bacterial lipocalin (Blc) and the insect Lazarillo protein (Charron *et al.*, 2005). Blc is very close to TILs and is far from other families. Blc is expressed under stress conditions such as starvation or high osmolarity and is thought to have an important role in membrane repair and maintenance by storage or transporting lipids (Campanacci *et al.*,

2004). Subcellular localization of TaTIL and AthTIL using green fluorescence protein (GFP) in the transient expression system with onion epidermal cells showed that this protein is localized in plasma membrane (Charron *et al.*, 2005). Also AthTIL protein was increased in leaf plasma membrane of *Arabidopsis* after cold acclimation as documented by mass spectrometric approaches (Kawamura and Uemura, 2003).

1.7 Objectives

Salt tolerance strategies of *P. euphratica* are not fully understood. Most studies to date have analysed plants exposed to salt shock. In this work, ecophysiological responses of *P. euphratica* and *P. x canescens* to salt stress were studied with emphasize on long term salt adaptation. In addition, the characteristics of two novel genes whose expression was salt-induced, were investigated. The objectives of this study were:

- to document ecophysiological responses to salt stress in *P. euphratica* and *P. x canescens*.
- to characterize novel salt-induced genes in *P. euphratica*
- to search homolog genes in the salt sensitive species *P. x canescens* and investigate gene expression.
- to characterise the role of these candidate genes in salt resistance using an integrative approach of loss of function and in silico analyses.

2

Materials and Methods

2.1 Plant materials and preparation

Populus euphratica Olivier (clone B2, Ein Avdat region, Israel; obtained from Prof. A. Altman, University of Jerusalem) and *Populus x canescens* (clone INRA717 1-B4, a hybrid poplar of *Populus alba* x *P. tremula*) were used in this work. Seeds of T-DNA insertional *Arabidopsis* mutant lines (At5g58070: Salk_136775 and At5g02020: SALK_146631) were ordered from the Nottingham Arabidopsis Stock Center (NASc, University of Nottingham, UK). The corresponding wild type Columbia 0 (ecotype Col-0) was received from the Max Planck Institute for breeding research (Cologne, Germany).

Propagation of *Populus* species was performed by *in-vitro* micropropagation according to a modified method of Leplé *et al.* (1992). Plants were maintained in a culture room (16 h light, 200 $\mu\text{mol PAR m}^{-2} \text{s}^{-1}$, 25°C, 60% relative air humidity). Clones of *P. euphratica* were maintained in half-MS propagation-medium (App. 7.1). Stems of stock plantlets (Figure 2A) were cut into fragments of *ca.* 2 cm length with at least 2 leaves and transferred to Petri plates (Schott Duran) containing WPM agar medium (App. 7.2) for 2 weeks (Figure 2B). After rooting, propagules were transferred to culture tubs (15 x 3cm) with

plastic lids (Kimax) containing propagation medium. After 4 weeks of growth under sterile conditions, plantlets were transferred to 50 ml Falcon tubes (Sarstedt) containing nutrient solution (App. 7.3) modified Long Ashton medium (Hewitt and Smith, 1975) so that the apical parts were exposed to open air under a glass plate. Glass plates were lifted gradually and after some days were removed completely. In order to avoid high transpiration half of the lamps were turned off and plants were observed periodically. If plants displayed symptoms of wilting, glass plates were replaced again. After two weeks, plants were transferred in 1.8 L pots containing nutrient solution (App. 7.3) and cultivated until an appropriate shoot length (20-25 cm) was reached. Finally plants were transferred in 20l boxes for hydroculture experiments or in 1.8 L pots containing soil (Frühstorfer Erde, Type N, Archut).



Figure 2. *Populus euphratica* stock (A) in a culture tube containing half MS agar medium and plantlets in rooting agar medium (WPM) in a Petri plate (B).

In case of *P. x canescens*, clones were maintained in propagation agar medium (App. 7.4). Stem tip cuttings of *P. x canescens* with at least 2 leaves were used as propagule. The cuttings were planted in Petri plates (Schott Duran) containing agar rooting medium (App. 7.5) under a clean bench (Bioquell). After 3 weeks, when roots were grown, they were transferred in 1.8 L pots containing nutrient solution (App. 7.3) with glass covers and adjusted to ambient conditions as described above.

A. thaliana plants were grown from seeds on agar plates (App. 7.5) as follows: Seeds were sterilized in 5% Ca(Cl₂O) (Merck) plus 0.02% Triton x-100 (Serva) for 5 min, and then rinsed 3 times with distilled water. Suspended seeds in water were pipetted on a sterile filter paper and picked one by one with a dissection needle and sown on agar plates. For

stratification, plates were placed at 4°C for 3 days horizontally. After stratification, plates were transferred into a culture room (16 h light, 200 $\mu\text{mol PAR s}^{-1} \text{cm}^{-2}$, 25°C, 60% relative air humidity) for 10 days. Seedlings were transferred either into soil or nutrient solution afterwards.

For *Arabidopsis* soil culture (Figure 3A), ten days old plants germinated on agar plates in culture room were transferred in small pots (25 cm^3) filled with soil (Fruhstorfer Erde, Type T 25, Archut) and grown in a green house under long day conditions (16 h light with approximately 150 $\mu\text{mol PAR s}^{-1} \text{cm}^{-2}$) or in a climate chamber under short day conditions (8 h light with 300 $\mu\text{mol PAR s}^{-1} \text{cm}^{-2}$ and 16 h dark, 20°C and a relative air humidity of 60%).

For *Arabidopsis* hydroponic culture, ten days old plants germinated on agar plates in culture room were transferred into 1.8 litter pots containing nutrient solution (App. 7.3) and grown in a climate chamber under short day conditions (8 h light with 300 $\mu\text{mol PAR s}^{-1} \text{cm}^{-2}$ and 16 h dark, 20°C and relative air humidity of 60%). Seedlings were placed on bored holes in PVC disks fixed over the nutrient solution surface with a PVC holder (Figure 3B).

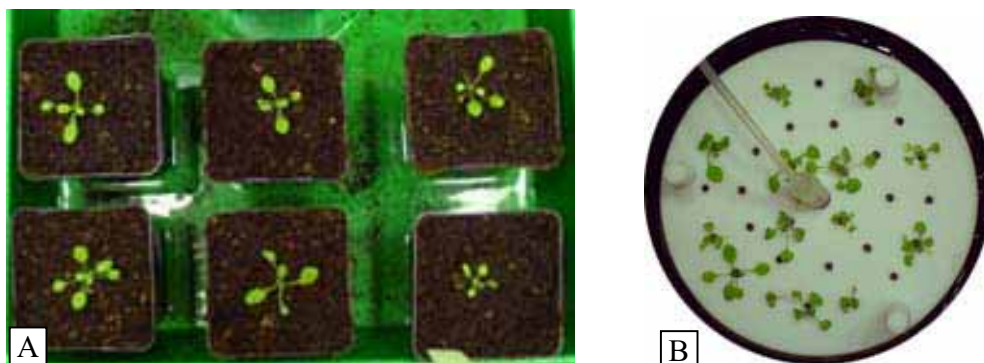


Figure 3. Cultures of *A. thaliana* in soil (A) and hydroponic (B).

2.2 Experimental treatments

2.2.1 Salt shock of *P. euphratica* and *P. x canescens*

For expression analysis of candidate genes in both poplar species the following experiments were conducted: Plants of *ca.* 25 cm stem height were exposed to 150 mM NaCl in hydroponic culture (16 h light, 200 $\mu\text{mol PAR s}^{-1} \text{cm}^{-2}$, 25°C, 60% relative air humidity). Harvests were conducted 0, 3, 6, 12 and 24 hours after adding 150 mM NaCl to the nutrient solution. To avoid a possible photoperiod effect, the lights remained on two days before harvest (Figure 4).

	1 st harvest	2 nd harvest	3 rd harvest	4 th harvest	5 th harvest
Time after adding 150 mM NaCl	0 (control)	----- 3h	-----6h	-----12h	-----24h

Figure 4. Scheme of salt shock experiments of *P. x canescens* and *P. euphratica* (n=5).

2.2.2 Short term salt adaptation of *P. euphratica* and *P. x canescens*

Poplar plants of *ca.* 40 cm height were acclimated to salinity in hydroponic culture. For *P. x canescens* the concentration of NaCl was increased weekly by 25 mM steps up to 75 mM. In case of *P. euphratica*, plants were divided in three salt adapted groups together with one control. Three groups were salt adapted to reach final concentrations of 25 mM, 100 mM and 200 mM, respectively, as shown in Figure 5. Harvests were conducted one week after reaching the target salt concentration. Nutrient solutions were exchanged two times per week.

a) <i>P. x canescens</i> salt adaptation				
		1 st week	2 nd week	3 rd week 4 rd week
Group 1: control	Without NaCl	-----	-----	-----Harvest
Group 2: Salt adaptation	Without NaCl	----- 25 mM	-----50mM	-----75 mM-- Harvest
b) <i>P. euphratica</i> salt adaptation				
		1 st week	2 nd week	3 rd week
Group 1: control	Without NaCl	-----	-----	----- Harvest
Group 2: Salt adaptation	Without NaCl	-----	----- 25 mM	----- Harvest
Group 3: Salt adaptation	Without NaCl	-----	----- 25 mM	-----100 mM ---- Harvest
Group 4: Salt adaptation	Without NaCl	-----	----- 25 mM	-----100 mM---- 200 mM ---- Harvest

Figure 5. Scheme of short term salt adaptation experiments conducted with of *P. x canescens* (n= 10) and *P. euphratica* (n=5), respectively.

To investigate expression levels of candidate genes, 3-month-old *P. euphratica* and *P. x canescens* were exposed to 25 mM NaCl in hydroponic culture (16 h light, 150 $\mu\text{mol PAR s}^{-1} \text{cm}^{-2}$, 25°C, 60% relative air humidity). One group was harvested after two weeks and the rest was exposed to 150 mM for more two weeks. Harvest was conducted after two weeks. At each harvest date non-treated samples were harvested as control. Four replications for each treatment were taken for expression analysis.

	Start	2 nd week	4 th week
Group 1: Control 1	-----	-----Harvest	
Group 2: Salt adaptation 1	25 mM NaCl-----	-----Harvest	
Group 3: Control 2	-----		----- Harvest
Group 4: Salt adaptation 2	25 mM NaCl -----		----- Harvest

Figure 6. Scheme of two weeks salt adaptation experiments conducted with of *P. x canescens* (n= 4) and *P. euphratica* (n=4).

2.2.3 Long term salt adaptation of *P. euphratica*

P. euphratica as a salt tolerant species was observed for long time periods (4 months). Plants of 30 cm height grown in hydroponic culture were acclimated to salinity in a green house (16 h light with approximately 150 $\mu\text{mol PAR s}^{-1} \text{cm}^{-2}$). For this purpose, the concentration of NaCl was increased weekly as up to 150 mM as shown in Figure 7. Harvests occurred 3 months after exposure to 150 mM NaCl. Nutrient solutions were exchanged two times per week.

	1 st week	2 nd week	3 rd week	4 th week	16 th week
Control	-----				----- Harvest
Salt adaptation	-----0-----	-----25mM -----	----- 50mM -----	-----100mM -----	----- 150mM ----- Harvest

Figure 7. Scheme of long term salt adaptation of *P. euphratica* in hydroculture (n=5).

Long term salt adaptation was also carried out with soil-grown plants (150 $\mu\text{mol PAR s}^{-1} \text{cm}^{-2}$, photoperiod 16 h light, 22°C). Plants of 30 cm height were subjected to 50 mM NaCl and the salt concentration was increased weekly with 50 mM steps to reach a final

concentration of 150 mM as shown in Figure 8. Plants were irrigated every day with 150 mM NaCl for 2 months. In the 3rd month plants were irrigated alternatively with 150 mM NaCl and with tap water. Finally, plants were irrigated for one further week with 150 mM NaCl and harvested.

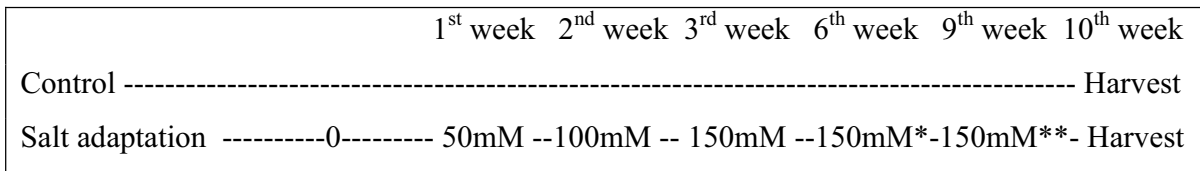


Figure 8. Scheme of long term salt adaptation of *P. euphratica* in soil (n=10).

* One day with 150 mM NaCl, one day with tap water ** Every day with 150 mM NaCl

2.2.4 Germination rate and root growth assays of *Arabidopsis thaliana*

For phenotypic characterisation of wild type and mutants of *Arabidopsis* under different stress conditions, wild type and knock out lines of *A. thaliana* were compared. For running *Arabidopsis* root assay experiments 12 x 12 cm sterile plastic plates (Sarstedt) containing rooting medium (App. 7.5) were used. 24 seeds were sown on each agar plate. For minimizing plate position effect seeds were sown in 3 alternating groups (8 seeds from wild type, 8 seeds from line At5g58070.1 Salk_136775 and 8 seeds from line At5g02020.1 Salk_146631). After stratification (3 days, 4°C), plates were transferred into a climate chamber and maintained with 16 h light of 300 $\mu\text{mol PAR s}^{-1}\text{cm}^{-2}$, 8 h dark, at 20°C and a relative air humidity of 60%. Plates were placed at an angle of *ca.* 65° in plastic holders to allow roots to grow on the surface of the media and also to allow condensed water to drop.

Stress assays were carried out with two NaCl concentrations (50 and 100 mM). For medium preparation, the desired concentration of NaCl was added to the basic media (App. 7.5) and autoclaved (121°C, 20min, HST 6x6x6, Zirbus).

12.5% (w/v) polyethylene glycol PEG 6000 was used to induce osmotic stress equivalent to 150 mM NaCl (according to practical measurements see Figure 47). For this purpose, 25% (w/v) PEG was prepared using rooting medium without agar and was autoclaved. This solution was poured on top of the solid agar plates (containing polymerized rooting medium with same volume as PEG solution) to allow diffusion of PEG in the media. After 24 hours, the PEG was poured off.

2.3 Ecophysiological measurements

2.3.1 Analysis of plant performance

Stem lengths, root collar diameters, leaf initiation rates and in some cases root lengths were measured regularly. Stem length was measured with a metric folding ruler from a point marked near to the root collar up to the apical bud. Root length was measured usually at harvest from a marked point near root collar down to the tip of the longest root. Root collar diameter was measured by a digital calliper placed vertically on a marked line close to the stem base.

At harvest fresh mass was separately determined for stems, leaves and roots and total fresh mass was calculated from these data. Dry mass was calculated by drying a representative sample of each tissue for one week at 40° C. Leaf area was measured by means of Win Dias Farb-Bildanalyse-System (UP) at harvest.

2.3.2 Membrane permeability

Damaged membranes release electrolytes that cause increases in electrical conductivity in the surrounding medium. To assess membrane injury of leaves, 10 leaf-disks (1 cm diameter) were cut out of one or two uppermost fully expanded leaves of *P. euphratica* with a cork borer. In *P. x canescens*, leaves were harvested in three positions: (a) 3rd to 5th leaf (=1-week-old leaves that were formed after reaching the final salt concentration), (b) 10th to 15th leaf (=3-week-old leaves that were formed during salt acclimation period) and (c) 20th to 25th leaf (=leaves that developed before the salt adaptation period). For other tissues (bark, xylem, root, shoot apex) *ca.* 0.5 g of tissues were weighted. Bark and xylem were harvested from bottom part of stem. Fine roots were immediately used for measurements. Also from each tissue a part was used to determine water content.

The leaf disks and other tissues were rinsed shortly in ddH₂O to remove solutes from both tissues surfaces and from cells damaged by cutting. The tissues were floated in 20 ml ddH₂O. The electrolyte conductivity was measured with a conductivity meter (LF 315/ Set, WTW) after 24 hours incubation at room temperature. At the end, the samples were boiled for 30 min at 100°C to achieve 100% electrolyte leakage and after cooling down to room

temperature total electrolyte conductivity was measured. Then the amount of electrolyte conductivity per water content was calculated. Finally the percentage of plasma membrane injury was calculated according to Blum and Ebercon (1981) with some modifications:

$$I\% = 1 - [1 - (T_{24}/T_{max})] / [1 - (C_{24}/C_{max})] \times 100$$

where I% is percentage of plasma membrane injury, T_{24} and T_{max} are electrolyte conductivity of the tissue water extract of salt treated plants after 24 h and after boiling, respectively, and C_{24} and C_{max} are the corresponding data for controls.

If this ratio is 0 %, electrolyte leakage of control and treated tissue from membrane are same and no stress-induced injury in plasma membrane is observed.

2.3.3 Leaf Water Potential

A Scholander pressure chamber (Soil Moisture) was used to measure the midday leaf water potential. For this purpose, the seventh leaf from the stem apex was cut and the blade was covered with an aluminium foil to protect water loss. The tip of the leaf petiole was sliced with a sharp razorblade and inserted through a gasket in the lid of the chamber. The lid was fixed over the chamber and consequently the leaf was enclosed with only the tip of its petiole. Air was gradually admitted to the chamber and increased in pressure. The cut-section was observed. The equilibrium pressure required to bring water to the cut surface of the petiole was recorded as leaf water potential.

2.3.4 Pigment analysis

Pigments were analyzed according to the procedure of Lichtenthaler and Wellburn (1983). Two leaf disks (0.8 cm diameter) cut out of tenth leaf from the stem apex were powdered with liquid nitrogen and weighted. The pigments were extracted in 80 % acetone. Chlorophyll a, chlorophyll b, and carotenoid contents were calculated by spectrophotometric absorbance measurement (Beckman) at 663, 646 and 470 nm according to following equations:

$$\text{Chlorophyll a} = 12.21A_{663} - 2.81A_{646} [\mu\text{g ml}^{-1}]$$

$$\text{Chlorophyll b} = 20.13A_{646} - 5.03A_{663} [\mu\text{g ml}^{-1}]$$

$$\text{Carotenoids} = (1000A_{470} - 3.27 \times \text{Chl a} - 104 \times \text{Chl b}) / 229 [\mu\text{g ml}^{-1}]$$

Finally the concentration was calculated based on leaf area and leaf fresh mass (Crowella et al., 2003).

2.3.5 Gas exchange measurements

Gas exchange of mature leaves (8th -10th leaf from the apex) was measured using a portable photosynthesis system (HCM-1000, Walz). For this purpose a measuring leaf was clamped in a cuvette exposed to an air flow. Gas exchange between the leaf and its surroundings was determined with help of an infrared gas analyser (IRGA) in this instrument. Transpiration and net photosynthesis together with stomatal conductivity were calculated according to given equations in the system automatically. Gas exchange in short term salt acclimated *P. x canescens* plants was measured one week after reaching 75 mM NaCl at times from 12:30 to 13:30 h with 687 $\mu\text{mol PAR m}^{-2} \text{s}^{-1}$ (n=3). In case of short term salt adapted *P. euphratica* plants, it was measured one week after reaching final concentrations of 25, 100 and 200 mM NaCl, respectively, at times from 10:00-16:00 h with 222 $\mu\text{mol PAR m}^{-2} \text{s}^{-1}$ (n=6).

2.3.6 Analysis of chlorophyll fluorescence

In all measurements, green and not affected upper leaves (6th to 10th leaf from the apex) of long term salt adapted *P. euphratica* (150 mM final concentration) were subjected to photosynthetic electron transport analysis (n=5). Leaves were dark adapted for 20 min and subjected to a short saturated light pulse (6000 $\mu\text{mol m}^{-2} \text{s}^{-1}$) and fluorescence emission changes were recorded by means of MINI-PAM fluorometer (Walz). Then the actinic light was turned on with a light intensity of ca. 160 $\mu\text{mol PAR m}^{-2} \text{s}^{-1}$ for 5 min and the leaf was exposed to another short saturated light pulse. The fluorescence was measured and recorded automatically before and after each saturated pulse. Following parameters were calculated:

$$\Phi\text{PSII (dark)} = (F_m - F_0) / F_m$$

$$\Phi\text{PSII (light)} = (F'_m - F') / F'_m$$

$$qP = (F'_m - F') / (F'_m - F'_0)$$

$$qN = (F_m - F'_m) / (F_m - F_0)$$

$$\text{NPQ} = (F_m - F'_m) / F'_m$$

where $\Phi\text{PSII}(\text{dark})$ = quantum yield of photosystem II, $\Phi\text{PSII}(\text{light})$ = actual quantum yield of photosystem II, qP = photochemical quenching, qN = non-photochemical quenching, NPQ = non-photochemical exciton quenching, F_m =maximal fluorescence in darkness, F_0 = basis fluorescence, F'_m = maximum fluorescence in light, F' = basis fluorescence in light, F'_0 = minimum fluorescence that can be achieved in far red light.

Because the Mini-PAM fluorometer had no far red light source, and because basis fluorescence doesn't change so much particularly at low qP values, F_0 was used instead of F'_0 for qP evaluation (Leipner, 2003).

2.3.7 Carbohydrate analysis

Leaf exudates of control and long-term salt-adapted *P. euphratica* plants (3 months at a concentration of 150 mM NaCl) were subjected to carbohydrate analysis using a combination of gas chromatography and mass spectrometry (GC/MS) at Beijing Forestry University by Prof. Jiang. To gain sufficient materials, leaf exudates of five plants were pooled and analyzed together. No biological or technical replication was conducted.

Briefly, the samples were acetyl-derivatized and were separated by a DB-17 capillary column (30 m, 0.25 mm, 0.25 μm) attached to a Finnigan Trace Gas Chromatograph Ultra (Thermo Finnigan), and detected and identified with a Finnigan Trace GC ultra-Trace DSQ GC/MS system (Thermo Finnigan). Ribitol, mannitol, galactose, sorbitol, fructose, inositol, glucose and trehalose were used as standards (Hu *et al.*, 2005).

2.4 Molecular biology

2.4.1 RNA handling

2.4.1.1 RNA extraction

Frozen samples, stored at -80°C , were ground at a speed of 60 rpm for 3 min with a mixer-ball-mill (MM 2, Retsch) in liquid nitrogen. A CTAB RNA extraction method was modified to extract total RNA (Chang *et al.*, 1993) as follows:

First day:

1. 100 mg of powdered samples were added to 600 μl extraction buffer (App. 7.8), pre-warmed to 65°C , in a 1.5 ml tube. Then 12 μl mercaptoethanol (Roth) was pipetted into each tube and samples were mixed for 15 min at 65°C (fume hood) with a thermo-mixer (Comfort).
2. 600 μl chloroform: isoamyl alcohol (24:1) was added and mixed for 15 min at room temperature. Then samples were centrifuged at 6000 rpm for 15 min at room temperature (5417 R, Eppendorf) and supernatants were pipetted to new tubes. Step 2 was repeated once.
3. 0.25 parts of 10 M LiCl, 4°C , was added and chilled on ice over night in fridge (4°C).

Second day:

4. Samples were centrifuged at 10000 rpm for 20 min at 4°C . The pellets were dissolved with 400 μl SSTE buffer (App. 7.9) for 5 min at 65°C by careful manual shaking.
5. 400 μl chloroform: isoamyl alcohol (24:1) was added and mixed for 5 min at room temperature. Then samples were centrifuged at 14000 rpm for 5 min at room temperature and supernatants were pipetted to new tubes. Step 5 was repeated once.
6. RNA was precipitated with 800 μl pre-cooled 96% ethanol (-20°C) for 1 h at -80°C (or 2 h at -20°C) and spun down at 14000 rpm for 20 min at 4°C .

7. To remove residual salts, pellets were washed twice with 70% ethanol.
8. Finally pellets were dried using a centrifugal vacuum concentrator (3501, Eppendorf) at 45°C for 3-5 min and then dissolved in 20 µl nuclease free water

2.4.1.2 Evaluation of RNA concentration and purity

RNA concentration was determined by a photometer (BioPhotometer, Eppendorf). A UV-Cuvette “micro” with minimum volume of 70 µl (Brand) was used for measuring nucleic acids. RNA extracts may contain contaminations such as proteins, phenols and other organic compounds, because of the extraction method, type of tissue and accuracy during extraction. Protein contamination was detected by calculating the absorbance ratio of $A_{260/280}$ (Clark, 1997). A value greater than 1.8 means that the RNA sample has a minimal amount of protein contamination (Sambrook *et al.*, 1989). However, the A_{260} measurement can be over estimated by presence of genomic DNA or phenols. Polysaccharide contamination was assessed by calculating the absorbance ratio $A_{260/230}$ (Puchood and Khoiratty, 2004). A ratio of $A_{260/230}$ greater than 1.8 indicates low polysaccharide contamination. Generally, pure RNA has $A_{260/230}$ equal to $A_{260/280}$ and greater than 1.8 (Sambrook *et al.*, 1989, Imbeaud *et al.*, 2005). Irrespective the measured ratios, all samples were included and a final decision for excluding a sample was conceded after performing gel electrophoresis.

2.4.1.3 RNA gel electrophoresis

Evaluation of RNA integrity was carried out by running RNA gel electrophoresis. In eukaryotes, intact total RNAs run on a denaturing gel will have at least two sharp, clear 28S and 18S rRNA bands. The 28S rRNA band should be approximately twice as intense as the 18S rRNA band. This 2:1 intensity ratio between 28S and 18S is a good indicator for intact RNA (Simmons *et al.*, 2004). Partially degraded RNA appears as a smear and lacks the sharp rRNA bands, or does not exhibit the 2:1 ratio of high quality RNA. Completely degraded RNA will appear as a very low molecular weight smear. Hence the RNA samples that showed smear or degradation were excluded. RNA gel electrophoresis was performed as follows:

1. 0.6 g agarose (Biozym) was dissolved in 35.2 ml ddH₂O and 4.8 ml 10x MOPS running buffer (App. 7.10) by heating in a microwave oven.
2. 10 ml of 37% formaldehyde solution (Merck) was added under a fume hood and mixed.
3. The solution was poured in a gel electrophoresis tray equipped with a comb and polymerisation took place at room temperature.
4. After removing the comb, gels were assembled in a tank containing MOPS running buffer.
5. 2 µl loading dye for RNA (App. 7.11) was applied to 2 µl RNA extract.
6. The mixture was heated for 10 min at 70°C and chilled on ice.
7. After loading the gel, electrophoresis was conducted with 100 A for 30-60 min. Finally gels were scanned (Fluor s-Multiimager, Biorad).

2.4.1.4 DNase treatment

Contaminating DNA was removed from RNA with DNaseI treatment (Turbo DNA-free kit, Ambion). This step was omitted in those cases where cDNA specific primers were used later on. The procedure was as follows:

1. The equivalent volume of 10 µg RNA was calculated. If the volume exceeded 44 µl, RNA extracts were concentrated by a centrifugal vacuum concentrator (3501, Eppendorf).
2. 5 µl of 10x Turbo DNase buffer and 1 µl of Turbo DNase (2U) were added and mixed.
3. Reactions were incubated at 37°C for 20 min.
4. 5 µl of resuspended DNase Inactivation Reagent was added and mixed.

5. Reactions were incubated at room temperature for 2 min and mixed 2-3 times during incubation.
6. Tubes were centrifuged at 10000x g for 2 min and supernatants were transferred to fresh tubes.

2.4.1.5 Synthesis of first strand cDNA

First-strand cDNA synthesis was carried out using RevertAid First Strand cDNA synthesis kit (Fermentas). 3 µg of total RNA and 1 µl oligo (dT) (0.5 µg/µl) primers (Fermentas) were mixed and DEPC-treated water was added to reach a volume of 12 µl. During this step the mixture was on ice. Then the mixture was incubated at 70°C for 5 min and afterwards chilled. Then 4 µl of 5x reaction buffers together with 1 µl RiboLock™ Ribonuclease Inhibitor (20 U/µl) and 2 µl of dNTP mix (10 mM) was added and mixed. After incubating at 37°C for 5 min, 1µl reverse transcriptase (200 U/µl) was added and then the mixture was incubated at 42°C for 60 min. The reaction was stopped by heating for 10 min, at 70°C. Finally the cDNA was diluted by adding 10 µl DEPC-treated water and stored at –20°C.

2.4.2 DNA handling

2.4.2.1 Genomic DNA extraction from Arabidopsis

This method was modified for genomic DNA extraction of *A. thaliana* leaves (Schneidereit, 2005). Genomic DNA was extracted as follows:

1. One half of a single *A. thaliana* leaf (fresh or frozen) was homogenized in a 1.5 ml tube with plastic pestle.
2. 400 µl extraction buffer (App. 7.20) was added to each tube and shortly mixed, centrifuged at 14000 rpm for 1 min at room temperature. 300 µl of the supernatant was transferred into a new tub.
3. 300 µl isopropanol was added to the supernatant, incubated for 2 min at room temperature and centrifuged at 14000 rpm for 5 min.

4. Pellets were dried in a centrifugal vacuum concentrator (3501, Eppendorf) and dissolved in 100 μ l 1x TE buffer (App. 7.21).

2.4.2.2 Primer design

For primer design some general recommendations were considered as follows:

1. To prevent non-specific priming on template DNA, primers with at least 18 nucleotides in length were designed.
2. Presenting C or G at 3' ends helps to stabilizing probes.
3. A single base, especially C or G, was not repeated consecutively more than 4 times.
4. Approximately same annealing temperature between 52-62°C for a primer pair was considered.
5. Melting temperature was calculated using this formula $(A+T)2+(C+G)4$.
6. To optimize the stability of primer-template duplex, GC content (percentage of G and C in primer) was kept around 50% (40%-60%).
7. Hairpin formation was prevented by avoiding the existence of complementary sequences within primers.
8. Primers were checked to prevent homo-dimer and hetero-dimer formation.
9. Specificity of primers was checked by performing a BLAST search against *P. trichocarpa* genome (JGI *P. trichocarpa* v1.0).
10. Finally, primers were tested by running a temperature-gradient PCR for optimizing annealing temperature.

The designed primers were analyzed with OligoAnalyzer3 online software (<http://eu.idtdna.com/analyzer/Applications/OligoAnalyzer>). All primers were ordered from MWG Biotech AG.

2.4.2.3 Polymerase chain reaction (PCR)

2.4.2.3.1 Standard PCR conditions

Specific fragments of DNA were amplified by polymerase chain reaction (PCR) using HotStarTaq® DNA polymerase (Qiagen; Table 3) and a Mastercycler Gradient (Eppendorf). PCR was performed according to the following steps: Initial DNA denaturation at 95°C for 15 min, 35 cycles of denaturation/annealing/elongation (95°C 30S/52-62°C 1 min/72°C 1 min) and final elongation at 72°C for 10 min and holding at 4°C. A negative control (without template DNA) was always used to check contaminations.

Table 3. Pipetting scheme for a standard PCR mix

Contents (μ l)	Concentration	Volume
PCR buffer	10x	2
MgCl ₂	25 mM	0.4
dNTP mix	each 10 mM	0.4
Forward primer	10 μ M	1.6
Reverse primer	10 μ M	1.6
Template		1
Taq DNA polymerase	5U/ μ l	0.1
ddH ₂ O		12.9

2.4.2.3.2 Quantitative real time PCR (qRT-PCR)

Relative expression levels of genes-of-interest in different samples were investigated with qRT-PCR. For this purpose total RNA of leaves and roots were isolated with CTAB-method (3.5.1.1) and after quality control of RNA by gel electrophoresis (3.5.1.3), 3 ng of RNA, calculated from original concentration of RNA, measured by photometer (3.5.1.2), and

converted to cDNA in a total volume of 30 μl (3.5.1.5). For each gene, a primer pair was designed so that one of the primers spans the introns to avoid amplification of contaminating genomic DNA. Samples were pipetted in 96-well PCR plates (Bio-Rad iCycler iQ) as shown in Table 4.

Table 4. Pipetting scheme for Real time PCR

Contents (μl)	Concentration	Volume
cDNA	0.1 $\mu\text{g}/\mu\text{l}$	2
Bio-Rad Mix	2x	12.5
Forward primer	10 μM	1
Backward primer	10 μM	1
ddH ₂ O		8.5

IQ Master Mix containing SYBR green I (BioRad), as nucleic acid stain was used for amplification and quantification dsDNA. Plates were covered with an optical tape (Bio-Rad iCycler iQ, Hercules, CA) and centrifuged by 1600 g for 3 min (5810R, Eppendorf). Quantitative real time PCR was run on iCycler MyiQ Single Colour Real Time PCR Detection System (BioRad, USA). In Table 5, cycling conditions of PCR are recorded. In each cycle, the emitted green light ($\lambda_{\text{max}} = 522 \text{ nm}$) was measured. Analyses of fluorescence curves of each sample were performed with MyIQ software based on '*PCR base line subtracted curve fit*' mode. The cycle when the fluorescence curve of a sample, crosses a threshold value is referred to as C_t (cycle threshold). Samples having high initial template concentration will have a small C_t value. Finally, extracted C_t data were analyzed with '*Relative expression software tool*' (REST) (Pfaffl, 2001; Pfaffl *et al.*, 2002). In this software expression ratio is calculated based on real-time PCR efficiency and mean crossing point deviation between the sample and control group.

Equation 1. Relative expression of one gene was computed based on real time PCR efficiencies (E) and the crossing time (Ct = PCR cycle in that the fluorescence of sample reach to a defined threshold level) difference (Δ) of an unknown sample versus control (house keeping gene).

$$\text{Relative expression} = \frac{(E_{\text{target}})^{\Delta C_t \text{ target (Mean control - Mean sample)}}}{(E_{\text{ref}})^{\Delta C_t \text{ target (Mean control - Mean sample)}}}$$

Target gene expression was normalized by actin gene expression known as a non-regulated housekeeping gene (App. 7.12, No. 5).

Table 5. Protocol of cycling conditions at RT-PCR

Amplification:

1 cycle

95°C for 03:00

45 cycles

94°C for 00:10

56°C for 00:30

72°C for 00:30

1 cycle

72°C for 01:00

Melt curve:

1 cycle

95°C for 01:00

1 cycle

50°C for 01:00

90 cycles

50°C for 00:10

Increase temperature 0.5°C every 10 seconds up to 95°C

1 cycle

25°C HOLD

2.4.2.4 DNA gel electrophoresis

DNA fragments with different sizes were separated by DNA gel electrophoresis together with λ Pst (App. 7.19) as the marker as follows:

1. 1 g agarose (Biozym) was dissolved in 100 ml 1x TBE running buffer (App. 7.17) by heating in a microwave (Siemens).
2. 5 μ l ethidium bromide (Carl Roth) was added to the liquid gel mixed and poured in a tray with a comb. The gels were polymerized at room temperature.
3. After removing the comb, gels were assembled in a tank containing TBE (1x) running buffer (App. 7.17).
4. 0.5 μ l loading dye (10x) for DNA (App. 7.18) was applied to 4.5 μ l DNA sample.
5. 2 μ l of λ Pst marker (App. 7.19) was used for product size definition.
6. Finally after loading the gel, electrophoresis was conducted with 100 A for 30-60 min and gels were scanned (Fluor s-Multiimager, Biorad).

2.4.2.5 Gel extraction

For extracting a specific DNA band, the band was excised from the gel using a razorblade on a UV-Transluminator (MW 312 nm, Konrad Benda) and extracted with QIAquick Gel Extraction Kit (QIAgene) using the “micro-centrifuge” method.

2.4.2.6 Sequencing

Sequencing of PCR products or plasmids was performed by SeqLab (Sequence Laboratories, Göttingen, Germany). DNA samples up to 300 bp were sequenced by “Hot Shot sequencing” service and samples up to 900 bp were sequenced by so called “extended Hot Shot sequencing” service. If the PCR product produced a sharp single band on an agarose gel, it was purified directly from the PCR mix with QIAquick PCR Purification Kit (QIAgene, Hilden, Germany). Otherwise bands with the expected size were extracted from gels (2.5.2.5). Plasmid purification for sequencing inserted DNA was carried out using “Miniprep-Plasmid Kit” (Seqlab, Göttingen).

2.4.3 *Arabidopsis* SALK line T-DNA knock out mutants

2.4.3.1 Selection of *Arabidopsis* mutants having T-DNA insertion

Searching for T-DNA insertional mutants of highly identical genes in the genome of *A. thaliana* was carried out with “SIGnAL T-DNA Express Arabidopsis Gene Mapping Tool” (Salk Institute Genomic Analysis Laboratory, <http://signal.salk.edu/cgi-bin/tdnaexpress>). Seeds were ordered from Nottingham Arabidopsis Stock Centre (NASc, <http://nasc.nott.ac.uk>). Transgenic plants were grown on rooting agar medium (App. 7.5) including kanamycin (0.05 g / ml). The NptII marker present in the T-DNA exhibits kanamycin resistance in mutants. This characteristic was used for pre-selection of T-DNA positive individuals of the Salk lines. Both homozygote and heterozygote plants showed antibiotic resistance. Wild type individuals can not survive on kanamycin.

2.4.3.2 PCR based screening for homozygous Salk lines

Homozygous mutants were identified by using two different primer combinations. In homozygous mutants, the combination of a primer against the left border of the T-DNA and a gene specific primer resulted in one single band of specific size. Primer combinations flanking the T-DNA integration site did not yield in amplicon when used on homozygous mutants. However, employing wild-type Col-0 DNA amplicons of the expected size could be detected. Accordingly, two bands, representing the wild-type and the insertion allele, could be displayed when using DNA from homozygous plants. SIGnAL iSect Tools software (<http://signal.salk.edu/cgi-bin/tdnaexpress>) was used to design genomic primers for verifying T-DNA insertions.

2.4.4 Vector transformation preparation

2.4.4.1 Preparation of electrocompetent *E. coli*

E. coli (strain Top 10, Invitrogene) electrocompetent cells were prepared as follows:

1. Electrocompetent *E. coli* cells were streaked out on SOB agar plates (+ tetracycline) (App. 7.22) using an inoculating loop and were grown over night at 37°C.

2. A single clone was removed using a sterile toothpick and incubated over night at 37°C in 500 ml Erlenmeyer flask containing 50 ml SOB (+ tetracycline) (App. 7.22).
3. 5 ml of over night culture was transferred in a 2 l flask containing 500 ml SOB medium (without tetracycline) and shaken at 37°C until an optical density of OD₅₇₈= 0.46 – 0.48 was reached (ca. 2 – 2.5 h). Pure SOB medium was used as a blank.
4. Cultures were chilled for 10 min on ice and distributed into two 250 ml centrifuge tubes (Nalgene).
5. Suspension cultures were centrifuged at 6000 rpm for 15 min at 4°C (J2-HS, Beckman).
6. Pellets were re-suspended in 250 ml ice cold ddH₂O and centrifuged at 6000 rpm for 15 min at 4°C and supernatants were collected in separate bottles for autoclaving.
7. Pellets were re-suspended in 125 ml ice cold ddH₂O and centrifuged at 6000 rpm for 15 min at 4°C and supernatants were collected in a separate bottle for autoclaving.
8. Pellets were suspended in 12.5 ml glycerine (10%, sterile and cold) and centrifuged at 6000 rpm for 15 min at 4°C.
9. Pellets were re-suspended in 0.5 ml glycerine (10%, sterile and cold).
10. 40 µl aliquots in sterile 1.5 ml tubes frozen in liquid nitrogen and stored at -80°C.

2.4.4.2 Preparation of electrocompetent *Agrobacterium*

1. *Agrobacterium* (GV3101) was streaked on YEB agar plates (+ Rifamycin and gentamycin) (App. 7.14) using an inoculating loop and were grown for 2 days at 28°C.
2. A single colony was removed with a sterile toothpick and 20 ml YEB medium (+ Rifamycin and gentamycin) was inoculated and incubated over night at 28°C.

3. 16 ml of over night culture was transferred in a 2 l flask containing 400 ml YEB medium (without Rifamycin and gentamycin) and shaken at 28°C until reaching $OD_{578} = 0.46 - 0.48$ (ca. 8 h). Pure YEB medium was used as a blank.
4. Cultures were chilled for 10 min on ice and distributed into two 250 ml centrifuge tubes (Nalgene).
5. Suspension cultures were centrifuged by 6000 rpm for 15 min at 4°C (J2-HS, Beckman).
6. Pellets were re-suspended in 100 ml 1mM Hepes (Roth) pH 7.5 (cold) and centrifuged at 6000 rpm for 15 min at 4°C and supernatants were collected in separate bottle for autoclaving.
7. Pellets were re-suspended in 50 ml 1mM Hepes pH 7.5 (cold) and centrifuged at 6000 rpm for 15 min at 4°C and supernatants were collected in separate bottle for autoclaving.
8. Pellets were re-suspended in 5 ml 10% glycerine in 1 mM Hepes pH 7.5 (cold) and centrifuged at 5000 rpm for 10 min at 4°C.
9. Pellets were re-suspended in 0.4 ml 10% glycerine in 1 mM Hepes pH 7.5 (cold).
10. 40 μ l aliquots were distributed into sterile 1.5 ml tubes, frozen in liquid nitrogen and stored at -80°C.

2.4.4.3 Electroporation

Plasmids were introduced to *E. coli* or *Agrobacterium* via an *E. coli* Pulser (Bio-Rad). For electroporation, 1 μ l of plasmid DNA was added to 40 μ l of electrocompetent cells that thawed on ice and applied to a pre-cooled electroporation cuvette with 1 mm electrode distance and the mix was exposed to 1.8 kV electric pulse. After signal was hold, 1 ml of SOC solution (App. 7.13) for *E. coli* or YEB medium (App. 7.14) for *Agrobacterium* was immediately added and incubated for 1 h at 37°C (2 h at 28°C for *Agrobacterium*). Then aliquots were streaked on LB agar plates plus ampicillin (App. 7.15) (YEB agar plates plus rifamycin, gentamycin and carbicillin (App. 7.14) for *Agrobacterium*) and incubated over

night at 37°C (or for 48 hours at 28°C for *Agrobacterium*). Single colonies were picked and inoculated in LB medium (App. 7.15) (or YEB medium (App. 7.14) for *Agrobacterium*) with the appropriate antibiotic. Presence of inserted DNA was checked by PCR and glycerin stocks were made.

2.4.5 PCR based gene isolation

All genes were isolated from cDNA by running PCR with primers (Table 6) that derived from a section within the UTR regions (approximately 30 bp from start and stop codons, respectively) of genes of interest from the *P. trichocarpa* genome available on the JGI server. (<http://genome.jgi-psf.org/cgi-bin/runAlignment?db=Poptr1>) (DOE Joint Genome Institute, 2004).

Table 6. List of genes cloned in this work from total cDNA.

Abb.	Description	Origin	Primers	Ta °C
PeuTIL	Temperature induced lipocalin like protein	<i>P. euphratica</i>	App.12-Nr.6	54
PcaTIL	Temperature induced lipocalin like protein	<i>P. x canescens</i>	App.12-Nr.6	54
PeuSIS	Salt induced serine rich protein	<i>P. euphratica</i>	App.12-Nr.7	54
PcaSIS	Salt induced serine rich protein	<i>P. x canescens</i>	App.12-Nr.7	54

2.4.6 Cloning genes of interest into pGEM T-vector

Genes of interest were amplified from *P. euphratica* and *P. x canescens* cDNA by PCR and the amplicons were checked by DNA gel electrophoresis. The PCR product was immediately used for ligation into the pGEM-T vector (Figure 9). After ligation, plasmids were transformed into *E. coli* Top10 competent cells (2.4.4.1). *E. coli* cells containing plasmid were selected with help of an ampicillin resistant gene. Resistant colonies containing an insert were selected with help of *LacZ* gene system that offers blue white screening (see 2.4.6.2). White colonies were picked and incubated in LB medium with ampicillin (App. 7.15) and maintained at –80°C as glycerine stocks.

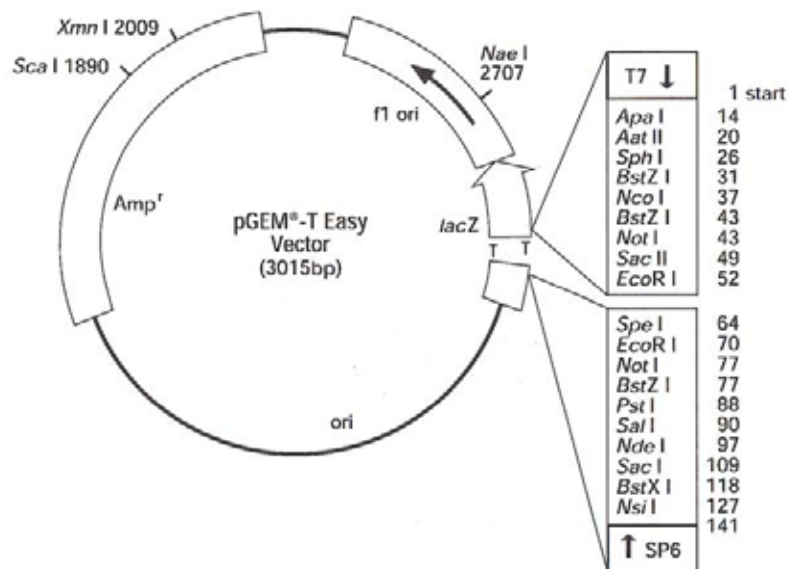


Figure 9. Plasmid map of pGEM-T Vector System I (Promega Corporation, Madison, WI, USA).

2.4.6.1 Ligation in pGEM-T Easy I vector

PCR products have adenine over-hang that formed by *Taq* DNA polymerase activity and can bind with thymine sticky ends of the pGEM-T vector. Hence, directly from PCR reaction tubes, 2 μ l of amplified DNA fragment with 5 μ l 2x Rapid ligation buffer[®] for T4 DNA Ligase, 1 μ l of linear pGEM-T vector and 1 μ l T4 DNA ligase (3U/ μ l) (MBI-Fermentas) were mixed and incubated at 37°C for 1 hour (alternatively at 4°C for 24 hours).

2.4.6.2 Blue-white screening

E. coli cells which are transformed with pGEM T-vectors, have an ampicillin resistance gene and a LacZ operon which encodes a β -galactosidase. LacZ expression is induced by IPTG, a lactose analogue that cannot be metabolized by *E. coli*. LacZ releases indole from the substrate X-gal (a glycoside composed of galactoside and indole). Indole molecules form dimers of blue colour. When pGEM T-vectors contain an insert in the cloning site, the *LacZ* gene gets interrupted and no colour will be produced. So blue colonies indicate re-closure of plasmid DNA resulting in *LacZ* gene function, whereas white colonies indicate that the DNA of interest was inserted into the plasmid and causes interruption of the *LacZ* gene. For blue-white screening 1 ml of grown cells were poured on indicator agar plates (App. 7.16). Plates were surface dried in the laminar air flow and incubated at 37°C over

night. Then, the white colonies were picked and grown in 3 ml LB + Ampicillin (App. 7.15) over night at 37°C.

2.4.6.3 Glycerine stock preparation

500 µl of bacterial culture was mixed with 500 µl of 30% glycerine and immediately frozen in liquid nitrogen. Stocks were kept at -80°C.

2.4.7 Cloning genes of interest in to a plant cloning vector

PeuTIL was cloned into pPCV702 (Figure 10), a binary vector. This vector consists of two main parts: a conditional mini-RK2 replicon and the T-DNA. The mini-RK2 segment consists of oriV and oriT that exhibit T-DNA stability in *E. coli* and *Agrobacterium*. T-DNA contains pg5, Ori_{pBR}, a β-lactamase gene, which confers resistance to ampicillin and carbenicillin (Ap^R / Cb^R) for selection in *E. coli* and *Agrobacterium*, CaMV35S promoter, pAnos, pnos, aph (3') II gene providing kanamycin resistance in transgenic plants and pAg4.

The pGEM-PeuTIL plasmid was extracted from over night culture of *E. coli*, restricted with BamHI and inserted between pCaMV35S promoter and poly-adenylation sequences from the nopaline synthase gene (pAnos) in BamHI cloning site.

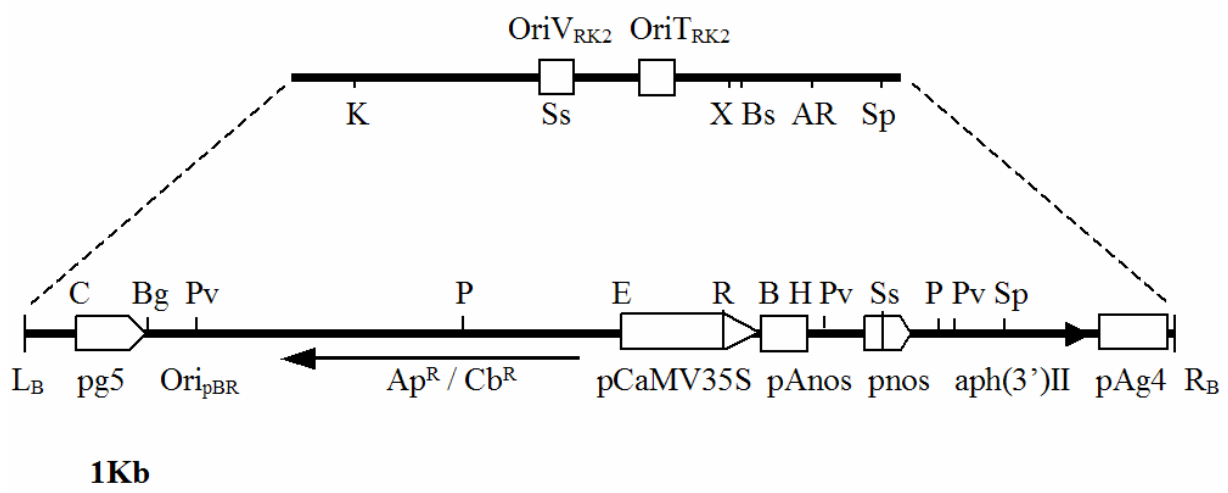


Figure 10. PCV702 vector. The upper lane shows mini-RK2 segment of PCV vectors and second lane displays the T-DNA.

2.4.7.1 Ligation of DNA fragment into plasmid

For this purpose an insert to vector molar ratio of 3:1 was calculated. 60 fmol of insert, 20 fmol vector, 1µl (5U) T4 DNA ligase (Fermentas) and 1µl 10x ligation buffer (Fermentas) in total volume of 10µl were incubated at 4°C for 24 hours (alternatively at 37°C for 2 hours). For calculation of molarities, the concentration of the insert and the linear plasmid DNA (see 2.4.7.2) were determined by photospectrometry (BioPhotometer, Eppendorf). Then the mass amount of insert and vector needed for ligation was calculated by multiplying the number of bases with average molar mass of dsDNA (660 g/mol) and with 60×10^{-15} (molar weight needed for insert) or 20×10^{-15} (molar weight needed for vector). Finally, the equivalent volume was calculated:

Equation 2. Calculating the volume of a DNA solution for ligation.

$$\text{DNA Volume}[\mu\text{l}] = \frac{\left(\frac{660 \text{ g DNA}}{1 \text{ mol bp DNA}} \right) \times \left(\frac{\text{Genome or plasmid size [bp]}}{1 \text{ copy}} \right) \times (\text{molar weight need [mol]})}{(\text{DNA concentration [ng}/\mu\text{l}]) \times \left(\frac{1 \text{ g}}{10^{+9} \text{ ng}} \right)}$$

2.4.7.2 Plasmid extraction by Mini-Prep (*E. coli* and *Agrobacterium*)

For extracting plasmid DNA, an alkaline lysis procedure modified by Birnboim and Dely (1979) was used. Plasmid DNA is separated from chromosomal DNA and proteins based on differences in topographic characteristics (see step 1 to 8). First of all the cells are lysed under alkaline conditions (step 3) and both nucleic acids and proteins become denatured. After neutralization with potassium acetate (step 4), plasmids re-nature correctly and remain in solution whereas chromosomal DNA, because of their huge sizes, can not re-nature properly and precipitates. The procedures are as follow:

1. *E. coli* stock cultures were picked in 5 ml "LB medium plus ampicillin" (App. 7.15) with a sterile toothpick and were grown over night at 37°C. *Agrobacterium* stock cultures were picked in 3 ml "YEB medium plus rifamycin, gentamycin and carbenicillin" (App. 7.14) with a sterile toothpick and were grown over night at 28°C.

2. 3 ml of over night incubated cultures were centrifuged (14000 rpm, 10 min) in 1.5 ml tubes (in two steps) and supernatants were discarded.
3. Pellets were suspended in 100 µl GTE buffer (App. 7.23) (150 µl GTE + Lysozyme for *Agrobacterium*) by mixing and incubated for 5 min at room temperature.
4. 200 µl of freshly made SDS/NaOH solution (300 µl for *Agrobacterium*) (App. 7.24) was added and mixed gently and chilled on ice for 5 minutes.
5. In order to neutralize the alkaline solution, 150 µl potassium acetate (5 M, pH 4.8-5.1) (225 µl for *Agrobacterium*) was added and mixed by pipetting up and down and chilled on ice for 5 minutes.
6. All wastes like proteins, chromosomal DNA, cell walls were precipitated by centrifugation at 14000 rpm (Eppendorf, 5417 R, Germany) for 3 min (10 min at 4°C for *Agrobacterium*). The supernatant was transferred in new 1.5 ml tubes.
7. 800 µl of pure ethanol was added to the solution, incubated for 2 minutes at room temperature and centrifuged 14000 rpm for 1 minute.
8. The pellets were washed with 1 ml of 70% EtOH to remove salts and afterwards air dried at 37°C for 2-3 minutes.
9. The pellets were re-dissolved in 30 µl ddH₂O and stored at -20°C.

Before ethanol precipitation (step 6) for *Agrobacterium* plasmid extraction, 700 µl chloroform : isoamylalcohol (24:1) was added, mixed by pipetting, centrifuged for 5 min at 14000 rpm and the supernatant was transferred in new 1.5 tubes. This step was continued until the middle phase disappeared.

2.4.8 In silico analysis

Similarity searches for nucleotide and amino acid sequences were carried out using the BLAST tool of NCBI GenBank (<http://www.ncbi.nlm.nih.gov/>). The *Arabidopsis* genome was searched using SeqViewer tool of TAIR (URL: <http://www.arabidopsis.org/>). Genomic DNA of *P. trichocarpa* was searched by performing BLAST algorithm at the JGI *P.*

trichocarpa v.1.0 database (URL: <http://www.jgi.doe.gov/poplar>). GeneDoc was used for performing and editing multiple sequence alignments (Nicholas *et al.*, 1997; URL: www.psc.edu/biomed/genedoc).

2.4.9 Phylogenetic analysis

Coding sequences of plant lipocalins were collected from NCBI data bank and saved as FASTA format in a file. Multiple sequence alignments were performed using ClustalW tools offered by EMBL-EBI (<http://www.ebi.ac.uk/>) by following parameters: gap opening penalty 5, gap extension penalty 0.05 and DNA identity matrix. The Kimura model was used (as default set of ClustalW) for estimating evolutionary distance (Kimura, 1980). The TREECON software 1.3b (beta version) was used for building NJ (neighbor joining) trees with 2000 samples for bootstrapping. (<http://bioinformatics.psb.ugent.be/psb/Userman-/treeconw.html>).

2.4.10 Protein sequence annotation

Presence of GPI anchor and cleavage sites were predicted using DGPI program (Kronegg and Buloz, 1999) (<http://www.expasy.org/tools/>) Topology prediction of putative membrane proteins were predicted using TopPred II and hydrophobicity profiles were calculated based on KD hydrophobicity scale (Kyte and Doolittle) for eukaryotes with upper cut-off 1.0 (Claros and von Heijne, 1994).

2.4.11 Promoter analysis

To analyze promoter elements, 627 bp upstream areas of candidate genes in *P. tremula* and *A. thaliana* were searched and the results were compared. Searching for motives in selected sequences was performed by SIGNAL SCAN: A computer program that scans DNA sequences for Cis-acting elements (Prestridge *et al.*, 1991) in plant cis-acting regulatory DNA elements database (PLACE) <http://www.dna.affrc.go.jp/PLACE/signalscan.html> (Higo *et al.*, 1999).

2.5 Statistical analyses

All statistical analyses were performed by SPSS software release 9.0.0, standard version (SPSS Inc.). Normal distribution of data was tested by Kolmogorov–Smirnov test. Two independent data sets were compared by t-test and more than two data sets were compared using Duncan multiple rang test. In figures and tables p-values ≤ 0.05 , 0.01, 0.001 are represented by one, two and three stars, respectively.

Outliers were detected using Grubb's outlier test ($p < 0.05$) with Graphpad software (<http://www.graphpad.com/quickcalcs/Grubbs1.cfm>) and removed.

3

Results

3.1 Ecophysiological characteristics of *P. euphratica* and *P. x canescens* during salt adaptation

3.1.1 Effect of short term salt adaptation on plant performance

The effect of NaCl as a growth limiting element was monitored in hydroponic cultures of *P. x canescens* and *P. euphratica* which are salt sensitive and salt tolerant species, respectively. To avoid symptoms of salt shock, plants were stepwise exposed to elevated salinity. *P. x canescens* plants were exposed to weekly increasing NaCl concentration up to 75 mM (25, 50 and 75 mM) and *P. euphratica* up to 200 mM (25, 100 and 200 mM).

Different salt exposure regimes were chosen, because of the differences in salt tolerance in both species. In *P. x canescens* stem elongation growth was reduced after one week of treating with 25 mM NaCl (Figure 11B). Further increases in salinity did not cause further significant reduction in the growth rate of the shoot apex. The overall growth was about 30 % lower than in controls (Figure 11B). As a result of changes in stem growth, a significant difference in total stem length was observed already after two weeks of salt treatment (Figure 11A).

The leaf initiation rate was already diminished at the lowest NaCl concentration in first week and remained at that level during the following experimental treatment (Figure 11D). The total leaf initiation was significantly reduced in third week at 75 mM NaCl (Figure 11C).

Increase in stem diameter in the transition zone between root and shoot, were defined as "collar diameter growth". Decreases in collar diameter occurred during the second week of NaCl treatment in *P. x canescens* (Figure 1F). Although the collar diameter growth was reduced, no significant difference in total collar diameter was observed during three weeks of salt adaptation (Figure 11E).

Stem length, initiation of new leaves and the collar diameter were also measured during weekly increases in salinity for *P. euphratica* (Figure 12A, C, and E). In *P. euphratica*, stem length growth was not affected during two weeks of salt increment up to 100 mM, but increasing the concentration to 200 mM NaCl reduced the growth rate severely (Figure 12B). Leaf initiation rate (Figure 12D) showed the same response to salt increment as stem growth whereas stem radial growth did not show a significant reduction (Figure 12F).

For this comparison, *P. x canescens* and *P. euphratica* plants of 40 cm stem length were used, as it is known that salt responses are also affected by the size of the plants. Under salt concentrations of up to 100 mM the performance of *P. euphratica* plants did not change but adding 200 mM NaCl caused significant growth losses. These observations suggest that for *P. euphratica* a final salt concentration between 100 and 200 mM would result in an effect comparable to that found in *P. x canescens* at 75 mM NaCl.

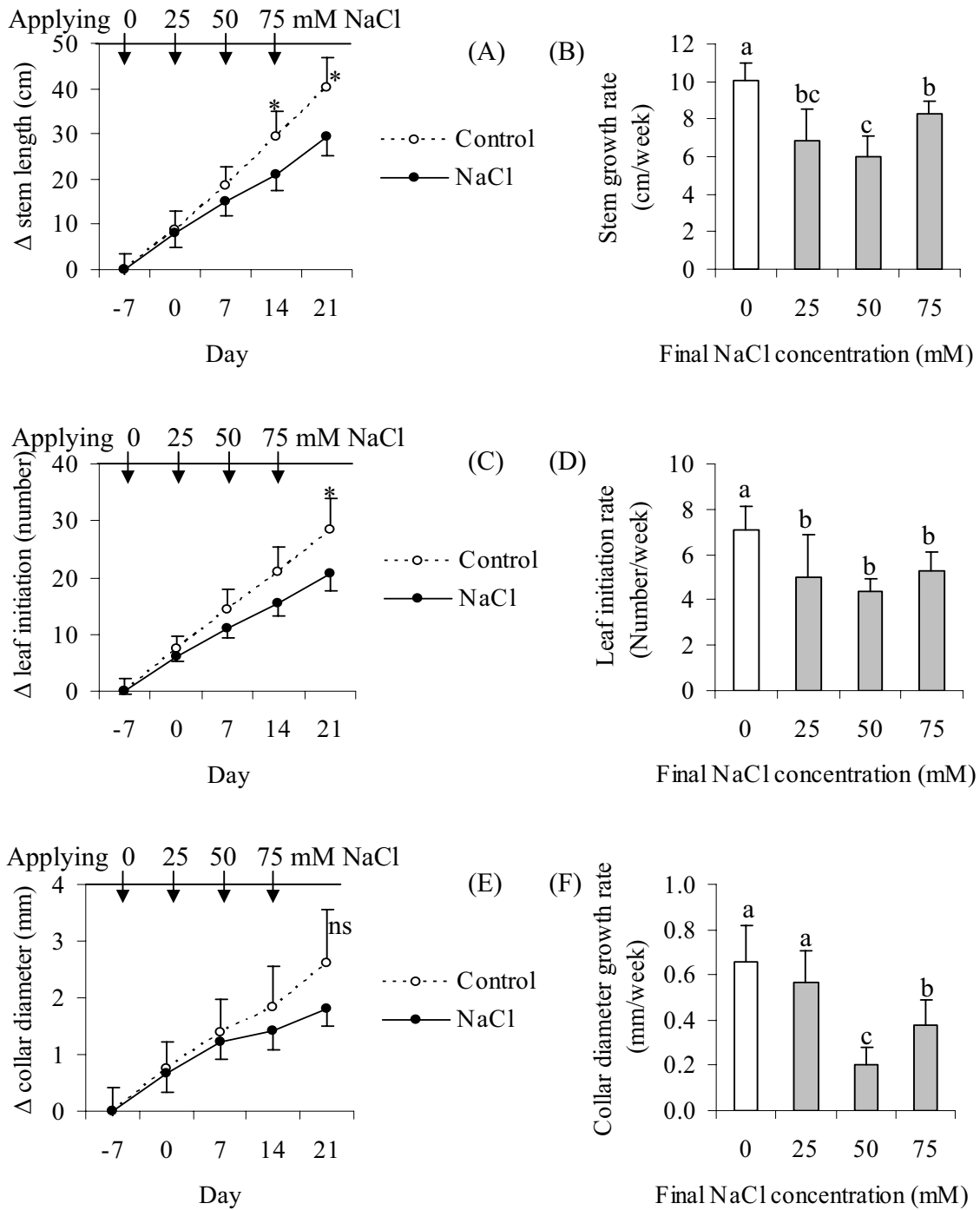


Figure 11. Performance of *P. x canescens* under saline and control conditions in hydroponic solution. Plants of 40 cm stem length were subjected to stepwise NaCl increments (25, 50 and 75 mM). Time of starting salt treatment was considered as day₀ and one week before salt treatment was considered as day₋₇. $\Delta = \text{day}_t - \text{day}_{-7}$. Growth rates were calculated as Δ / week . Stem length difference (A), stem growth rate (B); leaf initiation difference (C), leaf initiation rate (D) collar diameter difference (E), collar diameter growth rate (F); (n=5 \pm SD; ns: not significant; *: p \leq 0.05; **: p \leq 0.01).

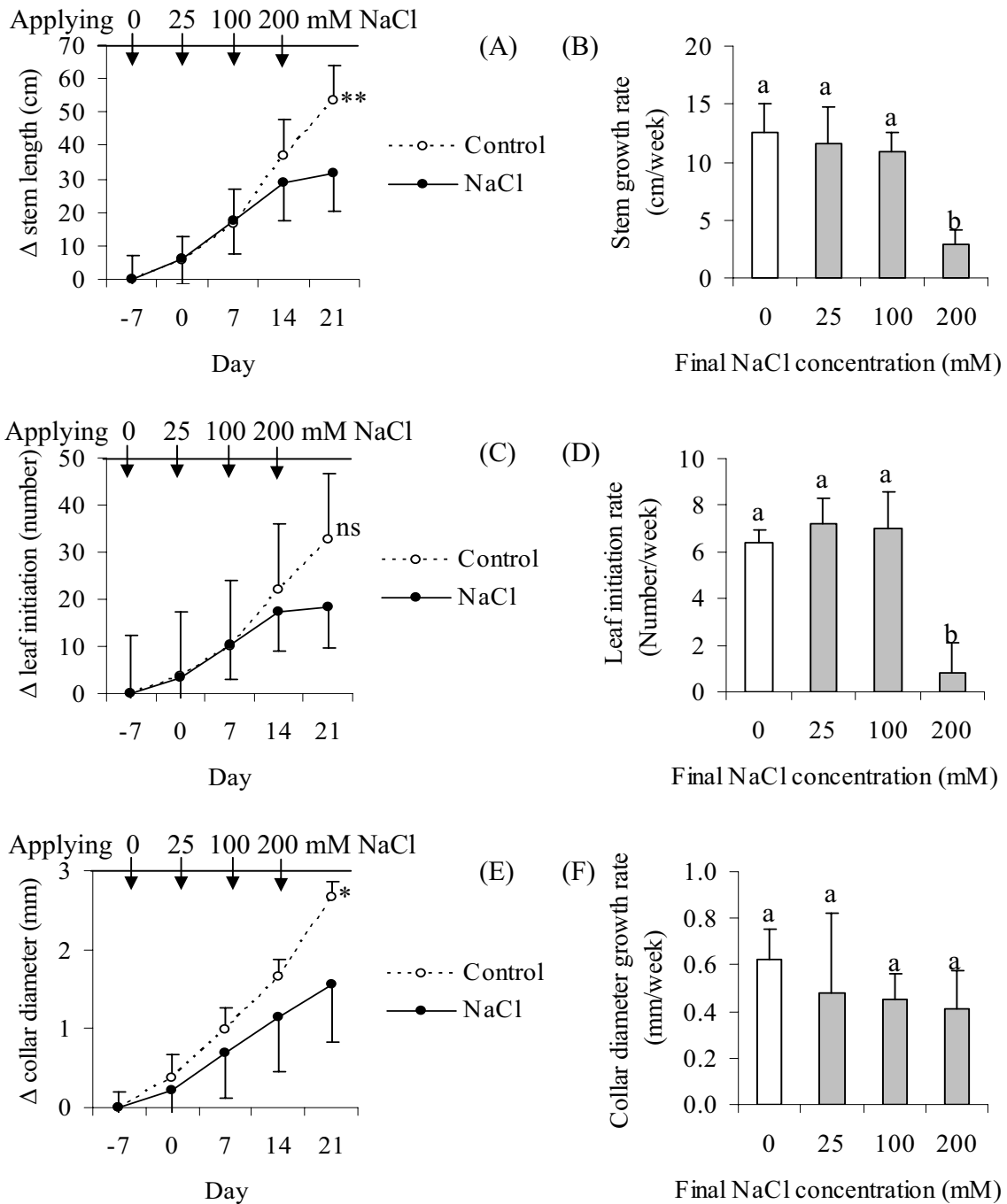
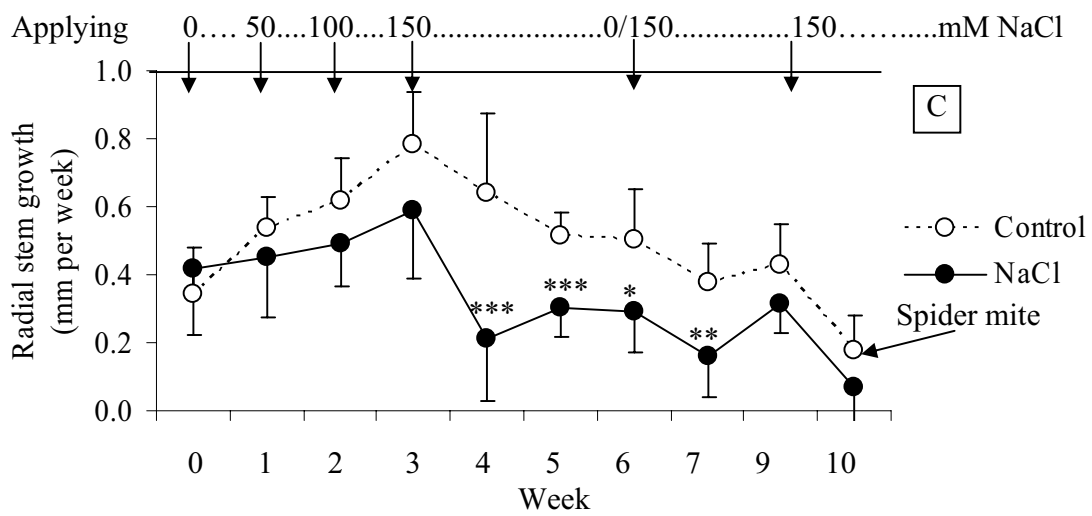
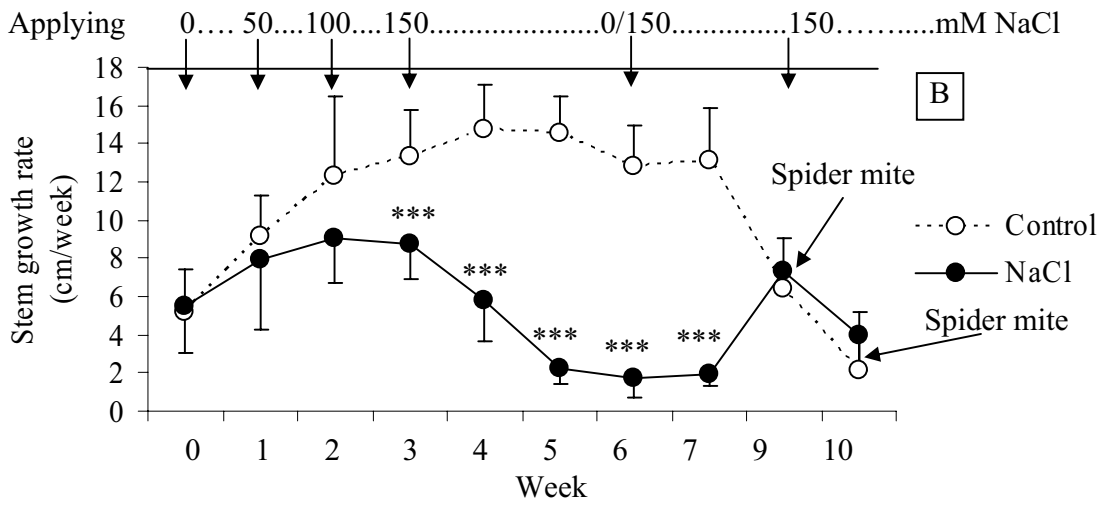
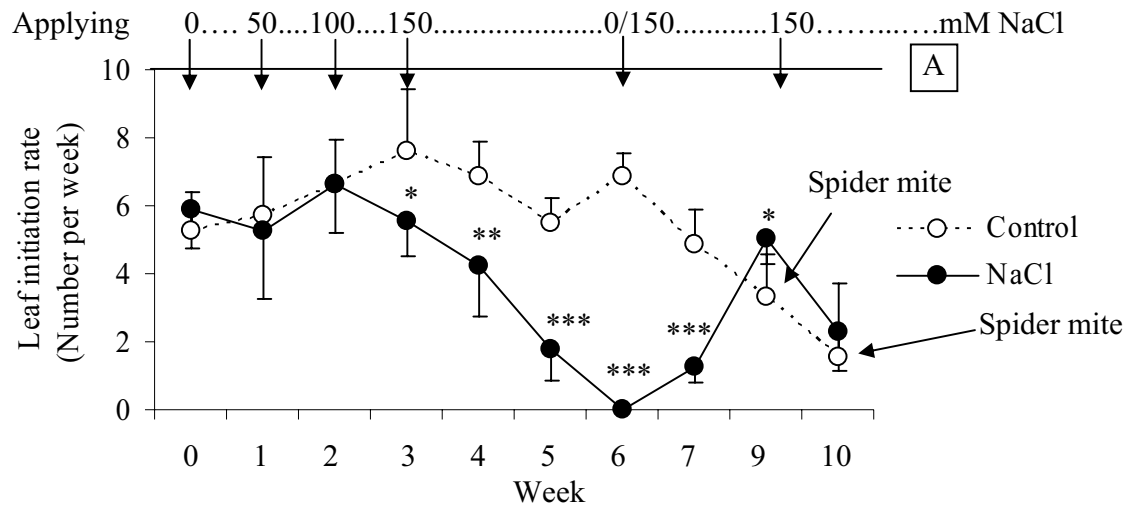


Figure 12. Performance of *P. euphratica* under saline and control conditions in hydroponic solution. Plants of 40 cm stem length were subjected to stepwise NaCl increments (25, 100 and 200 mM). Time of starting salt treatment was considered as day 0 and one week before salt treatment was considered as day (-7). $\Delta = \text{day}_t - \text{day}_{-7}$. Growth rates were calculated as Δ / week . Stem length difference (A), stem growth rate (B); leaf initiation difference (C), leaf initiation rate (D) collar diameter difference (E), collar diameter growth rate (F); (n=5 \pm SD; ns: not significant; *: p \leq 0.05; **: p \leq 0.01).

3.1.2 Performance of *P. euphratica* during long term salt adaptation

The performance of *P. euphratica* in a long term salt adaptation experiment was observed. Plants of *P. euphratica* in soil were subjected to a final concentration of 150 mM NaCl by stepwise weekly increases to 50, 100 and 150 mM. The leaf initiation rate was reduced one week after irrigating with 100 mM NaCl (Figure 13A). After three weeks irrigating with 150 mM NaCl, leaf generation stopped (Figure 13A). Alternative irrigation with 150 mM NaCl and tap water (one day saline water, one day tap water) caused resuming of the leaf generation rate. The same or even better performance as that observed in *P. euphratica* without salinity was regained during alternating irrigating with tap water and 150 mM saline water (Figure 13A). This finding suggests that *P. euphratica* has strategies to prevent lethal effects of high salinity. Daily irrigation with 150 mM NaCl for one week reduced the leaf initiation rate again. A significant reduction in stem length growth was observed one week after irrigating with 100 mM NaCl and showed a similar pattern as leaf initiation rate (Figure 13B). Radial stem growth was affected by salinity later than other parameters and declined one week after irrigating with 150 mM NaCl (Figure 13C). Alternative irrigation, conducted to stem radial growth increment of salt adapted plants (Figure 13C). Control plants were infected with spider mites at 9th and 10th week of the experiment that affected plant performance of control plants.

Salt treatment generally reduced the performance of the aerial parts of *P. euphratica* but did not affect root length and root dry mass (Figure 13D to I). Leaf expansion of salt adapted plants also was restricted so that in salt adapted plants leaf area, leaf length and leaf width decreased obviously (Figure 13J, K, L). Relative water content ($RWC = (FW - DW) / FW$) at the end of experiment was slightly reduced in both roots and leaves of salt adapted plants (Figure 13F). Despite significant reduction in water content, the plants exposed to salinity, still contained considerable amount of water in their tissues (Figure 13F).



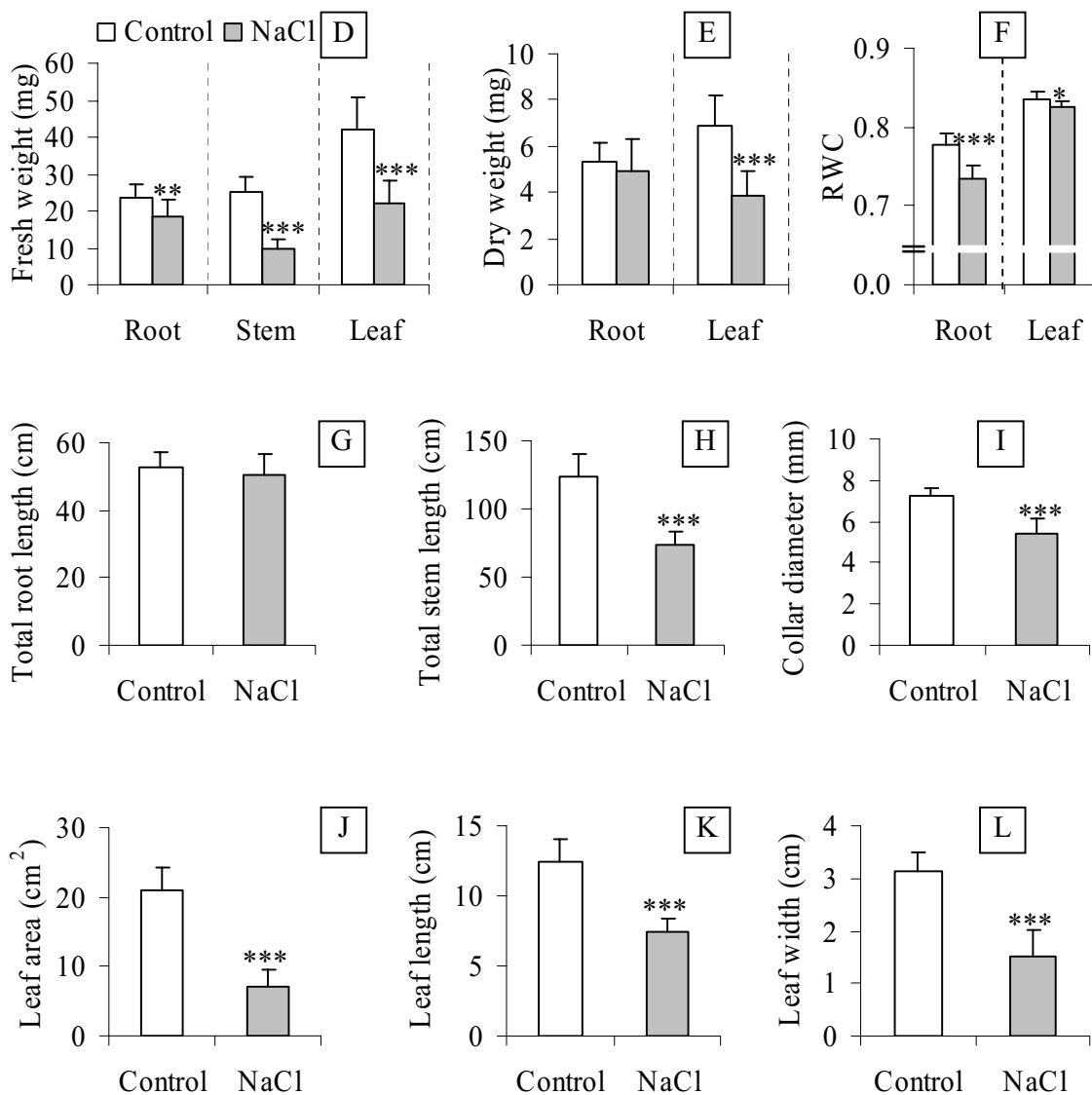


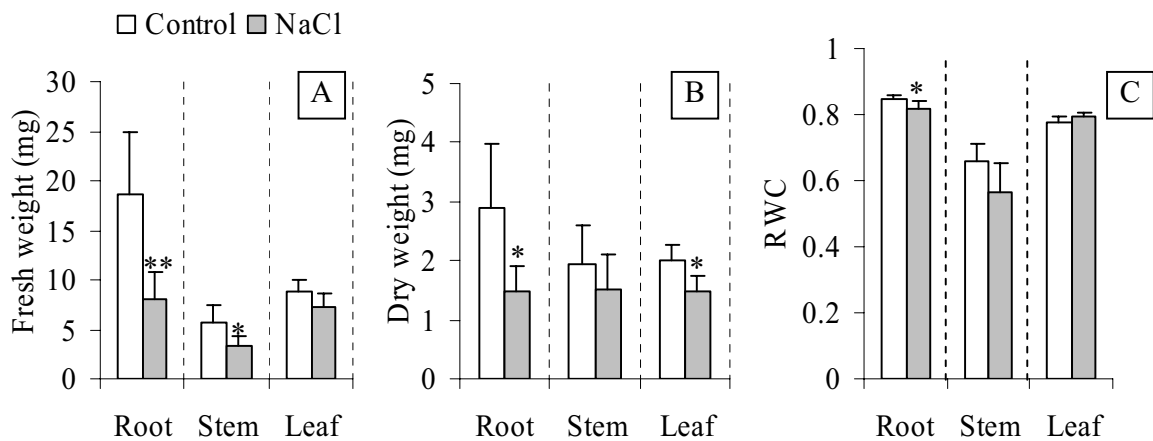
Figure 13. Performance of *P. euphratica* under saline and control conditions in soil. *P. euphratica* plants (about 30 cm height) were transferred in to soil and irrigated with either normal solution (Control) or with solution supplemented with NaCl (final concentration of 150 mM) ($150 \mu\text{mol s}^{-1} \text{cm}^{-2}$ PAR, photoperiod 16 h light, 22°C). Salt adaptation was performed weekly with 50, 100 and 150 mM NaCl. From 2th to 5th week salt adapted plants were irrigated with salty solution (150 mM). From 5th to 8th week plants were irrigated one day with salty solution (150 mM) and one day with tap water. Last week plants were irrigated again with solution containing 150 mM NaCl every day. From the 8th week control plants were infected with spider mite and affect on stem length growth and radial growth. 5-week-old leaves were subjected to morphological analysis at the end of experiment. FW: fresh weight, DW: dry weight. Bars indicate mean \pm SD; n= 8; *: $p \leq 0.05$; **: $p \leq 0.01$; ***: $p \leq 0.001$.

Since the control of salinity in soil was difficult, a further long term salt adaptation experiment was conducted in hydroponic solution. *P. euphratica* plants after weekly salt adaptation to 25, 50, 100 and 150 mM were grown for 3 months in the presence of 150 mM NaCl (see 2.2.3, *P. euphratica* in hydroponic).

Exposure to 150 mM NaCl for 3 months caused significant reductions in stem length and root length but no significant difference in collar diameter (Figure 14D, E, F). Also some necroses appeared due to salt exposure of upper leaves and spread from tip of a leaf to the petiole (Figure 14J, K). Roots of salt treated plants had less fresh and dry weight than controls and also the relative water content (RWC= (FW-DW)/FW) decreased in roots under salt treatment. Roots of salt adapted plants became thick (Figure 14I).

Stem fresh weight was slightly reduced but the stem dry weight and relative water content were not affected by exposure to NaCl (Figure 14B).

Despite lower leaf dry weight in salt adapted plants than controls (Figure 14B), no significant difference was observed in leaf fresh weight and relative water content (Figure 14A, C). This is due to the development of succulence in leaves of *P. euphratica* plants under salt stress as reported by Ottow *et al.* (2005).



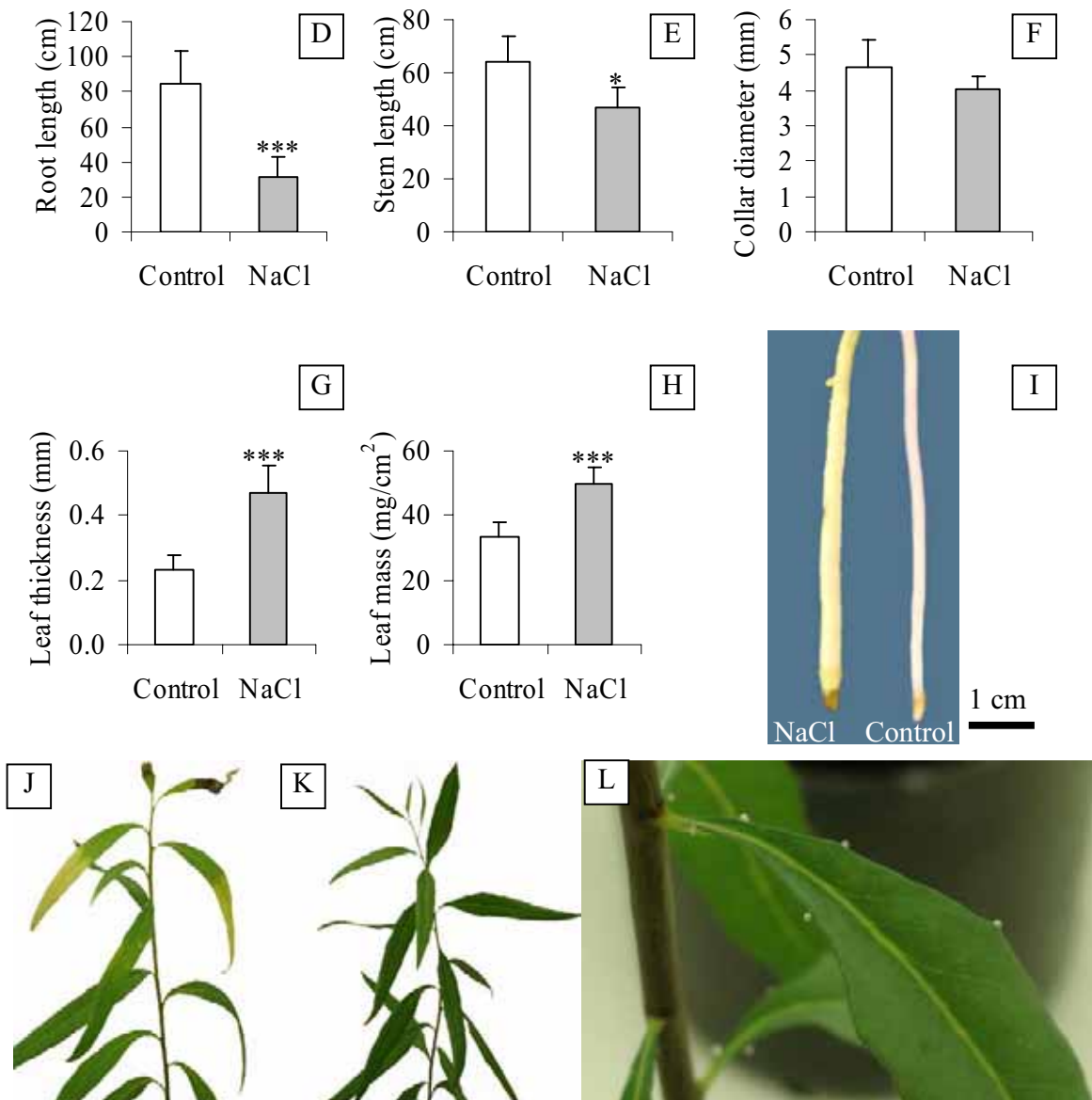


Figure 14. Plant performance of long term salt adapted *P. euphratica* after 3 months growth in 150 mM NaCl in hydroculture ($150 \mu\text{mol s}^{-1} \text{cm}^{-2}$ PAR, photoperiod 16 h light). Plants were grown in hydroponic medium and salt was applied by adding 25, 100 and 150 mM NaCl weekly. After 3 months growing in 150 mM NaCl, fully developed leaves from middle height (10th to 12th) were taken for measuring leaf thickness and leaf mass. I) Root tip of salt adapted and control *P. euphratica* J) Salt adapted plant, K) control plant, L) Leaf exudates at leaf edges (hydathodes).

3.1.3 Carbohydrates in leaf exudates

Leaf exudates of long term salt adapted *P. euphratica* (Figure 14) together with non-treated samples were subjected to carbohydrate analysis using GC/MS. Three sugars

(sucrose, glucose and fructose) together with one sugar-alcohol, inositol, were detected. Sucrose was the most abundant compound in both control and salt treated plants and was higher in exudates of salt adapted plants than in exudates of control plants (Figure 15).

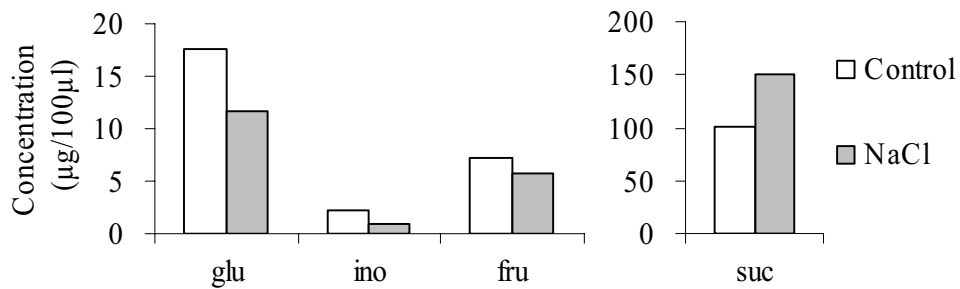


Figure 15. Carbohydrates in leaf exudates of control and salt adapted *P. euphratica* (150 mM, three month). One measurement was run for a pooled sample of five plants for each treatment. Glu: glucose, ino: inositol, fru: fructose, suc: sucrose.

3.1.4 Electrolyte conductivity as a measure for salt uptake and salt induced leaf injury

The presence of NaCl causes increases in the electrolyte conductivity of a solution. In Figure 16 this relationship is demonstrated.

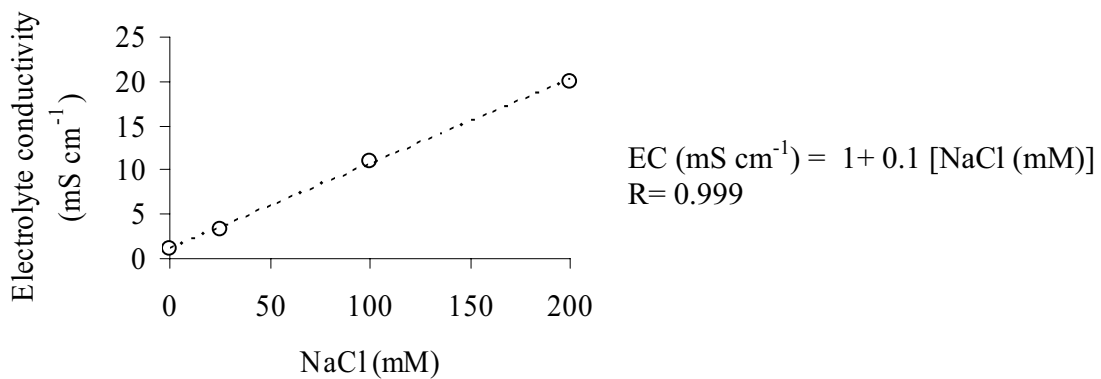


Figure 16. Relation between NaCl concentration and the electrical conductivity of a solution. Electrolyte conductivity was measured at different salt concentrations (0, 25, 100 and 200 mM) in ddH₂O.

Since growth of plants in saline solution leads to NaCl uptake, it was expected that this would lead to increases in EC of plant tissues. To investigate whether all plant tissues

increased EC under saline conditions xylem, root, shoot apex, bark and leaves of salt adapted *P. euphratica* with 25, 100 and 200 mM NaCl and controls were investigated (Figure 17). In roots only minor changes in electrolyte conductivity were observed, which were significant only in plants exposed to 100 mM NaCl. Leaf electrolyte conductivity increased with increasing salt concentrations (Figure 17). Electrolyte conductivity of bark did not change up to 100 mM salt adaptation and increased substantially after adaptation to 200 mM salt. Shoot apex showed slight increment in electrolyte conductivity by salt increment. In xylem no significant changes were observed up to 100 mM and raised up by 200 mM NaCl. All together treating with 25 mM NaCl for one week did not change the amount of electrolytes in whole plant. One week 25 mM followed by one week of 100 mM NaCl resulted in raising electrolyte conductivity in root and leaves. Growth at 200 mM caused a general increment of electrolyte conductivity in the whole plant except in roots.

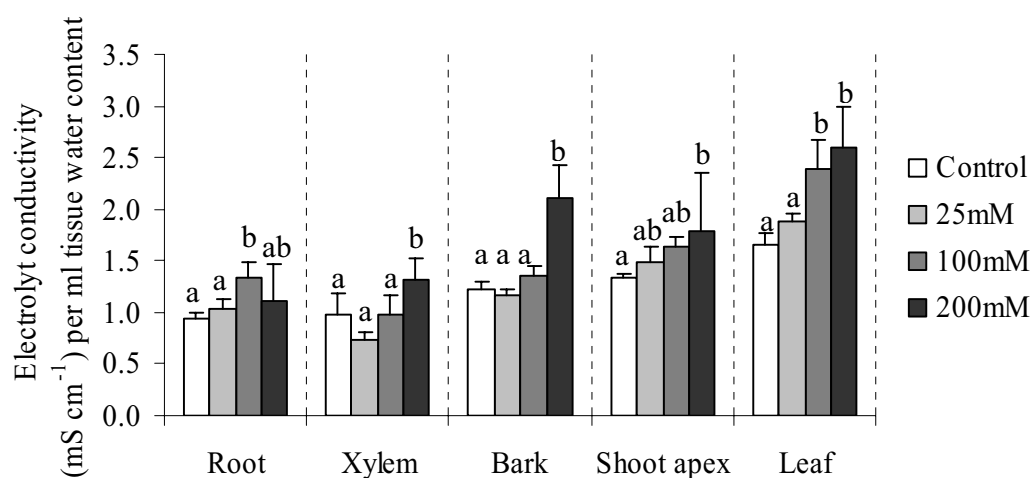


Figure 17. Maximum electrolyte conductivity different of tissues per ml tissue-water-content in *P. euphratica* under different NaCl concentration. Conductivity measurements were conducted in 20 ml ddH₂O extracts. Bars indicate means \pm SD (n=5). Different letters in each reticule show significant difference for $P \leq 0.05$ (see App. 7.28).

Correlation between electrolyte conductivity of tissues and growth medium in each adaptation step was calculated by Cendall's tau b nonparametric correlation. It should be considered that changes in electrolyte conductivity of plant tissues do not necessarily reflect direct changes of Na⁺ and Cl⁻ because such as K⁺ and Ca²⁺ may be affected as well.

Increasing the electrolyte conductivity of medium was positively correlated with changes in EC of leaves and apical shoots and negatively correlated with that of the xylem. No significant correlation was observed with root and bark (Table 7). The increment in electrolyte conductivity of the growth medium from 25 mM NaCl to 100 mM NaCl was highly and positively correlated with electrolyte conductivity changes of all plant tissues except shoot apex. Enhancing the electrolyte conductivity of growth medium under 100 to 200 mM NaCl was highly and positively correlated with electrolyte conductivity changes in bark but no significant correlation was observed with electrolyte conductivity changes in other tissues. These results indicate that NaCl uptake was probably higher when the salinity of the medium was increased from 25 to 100 mM than from 100 mM to 200 mM.

Table 7. Nonparametric correlation between changes in EC of growth medium and EC of plant tissues of *P. euphratica* in hydroponics (see 2.2.2).

	0-25 mM	25-100 mM	100-200 mM
Leaf	0.745**	0.745**	0.241
Bark	-0.370	0.724*	0.745**
Xylem	-0.754**	0.745**	0.671
Apical shoot	0.610*	0.396	0.392
Root	0.513	0.754**	-0.447

Measurements of relative electrolyte conductivity can also be used to assess plasma membrane injury as described in materials and methods (see 2.3.2). Plasma membrane permeability of salt shocked and salt adapted *P. x canescens* leaves were relatively higher than those of control leaves (Figure 18A). In *P. euphratica* plasma membrane permeability of salt shocked plants increased slightly (+10%) compared to control but not in salt adapted plants (Figure 18B). This shows that *P. euphratica* under short term stress can protect its photosynthetic tissue whereas in *P. x canescens*, the plasma membrane of leaf tissue severely suffers of salt. Also under salt adaptation, the plasma membrane of *P. euphratica* does not display as much damage as that of *P. x canescens*.

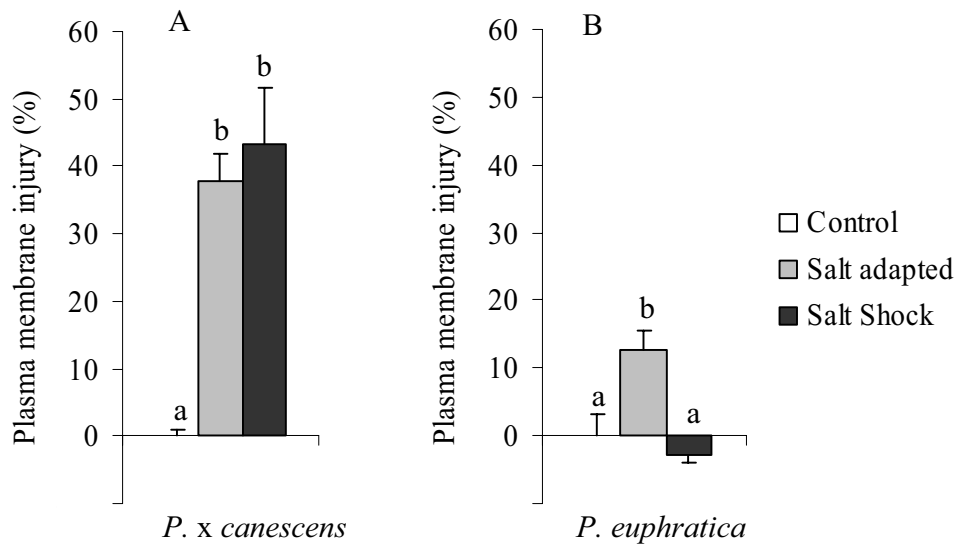


Figure 18. Plasma membrane injury in leaves of *P. x canescens* and *P. euphratica* after salt shock and salt adaptation. Stem length of *P. euphratica* was 23 cm and *P. x canescens* 20 cm at the time of salt treatment. Both species were gradually salt adapted (weekly salt increment as 25, 50, 100 and 150 mM NaCl) or exposed directly to 150 mM NaCl (salt shock). Leaves were harvested from the middle of the plants. Electrolyte leakage was measured in non-treated plants (control), one week after salt adaptation with 150 mM, and 24 h after salt shock with 150 mM NaCl. Bars indicate means \pm SD (n=3). Different letters show significant difference for $P \leq 0.05$.

Salt exposed plants have leaves of different types of salt adaptation. Some leaves are fully expanded at the time of salt exposure. Some leaves expand during salt adaptation and finally some leaves are initiated during salt adaptation. Leaves of *P. x canescens* in different developmental stages showed different responses to salt treatment. 3-weeks-old salt adapted leaves had higher increment in maximum electrolyte conductivity, suggesting probably higher NaCl uptake (Figure 19A). The leaves expanding during salt adaptation (3-week-old at time of harvest), exhibited symptoms of leaf necrosis after exposing to 25 mM NaCl. This symptom was neither observed in older leaves (5-week-old) nor in younger leaves (1-week-old). To find out whether salt stress is due to differences in plasma membrane injury in leaves of different age, relative electrolyte leakage (NaCl/Control) was determined (as described in 2.3.2). Relative electrolyte leakage of control and salt adapted leaves was measured and plasma membrane permeability was calculated. 3-week-old leaves had higher relative plasma membrane permeability than 1 and 5-week-old leaves (Figure 19B).

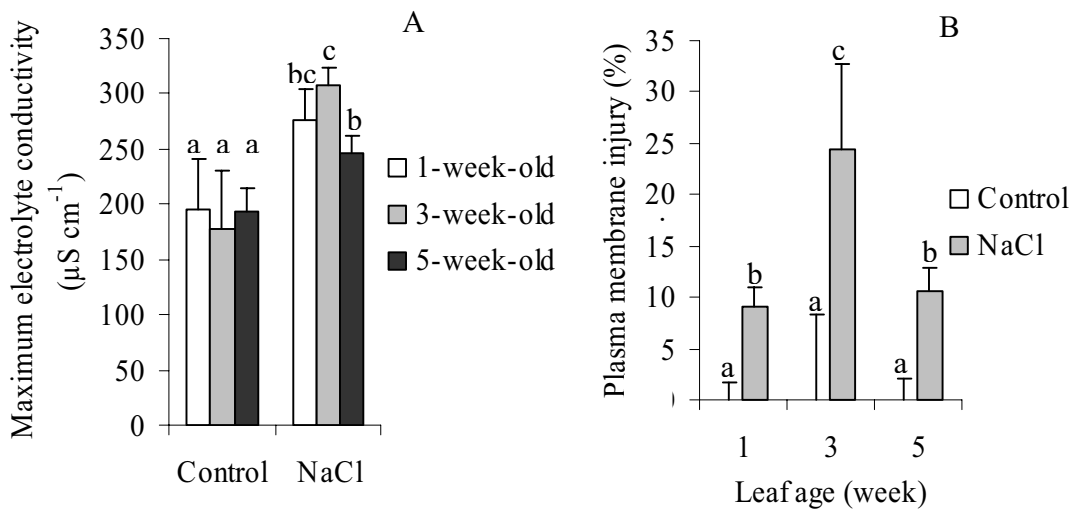


Figure 19. Maximum electrolyte conductivity (A) and relative plasma membrane injury of *P. x canescens* leaves of different age (B). Plants of 40 cm stem length were subjected to stepwise NaCl increments (25, 50 and 75 mM). Bars indicate means \pm SD (n=5). Different letters show significant difference for $P \leq 0.05$.

3.1.5 Leaf water potential under salt stress

Since salt stress has both osmotic and ionic effects and most of the physiological parameters like cell growth and photosynthesis are strongly influenced by water potential (Ψ), leaf water potential (Ψ_{leaf}) was measured in control and salt-adapted plants to assay osmotic changes due to salt stress (Figure 20).

Plants overcome osmotic stress via two possible basic strategies, dehydration avoidance and dehydration tolerance (Newton *et al.*, 1991). In both species, leaf water potential (Ψ_{leaf}) decreased in response to salt exposure. In *P. x canescens* a Ψ_{leaf} of -0.47 MPa dropped to -0.65 MPa after salt adaptation to 75 mM and in *P. euphratica*, Ψ_{leaf} decreased from -0.30 to -1.03 MPa in 150 mM salt adapted plants.

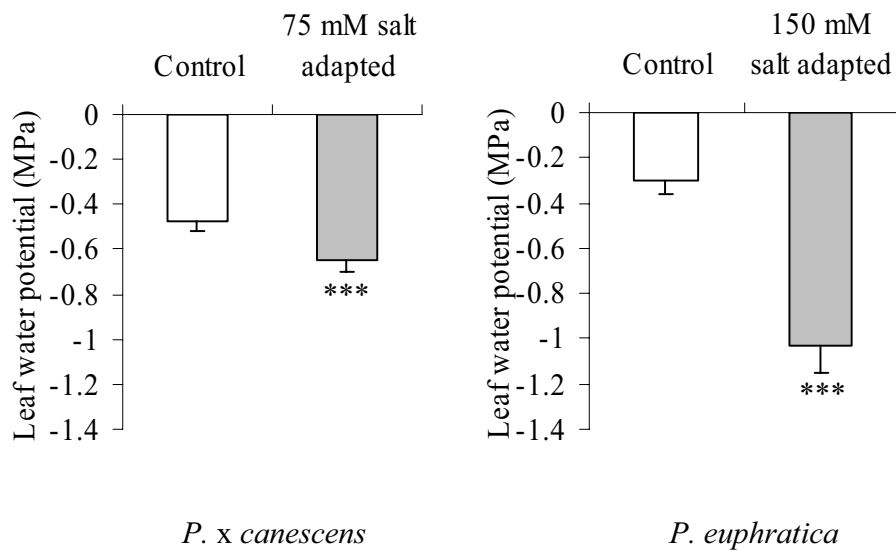


Figure 20. Leaf water potential of the seventh leaf from the top of *P. x canescens* and *P. euphratica*. *P. x canescens* in hydroponic (refer to 2.2.2, Fig. 5 a; n= 5); *P. euphratica* in soil (refer to 2.2.3, Fig. 8; n= 8). The measurements were done during day.

3.1.6 Pigment analysis

The concentration of Chl a, Chl b and Car were measured in *P. euphratica* in response to salinity. Plants were adapted stepwise to final concentration of 150 mM and maintained for 3 months at this level (see 2.2.3, *P. euphratica* in hydroculture). The pigment analysis was undertaken at the end of experiment. In salt adapted plants, where the leaves get succulent (Figure 14C, G, H), the concentrations of Chl a, Chl b and Car per fresh weight decreased (Figure 21A, B, C). Since the leaves showed significant increases in their thickness, per surface area no significant reduction are observed for Car and Chl a but the concentration of Chl b per leaf area was slightly decreased in salt affected plants (Figure 21D, E, F). This result shows that reduction in pigments especially Chl a and Car, in leaves of salt adapted *P. euphratica* are not the cause of degradation but caused by leaf succulence. Chl b was more sensitive than Chl a and is affected by salt stress in *P. euphratica*. The slight increment in Chl a/b ratio in salt adapted plants (Figure 22) suggests that PSII is relatively decreased to PSI in salt adapted plants (Špundová *et al.*, 2003).

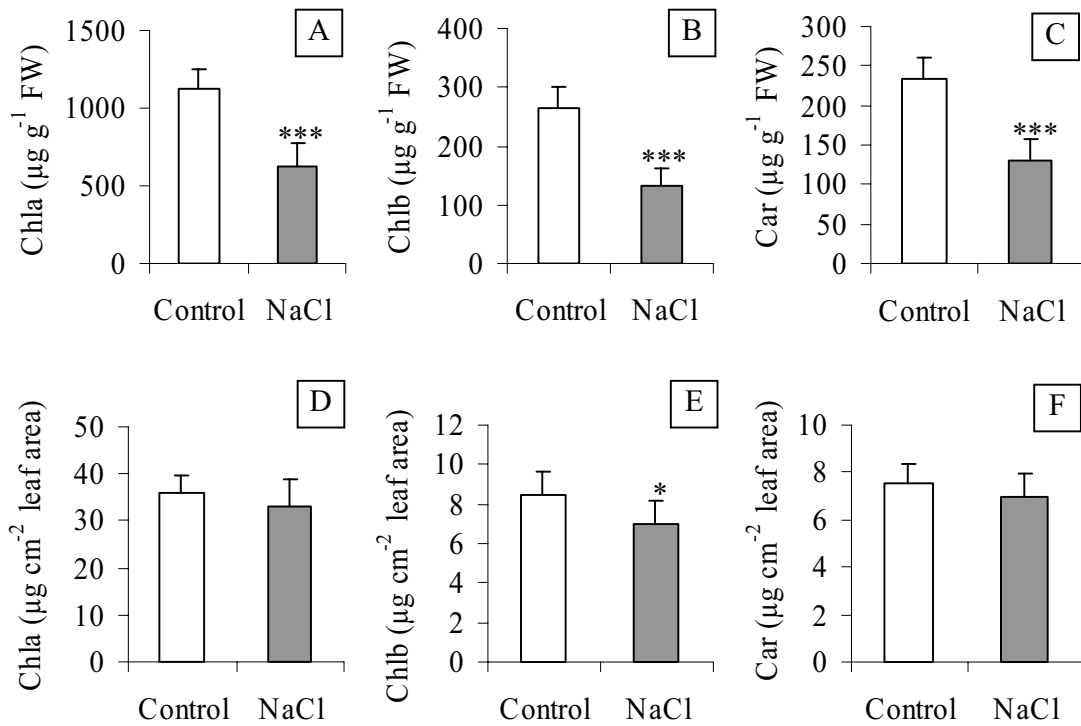


Figure 21. Leaf pigments of salt adapted and control plants of *P. euphratica*. Salt adapted *P. euphratica* were grown under 150 mM NaCl in hydroponic conditions for three months. Bars indicate means \pm SD (n=5).

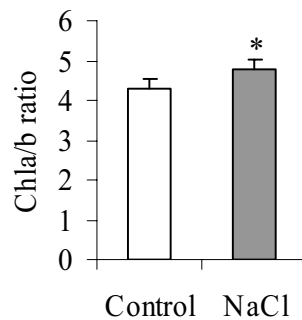


Figure 22. Chl a/b ratio in control and salt adapted *P. euphratica*. Ratios were calculated with the data from Figure 21.

3.1.7 Effect of salt adaptation on photosynthetic parameters of *P. x canescens* and *P. euphratica*

Since exposure to 75 mM NaCl and 200 mM NaCl of *P. x canescens* and *P. euphratica*, respectively, caused a significant growth reduction, a goal was to find out

whether these reductions were caused by negative effects of salt on photosynthesis in both species. Despite considerable reduction in transpiration and stomatal conductance of salt adapted *P. x canescens*, net photosynthesis rates did not change significantly (Figure 23).

It is surprising that CO₂ uptake was unchanged by salt increment. However, the analysis indicates that the gradient of P_{ca} and P_{ci} was much steeper under salt stress than under control conditions (Table 8) suggesting higher CO₂ flux into the leaf and a more efficient CO₂/H₂O balance.

In *P. euphratica* a slight decrease in transpiration rate and stomatal conductance was observed after one week in 100 mM NaCl and no significant reduction in photosynthesis was found (Figure 24). Increasing the salt concentration to 200 mM caused a severe decline in the transpiration rate and stomatal conductance and net photosynthesis was halved (Figure 24). Under these conditions the gradient of P_{ca} to P_{ci} also increased pointing to relatively higher water use efficiency (Table 8).

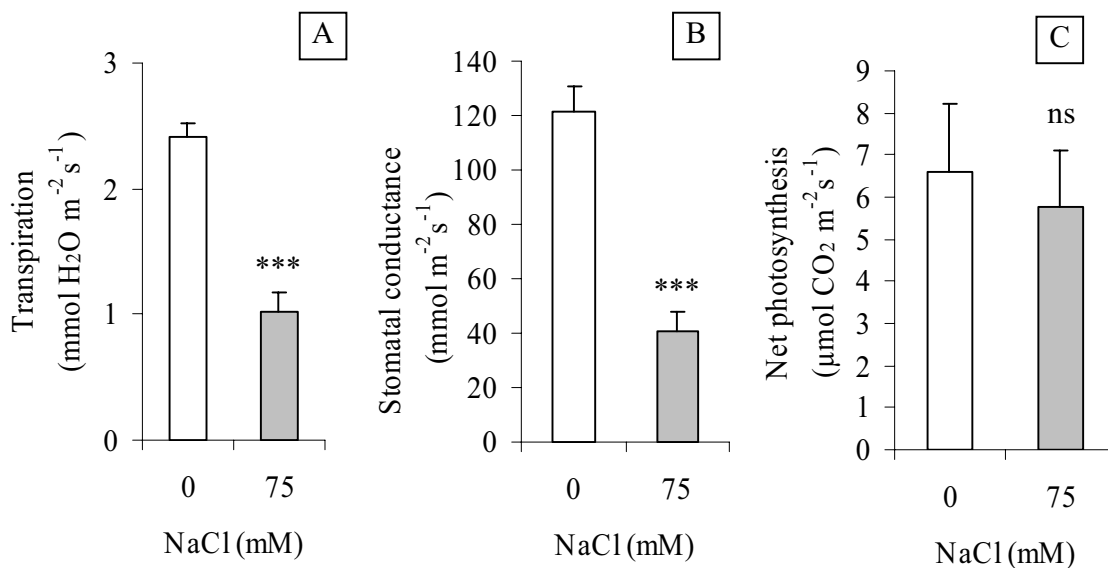


Figure 23. Photosynthetic parameters of control and salt adapted *P. x canescens* (75 mM NaCl, measured at 687 μmol PAR m⁻² s⁻¹). Bars indicate means ± SD (n=3). (ns: not significant; *: p<0.05; **: p<0.01; ***: p<0.001).

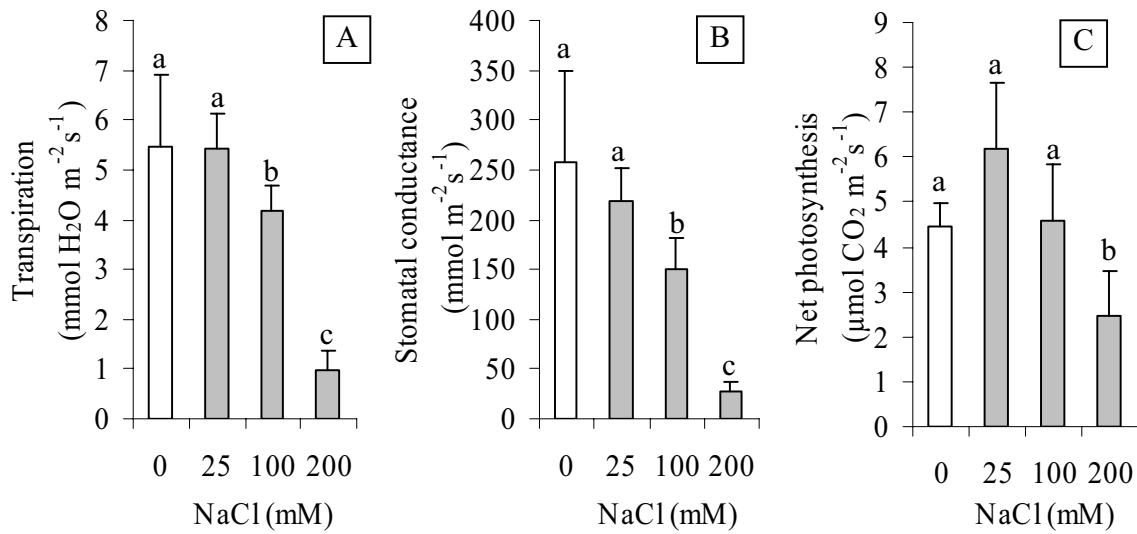


Figure 24. Photosynthetic parameters of *P. euphratica* exposed to different NaCl concentrations measured at 222 $\mu\text{mol PAR m}^{-2} \text{s}^{-1}$ (different letters indicate significant difference with 95% confidence). Bars indicate means \pm SD (n=6).

Table 8. Complementary data of gas exchange measurements presented in Figure 23 and Figure 24.

Species	NaCl (mM)	n	T (leaf) (°C)	CO ₂ abs ppm	RH%	Pci	Pca
<i>P. x canescens</i>	0	3	26.4 \pm 0.3	406 \pm 0	50.2 \pm 0.5	302 \pm 26	398 \pm 1
	75	3	28.1 \pm 0.2	406 \pm 0	46.0 \pm 0.8	169 \pm 21	399 \pm 1
<i>P. euphratica</i>	0	2	22.5 \pm 1.3	377 \pm 18	25.8 \pm 0.4	333 \pm 12	373 \pm 20
	25	7	23.7 \pm 0.9	386 \pm 9	20.9 \pm 3.0	323 \pm 19	382 \pm 10
	100	6	25.1 \pm 1.1	372 \pm 5	18.0 \pm 4.6	303 \pm 23	369 \pm 5
	200	5	28.6 \pm 0.5	382 \pm 3	16.3 \pm 0.9	235 \pm 39	381 \pm 3

3.1.8 Influence of salinity on chlorophyll fluorescence

Chlorophyll fluorescence was analyzed by a Mini-PAM fluorometer (Figure 25, Figure 26). The quantum yield efficiency of photosystem II of long term salt adapted *P. euphratica* to 150 mM (3 months) was enhanced in darkness and no significant differences were observed in light (Figure 25A and B). Photochemical quenching (qP) is related to relative portion of open PSII and was not affected by salinity (Figure 25C).

Non-photochemical quenching represents quenching of excess energy through heat dissipation of thylakoid membrane. Non-photochemical exciton quenching (NPQ) is particularly associated with energy dissipation as non-radiant heat through the xanthophyll cycle in antenna (Cruz *et al.*, 2005). As qN value is below 0.5, non photochemical quenching of excess light energy is mostly associated with heat dissipation and thylakoid membrane energization and the differences of NPQ after salt adaptation can not be considered as xanthophyll oxidation and photoinhibition (Figure 25E).

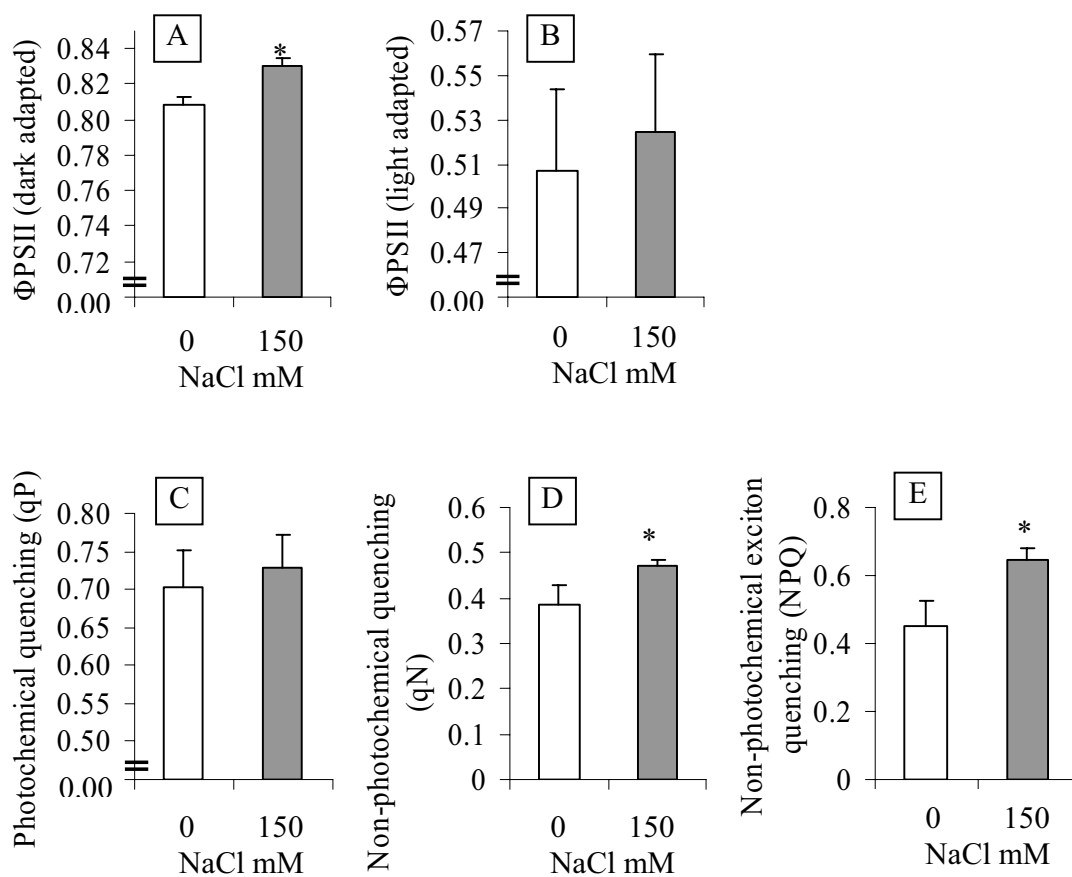


Figure 25. Potential and actual quantum yield efficiency of photosystem II (Φ PSII), photochemical (qP), non-photochemical quenching (qN) and non-photochemical exciton quenching (NPQ) in *P. euphratica* control and salt adapted leaves. Plants were adapted for 3 months to 150 mM in hydroponic conditions. (Act-width: 5:00 and Act-int: 5, measured at $157 \mu\text{mol m}^{-2} \text{s}^{-1}$ PAR). Bars indicate means \pm SD (n=5).

In *P. x canescens* exposed to 75 mM NaCl no changes in the quantum yield of photosystem II efficiency were observed in darkness, whereas in the light PSII efficiency was

decreased (Figure 26B). This indicates that quantum yield efficiency of PSII in salt adapted *P. x canescens* was restricted in light but recovered in darkness. This may be considered as a mechanism to protect PSII under salinity. As in *P. euphratica*, no significant change in photochemical quenching was observed (Figure 26C). As the qN value was below 0.5, the difference in NPQ value can not be considered to reflect xanthophyll oxidation and photoinhibition and may be associated with heat dissipation and thylakoid membrane energization.

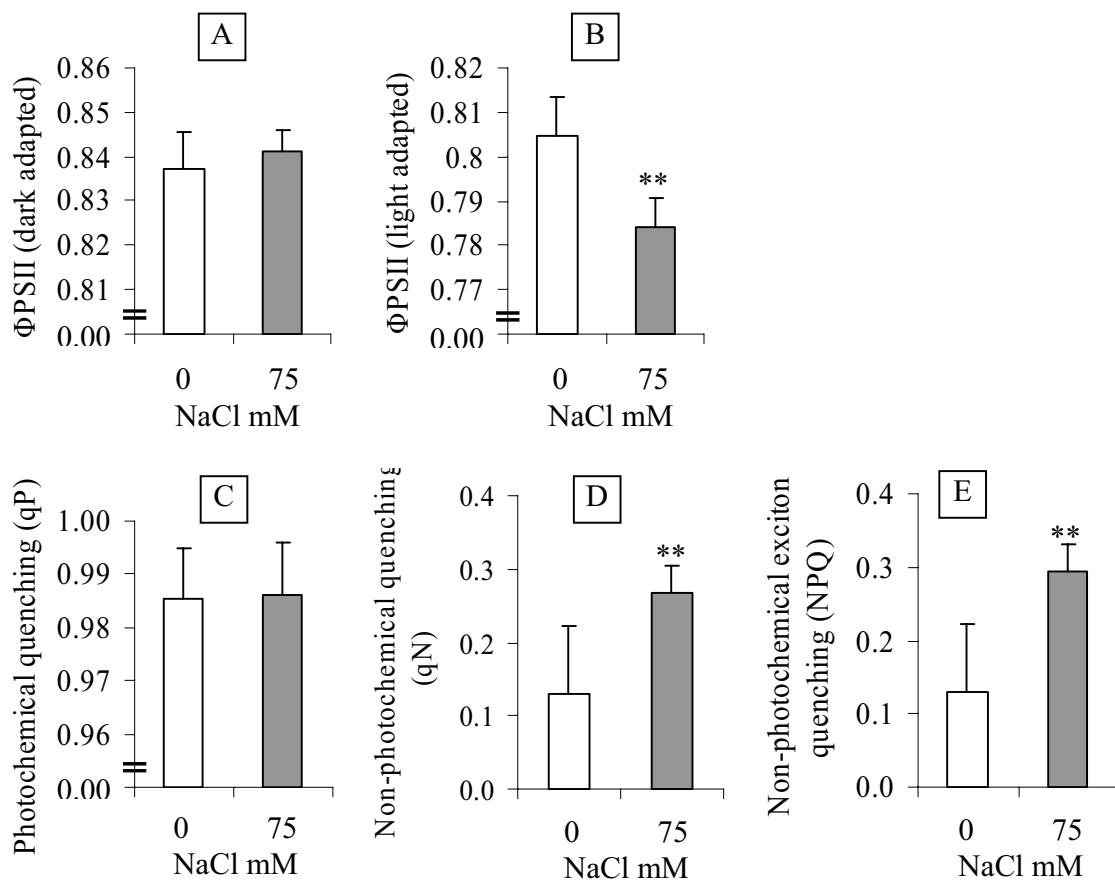


Figure 26. Potential and actual quantum yield efficiency of photosystem II (Φ PSII), photochemical (qP), non-photochemical quenching (qN) and non-photochemical exciton quenching (NPQ) in *P. x canescens* in control and after one week salt adaptation to 75 mM in hydroponic conditions. Dark adapted plants in night and subsequently light exposed plants in culture room with $150 \mu\text{mol m}^{-2} \text{s}^{-1}$ PAR (instrument has been detected maximum $10 \mu\text{mol m}^{-2} \text{s}^{-1}$ PAR it could be because of leaves shadow) were used for electron transport analysis. Bars indicate means \pm SD (n=6).

3.2 Selection of salt-related candidate genes

In a salt shock microarray experiment (Brinker and Polle, 2005) in which *P. euphratica* was exposed to 150 mM NaCl, the expression levels of 6340 genes were analyzed at different time points after salt stress. The microarray chip was constructed using cDNA libraries from control, stress-exposed and desert-grown *P. euphratica* trees (Brosché *et al.*, 2005). Plants were cultured in hydroponic condition (22°C, 150 $\mu\text{mol m}^{-2}\text{s}^{-1}$ PAR, at a photoperiod of 16h light/8h darkness) for 3.5 months. After reaching an average height of approximately 83 cm, plants were exposed to 150 mM NaCl. Roots and leaves of plants were harvested after 3h, 6h, 12h and 24h of salt stress. Among 67 ESTs, representing the salt regulated genes identified from salt microarray experiment only 24 were up-regulated. Based on results of ecophysiological studies and literature review, two of these upregulated and so far poorly characterised ESTs were selected for further investigations (Figure 27). One EST, AJ778489 that encodes a putative temperature induced lipocalin like protein was upregulated 3.3 fold after 3 h salt shock. *P. euphratica* was able to better protect its plasma membrane under salinity (Figure 18). As this protein is localized in plasma membrane (Kawamura and Uemura, 2003; Charron *et al.*, 2005), it may play an important role in plasma membrane protection under salinity. Another EST, AJ770289 that encodes an unknown protein, was upregulated 5.2 times in leaves after 24 hours salt shock and is completely uncharacterized.

>embl|AJ778489|AJ778489 Populus euphratica EST, clone P0000600001F02F1

```
[CGCGTCCG] GATGAGGCTAAACTCAAGGTCAAGTTTTATGTCCC GCCATTCTTGCCCATCA
TTCCTGTTGTTGGAGATTACTGGGTTCTGTCTCTTGATGATGATTATCAGTATGCTTTGATT
GGCCAGCCTAGCAGGAAATATCTCTGGATACTATGCAGGAAGACCCATATGGAGGATGAGAT
CTATAATCAGCTAGTGGAGAAGGCCGAAAGAACAGGGATATGATGTGGA
```

>embl|AJ770289|AJ770289 Populus euphratica EST, clone P0001100010A11F1

```
ACAACCTTGTCATCTTAGTTCATCAATCTATTATGGGGGTCAAGATATCTATCATCATCCTC
AGACTGCCCATACCTCAAGCATGAACCCAATGTTCAAAAAGGATGGACCTGAAGATGACACA
GGCAGTGCTTCAAGAGGAAATTGGTGGCAGGGGGGCCTTTATTACTAAGATCTCACGAGCCA
TGGCATATATATATATATATAGGTATAAAGGCAAGTTATAGGGTAGTAGTTTAATCTACCTT
TTGTTGTTGCAATAGGAAATATCAGTCAGCGTGTAGCGCAAAGCTGATTATTGTAATTCAC
CAGCCATGGAACAACACACACACACACACATATATGACAAGGCTATATGGCGCTTT
TTTTTATTTTGCTGTAAGGCAGATACATTATTTGGTCTTTTTGCAATAAAAGT
```

Figure 27. EST sequences of candidate genes obtained from EMBL Nucleotide Sequence Database (Brosché *et al.*, 2005). The first 8 nucleotides of AJ778489 belong to the cloning vector and were deleted in further analysis.

3.3 Identification and nomenclature of PeuTIL and PcaTIL (lipocalin like protein)

Real plant lipocalins were assigned to two groups: (a) the temperature induced lipocalins (TILs) and (b) chloroplastic lipocalins (CHLs) (see Introduction 1.6). Recent studies showed that TILs are induced by various stress factors and that they are not specifically temperature-induced proteins. Nevertheless this family is called ‘temperature-induced’. To prevent any confusion *P. euphratica* and *P. x canescens* lipocalins were called PeuTIL for *P. euphratica* temperature induced lipocalin like protein and PcaTIL for *P. x canescens* temperature induced lipocalin like protein.

3.4 Characterization of putative temperature induced lipocalin like proteins PeuTIL and PcaTIL

3.4.1 Gene expression analysis

3.4.1.1 Expression changes induced by salt shock

The promising results of the microarray experiment (Brinker and Polle, 2005) were confirmed by quantitative real time PCR (see 2.4.2.3.2). The transcription levels of PeuTIL 3, 6, 12 and 24 hours after salt shock (150 mM) were determined in relation to controls in leaves and roots of *P. euphratica* (Figure 28). Leaf PeuTIL was up-regulated 6 hours after salt shock (150 mM) and declined afterwards. In roots, PeuTIL transcripts were up-regulated at all time points.

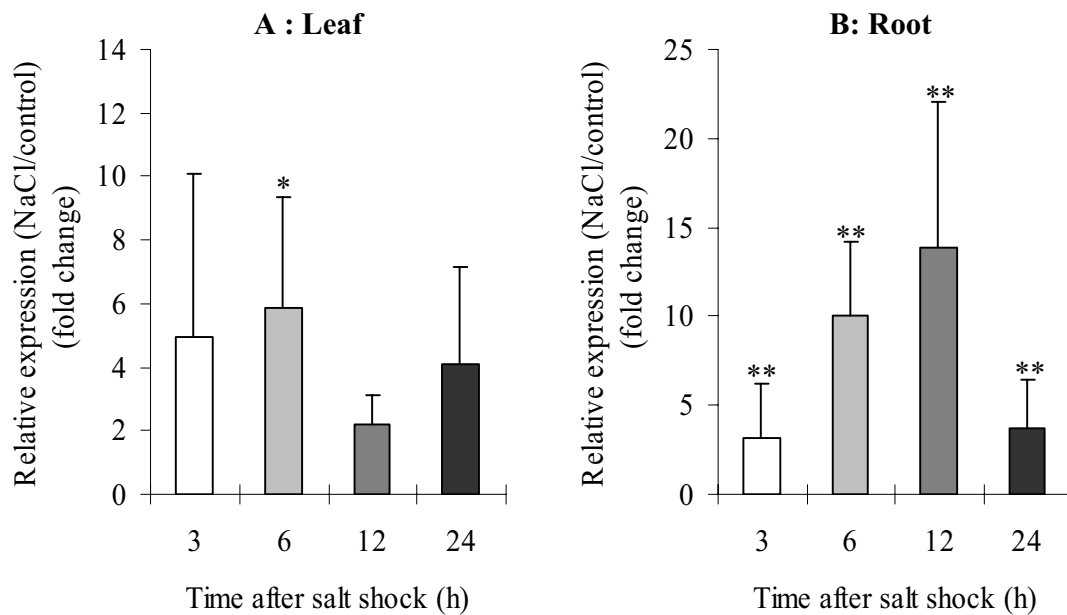


Figure 28. Expression (fold change) of PeuTIL in leaves (A) and roots (B) of *P. euphratica* relative to non treated plants after 3, 6, 12 and 24 hours of adding 150 mM NaCl. Stars show significant difference to non-treated plants. Data were normalized based on actin gene expression as house keeping gene. Bars indicate means \pm SE (n= 4).

Also the expression of PeuTIL in leaves was compared with its expression in roots in this salt shock experiment. It was found out that PeuTIL was differentially expressed in different tissue and that the amount of PeuTIL transcripts in leaves was even under control conditions relatively higher than that of roots (Figure 29).

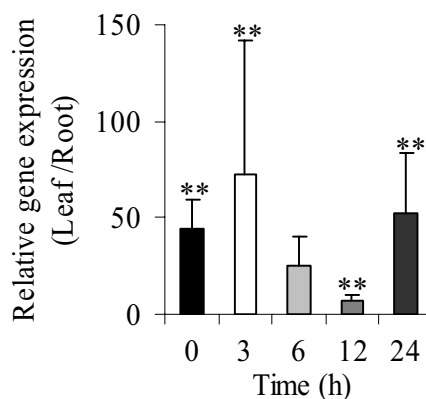


Figure 29. Relative transcript abundance of PeuTIL (leaf /root) before (0) and after 3, 6, 12 and 24 hours of salt stress with 150 mM NaCl in *P. euphratica*. Data were normalized based on actin gene expression as house keeping gene. Bars indicate means \pm SE (n= 4).

3.4.1.2 Expression changes induced by salt adaptation

To find out whether TILs play a role in long term salt adaptation, hydro-cultures of *P. euphratica* and *P. x canescens* were supplemented with 25 mM NaCl for two weeks. Then the salt concentration was increased to 100 mM for two further weeks. Real time PCR revealed that the transcript levels of both lipocalin genes (PcaTIL and PeuTIL) were unchanged relative to the controls after two weeks of growth in 25 or 100 mM NaCl (Figure 30).

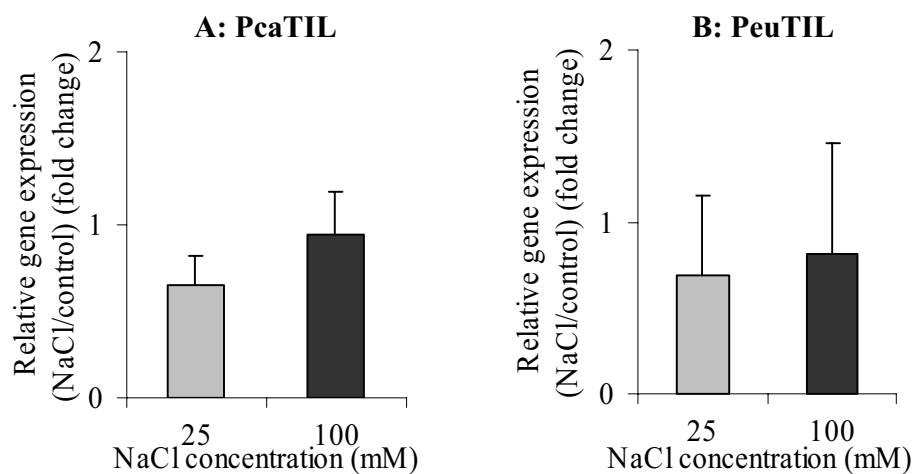


Figure 30. Relative expression of putative temperature induced lipocalin like gene of *P. x canescens* and *P. euphratica* in leaves after two weeks of salt adaptation to 25 and 100 mM NaCl, respectively, compared with non-treated plants. Plants were grown for two weeks in their final NaCl concentrations and all the leaves except 10% of shoot length from apex and base were harvested. Bars indicate means \pm SE (n= 3).

The expression ratio of PeuTIL was compared with the expression ratio of PcaTIL under control and salt adapted conditions in leaves of *P. euphratica* and *P. x canescens*. Data were normalized using actin gene expression. Under control conditions (without NaCl) lipocalin transcript levels in *P. euphratica* were obviously higher than in *P. x canescens* (Figure 31). Also after two weeks of adaptation to 25 mM NaCl, the amount of PeuTIL was significantly higher than that of PcaTIL in leaves (Figure 31). At 100 mM NaCl, the difference was not significant, probably because of the small number of replicates available.

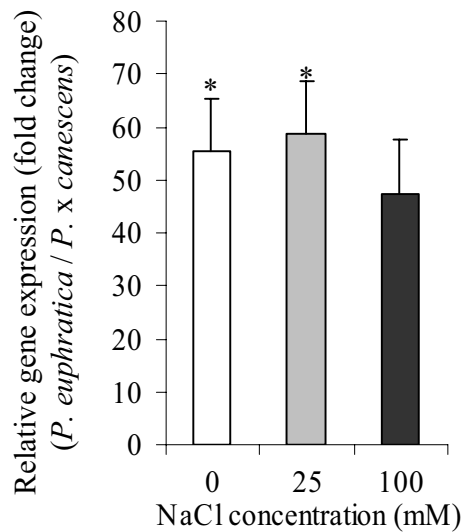


Figure 31. Relative expression ratio of *P. euphratica* TIL to *P. x canescens* TIL in leaves under different NaCl concentrations. Plants were grown for two weeks in their final NaCl concentrations and all leaves except 10 % of shoot length from apex and base were harvested. Stars means that *P. euphratica* TIL transcript abundance is significantly different in comparison with *P. x canescens*. Bars indicate means \pm SE (n= 3).

3.4.2 Gene isolation and sequencing

For isolating *PeuTIL* from *P. euphratica*, the presence of sequences corresponding to the EST was assessed in *P. trichocarpa* by running blast search on the JGI server against *P. trichocarpa* genome. All together one hit for AJ778489 (lipocalin EST) with 97.84% identity located on chromosome XVIII (JGI protein ID: 738040) was found (Figure 32). Cloning primers were designed in the UTR region of hit gene of *P. trichocarpa* (see 2.4.6). The primers contained BamHI as 5' extension to further cloning in pPCV702 containing 35S promoter for over- expression analysis.

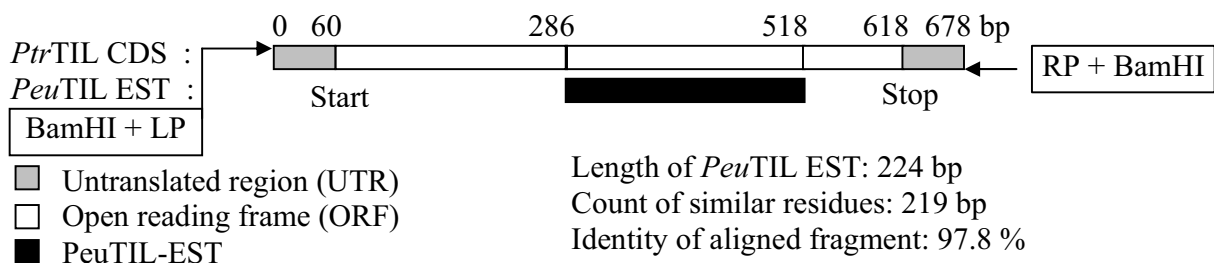


Figure 32. Alignment of *P. euphratica* lipocalin EST (*PeuTIL*-EST) and *PtrTIL* CDS. The location of the EST over *PtrTIL* CDS and cloning primers in untranslated region (UTR) has been shown schematically and the similarity of matched fragments is reported.

Both PeuTIL and PcaTIL were amplified with these primers (PeTIL_III_LP & RP) (App. 7.12) from cDNA. With respect to the product size of the *P. trichocarpa* cDNA of PtrTIL, fragments with 678 bp were expected and performing PCR fulfilled this expectation (Figure 33). All fragments were sequenced and cloned in the pGEM T-vector.

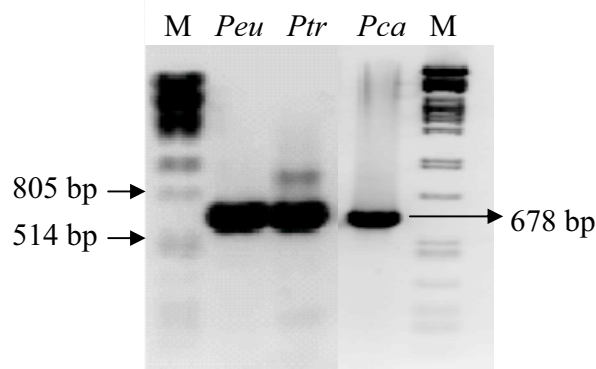


Figure 33. PCR products of full length coding sequence of temperature induced lipocalin like protein (TIL) in *P. euphratica*, *P. trichocarpa* and *P. x canescens*. Primers: (PeTIL-III-LP & RP) (App. 7.12). M: λ Pst marker.

3.4.3 Gain of function of PeuTIL in *A. thaliana* and *P. x canescens*

To do gain of function analysis of PeuTIL in *A. thaliana* and *P. x canescens*, it has been planned to insert the fragment in the binary plant vector pPCV702 containing 35S promoter at the BamHI insertion site and transform the construct in *Agrobacterium*. The first efforts to clone PeuTIL in pPCV702 were not successful and results of sequencing showed that it has been inserted in wrong direction. The proper transformation constructs will be send to Dr. R. Hänsch (Institut for Plant Biology, Technische Universität Braunschweig), who is responsible for poplar transformation in the frame work of poplar research group.

3.4.4 In silico analysis of temperature induced lipocalin like proteins

The open reading frame of PeuTIL contains 558 bp, with GC content of 44.6% (45.2% PcaTIL, 45.7% PtrTIL and 52% in AthTIL) and is predicted to encode a polypeptide of 185 amino acids with a theoretical isoelectric point (pI) of 5.73 and a molecular weight of 21.5 kDa. Comparing GC content of four selected TIL genes showed that AthTIL has higher GC content than poplar species. It is believed that direction of gene conversion might be

biased toward G and C. Also there are some evidences that the genes with higher GC content are more thermostable and also more stable under UV radiation (Eyre-Walker, 1993).

3.4.4.1 Amino acid distribution histogram

Amino acid composition of PeuTIL, PcaTIL, PtrTIL and AthTIL reveals that the amino acid frequency pattern of poplar TILs are similar and that AthTIL has more serines in comparison with poplar TILs (Figure 34).

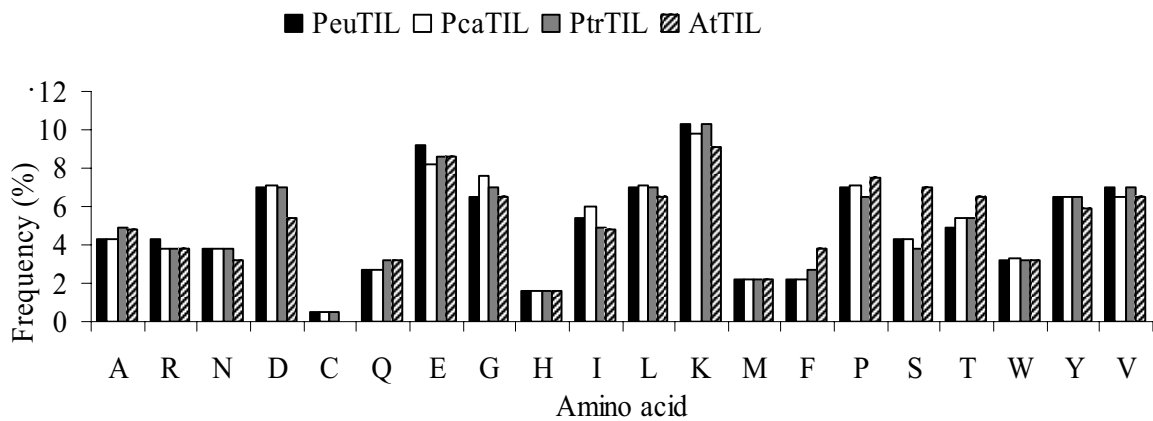


Figure 34. Amino acid composition of PeuTIL, PcaTIL, PtrTIL and AthTIL. Different amino acids have been demonstrated by IUPAC one code (App. 7.27).

To find out whether the amino acid frequency of PeuTIL is generally similar to other proteins or not, the amino acid composition of PeuTIL was compared with total amino acid composition of *A. thaliana* (derived from Banerjee *et al.*, 2006) using a histogram. This comparison shows that the amino acid frequency pattern of PeuTIL is similar to the general pattern observed in total amino acid composition of *A. thaliana* as plant model (Figure 35).

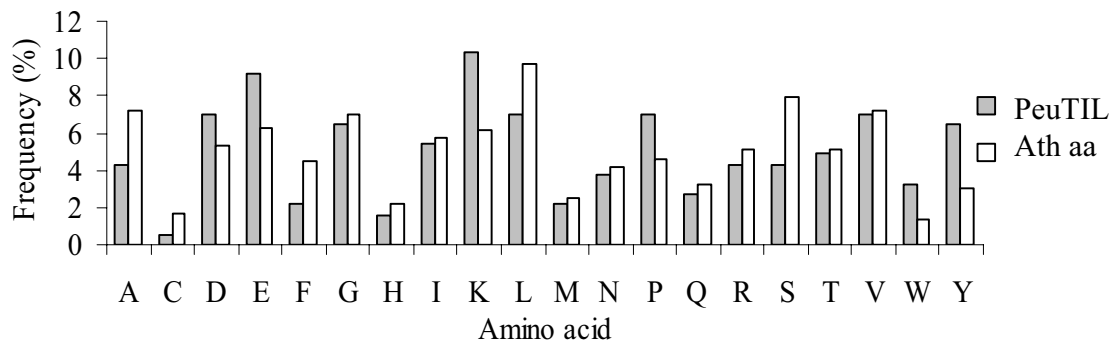


Figure 35. Amino acid composition of PeuTIL in comparison with amino acid composition pattern of *A. thaliana* genes. Different amino acids have been demonstrated by IUPAC one code (App. 7.27).

Multiple alignment of four plant lipocalin (PeuTIL, PcaTIL, PtrTIL and AthTIL) demonstrates the presence of three structurally conserved regions (SCR) (see 1.6) in all four species (Figure 36). Identity and similarity of sequences were determined using pair-wise comparisons (Table 9). PeuTIL has 95% identity and 97% similarity with PcaTIL and it has 76% identity and 88% similarity with AthTIL. Its similarity and identity with PtrTIL is higher than of PcaTIL. Most differences in the amino acid sequence of AthTIL with the three TIL of poplar are located in the SCR3 region and between 166 to 172 bp. To find out whether the structures of these proteins in determined regions are really conserved secondary structure of these proteins should be investigated. But one thing is clear that in all SCRs the consensus elements representing TILs are conserved in poplar TILs (see 1.6).

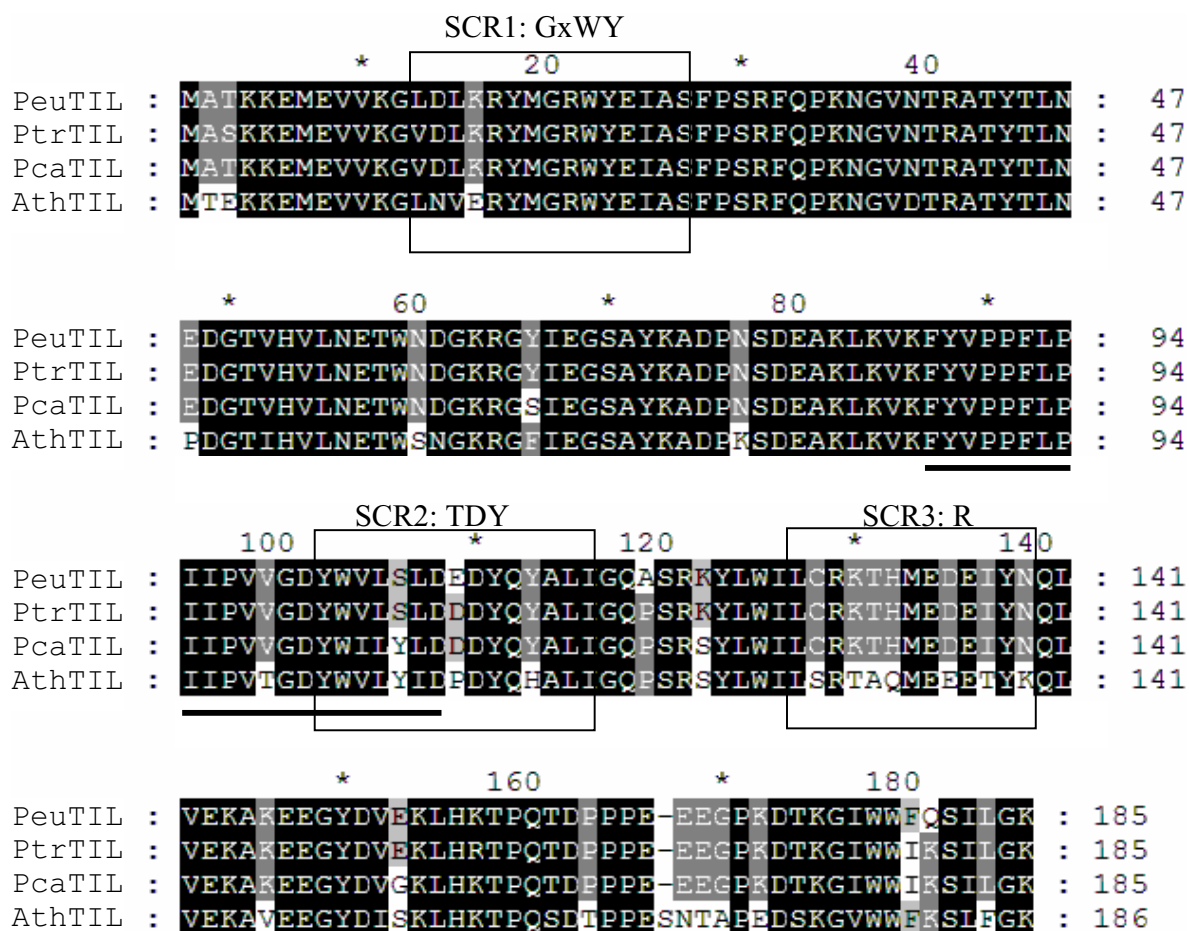


Figure 36. Multiple alignments of lipocalin amino acid sequences of *P. trichocarpa* (PtrTIL), *P. euphratica* (PeuTIL), *P. x canescens* (PcaTIL) and *A. thaliana* (AthTIL). SCRs are marked as boxes. Black line from 87-108 aa demonstrates putative transmembrane region predicted by TopPred (see 3.4.7). SCR= structural conserved region; GxWY, TDY and R are three known conserved sequences of lipocalins (see 7.27).

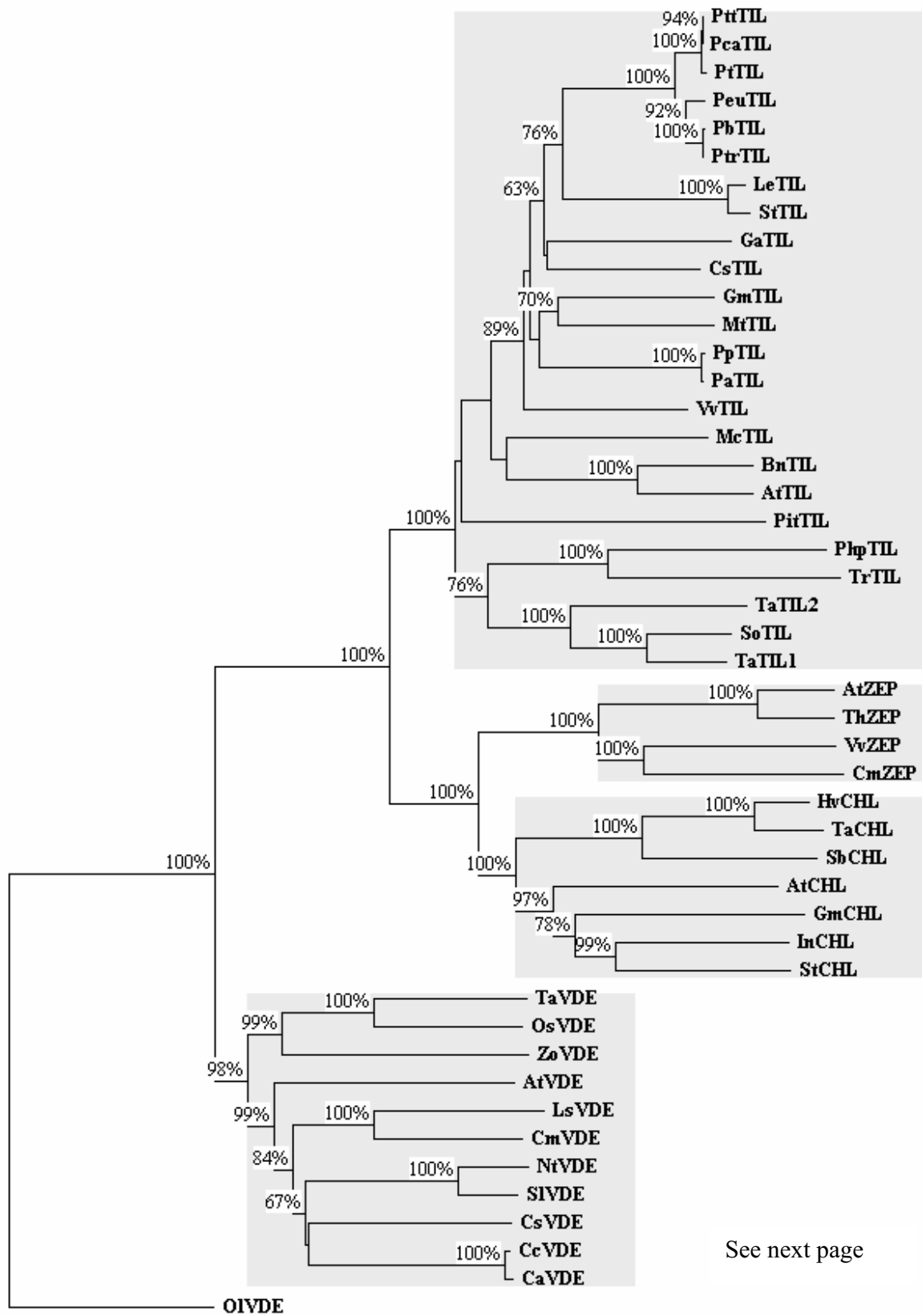
Table 9. Pair-wise comparison of four lipocalins (*P. trichocarpa*, *P. euphratica*, *P. x canescens* and *A. thaliana*). Matrix diameter shows number of amino acid. In each cell the first row shows identical residues, the second row shows similar residues and the third row shows residues lined up in a gap. Each number is expressed as absolute number of amino acid and as percentage on the different sides of the matrix diagonal.

	PtrTIL	PeuTIL	PcaTIL	AthTIL
PtrTIL	185	95% 98% 0%	94% 96% 0%	77% 88% 0%
PeuTIL	177 182 0	185	95% 97% 0%	76% 88% 0%
PcaTIL	175 179 0	177 180 0	185	78% 89% 0%
AthTIL	145 105 42	143 105 42	146 105 42	186

3.4.5 Phylogenetic studies of plant lipocalins

Protein sequence databank of NCBI was searched for four plant lipocalins (TILs, CHLs, ZEPs and VDES). After performing multiple alignment using ClustalW, the evolutionary distance was estimated by Kimura model and NJ tree demonstrated using TREECON program (see 2.4.9). VDE protein of *Ostreococcus lucimarinus*, an early-diverging class within the green plant lineage was selected as out group. Plant lipocalins cluster in four clades (Charron *et al.*, 2005). ZEPs and CHLs encoding zeaxanthin epoxidases and chloroplastic lipocalins are located closer to TILs than VDEs that encode violaxanthin de-epoxidases. Poplar TILs can be divided into two clades (bootstrap 100%). *P. trichocarpa* and *P. balsamifera* clustered with *P. euphratica* in one cluster (bootstrap 92%) whereas *P. tremula x tremuloides* and *P. tremuloides* clustered together with *P. canescens* (bootstrap 100%).

Distance 0.1



See next page

Figure 37. Neighbour-joining tree of nucleotide acid of plant lipocalins. Bootstrap values less than 50 % were removed. **AtCHL** : *Arabidopsis thaliana* , CAB41869 **AthTIL** : *Arabidopsis thaliana* , BAB10998 ;**AtVDE**: *Arabidopsis thaliana*, AY063067; **AtZEP** : *Arabidopsis thaliana* , AF283761; **BnTIL**: *Brassica napus*, DQ222996; **CaVDE**: *Coffea arabica*, DQ234768; **CcVDE**: *Coffea canephora*, DQ233246; **CmVDE**: *Chrysanthemum x morifolium*, AB205051; **CmZEP**: *Chrysanthemum x morifolium*, AB205053; **CsTIL**: *Citrus sinensis*, DQ223001; **CsVDE**: *Camellia sinensis*, AF462269; **GaTIL**: *Gossypium arboreum*, DQ223000; **GmCHL**: *Glycine max*, DQ223010; **GmTIL**: *Glycine max*, DQ222990; **HvCHL**: *Hordeum vulgare*, DQ223006; **InCHL**: *Ipomoea nil*, DQ223007; **LeTIL**: *Lycopersicon esculentum*, DQ222988; **LsVDE**: *Lactuca sativa*, U31462; **McTIL**: *Mesembryanthemum crystallinum*, DQ222999; **MtTIL**: *Medicago truncatula*, DQ222994; **NtVDE**: *Nicotiana tabacum*, U34817; **OIVDE**: *Ostreococcus lucimarinus*, XM_001421667; **OsVDE**: *Oryza sativa*, AF288196; **PaTIL**: *Prunus armeniaca*, DQ222998; **PbTIL**: *Populus balsamifera*, DQ223002; **PcaTIL**: *Populus x canescens*; **PeuTIL**: *Populus euphratica*; **PhpTIL**: *Physcomitrella patens*, DQ222991; **PitTIL**: *Pinus taeda*, DQ222992; **PpTIL**: *Prunus persica*, DQ222997; **PtTIL**: *Populus tremuloides*, DQ223003; **PtrTIL**: *Populus trichocarpa*, JGI-ID: 738040; **PttTIL**: *Populus tremula x tremuloides*, DQ223004; **SbCHL**: *Sorghum bicolor*, DQ223005; **SIVDE**: *Solanum lycopersicum*, AF385366; **SoTIL**: *Saccharum officinarum*, DQ222989; **StCHL**: *Solanum tuberosum*, DQ223008; **StTIL**: *Solanum tuberosum*, DQ222995; **TaCHL**: *Triticum aestivum*, DQ223009; **TaTIL1**: *Triticum aestivum*, AAL75812; **TaTIL2**: *Triticum aestivum*, DQ222977; **TaVDE**: *Triticum aestivum*, AF265294; **ThZEP**: *Thellungiella halophila*, AY842302; **TrTIL**: *Tortula ruralis*, DQ223011; **VvTIL**: *Vitis vinifera*, DQ222993; **VvZEP**: *Vitis vinifera*, AY337615; **ZoVDE**: *Zingiber officinale*, AY876286.

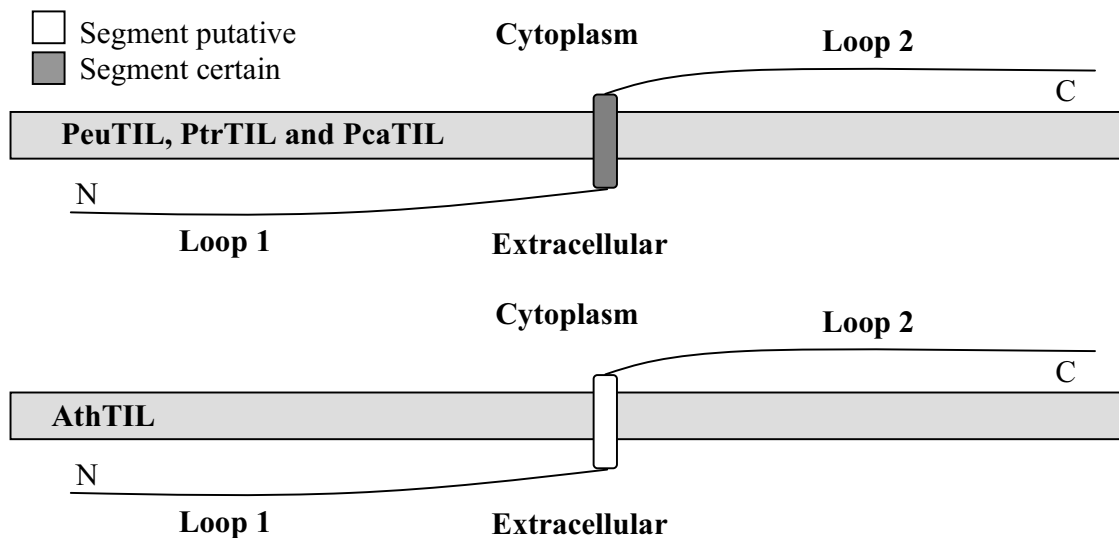
3.4.6 Topology and GPI anchor signal prediction

Topology prediction of PeuTIL, PtrTIL and PcaTIL using TopPred method that combines hydrophobicity analysis and positive-inside rule (the segment of membrane protein that have more positively charged residues is located inside the cell), detected a segment that certainly is able to penetrate membrane whereas the same segment in AthTIL is reported as putative transmembrane segment because of lower hydrophobicity (Figure 38A and Figure 39) (Wallin and von Heijne, 1998). The cytoplasmic C-terminus tails of candidate poplar TILs have more positively charged residues (arginine and lysine) than AthTIL (Figure 38B). This may increase contact with negatively charged phospholipid head groups (Ravichandran *et al.*, 1997). Also between poplar TILs, PcaTIL has one positively charged residue less than others (Figure 38B). None of the investigated proteins have GPI anchor signals and no cleavage site was detected.

3.4.7 Subcellular localization

Prediction of subcellular localization for PeuTIL, PtrTIL, PcaTIL and AthTIL was performed using TargetP 1.1 server (<http://www.cbs.dtu.dk/services/TargetP/>) with no cut-off setting and selecting ‘Plant’ option (Emanuelsson *et al.*, 2000). No target peptide for chloroplast transit peptide, mitochondrial targeting peptide, secretory pathway signal peptide or any other location was predicted in amino acid sequences of PeuTIL, PcaTIL and PtrTIL. It was already reported that despite the absence of a target peptide in AthTIL and TaTIL they are localized in plasma membrane (Kawamura and Uemura, 2003; Charron *et al.*, 2005). With respect to the results of topology prediction of a ‘certain transmembrane’ segment in poplar TILs in comparison with a ‘putative transmembrane’ segment in AthTIL a subcellular localization of poplar TILs in plasma membrane is expected. This is also supported by evidence for plasma membrane localization in *Arabidopsis*.

A: Topology of PeuTIL, PtrTIL, PcaTIL and AthTIL



B: Loop length and number of positively charged residues

	Loop 1		Loop 2	
	Length	KR	Length	KR
PeuTIL	87	15	77	12
PtrTIL	87	15	77	11
PcaTIL	87	15	77	11
AthTIL	87	15	78	9

Figure 38. Topology prediction of TIL proteins using TopPred. Demonstrating the topology of PeuSIS, PtrSIS and PcaSIS (A). Loop length and number of positively charged residues

(B). One transmembrane segment was detected in all species; however this segment is 'putative' in AthTIL (see also Figure 39). KR= number of lysine and arginine.

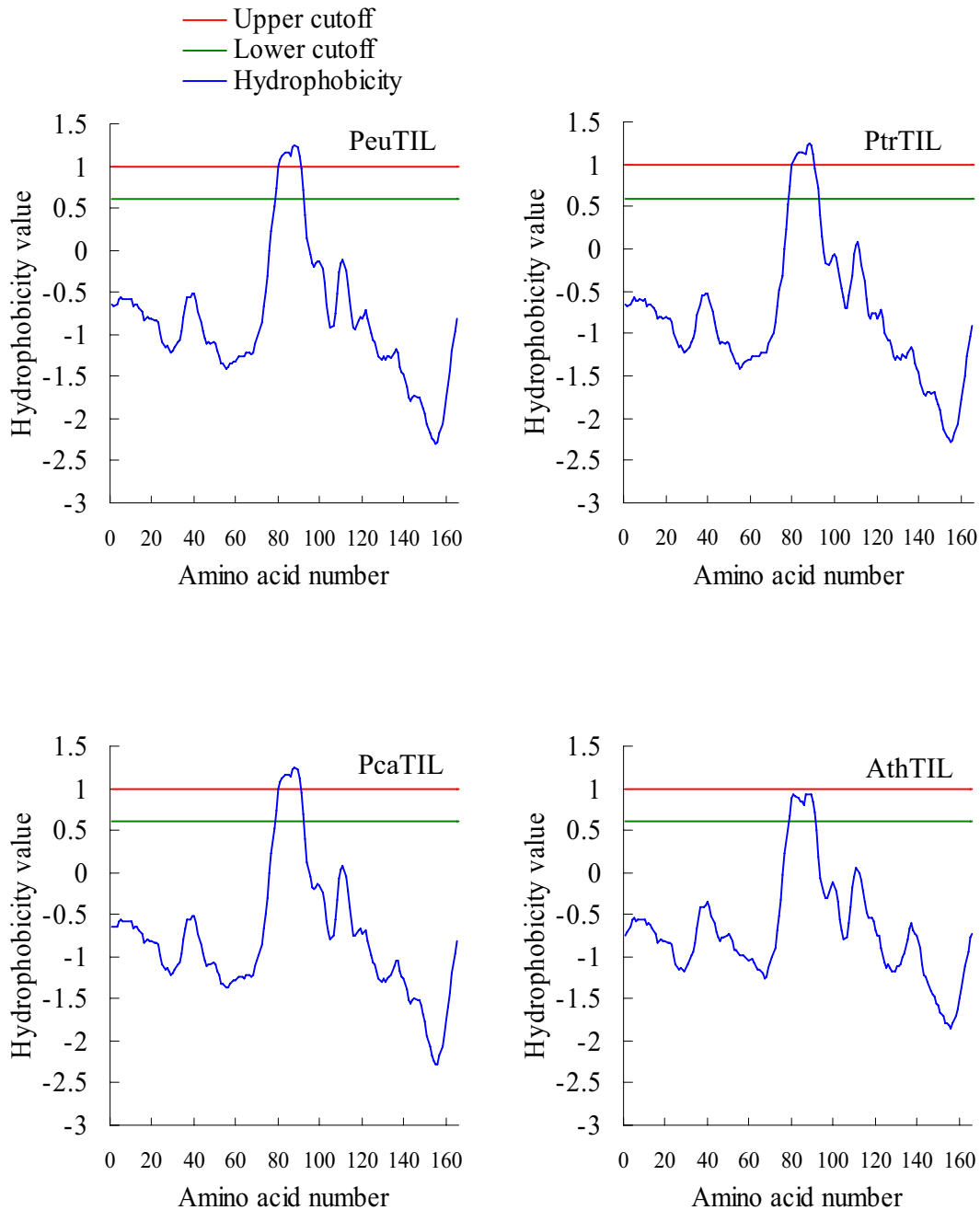


Figure 39. The hydrophobicity plot of TIL proteins based on Kyte-Doolittle scale. Hydrophobicity of PeuTIL, PtrTIL and PcaTIL exceed from the upper cutoff (hydrophobicity 1), whereas in AthSIS hydrophobicity profile does not reach to upper cutoff.

3.4.8 Promoter analysis of lipocalin

To analyze putative promoter elements 627 bp upstream of the PtrTIL and AthTIL genes were used, this avoids entering the coding region of the adjacent gene. These regions were searched against the PLACE database (a database of plant cis-acting regulatory DNA elements) and the results were compared (Table 10). Pairwise alignment showed 46% identity in this region. All together 67 elements only in *P. trichocarpa* and 46 regulatory elements only in *A. thaliana* were detected and 34 element were common in both species. Most abundant consensus sequences in both promoters were elements that are present in promoter areas of genes encoding storage proteins and seed specific genes (*i.e.* EBOXBNNAPA, POLLEN1LELAT52, SREATMSD). Promoters of both, PtrTIL and AthTIL, are rich of core sites required for binding of DOF (DNA binding with one finger) proteins (AAAG). DOF proteins belong to zinc finger transcription factor (TF) classes that bind to the AAAG motif. These TFs play a role in regulation of seed germination and development, guard cell specific functions, photosynthesis, phytohormone effects and plant-pathogen interaction (Plesch *et al.* 2001; Martinez *et al.*, 2004). The most abundant elements found in the promoter area of PtrTIL were related to ABA signalling and response to dehydration or light.

Table 10. Cis regulatory elements detected in 627 bp upstream region of PtrTIL and AthTIL. The frequency of regulatory elements in both (+) and (-) strands have been shown. Common elements between *P. trichocarpa* and *A. thaliana* with high frequency are sorted at the beginning of table, and then the elements that found just in *A. thaliana* and *P. trichocarpa* are sorted respectively. Y [TC] pYrimidine; R [AG] puRine; W [AT] Weak; S [GC] Strong; K [TG] Keto; M [AC] aromatic; B [TGC] not A; D [ATG] not C; H [ATC] not G; V [AGC] not T; N [ATGC]; Myb for avian MYeloBlastosis virus; MYC for avian myelocytomatosis viral oncogene.

Element	Sequence	Description	No. of elements	
			<i>Ptr</i>	<i>Ath</i>
EBOXBNNAPA	CANNTG	Storage protein promoter, ABA response	7-7+	2-2+
MYCCONSSENSUSAT	CANNTG	Early responsive to dehydration	7-7+	2-2+
DOFCOREZM	AAAG	Core site required for binding of DOF (DNA binding with one finger) proteins (endosperm-specific expression)	5-6+	5-12+
CAATBOX1	CAAT	LegA gene, seed storage	6-2+	3-3+
CACTFTPPCA1	YACT	mesophyll expression module1	4-3+	2-3+

		found in phosphoenolpyruvate carboxylase (ppcA1) of C4 dicots.		
GATABOX	GATA	Found in promoter of Petunia chlorophyll a/b binding protein	2-4+	2-4+
ARR1AT	NGATT	ARR1-binding; transcriptional activator; in promoter of rice non-symbiotic haemoglobin-2 gene	4-1+	9-5+
GT1CONSENSUS	GRWAAW	Light regulated genes	3-2+	5-6+
WRKY71OS	TGAC	Gibberellin signalling; Pathogenesis-Related genes	4-1+	2-
OSE2ROOTNODULE	CTCTT	Root nodule infected cell promoter	2-3+	1-1+
POLLEN1LELAT52	AGAAA	Regulatory element of Lat52 a heat stable protein in seed fertilizing and development	4-	3-5+
ROOTMOTIFTAPOX1	ATATT	Motif found in root elongation protein (RoLD)	1-2+	3-4+
GTGANTG10	GTGA	Found in the promoter of pectate lyase like gene; pollen	1-2+	4-
TAAAGSTKST1	TAAAG	found in promoter of KST1 gene encodes a K ⁺ influx channel of guard cells	1-2+	1-2+
TATABOX5	TTATTT	TATA box found in the 5'upstream region of glutamine synthetase gene;	3+	1-1+
WBOXNTERF3	TGACY	Translation release factor	2-1+	2-
MYBST1	GGATA	See MYB1AT	2-1+	1-
WBOXHVIS01	TGACT	In promoter of isoamylase gene	2-1+	1-
RAV1AAT	CAACA	Consensus of Rav1 a growth retardation protein	1-1+	3+
IBOXCORE	GATAA	Conserved sequence upstream of light induced genes	1-1+	1-2+
CCAATBOX1	CCAAT	Heat shock element	1-1+	2+
SREATMSD	TTATCC	sugar-repressive element; growth regulation; dormancy	1-1+	1+
SITEIIATCYTC	TGGGCY	Site II element found in the promoter regions of cytochrome genes in Arabidopsis	1-1+	1-
SEF4MOTIFGM7S	RTTTTTR	Seed specific transcript binding	1-	2-1+
GT1GMSCAM4	GAAAAA	Pathogen- and salt-induced	1+	2+
EECCRCAH1	GANTTNC	Periplasmic carbonic anhydrase enhancer	1-	2+
POLASIG3	AATAAT	Putative polyadenylation signals	1-	1-1+
MYBPLANT	MACCWAMC	In promoter of phenylpropanoid and lignin biosynthetic genes	1+	1+
MYCATERD1	CATGTG	Early responsive to dehydration	1+	1-
PYRIMIDINEBOXOSRAM Y1A	CCTTTT	Gibberellin-response found in the promoter of barley α -amylase	1+	1-

		gene		
MYCATRD22	CACATG	Early responsive to dehydration	1-	1+
NTBBF1ARROLB	ACTTTA	DOF binding site; Auxin induced	1-	1+
SORLIP1AT	GCCAC	Found in light induced promoters	1-	1+
INRNTPSADB	YTCANTYY	Light responsive element	1-	1-
NODCON1GM	AAAGAT	Nodulin gene consensus		2-3+
TATCCAOSAMY	TATCCA	alpha-amylase; MYB proteins; gibberellin; GA; sugar starvation;		1+
SEF3MOTIFGM	AACCCA	Seed specific transcript binding		1+
RYREPEATBNNAPA	CATGCA	ABA signalling; Required for seed specific expression		1+
RBCSCONSENSUS	AATCCAA	Rubisco consensus		1+
QELEMENTZM3	AGGTCA	Pollen specific		1+
PRECONSCRHSP70A	SCGAYNRN(15) HD	Plastid response element		1+
CIACADIANLELHC	CAANNNNATC	Promoter element of Light harvest centre gene		1+
-300ELEMENT	TGHAAARK	Seed storage protein, hordein		1+
-300CORE	TGTAAAG	Alfa-zein gene expression		1+
TBOXATGAPB	ACTTTG	Light activated gene encodes the B subunit of chloroplast glyceraldehyde-3-phosphate dehydrogenase		1-
TATABOXOSPAL	TATTTAA	found in the promoter of rice PAL gene encoding phenylalanine ammonia-lyase		1-
CGACGOSAMY3	CGACG	Seed storage, rice amylase genes		1-
AMMORESIIUDCRNIA1	GGWAGGGT	Ammonium response		1-
POLASIG1	AATAAA	Putative polyadenylation signals	3-	
WBOXATNPR1	TTGAC	Salicylic acid induced found in pathogenesis related genes	3-	
MYBCORE	CNGTTR	See MYB1AT	1-2+	
SORLIP2AT	GGGCC	Found in light induced promoters	1-2+	
BIHD1OS	TGTCA	Binding site of shoot apical meristem regulators	2+	
MARTBOX	TTWTWTTWTT	Scaffold attachment region	2+	
-10PEHVPSBD	TATTCT	Chloroplast gene expression	2-	
ABREZMRAB28	CCACGTGG	ABA and water stress responsive; CBF1 dependent low temperature signalling pathway in Populus spp.	1-1+	
CACGTGMOTIF	CACGTG	PhyA (Phytochrome)-responsive promoters	1-1+	
CATATGGMSAUR	CATATG	Auxin and protein-synthesis-inhibitor induced in SAUR (Small Auxin-Up RNAs) gene promoter	1-1+	
CURECORECR	GTAC	Copper and oxygen-deficiency response element	1-1+	

IRO2OS	CACGTGG	Fe deficiency induced	1-1+	
MYB1AT	WAACCA	Dehydration and ABA responsive in <i>A. thaliana</i> MYB gene controlling cell cycle	1-1+	
MYB2CONSENSUSAT	YAACKG	See MYB1AT	1-1+	
REALPHALGLHCB21	AACCAA	Required for phytochrome regulation, etiolation signalling	1-1+	
BOXIIPCCHS	ACGTGGC	Light responsive element	1+	
BOXLCOREDPCAL	ACCWWCC	phenylalanine ammonia-lyase (PAL1) promoter, light induced, phenylpropanoid pathway	1+	
EMBP1TAEM	CACGTGGC	ABA signalling	1+	
GBOXLERBCS	MCACGTGGC	Light regulated genes	1+	
LREBOXIIPCCHS1	TCCACGTGGC	Light responsive element	1+	
LRENPCABE	ACGTGGCA	Light responsive element	1+	
LTRECOREATCOR15	CCGAC	Low temperature responsive	1+	
MYB2AT	TAACTG	See MYB1AT	1+	
MYBCOREATCYCB1	AACGG	See MYB1AT	1+	
MYBPZM	CCWACC	See MYB1AT, gene specifies red pigmentation of kernel pericarp	1+	
SURECOREATSULTR11	GAGAC	Sulfur-responsive element (SURE)	1+	
CBFHV	RYCGAC	dehydration-responsive element	1-	
IBOX	GATAAG	Conserved sequence upstream of light induced genes	1-	
IBOXCORENT	GATAAGR	See IBOX	1-	
SP8BFIBSP8BIB	TACTATT	Found in promoters of sporamin (a vacuolar protein of the sweet potato) and beta-amylase genes	1-	
SV40COREENHAN	GTGGWWHG	light-responsive elements of RuBisCo gene	1-	
UP1ATMSD	GGCCCAWWW	Growth regulation; dormancy	1-	
WBBOXPCWRKY1	TTTGACY	Found in amylase gene	1-	

3.4.9 Loss of function analysis

3.4.9.1 Characterisation of AthTIL knock out lines

The *Arabidopsis* genome was searched to find homolog gene of PeuTIL by performing a blast with PeuTIL protein sequence using the 'tblastn protein' program which had been used for the in silico analysis (3.4.5). One hit with 76% identity and 88% similarity in the predicted amino acid sequence was found. Among the available *Arabidopsis* Salk lines of At5g58070, the transgenic SALK T-DNA knockout line of At5g58070.1 - SALK_136775

with the T-DNA insertion in the intron was ordered from the Nottingham *Arabidopsis* stock centre (NASC) (Figure 40).

```
>At5g58070
ATGACAGAGAAGAAAGAGATGGAAGTGGTGAAGGGCTCAACG
TGGAGAGATACATGGGCCGTTGGTACGAGATTGCTTCTTTCCC
ATCAAGGTTTTAGCCAAAGAACGGCGTCGACACTCGCGCCACC
TACACCCTTAACCCCGACGGTACCATACACGTCTTGAACGAAA
CGTGGAGCAACGGGAAGAGGGGTTTTATCGAAGGCAGCGCCTA
TAAGGCCGATCCTAAAAGCGACGAAGCCAAGCTCAAAGTCAAG
TTCTATGTCCCTCCTTTCCCTCCAATCATTCCCGTCACCGGAG
ACTACTGGGTGCTCTACATCGATCCTGACTACCAGCACGCTCT
CATTGGCCAGCCTTCCAGGAGTTATCTCTGGATATTGAGCAGG
ACGGCGCAAATGGAGGAAGAGACGTATAAGCAGCTGGTGGAGA
AGGCAGTGGAGGAAGGTTATGACATCAGCAAGCTTCACAAGAC
TCCTCAGAGTGACACACCACCTGAGTCCAACACTGCCCTGAA
GACTCCAAGGGCGTTTGGTGGTTCAAATCTCTCTTCGGCAAAT
AG
```

Figure 40. Coding sequence of At5g58070. The insertion site of the T-DNA has been shown by a triangle and the flanking sequence has been highlighted by grey colour.

Seeds of this Salk-line were grown on agar plates containing 1% kanamycine. The seeds that contained no T-DNA were not able to develop in presence of kanamycine (Figure 41A)

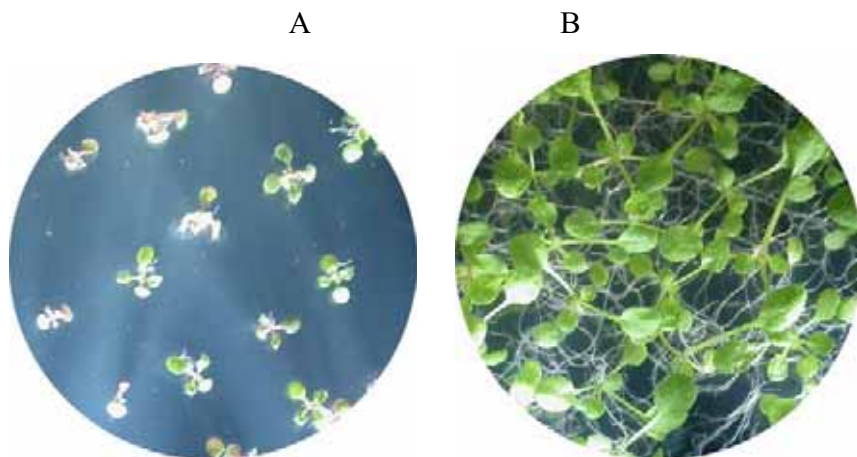


Figure 41. The individuals having T-DNA are kanamycine resistant. A) Wild type *A. thaliana* on agar containing 1% kanamycine. B) Salk T-DNA mutant *A. thaliana* At5g58070.1 - Salk_136775 growth on agar containing 1% kanamycine.

After transferring the seedlings in soil, homozygote individuals were selected by a PCR method using a combination of left and right gene specific primers (AtTIL136775-LP

and RP) (App. 7.12), and also the left border T-DNA specific primer (Lba1) and right gene specific primer (RP) (Figure 42) as described under 2.4.2.3. No product with the LP-RP combination was observed in the Salk lines and the correct size of 1141 bp was achieved in the wild type. Running PCR with the Lba1-RP combination and the Salk line genomic DNA as template produced the expected fragment of 705 bp and no product was observed in wild type. As result the tested Salk lines 1, 2 and 3 are homozygous for the T-DNA insert.

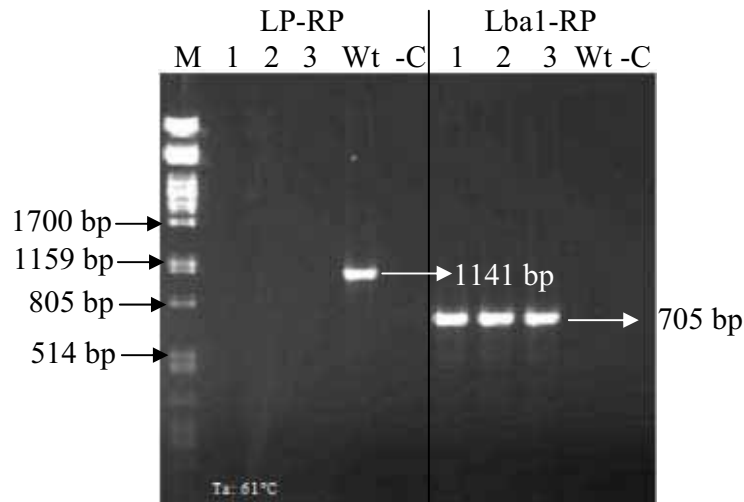


Figure 42. PCR based selection of homozygote Salk lines. Three Salk lines (1, 2 and 3) together with wild type (Wt) and negative control (-C: no DNA) were subjected to PCR with to different primer combinations (LP-RP and Lba1-RP). LP: left primer of gene of interest, RP: right primer of gene of interest, Lba1: left border primer a1 anneals on TDNA insertion and M: λ Pst marker. (For primers sequences see App. 7.12).

To ensure the location of the T-DNA, PCR products of Lba1-RP were sequenced and the flanking sequences were blasted against the *A. thaliana* genome (Figure 43).

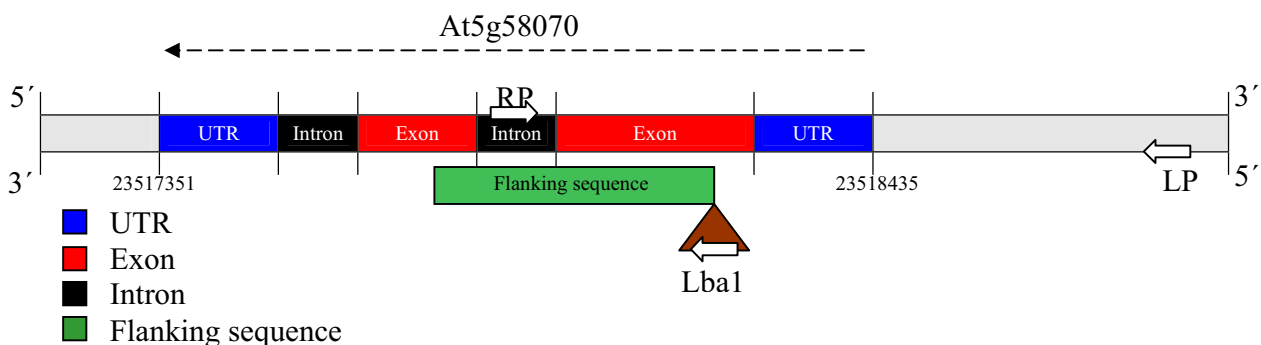


Figure 43. Location of AthTIL (At5g58070), the insert T-DNA and primers in the *Arabidopsis* genome. The Salk line Salk_136775 was used. T-DNA is indicated by a triangle. White arrows show the position of primers.

In homozygote transgenics, with the inserted T-DNA in the exon, no transcript is expected. To be sure that no transcript of AthTIL is existing in its knockout line (At5g58070.1 - SALK_136775), a PCR was run using cDNA as template and with the primer combination of LBa1 and AtTILexpRP (see App. 7.12). Also genomic DNA was used as positive control. Despite the inserted T-DNA, a fragment was produced with cDNA (Figure 44). The smaller size of the cDNA than that of the gDNA reveals that this fragment is most likely not from contaminating genomic DNA and it matched with the expected transcript size. If this fragment is a transcript of AthTIL together with the T-DNA, it can not be translated into a functional protein because of the presence of a number of stop codons in the T-DNA.

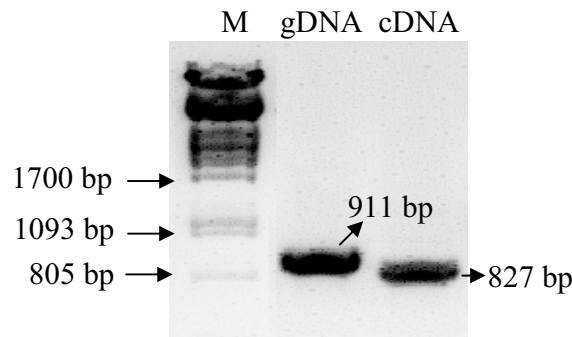


Figure 44. Evaluation of the transcript level of AthTIL in Salk line. M= λ Pst DNA ladder, gDNA= genomic DNA of At5g58070.1 – Salk 136775, cDNA= cDNA of At5g58070.1 – Salk 136775. Primer combination= LBa1 and AtTILexpRP (see App. 7.12, also see Figure 45).

The T-DNA was located 34 bp after the start codon in exon region. An intron with 84 bp is located between RP gene specific primer and Lba1 from TDNA (Figure 45). Hence a fragment that is amplified from cDNA is 84 bp shorter than that from gDNA.

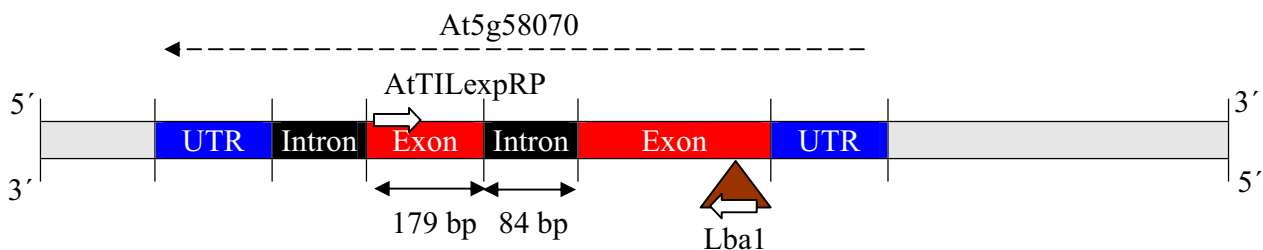


Figure 45. Position of primers used for testing cDNA of lipocalin Salk line on genomic DNA with emphasize on the length of intron between two primers. T-DNA has been demonstrated by a triangle.

3.4.9.2 Phenotypic analysis of AthTIL knock out lines

For investigating the phenotype of AthTIL knock-out lines, knock-out and wild type plants were grown in soil for 10 weeks (8 h light, 16 h dark, 20° C) (see 2.1). Maximum inflorescence bolting time of AthTIL knock out lines was 11 days sooner than that of wild type. At the time of inflorescence bolting, the number of leaves per rosette was counted. AthTIL knock out lines had less leaves per rosette at the time of bolting (Figure 46A). No significant differences were observed in seed number per silique, inflorescence height and rosette fresh mass 10 weeks after growing in short day conditions (Figure 46B, C and D).

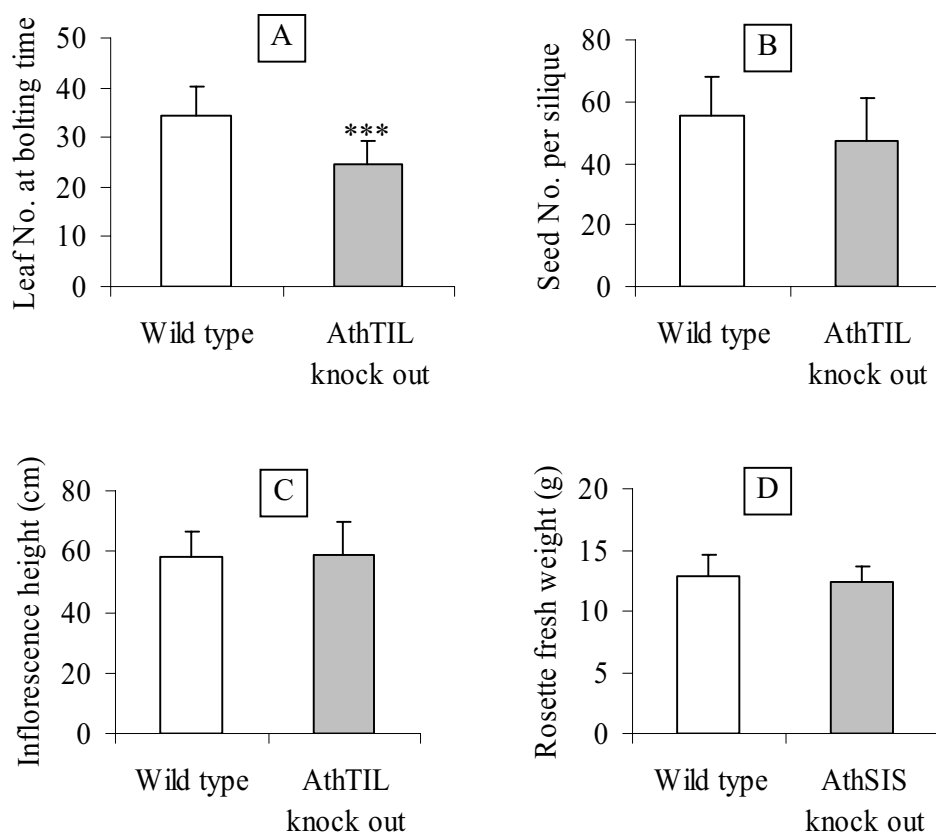


Figure 46. Morphology of AthTIL knock out line and wild type. Leaf number at bolting time (A), seed number (B), inflorescence height (C) and rosette fresh weight. Plants were cultivated in soil and short day conditions (8 h light, 16 h dark, 20° C). Bars indicate means \pm SD (n= 12).

3.4.9.3 Performance of AthTIL knock out lines under stress

The effect of different kinds of stresses like salt stress, osmotic stress, cold stress and heat stress on root growth of *A. thaliana* wild type and AthTIL knock out line were tested. To apply NaCl and PEG at similar osmotic pressure, the osmotic pressure of both PEG and NaCl at different concentrations were determined, and regression between NaCl and osmotic pressure was determined (Figure 47A). Using osmotic pressure of PEG in different concentration (Figure 47B) and regression model, equilibrium osmotic pressure between PEG (%) and NaCl (mM) was calculated (Figure 47C).

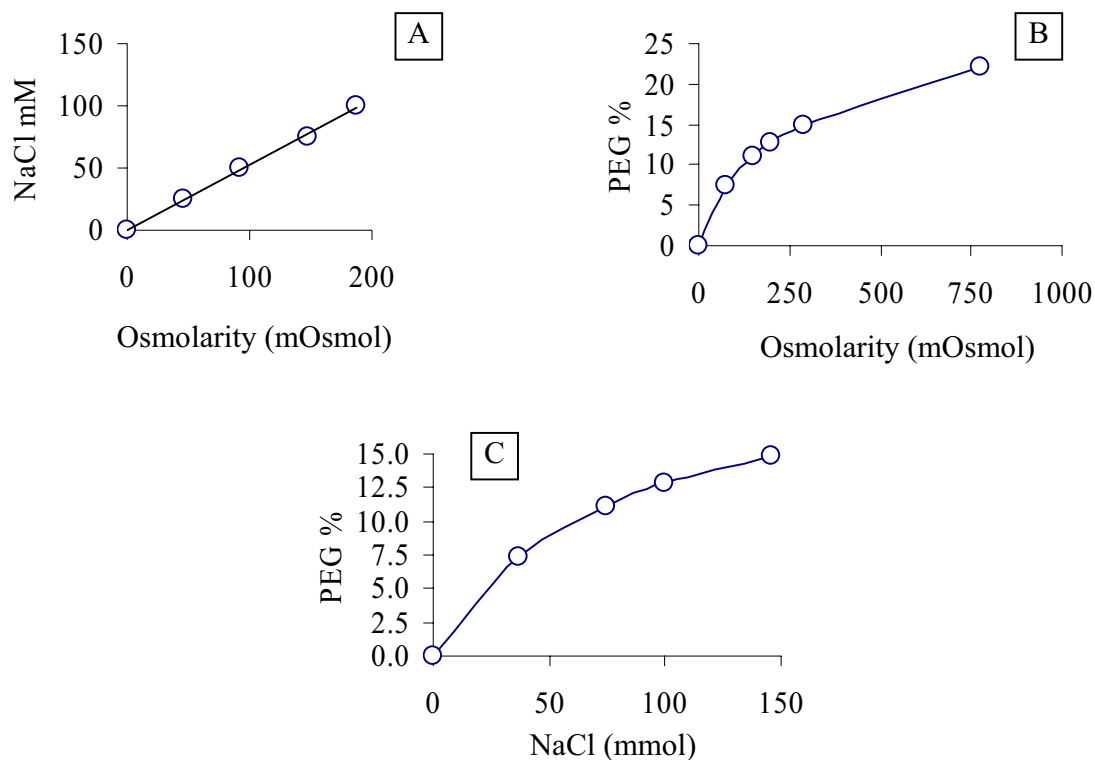


Figure 47. Calculation of equilibrium osmotic pressure induced by different concentration of NaCl and PEG. Osmotic pressure of NaCl in different concentration (A) Osmotic pressure of PEG in different concentration (B) and equilibrium line between PEG (%) and NaCl (mM) in that the osmotic pressure is same (C).

In the AthTIL knock out line (At5g58070.1 - Salk_136775) root length reduction under 100 mM NaCl was significantly higher than in the wild type. No significant difference was observed in 12.5 % PEG between AthTIL knock out line and wild type (Figure 48).

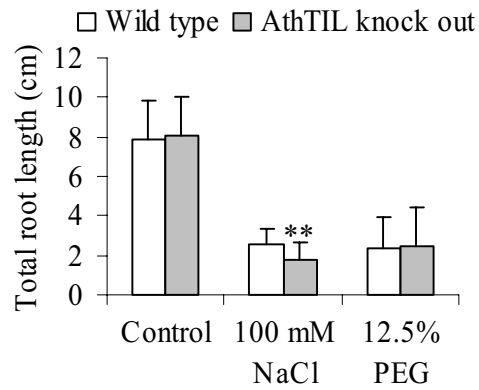


Figure 48. Root lengths of *A. thaliana* wild type and AthTIL knock out lines under different stress conditions (control, 100 mM NaCl and 12.5% PEG). Bars indicate means \pm SD (n= 24).

Also no significant differences between AthTIL knock out lines and wild types were observed at different temperatures (Figure 49).

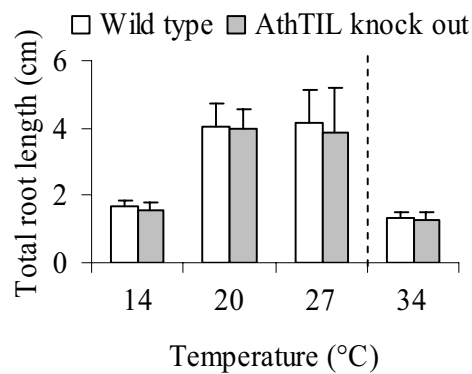


Figure 49. Root length comparisons between AthTIL knock out lines and wild types at different temperature (14, 20 and 27°C) after one week. One week after treating at 14°C, the temperature was switched to 34°C and the additive root growth has been reported. Bars indicate means \pm SD (n= 24).

3.5 Characterization of salt induced serine rich proteins PeuSIS and PcaSIS

3.5.1 Identification and nomination of SIS

An EST (EMBL, AJ770289), encoding a gene of unknown function was over expressed in salt shock microarray experiment (Brinker and Polle, 2005). This gene was called SIS because it was a Salt-Induced Serine rich protein according to the results of expression analysis and amino acid frequency of the translated full-length cDNA clone of the related gene in *P. euphratica* (see below).

3.5.2 Expression analysis

3.5.2.1 Expression changes induced by salt shock

The results of the microarray experiment (Brinker and Polle, 2005) were confirmed by quantitative real time PCR (see 2.4.2.3.2). The transcription levels of PeuSIS 3, 6, 12 and 24 hours after salt shock (150 mM) were determined in comparison with controls in leaves and roots of *P. euphratica*. Leaf PeuSIS was up-regulated 6 hours after salt shock (150 mM) and declined afterwards. In roots, PeuSIS transcripts were up-regulated at all time points.

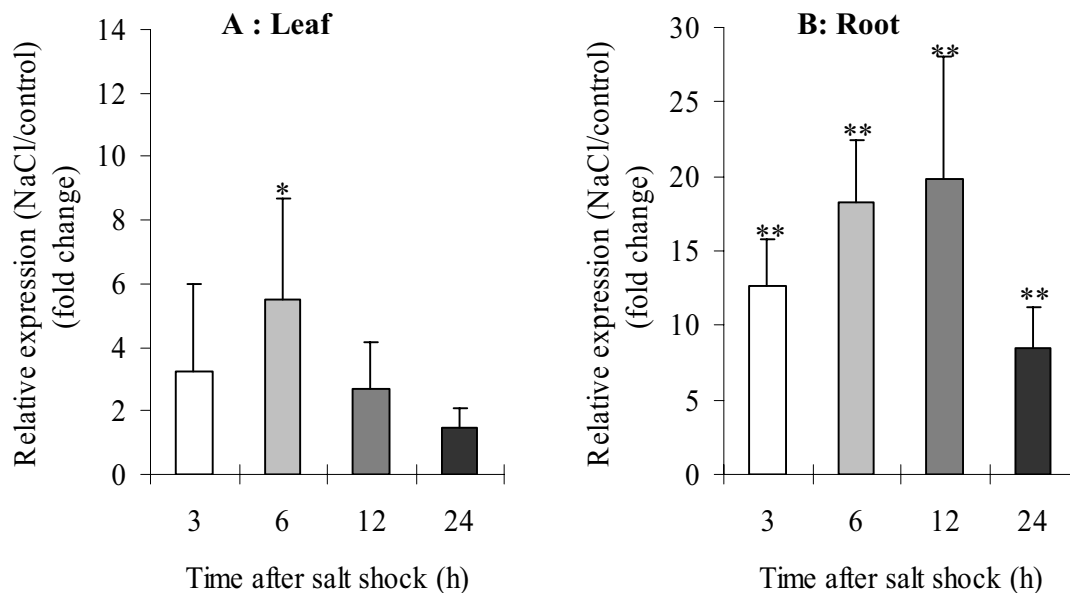


Figure 50. Relative expression (fold change) of PeuSIS in leaves (A) and roots (B) of *P. euphratica* relative to non treated plants after 3, 6, 12 and 24 hours of adding 150 mM NaCl. Stars show significant difference to non-treated plants. Data were normalized based on actin gene expression as house keeping gene. Bars indicate means \pm SE (n= 4).

Also the expression of *PeuSIS* in leaves was compared with its expression in roots in this salt shock experiment. No significant differences were detected between amount of *PeuSIS* transcripts in leaves and roots (Figure 51).

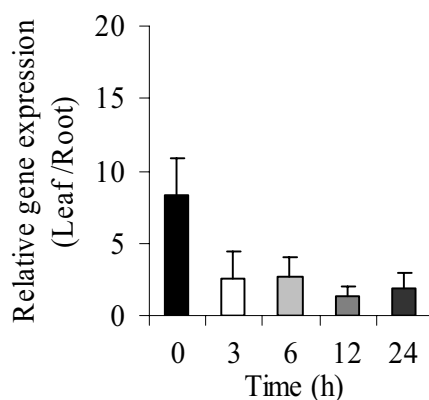


Figure 51. Relative transcript abundance of *PeuSIS* (leaf /root) before (0) and after 3, 6, 12 and 24 hours of salt stress with 150 mM NaCl in *P. euphratica*. Data were normalized based on actin gene expression as house keeping gene. Bars indicate means \pm SE (n= 4).

3.5.2.2 Expression changes induced by salt adaptation

To find out whether SISs play a role in long term salt adaptation, hydro-cultures of *P. euphratica* and *P. x canescens* were supplemented with 25 mM NaCl for two weeks. Then the salt concentration was increased to 100 mM for two further weeks. Real time PCR revealed that the transcript levels of both SIS genes (*PcaSIS* and *PeuSIS*) were unchanged relative to the controls after two weeks growing in 25 or 100 mM NaCl (Figure 52).

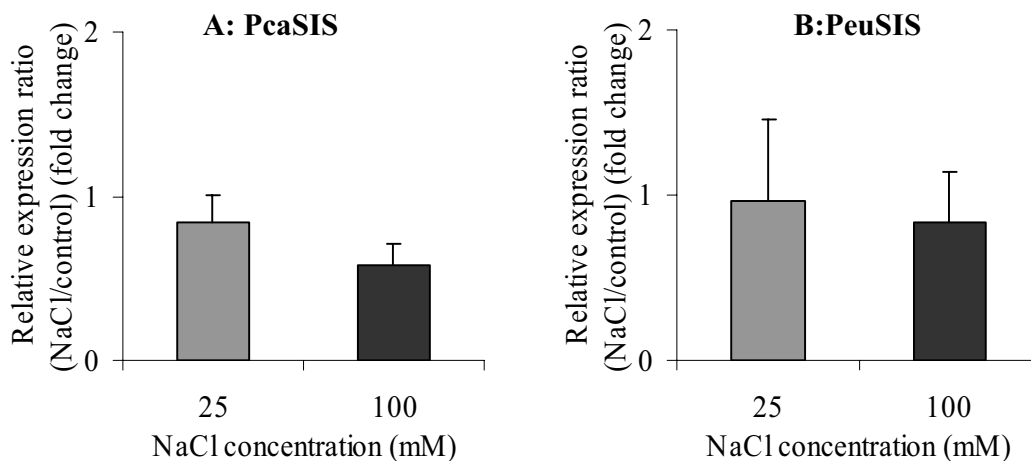


Figure 52. Relative expression of salt-induced serine rich gene of *P. x canescens* and *P. euphratica* in leaves after two weeks salt adaptation to 25 and 100 mM NaCl, respectively, compared with non-treated plants. Plants were grown for two weeks in their final NaCl concentrations and all the leaves except 10% of shoot length from apex and base were harvested. Bars indicate means \pm SE (n= 3).

The expression ratio of PeuSIS was compared with the expression ratio of PcaSIS under control and salt adapted conditions in leaves of *P. euphratica* and *P. x canescens*. Data were normalized using actin gene expression. No differences between transcript levels of PeuSIS and PcaSIS under different salt concentrations were observed (Figure 53).

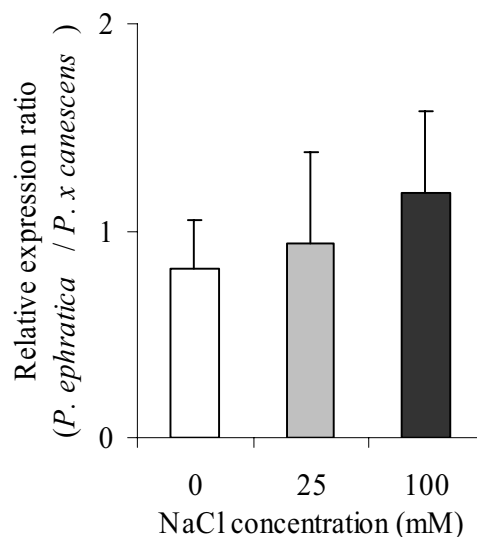


Figure 53. Relative expression ratio of *P. euphratica* SIS to *P. x canescens* SIS in leaves under different NaCl concentrations. Plants were grown for two weeks in their final NaCl concentrations and all leaves except 10 % of shoot length from apex and base were harvested. Bars indicate means \pm SE (n= 3).

3.5.3 Gene isolation and sequencing

For isolating *PeuSIS* from *P. euphratica*, the presence of sequences corresponding to the EST was assessed in *P. trichocarpa* by running blast search on the JGI server against *P. trichocarpa* genome. All together one hit for AJ770289 (Salt induced serine rich EST) with 98.68% located on chromosome VI (JGI protein ID: 560836) was found (Figure 54). Cloning primers were designed in UTR regions of hit gene of *P. trichocarpa* (see 2.4.6). The primers contained BamHI as 5' extension to further cloning in pPCV702 containing 35S promoter for over- expression analysis.

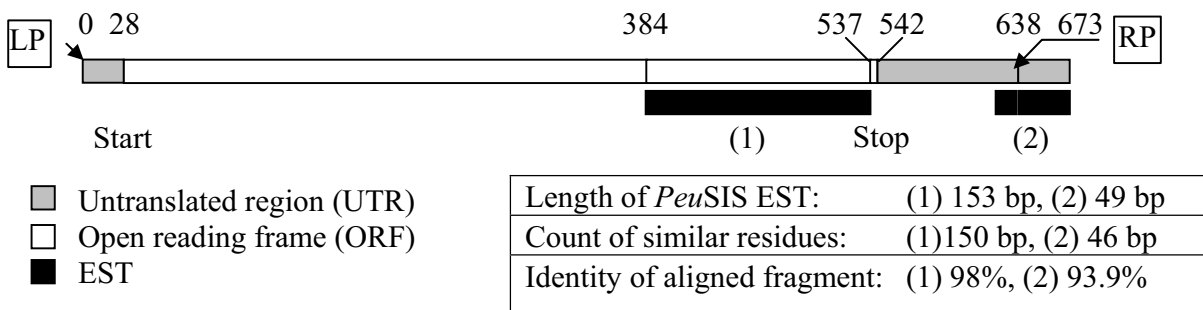


Figure 54. Alignment of *P. euphratica* SIS EST (*PeuSIS*-EST) and its homolog in the coding sequence of *P. trichocarpa*. The location of the EST in template (*PtrSIS* CDS) and cloning primers in untranslated region (UTR) has been shown schematically and the similarity of matched fragments is reported.

Both *PeuSIS* and *PcaSIS* were amplified with these primers (*TrUnk*-I-LP & RP) (App. 7.12) from cDNA. With respect to the product size of *P. trichocarpa* cDNA of *PtrSIS*, fragments with 638 bp were expected and performing PCR fulfilled this expectation (Figure 55). All fragments were sequenced and cloned in pGEM T-vector.

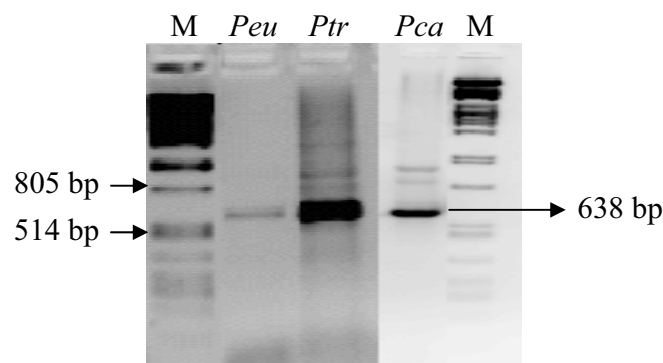


Figure 55. PCR products of full length coding sequence of salt induced serine rich protein (SIS) in *P. euphratica*, *P. trichocarpa* and *P. x canescens*. Primers: (*TrUnk*-I-LP & RP) (App. 7.12). M: λ Pst marker.

3.5.4 In silico analysis of salt induced serine rich proteins

The open reading frame of PeuSIS contains 474 bp, with GC content of 45.6% (44.6% PcaSIS, 44.9% PtrSIS and 44.9% in AthSIS) and predicted to encode a polypeptide of 158 amino acids with theoretical isoelectric point (pI) of 5.30 and a molecular weight of 17.16 kDa.

3.5.4.1 Amino acid distribution histogram

Amino acid composition of PeuSIS, PcaSIS, PtrSIS and AthSIS showed similar profiles (Figure 56) and serine content was obviously high.

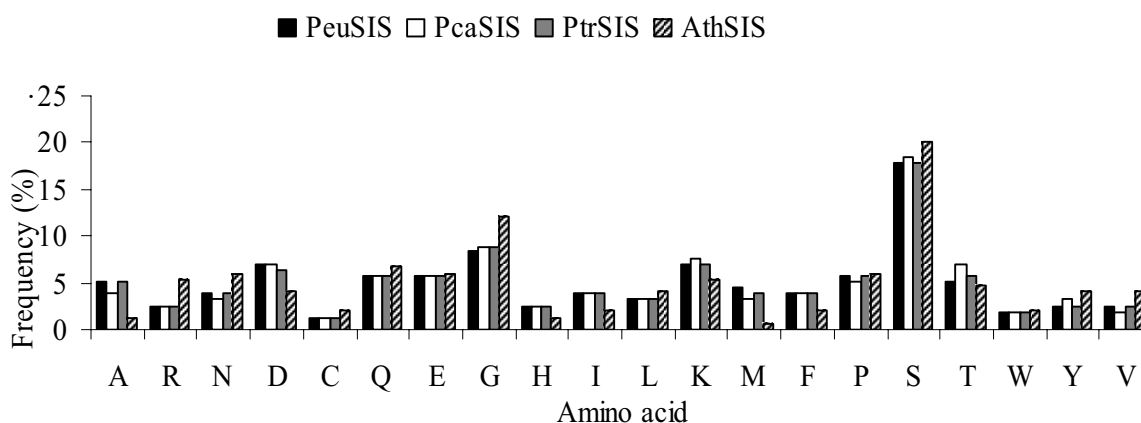


Figure 56. Amino acid composition of PeuSIS, PcaSIS, PtrSIS and AthSIS. Different amino acids have been demonstrated by IUPAC one code system (App. 7.27).

Also comparison of amino acid profile of PeuSIS and total amino acids of *A. thaliana* (derived from Banerjee *et al.*, 2006) revealed that the frequency of serine is obviously (17.7% versus 7%) higher than in amino acids of *A. thaliana* (Figure 57).

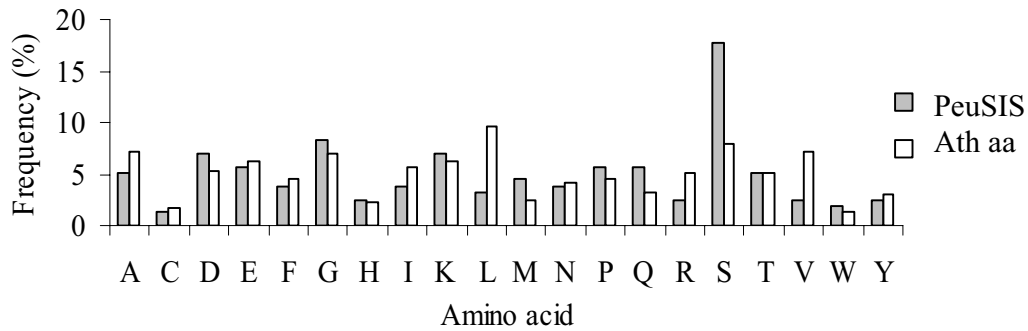


Figure 57. Amino acid composition of PeuSIS in comparison with the amino acid composition pattern of *A. thaliana* proteins. Different amino acids have been demonstrated by IUPAC one code system (App. 7.27).

Multiple alignments of two cloned genes (PeuSIS and PcaSIS) and four other top hit genes (PtrSIS, VviSIS, AthSIS and MtrSIS), demonstrate the presence of conserved regions, especially from 155 to 163 aa and from 196 to 207 aa (Figure 58). Similarity and identity of sequences were determined using pair-wise comparisons (Table 11). PeuSIS has 98% similarity and 98% identity with PtrSIS, 94% similarity and 94% identity with PcaSIS and 52% similarity and 63% identity with AthSIS (Table 11).

```

                *           20           *           40
PtrSIS : ME-G-KKQTGS--SS--SS-FTSDLF-----GS-----K : 22
PeuSIS : ME-G-KKQTGS--SS--SS-FTSDLF-----GS-----K : 22
PcaSIS : ME-G-KKQTGS--SS--SS-FTSDLF-----GS-----K : 22
VviSIS : ME-G-KKRAGS--SS--SSSEATDLF-----GS-----K : 23
AthSIS : ME-GRKKKASS--SSPCSSSSLTSELF-----GS-----R : 27
MtrSIS : MEVGGAE--GSRCSHHHKRRLHLKMYWIPGGGGEFCVERWQRK : 42

                *           60           *           80
PtrSIS : EN-S-----PSS---MGIFGS-IFAPA-SP--K-V--LG--- : 45
PeuSIS : EN-S-----PSS---MGIFGS-IFAPA-SP--K-V--LG--- : 45
PcaSIS : EY-S-----SSS---TGIFGS-IFAPA-SP--K-V--LG--- : 45
VviSIS : ES-S---YPS-PSS---TGIFAS-IFSTS-S---K-V--LG--- : 48
AthSIS : ENPS-----SPSS---SGILGS-IFPEP-S---K-V--LG--- : 51
MtrSIS : ETLKVRVFEDPSTPTFFQGKYGDGV--EAHNPTIKLVNDLGDNV : 84

                *           100           *           120           *
PtrSIS : -RESLRFEVAEKKQDS-ADDAWNTKSGTEASDLT SKMNEGESQS : 87
PeuSIS : -RESLRFEVAEKKQDS-ADDAWNTKSGIPASDLT SKMNEDESQS : 87
PcaSIS : -RESLRFEVDEKKQDS-ADDAWNTKSGTPTS DLT SKMNEGESQS : 87
VviSIS : -RESLRPDLTKKKQDS-GNEVWNAKPGTTENAL--QQSEGESQS : 88
AthSIS : -RESVR-----QETVTGGCWNKTSKTGGNV--DRNR-EQQE : 84
MtrSIS : FR--VRVSIPEP-----MPLNDI-SKIHENQSHI : 110

                140           *           160           *
PtrSIS : VPKND--MSSIYQE-QRVQPCHLSSSIYYGGQDI-YHHP-QTAH : 126
PeuSIS : VPKND--MSSIYQE-QRVQPCHLSSSIYYGGQDI-YHHP-QTAH : 126
PcaSIS : IPKND--MSSIYQE-QRVQPCHLSSSIYYGGQDI-YHHP-QTAH : 126
VviSIS : ISNRD--TGSEYQE-QRVQPCHLSSSIYYGGQDI-YFHP-QNSQ : 127
AthSIS : --NH---GSGYQQDQRVQPCHLSSSIYYGGEDV-YFQP-QNS- : 119
MtrSIS : --NKVKVTSSEIFQD-QIIGPCNLSSSIYYGGQDILY--PAQNAR : 149

                180           *           200           *           220
PtrSIS : -TSSINP-MFKK-D-GPE-DDTGSASRGNWW---Q--GMT--C : 157
PeuSIS : -TSSMNP-MFKK-D-GPE-DDTGSASRGNWW---Q--GMT--C : 157
PcaSIS : -TSSKNP-MFKK-D-GPE-DDTGSASRGNWW---Q--GMT--C : 157
VviSIS : -SSGM-PSMLKK-DSG-E-DDTGSASRGNWW---Q--G-SLYY : 159
AthSIS : -TS--N-STNKK-DGG-E-DDSGSASRGNWW---Q--G-SLYY : 149
MtrSIS : LTS-----LKKYDW--ENDDSGVASRGDWWKDISQNLG--DA : 182

```

Figure 58. Multiple alignments of SIS amino acid sequences of *P. trichocarpa* (PtrSIS), *P. euphratica* (PeuSIS), *P. x canescens* (PcaSIS), *Vitis vinifera* (VviSIS), *A. thaliana* (AthSIS) and *Medicago truncatula* (MtrSIS).

Table 11. Pair-wise comparison of four SISs (*P. trichocarpa*, *P. euphratica*, *P. x canescens* and *A. thaliana*). Matrix diameter shows number of amino acid. In each cell first row shows identical residues, the second row shows similar residues and the third row shows residues lined up in gap. Each number is expressed as absolute number of amino acid and as percentage on the different sides of the matrix diagonal.

	PtrSIS	PeuSIS	PcaSIS	VviSIS	AthSIS	MtrSIS
PtrSIS	157	98% 98% 0%	95% 96% 0%	64% 77% 8%	52% 63% 18%	33% 44% 43%
PeuSIS	154 155 0	157	94% 94% 0%	64% 76% 8%	52% 63% 18%	33% 45% 43%
PcaSIS	150 151 0	148 149 0	157	65% 76% 8%	51% 63% 18%	32% 43% 43%
VviSIS	107 128 14	106 126 14	108 126 14	159	56% 67% 15%	28% 42% 40%
AthSIS	89 108 32	89 108 32	87 107 32	94 113 26	149	27% 36% 43%
MtrSIS	72 96 93	72 98 93	71 95 93	62 91 87	57 78 91	182

3.5.5 Phylogenic studies of salt induced serine rich like proteins

Translated amino acids of SIS like genes of six plants were subjected to phylogenetic analysis. Three SIS like proteins of poplar species were clustered in one clade with least genetic distance. Within these SIS genes, PtrSIS, PeuSIS and PcaSIS are from poplar trees and clustered in one group. MtrSIS because of lower identity than other amino acids was selected as out-group.

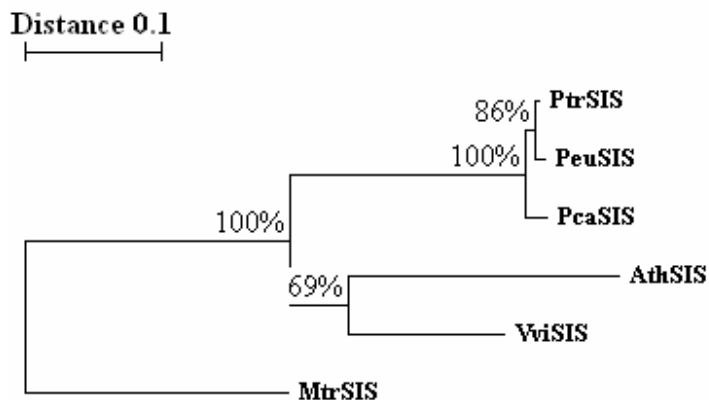


Figure 59. Neighbour-joining tree of nucleotide acid of salt induced serine rich like proteins (SISs). Bootstrap values less than 50 % were removed. **PtrSIS** : *Populus trichocarpa*; **PeuSIS** : *Populus euphratica*; **PcaSIS** : *Populus x canescens*; **MtrSIS**, *Medicago truncatula*; **AthSIS** : *Arabidopsis thaliana*; **VviSIS** : *Vitis vinifera*.

3.5.6 Topology prediction

Topology prediction of PeuSIS, PtrSIS, PcaSIS using TopPred method that combines hydrophobicity analysis and positive-inside rule, detected a segment that putatively is able to penetrate membrane (Figure 60) (Wallin and von Heijne, 1998). It is called putative because the hydrophobicity profile of this segment does not reach to upper cutoff level (hydrophobicity value 1) (Figure 61). The extracellular C tail of PcaSIS has one positively charged residue more than that of PeuSIS and PtrSIS but this difference did not change the predicted orientation of this protein. No trans-membrane segment was detected in AthSIS (Figure 60).

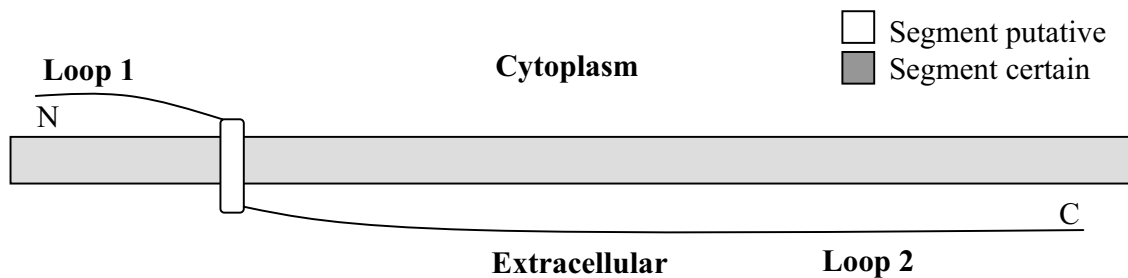
3.5.7 Subcellular localization

Prediction of subcellular localization for PeuSIS was performed using TargetP 1.1 server (<http://www.cbs.dtu.dk/services/TargetP/>) with no cut-off setting and selecting 'Plant' option (Emanuelsson *et al.*, 2000). A chloroplast target peptide was predicted with reliability class 3 (out of 5; 1 indicates the strongest prediction) in sequence of PeuSIS. If we put the results of subcellular localization using TargetP and hydrophobicity profile of investigated SIS proteins, its unlikely that this protein be localized in plasma membrane.

3.5.8 Investigating phosphorylation sites

Sequence analysis of PeuSIS using the NetPhosK 1.0 (<http://www.cbs.dtu.dk/services/NetPhosK/>) and NetPhos 2.0 server (<http://www.cbs.dtu.dk/services/NetPhos/>), identified several putative phosphorylation sites by protein kinase C (PKC) (25% of phosphorylation sites were PKC with highest score) which suggested PeuSIS activity may regulated by PKC. PKC is induced by many extracellular signals. It was first described as calcium activated and phospholipid-dependent serine/threonine protein kinase, and plays a critical role in many signal-transducing pathways in the cell (Toker, 1998).

A: Topology of PeuSIS, PtrSIS and PcaSIS



B: Loop length and number of positively charged residues

	Loop 1		Loop 2	
	Length	KR	Length	KR
PeuSIS	25	3	111	12
PtrSIS	25	3	111	12
PcaSIS	25	3	111	13
AthSIS	No trans-membrane segment was predicted			

Figure 60. Topology prediction of SIS proteins using TopPred. Demonstrating the topology of PeuSIS, PtrSIS and PcaSIS (A). Loop length and number of positively charged residues (B). One putative transmembrane segment was detected in PeuSIS, PtrSIS and PcaSIS but no transmembrane segment was predicted in AthSIS (see also Figure 61). KR= number of lysine and arginine.

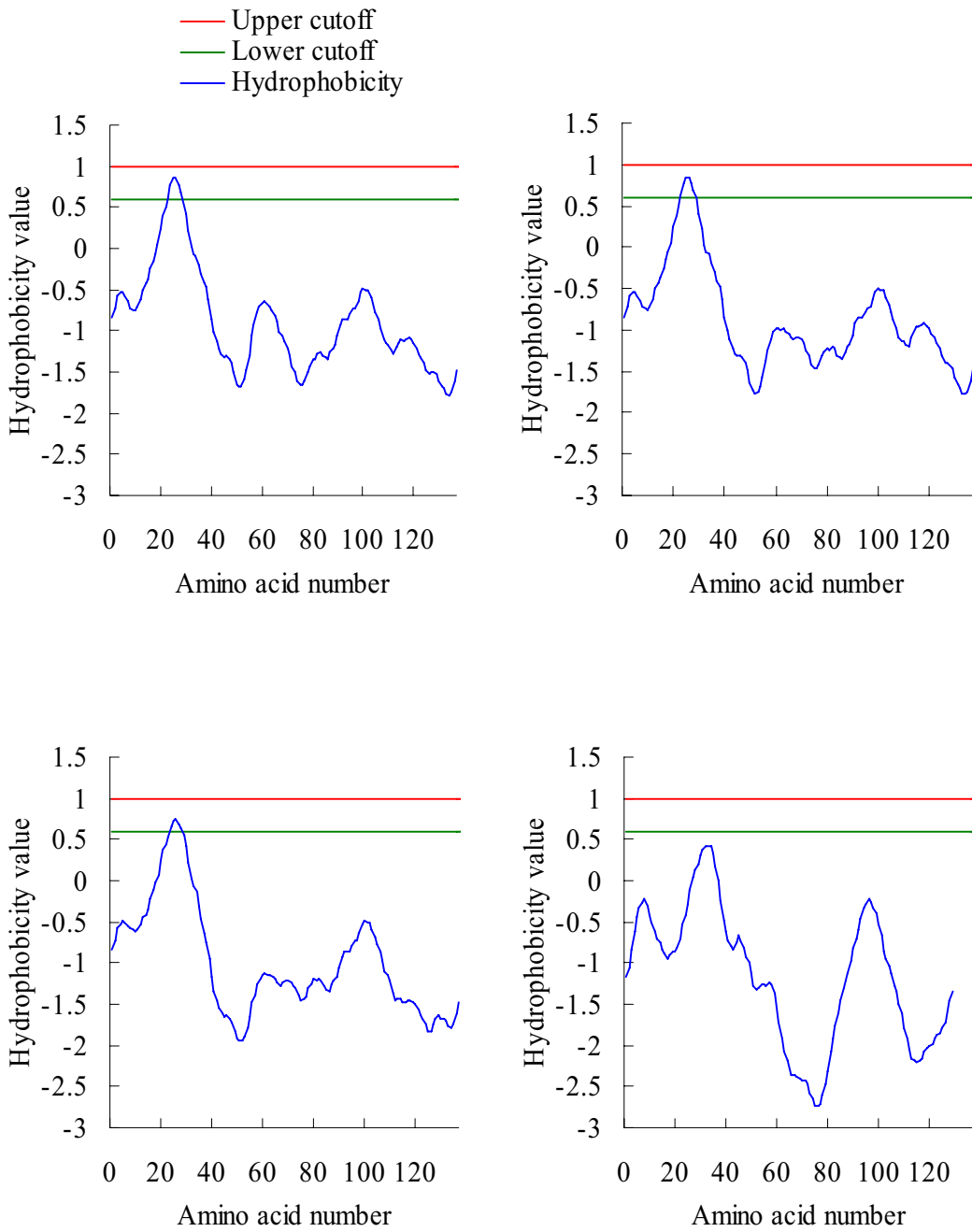


Figure 61. Hydrophobicity plot of SIS proteins based on Kyte-Doolittle scale. Hydrophobicity of PeuSIS, PtrSIS and PcaSIS only exceed from the lower cutoff (hydrophobicity 0.6) and does not reach to upper cutoff (hydrophobicity 1). AthSIS hydrophobicity profile even does not reach to lower cutoff.

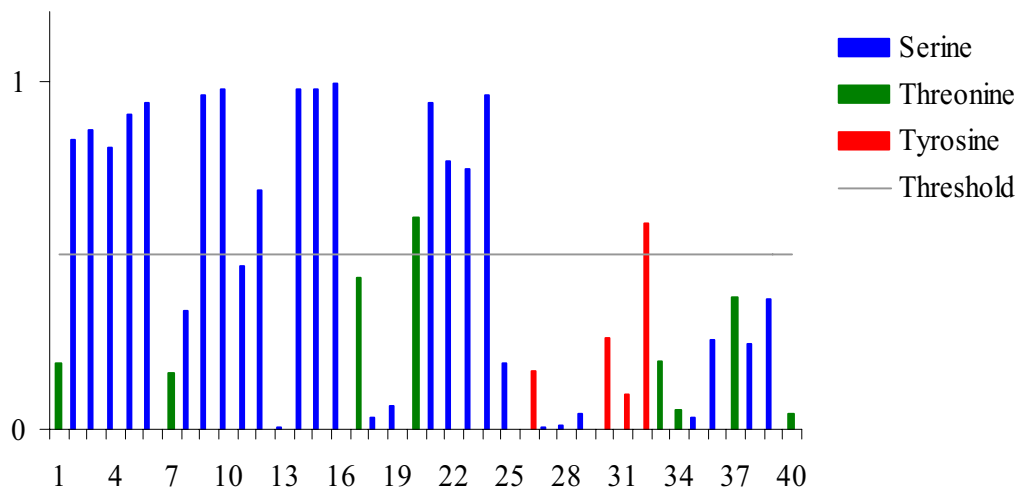


Figure 62. Generic phosphorylation sites of PeuSIS predicted by NetPhos 2.0 server provided for phosphorylation sites in eukaryotic proteins

3.5.9 Promoter analysis of salt induced serine rich protein

To analyze putative promoter elements, 627 bp upstream regions of the PtrSIS and AthSIS to avoid entering the coding region of adjacent gene, were searched against the PLACE database (a database of plant cis-acting regulatory DNA elements) and the results were compared (Table 12). Pairwise alignment showed 48% identity in this region. All together 43 elements only in *P. trichocarpa* and 23 regulatory elements only in *A. thaliana* were detected and 29 element were common in both species. Both PtrSIS and AthSIS are rich of motives that are involved in regulation of genes related with seed storage, light signalling, ABA and dehydration signalling. Also one salt induced motif (GT1GMSCAM4, GAAAAA) is present in upstream sequence of both PtrSIS and AthSIS. In PtrSIS promoter region, many light induced elements are present that are lacking in promoter region of AthSIS.

Table 12 Cis regulatory elements detected in 627 bp upstream region of PtrTIL and AthTIL. The frequency of regulatory elements in both (+) and (-) strands have been shown. Common elements between *P. trichocarpa* and *A. thaliana* with high frequency are sorted at the beginning of table, and then the elements that found just in *A. thaliana* and *P. trichocarpa* are sorted respectively. Y [TC] pYrimidine; R [AG] puRine; W [AT] Weak; S [GC] Strong; K [TG] Keto; M [AC] aromatic; B [TGC] not A; D [ATG] not C; H [ATC] not G; V [AGC] not T; N [ATGC]; Myb for avian MYeloBlastosis virus; MYC for avian myelocytomatosis viral oncogene.

Element	Sequence	Description	No. of elements	
			<i>Ptr</i>	<i>Ath</i>
NODCON2GM	CTCTT	Root nodule infected cell promoter	12-	2-
DOFCOREZM	AAAG	Core site required for binding of DOF (DNA binding with one finger) proteins	3-6+	4-4+
ARR1AT	NGATT	ARR1-binding; transcriptional activator; in promoter of rice non-symbiotic haemoglobin-2 gene	3-5+	2-2+
POLLEN1LELAT52	AGAAA	Regulatory element of Lat52 a heat stable protein in seed fertilizing and development	4-4+	1+
CACTFTPPCA1	YACT	mesophyll expression module1 found in phosphoenolpyruvate carboxylase (ppcA1) of C4 dicots.	4-3+	6-3+
GT1CONSENSUS	GRWAAW	Light regulated genes	2-5+	3-5+
EBOXBNNAPA	CANNTG	Storage protein promoter, ABA response	3-3+	3-3+
CAATBOX1	CAAT	LegA gene, seed storage	4-1+	5-5+
GATABOX	GATA	Found in promoter of Petunia chlorophyll a/b binding protein	2-3+	3-4+
POLASIG1	AATAAA	Putative polyadenylation signals	2-3+	2+
ACGTATERD1	ACGT	Light regulation	3-3+	2-2+
GTGANTG10	GTGA	Found in the promoter of pectate lyase like gene; pollen	2-2+	2-2+
CBFHV	RYCGAC	dehydration-responsive element	1-3+	1+
PRECONSCRHSP70A	SCGAYNRNNN NNNNNNNNNN NNHD	Plastid response element; chlorophyll	4+	1+
GT1GMSCAM4	GAAAAA	Pathogen- and salt-induced	1-2+	2+
IBOXCORE	GATAA	Conserved sequence upstream of light induced genes	1-2+	1-1+
TATABOX5	TTATTT	TATA box found in the 5'upstream region of glutamine synthetase gene;	3-	1-
ROOTMOTIFTAPOX1	ATATT	Motif found in root elongation protein (Rold)	1-1+	3-4+

MARTBOX	TTWTWTTWTT	Scaffold attachment region	2-	2-1+
MYB1AT	WAACCA	Dehydration and ABA responsive in <i>A. thaliana</i> MYB gene controlling cell cycle	2-	1-1+
LTRECOREATCOR15	CCGAC	Low temperature responsive	2+	1+
MYBST1	GGATA	Dehydration and ABA responsive in <i>A. thaliana</i> MYB gene controlling cell cycle	1-1+	1-
DRECRTCOREAT	RCCGAC	Dehydration-responsive element	2+	1+
SEF4MOTIFGM7S	RTTTTTR	Seed specific transcript binding	1-	2-
WBOXATNPR1	TTGAC	Salicylic acid induced found in pathogenesis related genes	1+	2-
REALPHALGLHCB21	AACCAA	Required for phytochrome regulation, etiolation signalling	1-	1-
DRE2COREZMRAB17	ACCGAC	ABA; drought response	1+	1+
CGACGOSAMY3	CGACG	Seed storage, rice amylase genes	1+	1+
SREATMSD	TTATCC	sugar-repressive element; growth regulation; dormancy	1+	1+
RAV1AAT	CAACA	Transcription factor binding consensus		3-1+
ACGTABOX	TACGTA	Sugar repression		2-2+
BIHD1OS	TGTC A	Binding site of shoot apical meristem regulators		2-1+
CARGCW8GAT	CWWWWWWW WG	Flowering; low temperature induced		1-1+
ANAERO1CONSENSUS	AAACAAA	In promoters of anaerobic genes involved in the fermentative pathway		1+
POLASIG3	AATAAT	Polyadenylation		1+
PREATPRODH	ACTCAT	Found in promoter region of proline dehydrogenase (ProDH) gene		1+
NTBBF1ARROLB	ACTTTA	Dof binding site of rol gene; auxin induced		1-
S1FBOXSORPS1L21	ATGGTA	Down-regulating genes encoding the plastid ribosomal protein S1 and L21		1+
MYCATERD1	CATGTG	Early responsive to dehydration		1-
PYRIMIDINEBOXOSRAM Y1A	CCTTTT	GA responsive in alpha amylase gene; sugar repressive		1+
5659BOXLELAT5659	GAAWTTGTGA	Pollen		1+
EECCRCAH1	GANTTNC	Low CO ₂		1+
MYB26PS	GTTAGGTT	In promoter of phenylpropanoid biosynthetic genes		1+
GT1MOTIFPSRBCS	KWGTGRWAA WRW	Light induced		1-
MYBPLANT	MACCWAMC	phenylpropanoid and lignin		1-

		biosynthesis		
TAAAGSTKST1	TAAAG	In promoters of guard cell specific gene encodes a K ⁺ influx channel		1+
NAPINMOTIFBN	TACACAT	Seed; storage protein; napin		1+
TATABOX2	TATAAAT	TATA; legA; phaseolin;		1+
ANAERO3CONSENSUS	TCATCAC	In promoters of anaerobic genes involved in the fermentative pathway		1-
ASF1MOTIFCAMV	TGACG	Transcriptional activation of many genes; auxin; salicylic acid; light induced		1-
-300ELEMENT	TGHAAARK	Seed; storage protein; hordein		1-
MYCATRD22	CACATG	Early responsive to dehydration		1+
CACGTGMOTIF	CACGTG	PhyA (Phytochrome)-responsive promoters	2-2+	
ABRELATERD1	ACGTG	Early responsive to dehydration; etiolation induced	2-2+	
CURECORECR	GTAC	Copper and oxygen-deficiency response element	2-2+	
CCAATBOX1	CCAAT	Heat shock element	2-1+	
ABRERATCAL	MACGYGB	ABA responsive present in upstream region of calcium responsive upregulated genes	1-2+	
SEF3MOTIFGM	AACCCA	Seed specific transcript binding	2-	
POLASIG2	AATTAAG	Poly A signal found in alpha amylase gene	2+	
DPBFCOREDCDC3	ACACNNG	ABA-responsive and embryo-specification elements	1-1+	
SORLIP1AT	GCCAC	Found in light induced promoters	2-	
P1BS	GNATATNC	Present in phosphate starvation responsive genes	1-1+	
CRTDREHVCBF2	GTCGAC	Low temperature induced	1-1+	
RHERPATEXPA7	KCACGW	Root Hair Cell-Specific cis-Element	1-1+	
INRNTPSADB	YTCANTYY	Light responsive element	1-1+	
MYBCORE	CNGTTR	Dehydration induced	1+	
BOXIIPCCHS	ACGTGGC	Light responsive element	1+	
ACGTABREMOTIFA2OSEM	ACGTGKC	ABA responsive	1+	
ABREOSRAB21	ACGTSSSC	Regulation of abscisic acid-induced transcription	1+	
TBOXATGAPB	ACTTTG	Light activated gene encodes the B subunit of chloroplast glyceraldehyde-3-phosphate dehydrogenase	1+	
BOXIINTPATPB	ATAGAA	Required for expression of plastid genes	1+	

ERELEE4	AWTTCAA	Early responsive to dehydration; fruit	1-	
CIACADIANLELHC	CAANNNNATC	Promoter element of Light harvest centre gene	1-	
IRO2OS	CACGTGG	Fe deficiency induced	1+	
EMBP1TAEM	CACGTGGC	ABA signalling	1+	
HEXAMERATH4	CCGTCCG	Histon promoter; meristem	1-	
MYBPZM	CCWACC	See MYB1AT, gene specifies red pigmentation of kernel pericarp	1-	
MYBATRD22	CTAACCA	Dehydration-responsive gene; ABA induction	1-	
SURECOREATSULTR11	GAGAC	Sulfur-responsive element (SURE)	1-	
SORLIP5AT	GAGTGAG	Over-represented in light-induced genes; cotyledon-specific and root-specific genes	1+	
IBOX	GATAAG	Conserved sequence upstream of light induced genes	1+	
IBOXCORENT	GATAAGR	Conserved sequence upstream of light induced genes	1+	
SORLIP2AT	GGGCC	Found in light induced promoters	1+	
GBOXLERBCS	MCACGTGGC	Light regulated genes	1+	
TATCCAOSAMY	TATCCA	α -amylase; MYB proteins; gibberellin (GA); sugar starvation;	1+	
TATCCACHVAL21	TATCCAC	Gibberellin responsive element	1+	
TATCCAYMOTIFOSRAM Y3D	TATCCAY	Found in alpha amylase genes; sugar repression	1+	
-10PEHVPSBD	TATTCT	Chloroplast gene expression	1-	
WBOXNTERF3	TGACY	Translation release factor	1+	
SITEIIATCYTC	TGGGCY	Site II element found in the promoter regions of cytochrome genes in Arabidopsis	1+	
ELRECOREPCR1	TTGACC	Elicitor Responsive Element; pathogen- and wound-induced	1+	
ABREATCONSENSUS	YACGTGGC	ABA responsive element	1+	
MYBCOREATCYCB1	AACGG	Dehydration and ABA responsive in <i>A. thaliana</i> MYB gene controlling cell cycle	1+	
RBCSCONSENSUS	AATCCAA	Rubisco consensus	1+	
RAV1BAT	CACCTG	Binding consensus sequence of a transcription factor	1-	

3.5.10 PatMatch analysis for identification of SIS protein

To find out a conserved region in PeuSIS protein, PatMatch program from TAIR tools was used. For this purpose amino acid sequence of PeuSIS was divided in to small peptides with 5 aa length and a blast search against GeneBank plant protein database was performed (Table 13). The AthSIS gene (At5g02020) was the only hit with exactly 4 identical patterns for the SIS protein of *P. euphratica*.

Table 13. PatMatch analysis of SIS protein of *P. euphratica* with 5 aa length patterns.

Sequence Name	Identification	Hit pattern
<i>Arabidopsis thaliana</i> At5g02020	SIS protein	ASRGN
		HLSSS
		IYYGG
		RVQPC

3.5.11 Loss of function analysis

3.5.11.1 Characterisation of AthSIS knock out lines

The *Arabidopsis* genome was searched to find homolog gene of PeuSIS by performing a blast with PeuSIS protein sequence using the ‘tblastn protein’ program which had been used for the in silico analysis (3.4.5). The most identical gene was At5g02020 with 57% identity in nucleotide level and 52% identity and 63% similarity in amino acid sequence. Among the available *Arabidopsis* Salk lines of At5g02020, the transgenic Salk T-DNA knockout line of At5g02020- Salk_146631 with the T-DNA insertion in the intron was ordered from the Nottingham *Arabidopsis* stock centre (NASC) (Figure 63).

```

>At5g02020
  ▽
ATGGAAGGAAGAAAGAAGAAAGCTTCGTCTTCCTCTCCTTGTT
CTTCTTCCTCGTTAACCTCTGAGCTTTTTGGTTCCAGAGAAAA
CCCTTCTTCTCCTTCCTCTTCTGGTATTCTCGGATCCATTTTT
CCTCCTCCTTCTAAGGTTTTGGGAAGAGAATCTGTGCGACAAG
AGACTGTGACTGGTGGTTGCTGGAACGAGAAAACCTCCAAGAC
TGGTGGTAATGTTGATAGAAACAGGGAACAACAGGAGAATCAT
GGTTCAGGTTATCAGCAGGATCAGAGAGTACAACCCTGTCATC
TGAGTTCTTCCATCTATTACGGTGGTCCCTGATGTTTATTTCCA
GCCTCAA AATTCCACCAGCAACTCTACGAACAAGAAAGATGGA
GGCGAAGATGATTCCGGAAGTGCCTCAAGAGGAAATTGGTGGC
AAGGGTCTCTGTATTACTAA

```

Figure 63. Coding sequence of At5g02020. The insertion site of the T-DNA has been shown by a triangle and the flanking sequence has been highlighted by grey colour.

After transferring the seedlings in soil, homozygote individuals were selected by a PCR method using a combination of left and right gene specific primers (Unknown-IX-LP and RP) (App. 7.12), and also the left border T-DNA primer and right gene specific primer (Lba1-RP) (Figure 64) as described under 2.4.2.3. No product with the LP-RP combination was observed in the Salk lines and the correct size of 1202 bp was achieved in the wild type. Running PCR with the Lba1-RP combination and the Salk line genomic DNA as template produced the expected fragment of 703 bp and no product was observed in wild type. As result the tested Salk lines 1, 2 and 3 are homozygous that means the T-DNA insertions were present in both chromosomes.

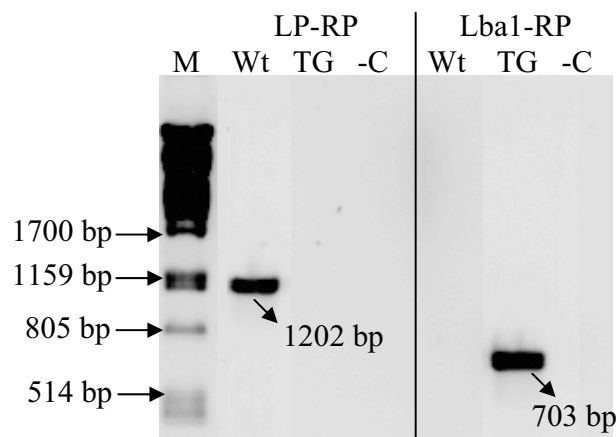


Figure 64. PCR based selection of homozygote Salk lines. One Salk line (TG), together with wild type (Wt) and negative control (-C: no DNA) were subjected to PCR with to different primer combinations (LP-RP and Lba1-RP). LP: left primer of gene of interest, RP: right primer of gene of interest, Lba1: left border primer a1 anneals on TDNA insertion and M: λ Pst marker. (For primers sequences see App. 7.12).

To ensure the location of the T-DNA, PCR products of Lba1-RP were sequenced and the flanking sequences were blasted against the *A. thaliana* genome (Figure 65).

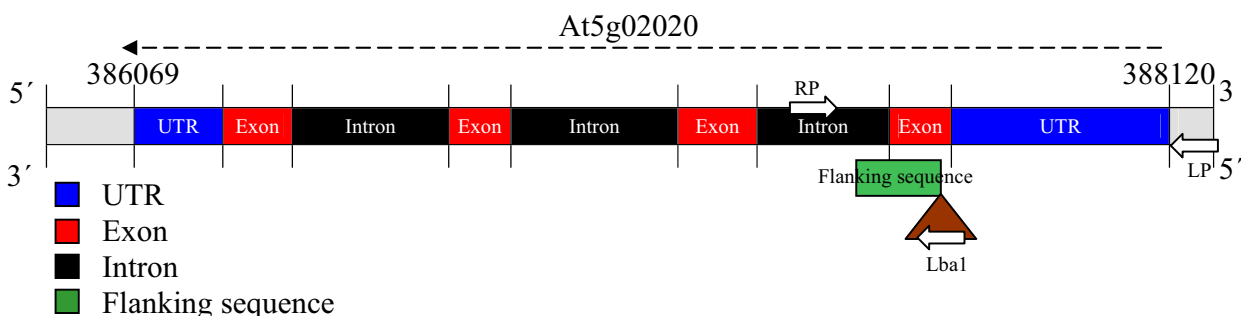


Figure 65. Location of AthTIL (At5g02020), the insert T-DNA and primers in the *Arabidopsis* genome. The Salk line Salk_146631 was used. T-DNA is indicated by a triangle. White arrows show the position of primers.

In homozygote transgenics, with the inserted T-DNA in the exon, no transcript is expected. To be sure that no transcript of AthSIS is existing in its knockout line (At5g02020.1 - Salk_146631), a PCR was run using cDNA as template and with the primer combination of LBA1 and AtUnkexpRP (see App. 7.12). As expected with using cDNA as template no product was observed and using gDNA as template a fragment of 1082 bp was obtained which has the correct size.

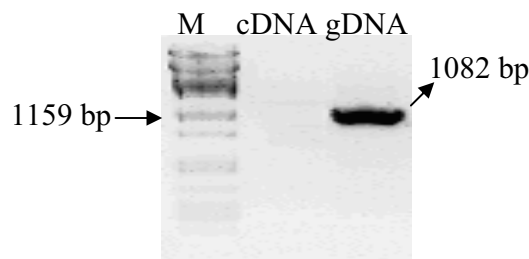


Figure 66. Evaluation of the transcript level of AthSIS in Salk line. M= λ Pst DNA ladder, cDNA= cDNA of At5g02020.1 – Salk 146631 (lipocalin knock out), gDNA= genomic DNA of At5g02020.1 – Salk 146631. Primer combination= LBA1 and AtTILexpRP (see App. 7.12).

3.5.11.2 Phenotypic analysis of AthSIS knock out lines

For investigating the phenotype of AthSIS knock-out lines, knock-out and wild type plants were grown in soil for 10 weeks (8 h light, 16 h dark, 20° C) (see 2.1). Maximum inflorescence bolting time of AthSIS knock out lines was 11 days sooner than that of wild type. At the time of inflorescence bolting, the number of leaves per rosette was counted. AthSIS knock out lines had less leaf per rosette at the time of bolting (Figure 67A). No significant differences were observed in seed number per silique, inflorescence height and rosette fresh mass 10 weeks after growing in short day conditions (Figure 67B, C and D).

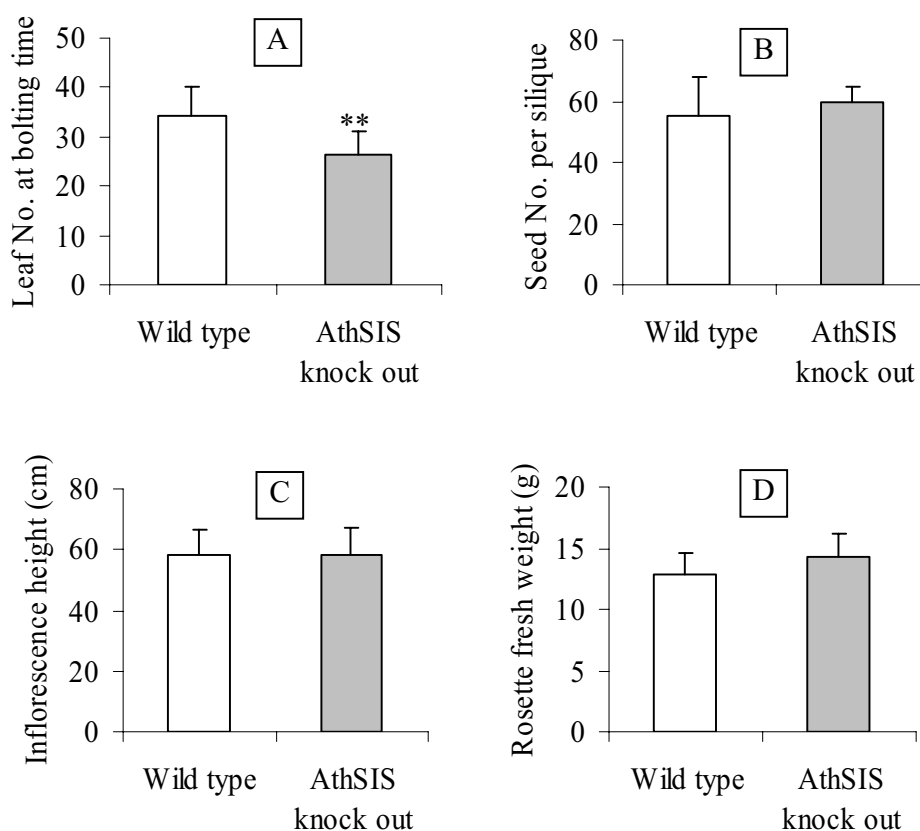


Figure 67. Morphology of AthSIS knock out line and wild type. Leaf number at bolting time (A), seed number (B), inflorescence height (C) and rosette fresh weight. Plants were cultivated in soil and short day conditions (8 h light, 16 h dark, 20° C). Bars indicate means \pm SD (n= 12).

3.5.11.3 Performance of AthSIS knock out lines under stress

The effect of different kinds of stresses like salt stress, osmotic stress, cold stress and heat stress on root growth of *A. thaliana* wild type and AthSIS knock out lines were tested. No significant differences were observed under 12.5% PEG and 100 mM NaCl between AthSIS knock out line and wild type line (Figure 68). Also no significant differences between AthSIS knock out lines and wild types were observed at different temperature (Figure 69).

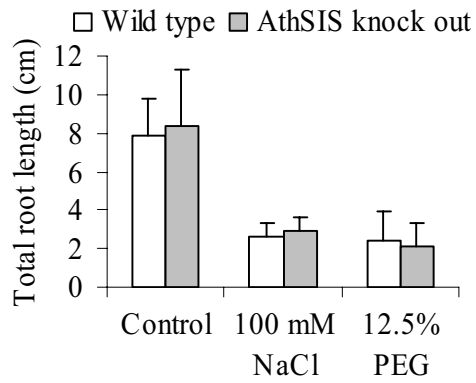


Figure 68. Root lengths of *A. thaliana* wild type and AthSIS knock out lines under different stress conditions (control, 100 mM NaCl and 12.5% PEG) Bars indicate means \pm SD (n= 24).

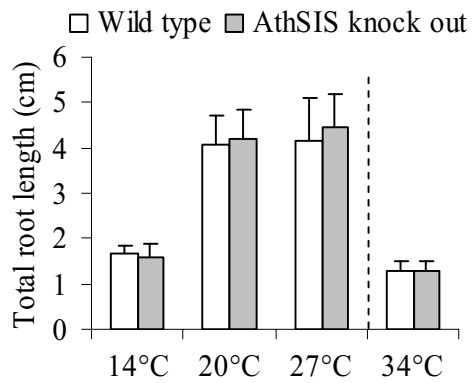


Figure 69. Root length comparisons between AthSIS knock out lines and wild types at different temperature (14, 20 and 27°C) after one week. One week after treating at 14°C, the temperature was switched to 34°C and the additive root growth has been reported. Bars indicate means \pm SD (n= 24).

4

Discussion

4.1 Ecophysiological characteristics of *P. euphratica* and *P. x canescens* during salt adaptation

4.1.1 Effect of salinity on plant performance and morphology

According to the general classification of salinity (see introduction), the experiments performed in this thesis covered none saline (control), weakly saline (25 mM), moderately saline (75 mM), strongly saline (150 mM) to very strongly saline (200 mM) conditions (U.S. Salinity Laboratory Staff classification). Salinity limits vegetative growth and fertility of all plants except some halophytes. One of the key parameters to assay vegetative activity of plants is the leaf initiation rate. This parameter is associated with shoot apical meristem activity that regulates lateral organ initiation (Miyoshi *et al.*, 2004). Leaf initiation rates vary from species to species and are also age-dependent. *P. euphratica* and *P. x canescens* of similar stem height had approximately the same leaf initiation rate (about 6 leaves per week). When both species were exposed to stepwise salt increment reductions in the performance of *P. euphratica* at 100 to 200 mM were similar to those in *P. x canescens* found at 75 mM NaCl.

Reversibility of negative effects of salt stress on *P. euphratica* was investigated after long term salt adaptation in soil. Leaf initiation rate decreased by irrigating with 150 mM and stopped within three weeks but recovered after alternative daily irrigation with none saline water and 150 mM NaCl. Plant performance of *P. euphratica* in response to gradually

increasing water deficit and recovery was investigated by Bogeat-Triboulot *et al.* (2007) and showed a very steep decline in stem height growth (50% reduction) and diameter growth (80% reduction) at 35% relative extractable soil water. After rewatering, the plants were able to recover their growth. This suggests that *P. euphratica* can tolerate periodic salinity or water deficits for example in areas that suffer high saline water table. This could be one of the reasons why *P. euphratica* can form pre-dominant population in regions with periodic water-logging (Wang *et al.*, 1996; Khamzina *et al.*, 2006).

Salinity decreases the water potential and thus decreases the available water for plants. Leaf elongation and expansion of *P. euphratica* was reduced during salt adaptation (Figure 3J, K, L). Munns *et al.* (2000) placed roots of plants exposed to salt in a pressure chamber to maintain fully turgid plants and thereby proved that changes in leaf elongation and expansion were caused by water deficit.

During three months growth at 150 mM NaCl in hydroponic solution leaves of *P. euphratica* became thicker and heavier than those of the controls, *i.e.* developed succulence (Figure 4G, H). Leaf succulence in *P. euphratica* under salinity is due to increasing the number of cell layers in the mesophyll (Ottow, 2004). Leaf succulence in saline conditions may contribute to salt tolerance by reducing water loss and also reducing salt uptake (Welch and Rieseberg, 2002). Salt induced leaf succulence plays an important role in maintaining gas exchange of C4 plants (Kemp and Cunningham, 1981).

According to Junghans *et al.* (2006) salinity reduces vessel lumen area and increases cell wall thickness in *P. euphratica*. By investigating wood anatomy of *P. euphratica* under water deficit the same effect as under salinity was observed (Bogeat-Triboulot *et al.*, 2007). Decreasing vessel lumen area and increasing wood density reduce hydraulic vulnerability of plant to cavitations and contributes to continued water transport. Furthermore it was observed that despite reduction in vessel lumen area the predicted hydraulic conductivity did not change in *P. euphratica* under salt, whereas in *P. x canescens* both vessel lumen area and hydraulic conductivity decreased (Junghans *et al.*, 2006).

4.1.2 Salinity and osmotic adjustment

Plants exposed to salt increase osmotic pressure of cells by increasing organic and inorganic contents. Increases in inorganic osmolytes like sodium and chloride in cytoplasm inhibit enzymatic activities. Ions are accumulating in vacuoles where cell metabolism is less

intensive than in the cytoplasm. But in cytoplasm the amount of organic osmolytes increases to balance osmotic pressure between cytoplasm and vacuole (Greenway and Munns, 1980). In salt exposed *P. euphratica* the amount of proline in both young and old leaves increased (Watanabe *et al.*, 2000). Also in leaf exudates of *P. euphratica* a high amount of carbohydrate compounds like sucrose, glucose and fructose together with one sugar-alcohol (inositol) was detected that can help the plant to cope with high osmotic stress induced by salinity and that also may help to exclude excess ions from the apoplast. According to Bogeat-Triboulot *et al.* (2007) inositol, salicin, glucose, fructose, sucrose, and galactose were major osmotic compounds present in the leaves of *P. euphratica*. All together *P. euphratica* is able to produce many metabolites to adjust the osmotic pressure and reduce ion toxicity. As a result of decreasing stomatal conductivity (Figure 25B), accumulation of high amounts of inorganic osmolytes like Na⁺ and Cl⁻ in apoplast and vacuoles (Ottow, 2004), and increasing metabolites like proline and soluble carbohydrates (Bogeat-Triboulot *et al.* 2007; Watanabe *et al.*, 2000), *P. euphratica* is able to keep water available for its cells. This results in decreases of leaf water potential in *P. euphratica* (Figure 20).

4.1.3 Electrolyte leakage and plasma membrane injury

Investigating the relationship of salt increment with changing of electrolyte conductivity in leaves of *P. euphratica* revealed that the amount of electrolytes in leaves and shoots increased whereas it decreased in xylem sap (3.1.4; Table 7). This suggests unloading of electrolytes from xylem to the leaves and shoot apex to build up an osmotic gradient. Changes in electrolyte conductivity of bark and xylem were positively correlated with salt increment in growth medium showing an increment in electrolyte flux into the root and continued accumulation of electrolytes in leaves. By increasing salinity of the growth medium from 100 to 200 mM the amount of electrolytes increased only in xylem and bark and no further increment in roots and leaves was observed. At this stress level also a steep drop in transpiration and stomatal conductance was found (Figure 24).

The plasma membrane of *P. x canescens* was severely injured in both salt shocked and salt adapted plants whereas in *P. euphratica* the permeability of the plasma membrane did not change under salt shock and it was only slightly injured (10%) one week after treating with 150 mM NaCl. *P. euphratica* plasma membrane also has high thermostability since

exposure of plants to 42°C for 54 h did not change plasma membrane permeability (Ferreira *et al.*, 2006).

Leaves located at different positions, age or developmental stages showed different responses to salinity. Investigating plasma membrane injury of *P. x canescens* in three different leaf ages showed that the leaves that were expanding during salt increment (3 week old leaves) were injured more than other leaves (1 and 5 week old) (Figure 19).

4.1.4 Performance of photosynthesis in response to salinity

Evaluation of the efficiency of photosystem II in long term (3 months) salt adapted *P. euphratica* (150 mM in hydroponic condition) revealed that this species is able to enhance the efficiency of photosystem II centre in dark conditions (Figure 25A). During the day when all photosynthetic enzymes were active no changes in the efficiency of photosystem II were observed under salt stress. It can be concluded that salt did not disturb the photosynthetic apparatus of *P. euphratica*. According to Wang *et al.* (2007) no change in maximum photosystem II efficiency of *P. euphratica* exposed to 200 mM NaCl was observed after 12 days.

But there is some evidence of beginning PSII damage since Chl b was slightly decreased. It is known that Chl b is more susceptible than Chl a and is unstable in alkaline conditions (Hojnik *et al.*, 2007). The Chl a/b ratio in *P. euphratica* slightly increased after 3 months growth in 150 mM NaCl (Figure 12B) due to decrease of Chl b content (Figure 21B and E) indicating initial degradation of PSII (Špundová *et al.*, 2003).

In case of *P. x canescens* supplemented with 75 mM NaCl for one week no difference in maximum efficiency of photosystem II was observed (Figure 16A), however efficiency of photosystem II was decreased in the light (Figure 26B). This reduction in light condition was observed despite very low PAR intensity ($10 \mu\text{mol m}^{-2} \text{s}^{-1}$ PAR) caused by shadowing of *P. x canescens* canopy.

By increasing salinity up to 100 mM in *P. euphratica* transpiration rate and stomatal conductance slightly decreased but no change in net photosynthesis was observed. Increasing salinity up to 200 mM decreased net photosynthesis (Figure 24A, B, C). However Ma *et al.* (1997) showed that the amount of photosynthesis in *P. euphratica* irrigating with 200 mM NaCl decreased and was recovered after three weeks, suggesting that *P. euphratica* may be able to enhance its photosynthetic activities in long term salt exposure.

4.2 Molecular characteristics of temperature induced lipocalin like proteins

Plant lipocalins have been well classified by Charron *et al.* (2005). The first temperature-induced lipocalin (TIL) was identified from an EST databank of cold-acclimated wheat and other homologues were named based on the characteristics of the first member of this family. No signal peptide was detected in TILs (Charron *et al.*, 2005). But in an effort to identify the subcellular localization of TILs, Charron *et al.* (2005) transformed plasmids carrying GFP-AthTIL (*Arabidopsis*) and GFP-TaTIL (wheat) fusions into onion epidermal cells. Both AthTIL and TaTIL were localized in the plasma membrane of onion epidermis (Charron *et al.*, 2005). Kawamura and Uemura (2003) found out that the amount of lipocalin protein in plasma membranes increased one day after cold acclimation. Gu *et al.* (2004) subjected *P. euphratica* plants to gradual salt increment over 3 h to a final concentration of 300 mM and observed transcript profiles at intervals from 0.5 to 72 h of salt stress and 1 to 48 h of recovery. A catalytic polypeptide-like protein (AJ534506) an editing enzyme for human apolipoprotein B mRNA was identified as a significantly upregulated gene during salt stress and recovery. Increased expression of lipocalin induced by salt stress and salt induction of an editing enzyme for lipoprotein supports the hypothesis that PeuTIL plays an important role in membrane biogenesis and repair under salt stress in *P. euphratica*. Searching stress specific expression profiles present in Genevestigator (Zimmermann *et al.*, 2004) showed that AthTIL expression is induced by various stress factors like syringol, anoxia, hypoxia, cold, heat, osmotic and salt. This suggests that TIL like proteins are involved also in other kinds of stresses. By searching the amino acid sequences of PeuTIL, PcaTIL and AthTIL for candidate membrane-spanning segments using TopPred program (Heijne, 1994) and KD-scale (Kyte and Doolittle), one segment in each lipocalin candidate was found that can penetrate the plasma membrane. Comparison between TILs of with *Arabidopsis* and poplar showed that these trans-membrane segments of PeuTIL and PcaTIL have higher hydrophobicity than AthTIL and were evaluated as "certain" segment, that its hydrophobicity profile exceeds the upper cut off, whereas in case of AthTIL this segment is reported as "putative" trans-membrane segment (Figure 40 and Figure 41).

PeuTIL transcript levels in leaves of *P. euphratica* are higher than those in roots in both control and saline conditions (Figure 29). Therefore, a specific function of TIL in leaves may be assumed. Also the amount of TIL transcript in *P. euphratica* is about 50 fold higher

than TIL in *P. x canescens* (Figure 31). These results are in accordance with results on plasma membrane injury of *P. euphratica* and *P. x canescens* under salt shock and salt adaptation that suggest that plasma membranes of *P. x canescens* were injured more than that of *P. euphratica*. This supports a role of TILs in plasma membrane maintenance and repair (Figure 18).

In the 5' upstream region of PtrTIL and AthTIL, consensus elements related to ABA signalling, early response to dehydration, endosperm specific expression (DOF-binding site) and seed storage regulation are common and highly present (Table 10). Elements known to be involved in binding of transcription factors such as ABA signalling elements and early responses to dehydration elements in the promoter region were obviously more frequent in PtrTIL than in AthTIL. This suggests an increased efficiency of transcriptional regulation of this TIL gene in poplar under osmotic stress conditions like salt stress and cold stress than in *Arabidopsis*. The presence of consensus controlling seed storage regulation and endosperm specific expression in AthTIL is relatively increased compared with PtrTIL. This observation is in accordance with a predominant up-regulation of TIL in *Arabidopsis* in seeds as observed in Genevestigator (Zimmermann *et al.*, 2004). Also dehydration is an important feature of salt stress and several dehydration related proteins have been initially found in seed (Ingram and Bartels, 1996). ABA signalling has an important role in enhancing stress tolerance in plants (Kim, 2004). Montero *et al.* (1997) showed that ABA inhibited Cl⁻ and Na⁺ uptake and stimulated the uptake of K⁺ in the NaCl tolerant bush bean. In *P. euphratica* the concentration of ABA in xylem increased more rapidly than in other salt-sensitive poplar genotypes (Chen *et al.*, 2001; Chen *et al.*, 2002). The high frequency of ABA consensus element in the 5' upstream region of TILs, especially in PtrTIL, suggests that the expression of this gene is highly responsive to ABA signalling.

To investigate the function of TILs in plant, a homolog knock out T-DNA mutant (At5g58070.1 - SALK_136775) in *Arabidopsis* was examined using root length assays under different stress conditions. The knock out mutants were compared with the wild types as reference. If lipocalin helps plant to tolerate stress conditions, it is expected that knock out mutants become more sensitive than wild type. Under control conditions root lengths of both knock out mutants and wild type plants were similar whereas under salt stress (100 mM NaCl) root lengths of AthTIL knock out mutants were significantly smaller than those of the wild type (Figure 50). This shows that the absence of lipocalin makes the plants more salt

sensitive. When performing root assays under similar osmotic stress using PEG (12.5 % w/v) no difference between AthTIL knock out mutants and wild type plants was observed. It can be concluded that the reduction of root lengths in salt- stressed AthTIL knock out mutants is mostly associated with ion toxicity not with osmotic stress. Also no significant differences were observed under cold stress (14 °C) and heat stress (27° C and 34°C) between AthTIL knock out mutants and wild types. However to better understanding the regulation and function of this gene, further experiments in soil or hydroponic conditions to characterize the function of this gene in relation with stress are necessary.

Knock out mutants of AthTIL showed a similar phenotype as the wild type for seed number per silique, rosette fresh weight and inflorescence height, but bolting in knock out mutants occurred much earlier than the wild type (Figure 48). According to Ye *et al.* (2000), in the pre-bolt stage of *Arabidopsis* the ratio of enzymatic to non-enzymatic lipid peroxidation is approximately one. This ratio is normal during the vegetative growth stage because membrane lipids in wild type are supported with lipocalin and are presumably more stable than knock out mutant against lipid peroxidation. But it is suspected that in AthTIL knock out mutants lipid peroxidation is high because of the lack of lipocalins to support membrane lipids. Subsequently lipid peroxidation may initiate the synthesis of a lipid derived secondary messenger (Ye *et al.*, 2000). Jasmonic acid is one of such messengers that activate bolting (McGurl *et al.*, 1994). In the mutants this may occur earlier than wild type and leading to the early-bolting phenotype of AthTIL knock out mutants. However, whether silencing of AthTIL increased lipid peroxidation is not known. Taking all data together it can be concluded that temperature induced lipocalin like proteins (TILs) are involved in mediating salt tolerance. It is possible that up-regulation of this gene can help plant to prevent lipid peroxidation of membranes and protect against injury.

4.3 Molecular characteristics of salt induced serine rich proteins

The PeuSIS open reading frame encodes a 17 kDa serine rich protein (17.8%) comprised of 157 amino acids with a predicted chloroplast target peptide. It was reported that this gene was up-regulated up to 5.2 fold in leaves of *P. euphratica* after 24 h salt shock (Brinker and Polle, 2005). To verify salt induction of the PeuSIS gene, plants of *P. euphratica* were exposed to 150 mM NaCl and the expression of PeuSIS was investigated using real time PCR. Expression analysis showed that transcript levels of PeuSIS in leaves

were up-regulated after 6 h exposure to 150 mM NaCl and decreased again to control levels after 12 h. In roots, 3h after salt stress *PeuSIS* was up-regulated and increased up to 12 h and decreased at 24h; however it still remained up-regulated. After long term exposure to 150 mM no change in transcript levels between control and salt-treated plants were observed. This suggests a potential role of this gene in early response to salinity. Also no significant differences between leaves and roots in transcription levels at different time points after exposing to NaCl were observed. Serine-rich proteins, such as transcription or splicing factors are often involved in RNA/DNA binding (Horie *et al.*, 1998).

The 627 bp upstream regions of *PtrSIS* and *AthSIS* were selected to avoid interference with adjacent genes and searched against the PLACE database. Upstream regions of both *PtrSIS* and *AthSIS* are rich in transcription factor binding consensus elements such as light induced elements, seed storage protein promoter elements and chloroplast gene expression elements. Early response to dehydration and ABA response elements were mostly present in the upstream region of *PtrSIS* but less in *AthSIS*. Probably because of the high presence of dehydration responsive elements and ABA signalling induced elements, the *SIS* gene of *P. trichocarpa* may be more responsive to stress than that of *A. thaliana*. However this is currently a speculation that would need to be analysed further.

To characterize the function of the *SIS* protein, root assays were undertaken with *SIS* knock out mutant of *A. thaliana*. However no differences between knock out and wild type plants were found under osmotic or salt stress and also at different temperatures (14, 20, 27 and 34°C) (Figure 70 and 71). Phenotype comparisons revealed that the *AthSIS* SALK line bolted earlier than the wild type but no differences in seed number per silique, inflorescence height and rosette fresh weight were observed (Figure 69).

The *SIS* protein because of its high amount of serine is a putative target protein for kinase proteins. In silico analysis using NetPhos 2.0 and NetPhosK 1.0 showed that the most frequent and highest scores belonged to PKC that is induced by many extracellular signalling (Figure 64). Many serine rich proteins are splicing factors or transcription factors but none of them had high similarity with *SIS*s. To elucidate the role of the low number of ABA signalling elements in the upstream region of *AthSIS* in comparison with *PtrSIS*, further studies need to be done to unravel whether this responds to ABA signalling.

4.4 Outlook

It was found that the expression level of *PeuTIL* transcripts in control and after salt adaptation was higher than that of *PcaTIL*. Therefore looking at regulatory elements, present in the upstream regions of *TIL* like genes in these two species, can give us valuable information about the specific inducers of *TIL* in *P. euphratica*. In this study, the upstream region of *AthTIL* and *PtrTIL* were compared and it was found that *PtrTIL* contained a considerably higher number of ABA signaling and early response to dehydration elements than *AthTIL*.

Over expression of *PeuTIL* in *P. x canescens* to conduct „gain of function” analysis is ongoing and to continue this task a part of cDNA containing open reading frame together with a part of UTR region of *PeuTIL* has been amplified using PCR and cloned in the pGEM-Tvector.

To perform loss of function analysis for *AthTIL*, one homozygote Salk line was investigated. In this line *AthTIL* transcript was present but it is expected that no functional protein can be formed because this transcript is together with T-DNA and also the T-DNA is located near to start codon. Root assay experiments revealed that *AthTIL* knock out lines growing in 100 mM NaCl, became more salt sensitive but no different in equimolar osmotic stress induced by 12.5 % (w/v) PEG between wild type and *AthTIL* knock out lines was observed. Since this gene was also upregulated under developing drought stress in *P. euphratica*, it seems that *AthTIL* knock out mutants become more susceptible than wild types to higher osmotic stress.

It was speculated that the lack of *AthTIL* caused to increasing lipid peroxidation in the prebolting stage and induced bolting by a lipid driven secondary messenger like jasmonic acid. To check the validity of this conclusion, performing further analysis, e.g. of jasmonic acid and malondialdehyde to assess lipid peroxidation are necessary.

5

Summary

Salt tolerance is a complex trait that involves biochemical, physiological and morphological modifications that are regulated at the molecular level. The aim of this work was to understand the effects of salinity on *P. euphratica*, a salt tolerant species. For this purpose ecophysiological and molecular methods were applied and necessary comparisons were conducted with *P. x canescens*, a salt sensitive species or *A. thaliana*, the model plant for herbaceous species.

The present work shows that *P. euphratica* under salinity is able to protect its plasma membrane and maintain quantum yield efficiency of PSII.

Molecular analysis showed that the expression levels of two genes were increased in response to salinity (TIL and SIS) in both *P. euphratica* (PeuTIL) and *P. x canescens* (PcaTIL). These genes were characterized to study their functions with respect to salt tolerance.

In both root and leaf, PeuTIL was up-regulated after salt stress and decreased to the control level within few hours. Comparison of PeuTIL and PcaTIL showed that the transcript level of TIL in *P. euphratica* was significantly higher than that of its homolog in *P. x canescens* both under control conditions and salt stress. It has also been found that the expression of PeuTIL in leaves was considerably higher than in roots. In silico analysis of

PeuTIL revealed evidence for a transmembrane segment. The homolog segment in AthTIL exhibited lower hydrophobicity than that of PeuTIL and PcaTIL, respectively.

To obtain evidence for factors controlling gene expression of TILs, the upstream regions of AthTIL and PtrTIL were searched for cis-acting elements and the results were compared. Elements related to ABA signalling, early response to dehydration, endosperm specific expression (DOF-binding site) and seed storage regulation were common and highly present in the upstream regions of both genes. ABA signalling and early response to dehydration elements were more frequently present in the PtrTIL upstream region suggesting a higher efficiency of transcriptional control in *P. trichocarpa* than in *A. thaliana* in response to stress.

To characterize the function of TIL in plants, knock-out mutants of its homolog in *A. thaliana* were investigated. The mutants and controls were subjected to different stress factors. Knock out mutants of AthTIL were more salt sensitive than the wild type but no differences were observed under equivalent osmotic stress induced by PEG. Also different temperatures in a range of 14°C to 34°C did not reveal any differences between knock out mutants of AthTIL and wild type plants.

AthTIL knock out mutants showed an early bolting phenotype. Since increased lipid peroxidation induces lipid-derived-signalling leading to bolting in *Arabidopsis*, it can be speculated that the absence of TIL, may affect plasma membrane lipids and that may induce early-signalling and bolting. However, further investigations need to be done, especially comparing lipid peroxidation in the vegetative stage.

PeuSIS is a gene encoding a protein of yet completely unknown functions. The gene was cloned together with its homolog of *P. x canescens* (PcaSIS) and subjected to loss of function experiments and in silico analysis. Expression studies revealed that PeuSIS was upregulated shortly after salt shock and decreased to the control level within a few hours. There were no differences in gene expression between leaves and roots and also not between *P. x canescens* and *P. euphratica*.

All together 4 hits for this gene were found in NCBI data bank. All of the SIS genes show a high frequency of serines and display high similarity in the last 50 amino acids out of 157 amino acids. Based on SignalP and Netphos prediction, this protein is localized in chloroplast and has ample phosphorylation sites, which might tie in this protein into the signaling chain.

Also the upstream regions of both PtrSIS and AthSIS were searched for putative transcription factor binding sites that may be involved in controlling gene expression. It was found that this region is rich of potential transcription factor binding sites for light induced elements, seed storage protein promoter elements and chloroplast gene expression elements in both species. The upstream region of PtrSIS contains a considerable amount of early response to dehydration, ABA response elements and light responsive elements in comparison with AtSIS.

This study assigns a novel function to TIL by showing that TIL may play a role in salt tolerance in *P. euphratica* during short term salt adaptation by protecting the plasma membrane.

6

References

- Ashby WC and Beadle NCW** (1957) Studies halophyte. III Salinity factors in the growth of Australian salt bushes. *Ecology* **38**: 344-352
- Ashraf M and Orooj A** (2006) Salt stress effects on growth, ion accumulation and seed oil concentration in an arid zone traditional medicinal plant ajwain (*Trachyspermum ammi* [L.] –Sprague). *J Arid Environ* **64**: 209-220
- Banerjee T, Gupta SK and Ghosh TC** (2006) Compositional transitions between *Oryza sativa* and *Arabidopsis thaliana* genes are linked to the functional change of encoded proteins. *Plant Sci Lett* **170**: 267–273
- Benedict C, Skinner JS, Meng R, Chang Y, Bhalerao R, Huner NPA, Finn CE, Chen THH and Hurry V** (2006) The CBF1-dependent low temperature signalling pathway, regulon, and increase in freeze tolerance are conserved in *Populus* spp. *Plant Cell Environ* **29**: 1259–1272
- Birnboim and Doly** (1979) Plasmid DNA Isolation, Alkaline Lysis. *Nucleic Acid Res* **7**: 1513-1523
- Bishop RE** (2000) The bacterial lipocalin. *Biochim Biophys Acta* **1482**: 73-83
- Bishop RE, Penfold SS, Frost LS, Holtje JV and Weiner JH** (1995) Stationary Phase Expression of a Novel *Escherichia coli* Outer Membrane Lipoprotein and Its Relationship with Mammalian Apolipoprotein D. Implications for the origin of lipocalins. *J Biol Chem* **270**: 23097-23103

- Black RF** (1960) Effects of NaCl on the ion uptake and growth of *Atriplex vesicaria* Howard. *Aust J Biol Sci* **13**: 249-266
- Blom N, Sicheritz-Ponten T, Gupta R, Gammeltoft S and Brunak S** (2004) Prediction of post-translational glycosylation and phosphorylation of proteins from the amino acid sequence. *Proteomics* **4**: 1633-49
- Blum A and Ebercon A** (1981) Cell membrane stability as a measure of drought and heat tolerance in wheat. *Crop Sci* **21**: 43-47
- Blumwald E** (2000) Sodium transport and salt tolerance in plants. *Curr Opin Cell Biol* **12**: 431-434.
- Bogeat-Triboulot MB, Brosche M, Renaut J, Jouve L, Thiec D, Fayyaz P, Vinocur B, Witters E, Laukens K, Teichmann T, Altman A, Hausman JF, Polle A, Kangasjärvi J and Dreyer E** (2007) Gradual soil water depletion results in reversible changes of gene expression, protein profiles, ecophysiology, and growth performance in *Populus euphratica*, a poplar growing in arid regions. *Plant Physiol* **143**: 876-892
- Bolu WH and Polle A** (2004) Growth and stress reactions in roots and shoots of a salt-sensitive poplar species (*Populus x canescens*). *J Trop Ecol* **45**: 161-171
- Bradshaw HD, Ceulemans R, Davis J, Stettler R** (2000) Emerging model systems in plant biology: poplar (*Populus*) as a model forest tree. *J Plant Growth Regul* **19**:306-313
- Brosché M, Vinocur B, Alatalo ER, Lamminmäki A, Teichmann T, Ottow EA, Djilianov D, Afif D, Bogeat-Triboulot MB, Altman A, Polle A, Dreyer E, Rudd S, Paulin L, Auvinen P and Kangasjärvi A** (2005) Gene expression and metabolite profiling of *Populus euphratica* growing in the Negev desert. *Genome Biol* **6/R101**: 2-17
- Bugos RC, Hieber AD, Yamamoto HY** (1998) Xanthophyll cycle enzymes are members of the lipocalin family, the first identified from plants. *J Biol Chem* **273**: 15321-15324
- Brinker M and Polle A** (2005) unpublished data, Forest Botanical Institute, Göttingen, Germany
- Campanacci V, Nurizzo D, Spinelli S, Valencia C, Tegoni M and Cambillau C** (2004) The crystal structure of the Escherichia coli lipocalin Blc suggests a possible role in phospholipids binding. *FEBS Lett* **562**:183-188
- Ceulemans R and Deraedt W** (1999) Production physiology and growth potential of poplars under short-rotation forestry culture. *For Ecol Manage* **121**: 9-23
- Chang S, Puryear J and Cairney J** (1993) A simple and efficient method for isolating RNA from pine trees. *Plant Mol Biol Rep* **11**: 113-116

- Charron J, Ouellet F, Pelletier M, Danyluk J, Chauve C and Sarhan F** (2005) Identification, expression, and evolutionary analyses of plant lipocalins. *Plant Physiol* **139**: 2017-2028
- Charron J and Sarhan F** (2006) Plant lipocalins. In: Åkerström B, Borregaard N, Flower D and Salier J (editors) Lipocalins. Landes Bioscience, Georgetown TX USA **204**: 40-48
- Chaves MM and Oliveira MM** (2004) Mechanisms underlying plant resilience to water deficits: prospects for water-saving agriculture. *J Exp Bot* **407**: 2365-2384
- Chen S, Li J, Wang S, Hüttermann A and Altman A** (2001) Salt, nutrient uptake and transport, and ABA of *Populus euphratica*; a hybrid in response to increasing soil NaCl. *Trees* **15**: 186-194
- Chen S, Li J, Wang T, Wang S, Polle A and Hüttermann A** (2002) Osmotic stress and ion-specific effects on xylem abscisic acid and the relevance to salinity tolerance in poplar. *J Plant Growth Regul* **21**: 224-233
- Clark MS** (1997) In: Plant Molecular Biology - A Laboratory Manual, Springer-Verlog Berlin Heidelberg, New York: 305-328
- Claros MG and von Heijne G** (1994) TopPred II: an improved software for membrane protein structure predictions. *Comput Appl Biosci* **10**: 685-686
- Colmenero-Flores JM, Martínez G, Gamba G, Vázquez N, Iglesias DJ, Brumós J and Talón M** (2007) Identification and functional characterization of cation-chloride cotransporters in plants. *Plant J* **50**: 278-292
- Crowella DN, Packarda CE, Piersona CA, Ginerb JL, Downesa BP and Charya SN** (2003) Identification of an allele of CLA1 associated with variegation in *Arabidopsis thaliana*. *Physiol Plant* **118**: 29-37
- Cruz JA, Avenson TJ, Kanazawa A, Takizawa K and Edwards GE** (2005) Plasticity in light reactions of photosynthesis for energy production and photoprotection. *J Exp Bot* **56**: 395-406
- Demmig-Adams B** (1990) A carotenoids and photoprotection in plants: a role for the xanthophyll zeaxanthin. *Biochim Biophys Acta* **1020**: 1-24
- Emanuelsson O, Nielsen H, Brunak S and Heijne G** (2000) Predicting subcellular localization of proteins based on their N-terminal amino acid sequence. *J Mol Biol*, **300**: 1005-1016
- Epstein E and Rains DW** (1987) Advances in salt tolerance. *Plant Soil* **99**: 17-29
- Ferreira S, Hjern K, Larsen M, Wingsle G, Larsen P, Fey S, Roepstorff P and Pais MS** (2006) Proteome profiling of *Populus euphratica* Oliv. upon heat stress. *Ann Bot (Lond)* **98**: 361-377

- Flower DR** (1996) The lipocalin protein family: structure and function. *Biochem J* **318**: 1-14
- Flower DR, North ACT and Attwood TK** (1993) Structure and sequence relationships in the lipocalins and related proteins. *Protein Sci* **2**: 753-761
- Flower DR, North ACT and Sanson CD** (2000) The lipocalin protein family: structural and sequence overview. *Biochim Biophys Acta* **1482**: 9-24
- Flowers TJ** (1977) The mechanism of salt tolerance in halophytes. *Annu Rev Plant Physiol* **28**: 89-121
- Glenn EP, Brown JJ and Blumwald E** (1999) Salt tolerance and crop potential of halophytes. *CRC Crit Rev Plant Sci* **18**: 227-255
- Greenway H and Munns R** (1980) Mechanisms of salt tolerance in nonhalophytes. *Annu Rev Plant Physiol* **31**: 149-190
- Gruenberg-Fertig I** (1996) List of Palestine plants with data on their geographical distribution. Ph.D. thesis, The Hebrew University, Jerusalem.
- Gu R, Fonseca S, Puskás L, László Hackler JR, Zvara Á, Dudits D and Pais MS** (2004) Transcript identification and profiling during salt stress and recovery of *Populus euphratica*. *Tree Physiol* **24**: 265-276.
- Hajar AS, Zidan MA and Al-Zahrani HS** (1996) Effect of salinity stress on the germination, growth and some physiological activities of black cumin (*Nigella sativa* L.). *Arab Gulf J Sci Res* **14**: 445-454
- Hewitt EJ and Smith TA** (1975) Plant mineral nutrition, English University Press, London
- Higo, K, Ugawa Y, Iwamoto M and Korenaga T** (1999) Plant cis-acting regulatory DNA elements (PLACE) database:1999. *Nucleic Acids Research* **27(1)**: 297-300
- Hojnika M, Škergeta M and Knez Ž** (2007) Isolation of chlorophylls from stinging nettle (*Urtica dioica* L.) *Separ Purif Tech* **57**: 37-46
- Horie S, Watanabe Y, Tanaka K, Nishiwaki S, Fujioka H, Abe H, Yamamoto M and Shimoda C** (1998) The Schizosaccharomyces pombe mei4(+) gene encodes a meiosis-specific transcription factor containing a forkhead DNA-binding domain. *Mol Cell Biol* **18**: 2118–2129
- Hu L, Lu H, Liu Q, Chen X and Jiang X** (2005) Overexpression of mtID gene in transgenic *Populus tomentosa* improves salt tolerance through accumulation of mannitol. *Tree Physiol* **25**:1273-81
- Hunte C, Screpanti E, Venturi M, Rimón A, Padan E and Michel H** (2005) Structure of a Na⁺/H⁺ antiporter and insights into mechanism of action and regulation by pH. *Nature* **435**: 1197-1202

- Imbeaud S, Graudens E, Boulanger V, Barlet X, Zaborski P, Eveno E, Mueller O, Schroeder A and Auffray C** (2005) Towards standardization of RNA quality assessment using user-independent classifiers of microcapillary electrophoresis traces. *Nucleic Acids Res* **33**: 56
- Ingram J and Bartels D** (1996) The molecular basis of dehydration on plants. *Annu Rev Plant Physiol* **47**: 377–403
- James DW, Hanks RJ and Jurinak JJ** (1982) Modern irrigated soils. New York: John Wiley.
- Johnson MK, Johnson EL, MacElroy RD, Speer HL and Bruff BS** (1968) Effect of salts on the halophilic alga *Dunaliella viridis*. *J Bacteriol* **95**: 1461-6
- Junghans U, Polle A, Düchting P, Weiler E, Kuhlman B, Gruber and Teichmann T** (2006) Adaptation to high salinity in poplar involves changes in xylem anatomy and auxin physiology. *Plant Cell Environ* **29**: 1519–1531
- Kariola T, Brader G, Li J and Palva ET** (2005) Chlorophyllase 1, a damage control enzyme, affects the balance between defence pathways in plants. *Plant Cell* **17**: 282–294
- Katerji N, Hoorn JW, Hamdy A and Mastrollili** (2000) Salt tolerance classification of crops according to soil salinity and to water stress day index. *Agric Water Manage* **43**: 99-109
- Kawamura Y and Uemura M** (2003) Mass spectrometric approach for identifying putative plasma membrane proteins of Arabidopsis leaves associated with cold acclimation. *Plant J* **36**: 141-154
- Kemp PR and Cunningham GL** (1981) Light, Temperature and Salinity Effects on Growth, Leaf Anatomy and Photosynthesis of *Distichlis spicata* (L.) Greene. *Am J Bot* **68**: 507-516
- Khamzina A, Lamers JPA, Worbes M, Botman E and Vlek PLG** (2006) Assessing the potential of trees for afforestation of degraded landscapes in the Aral Sea Basin of Uzbekistan. *Agrofor Syst* **66**: 129–141
- Kim SY** (2004) Enhancing stress tolerance by regulon engineering of ABA-Responsive genes. ISB News Report
- Kimura M** (1980) A simple method for estimating evolutionary rates of base substitutions through comparative studies of nucleotide sequences. *J Mol Evol* **16**: 111-120
- Kronegg J and Buloz D** (1999) Detection/prediction of GPI cleavage site (GPI-anchor) in a (DGPI). <http://www.expasy.ch/tools/>.
- Kulshrestha S, Mishra DP and Gupta RK** (1987) Changes in contents of chlorophyll, proteins and lipids in whole chloroplast membrane fractions at different leaf water

- potentials in drought resistant and sensitive genotype of wheat. *Photosynthetica* **21**: 65–70
- Landis TD** (1988) Management of forest nursery soils dominated by calcium salts. *New Forests* **2**: 173-193
- Leipner J** (2003) Chlorophyll a fluorescence measurements in plant biology, ETH Federal Institute of Technology Zurich - Institute of Plant Sciences - Agronomy and Plant Breeding (Online)
- Leplé JC, Brasiliero A, Michel MF, Delmotte F and Jouanin L** (1992) Transgenic poplars: expression of chimeric gens using four different constructs. *Plant Cell Rep* **11**: 137-141
- Lichtenthaler HK and Wellburn A** (1983) Determination of total carotenoids and chlorophyll a and b of leaf extracts in different solvents. *Biochem Soc Trans* **11**: 591
- Lledo MD, Crespo MB and AmoMarco JB** (1995) The role of cytokinins and ethylene inhibitors on lenticel hypertrophy generation and ethylene production in in-vitro cultures of *Populus euphratica* Olivier. *Isr. J. Plant Sci.* **43**: 339-345
- Ma HC, Fung L, Wang SS, Altman A and Hütermann A** (1997) Photosynthetic response of *Populus euphratica* to salt stress. *For Ecol Manage* **93**: 55-61
- Mansour MMF** (1998) Protection of plasma membrane of onion epidermal cells by glycinebetaine and proline against NaCl stress. *Plant Physiol Biochem* **36**: 767-772
- Martínez M, Rubio-Somoza I, Fuentes R, Lara P, Carbonero P and Diaz I** (2005) The barley cystatin gene (Icy) is regulated by DOF transcription factors in aleurone cells upon germination. *J Exp Bot* **56**: 547–556
- MCGurl B, Pearce G, Orozco-Cardenas M, and Ryan CA** (1992) Structure, expression, and antisense inhibition of the systemin precursor gene. *Science* **255**:1570-1573
- Meloni DA, Oliva MA, Ruiz HA and Martinez CA** (2001) Contribution of proline and inorganic solutes to osmotic adjustment in cotton under salt stress. *J Plant Nutr* **24**: 599 – 612
- Miyoshi K, Ahn B, Kawakatsu T, Ito Y, Itoh JI, Nagato Y and Kurata N** (2004) Plastochron1, a timekeeper of leaf initiation in rice, encodes cytochrome P450. *Proc Natl Acad Sci U S A* **101**: 875–880
- Montero E, Cabot C, Barcelo J and Poschenrieder C** (1997) Endogenous abscisic acid levels are linked to decreased growth of bush bean treated NaCl. *Physiol Plant* **101**: 17–22
- Montfort C, Brandup W** (1927) Physiologische und pflanzengeographische Seesalzwirkungen. II Ökologische Studien über Keimung und erste Entwicklung bei Halophyten. *Jahrb Wiss Bot* **66**: 902-46

- Munnus R, Passiora JB, Guo J, Chazen O and Cramer GR** (2000) Water relations and leaf expansion: importance of time scale. *J Exp Bot* **51**: 1495-1504
- Newton RJ, Funkhouser EA, Fong F, Tauer CG** (1991) Molecular and physiological genetics of drought tolerance in forest species. *For Ecol Manage* **43**:225–250
- Ottow EA** (2004) Molecular and ecophysiological responses of *Populus euphratica* (Oliv.) and *Arabidopsis thaliana* (L.) to salt stress, Ph.D. thesis, Göttingen University, Germany.
- Ottow EA, Brinker M, Teichmann T, Fritz E, Kaiser W, Brosché M, Kangasjärvi J, Jiang X, and Polle A** (2005) *Populus euphratica* displays apoplastic sodium accumulation, osmotic adjustment by decreases in calcium and soluble carbohydrates, and develops leaf succulence under salt stress. *Plant Physiol* **139**: 1762–1772
- Ouyang Y** (2002) Phytoremediation: modeling plant uptake and contaminant transport in the soil–plant–atmosphere continuum. *J Hydrol* **266**: 66–82
- Parida AK and Das AB** (2005) Salt tolerance and salinity effects on plants: a review. *Ecotoxicol Environ Saf* **60**: 324–349
- Parida AK, Das AB and Mitra B** (2004) Effects of salt on growth, ion accumulation, photosynthesis and leaf anatomy of the mangrove, *Bruguiera parviflora*. *Trees* **18**:167-174
- Pfaffl MW** (2001) A new mathematical model for relative quantification in real-time RT-PCR. *Nucleic Acids Res* **29**: 2002-2007
- Pfaffl MW, Graham WH and Dempfle L** (2002) Relative expression software tool (REST©) for group-wise comparison and statistical analysis of relative expression results in real-time PCR. *Nucleic Acids Res* **30**: 1-10
- Prathapar S, Aslam M, Kahlown K, Iqbal Z and Qureshi A** (2005) Mechanically reclaiming abandoned saline soils in Pakistan. *Irrigation and Drainage* **54**: 519–526
- Prestridge DS** (1991) SIGNAL SCAN: A computer program that scans DNA sequences for eukaryotic transcriptional elements. *Comput Appl Biosci* **7**: 203-206
- Puchood D and Khoyratty S** (2004) Genomic DNA extraction from *Victoria amazonica*. *Plant Mol Biol Rep* **22**: 195-195
- Ruiz D, Martinez V and Cerdá A** (1999) Demarcating specific ion (NaCl, Cl⁻, Na⁺) and osmotic effects in the response of two citrus rootstocks to salinity. *Sci Hort* **80**: 213-224
- Sambrook J, Fritsch EF and Maniatis T** (1989) *Molecular Cloning: A Laboratory Manual*, 2nd edn, NY Cold Spring Harbor Laboratory Press

- Sánchez D, Ganfornina MD, Gutiérrez G and Marín A (2003)** Exon-intron structure and evolution of the lipocalin gene family. *Mol Biol Evol* **20**: 775-783
- Schneidereit A (2005)** Untersuchungen zur transkriptionellen Regulation des AtSUC2-Promotors beim Sink/Source-Übergang im Blatt und Analyse der Gene AtINT2 und AtINT4. Dissertation, Friedrich Alexander Universität, Erlangen, Nürnberg, pp. 117
- Simmons CA, Zilberberg J and Davies PF (2004)** A rapid, reliable method to isolate high quality endothelial RNA from small spatially-defined locations. *Ann Biomed Eng* **32(10)**: 1453–1459
- Sixto H, Grau JM, Alba N and Alia R (2005)** Response to sodium chloride in different species and clones of genus *Populus* L. *Forestry* **78(1)**: 93-104
- Wallin E and von Heijne G (1998)** Genome-wide analysis of integral membrane proteins from eubacterial, archaean, and eukaryotic organisms. *Protein Sci* **7**: **1029-1038**
- Špundová M, Popelková H, Ilík P, Skotnica J, Novotný R, Nauš J (2003)** Ultra-structural and functional changes in the chloroplasts of detached barley leaves senescing under dark and light conditions. *J Plant Physiol* **160**: 1051–1058
- Steudle E (1996)** Water transport in plants: Role of the apoplast. *Plant Soil* **187**: 67-79
- Steudle E (2000)** Water uptake by plant roots: an integration of views. *Plant Soil* **226**: 45-56
- Sudhir P and Murthy SDS (2004)** Effects of salt stress on basic processes of photosynthesis. *Photosynthetica* **42**: 481-486
- Tholakalabavi A, Zwiazek J, and Thorpe T (1994)** Effect of mannitol and glucose-induced osmotic stress on growth, water relations, and solute composition of cell suspension cultures of poplar (*Populus deltoides* var. *occidentalis*) in relation to anthocyanin accumulation. *In Vitro Cell Dev Biol* **30**: 164-170
- Toker A (1998)** Signaling through protein kinase C. *Front Biosci* **3**: 1134-1147
- U.S. Salinity Laboratory Staff (1969)** Diagnosis and improvement of saline and alkali soils. U.S. Superintendent of Documents, Washington, DC. Agriculture Handbook 60.160
- Venkatesan A, Manikandan T and Natarajan S (2005)** Bioreclamation of saline soil under *Salicornia brachiata* Roxb., A halophyte, book of abstract; third international conference on plants and environmental pollution (ICEP-3), Lucknow, India pp 49
- Wan D, Li H, Zhou G, Liang H, Zhang L (2004)** Effect of insect pest on activated oxygen metabolism in lanceolate leaves of *Populus euphratica* under different water condition. *The Journal of Applied Ecology* (Chinese) **15**:849-52
- Wang L, Chen L and Jacob T (2000)** The role of ClC-3 in volume-activated chloride currents and volume regulation in bovine epithelial cells demonstrated by antisense inhibition. *J Physiol* **524**:63-75

- Wang R, Chen S, Deng L, Fritz E, Hüttermann A and Polle A** (2007) Leaf photosynthesis, fluorescence response to salinity and relevance to chloroplast salt compartmentation and anti-oxidative stress in two poplars. *Trees* **21**: 581-591
- Wang S, Chen B and Li H** (1996) Euphrates poplar forest. China Environmental Science Press, Beijing, 212 p
- Watanabe S, Kojima K, Ide Y and Sasaki S** (2000) Effects of saline and osmotic stress on proline and sugar accumulation in *Populus euphratica* in vitro. *Plant Cell Tissue Organ Cult* **63**: 199–206
- Welch ME and Rieseberg LH** (2002) Habitat divergence between a homoploid hybrid sunflower species, *Helianthus paradoxus* (Asteraceae), and its progenitors. *Am J Bot* **89**(3): 472–479
- Wyn Jones RG and Pollard A** (1983) Proteins, enzymes and inorganic ions. In: Laüchli A and Pirson A (editors). Encyclopedia of plant physiology. Springer Press, Berlin, Germany **15B**: 528-562
- Xu WY** (1988) Poplar (in Chinese). Heilongjiang People's Press, Harbin, China 167 pp.
- Yamaguchi T and Blumwald E** (2005) Developing salt-tolerant crop plants: challenges and opportunities. *Trends in Plant Sci* **10**: 615-620
- Ye Z, Rodriguez R, Tran A, Hoang H, de los Santos D , Brown S and Vellanoweth RL** (2000) The developmental transition to flowering represses ascorbate peroxidase activity and induces enzymatic lipid peroxidation in leaf tissue in *Arabidopsis thaliana*. *Plant Sci* **158**(13): 115-127
- Yeo A** (1998) Molecular biology of salt tolerance in the context of whole-plant physiology. *J Exp Bot* **323**: 915–929
- Zhu JK** (2001) Plant salt tolerance. *Trends Plant Sci* **6**: 66-71
- Zimmermann P, Hirsch-Hoffmann M, Hennig L and Gruissem W** (2004) Genevestigator. Arabidopsis microarray database and analysis toolbox. *Plant Physiol* **136**: 2621-2632

7

Appendix

App. 7.1. Half MS (Murashige and Skoog) medium for *Populus euphratica*

Stocks	Types	Amount	
Macros	MS (App. 7.7.1)	50	ml/l
Micros	MS (App. 7.7.2)	0.5	ml/l
Vitamin	MS (App. 7.7.3)	1	ml/l
Glycine	MS (App. 7.7.4)	1	ml/l
Inositol	MS (App. 7.7.5)	5	ml/l
Iron	MS (App. 7.7.6)	5	ml/l
Sucrose		20	g/l
Gelrite		3	g/l

Note: Adjust medium to pH 5.8 before adding gelrite.

App. 7.2. WPM medium for *Populus euphratica*

Stocks	Types	Amount	
WPM (+ vitamin)		2462.6	mg/l
Myo inositol		100	mg/l
Vitamin	MS (App. 7.7.3)	1	ml/l
NAA (stock) *		1	ml/l
DMSO (stock) **		1	ml/l
Ascorbic acid		10	mg/l
Sucrose		30	g/l
Agar		8	g/l

Note: Adjust medium to pH 5.8 before adding agar.

* NAA 1 mg/ml

** DMSO 75 mM

App. 7.3. Nutrient solution for hydroculture modified according to Long Ashton

Stocks*	Salts	Amount (g/l)
A	KNO ₃	50.55
B	Ca(NO ₃) ₂ ·4H ₂ O	106.27
C	MgSO ₄ ·7H ₂ O	37
D	KH ₂ PO ₄	40.82
	K ₂ HPO ₄	3.6
E	Fe-EDTA	1.8355
F	MnSO ₄ ·H ₂ O	0.1690
	H ₃ BO ₃	0.3090
	Na ₂ MoO ₄ ·2H ₂ O	0.8460
	CoSO ₄ ·7H ₂ O	0.0056
	ZnSO ₄ ·7H ₂ O	0.0288
	CuSO ₄ ·5H ₂ O	0.0160

* 400 ml from each stock diluted 200 liter ddH₂O.

App. 7.4. Propagation medium for *Populus x canescens*

Stocks	Types	Amount
Macros	MS (App. 7.7.1)	100 ml/l
Micros	MS (App. 7.7.2)	1 ml/l
Vitamin	MS (App. 7.7.3)	1 ml/l
Glycine	MS (App. 7.7.4)	1 ml/l
Inositol	MS (App. 7.7.5)	5 ml/l
Iron	MS (App. 7.7.6)	5 ml/l
BAP*		0.8 ml/l
Sucrose		20 g/l
Gelrite		3 g/l

Note: Adjust medium to pH 5.8 before adding gelrite.

* For BAP stock, add 25 mg BAP in 50ml ethanol, reach to 100 ml by ddH₂O.

App. 7.5. Rooting medium for *Populus x canescens* and *Arabidopsis thaliana*

Stocks	Types	Amount
Macros	SH (App. 7.7.7)	100 ml/l
Micros	GD (App. 7.7.9)	1 ml/l
Vitamin	MS (App. 7.7.3)	1 ml/l
Glycine	MS (App. 7.7.4)	1 ml/l
Inositol	MS (App. 7.7.5)	5 ml/l
Iron	MS (App. 7.7.6)	5 ml/l
Sucrose		25 g/l
Gelrite		2.8 g/l

Note: Adjust medium to pH 5.8 before adding gelrite.

App. 7.6. Rooting medium for *Arabidopsis thaliana* (produce less lateral root)

Stocks	Types	Amount	
Micros MS	[1000x]	1	ml
NH ₄ NO ₃	[1M]	5	ml
KNO ₃	[1M]	5	ml
CaCl ₂ .2H ₂ O		0.22	g
MgSO ₄ .7H ₂ O		0.18	g
KH ₂ PO ₄		1.7	g
MES [2-(Nmorpholino) ethanesulfonic acid]		0.5	g
Sucrose		45	g
Agar		0.7%	
ddH ₂ O		up to 1	L

Note: Adjust pH 5.7 by 1N KOH and add Agar afterward.

App. 7.7- Stock solutions for micro propagation and rooting mediums

7.7.1. Macronutrients-MS 10x concentration	(g/l)
NH ₄ NO ₃	16.5
KNO ₃	19.0
CaCl ₂ .2H ₂ O	4.4
MgSO ₄ .7H ₂ O	3.7
KH ₂ PO ₄	1.7

7.7.2. Micronutrients-MS 1000x concentration	(mg/100 ml)
H ₃ BO ₃	620
Na ₂ MoO ₄ .2H ₂ O	25
KJ	83
MnSO ₄ .H ₂ O	1000
ZnSo4.7H ₂ O	860
CoCl ₂ .6H ₂ O	2.5
CuSO ₄ .5H ₂ O	2.5

7.7.3. Vitamins-MS 1000x concentration	(mg/100 ml ddH₂O)
Nicotinic acid	50
Pyridoxine-HCl	50
Thiamine-HCl	10

7.7.4. Glycine-MS 1000x concentration	(mg/100 ml)
Glycine	200

7.7.5. Inositol-MS 500x concentration	(mg/100 ml)
Inositol	2000

7.7.6. Fe-Solution-MS	500x concentration	(mg/100 ml)
EDTA ferric sodium salt		734

7.7.7. Macronutrients-SH	(g/l)
KNO ₃	25
CaCl ₂ ·2H ₂ O	2
MgSO ₄ ·7H ₂ O	4
NH ₄ H ₂ PO ₄	3

7.7.8. Macronutrients-GD	(g/l)
(NH ₄) ₂ SO ₄	2
KCl	3
KNO ₃	10
MgSO ₄ ·7H ₂ O	2.5
Na ₂ HPO ₄ ·7H ₂ O	0.3
NaH ₂ PO ₄ ·H ₂ O	0.9
CaCl ₂ ·2H ₂ O	1.5

7.7.9. Micronutrients-GD	(mg/100 ml)
H ₃ BO ₃	300
Na ₂ MoO ₄ ·2H ₂ O	25
KJ	75
MnSO ₄ ·H ₂ O	1000
ZnSO ₄ ·7H ₂ O	300
CoCl ₂ ·6H ₂ O	125
CuSO ₄ ·5H ₂ O	25

App. 7.8. Extraction buffer for RNA

H ₂ O		205	ml	
CTAB*		10	g	Roth
Tris-HCl (pH 8.0)	[1M]	50	ml	Sigma
EDTA	[0.5M]	25	ml	Sigma
NaCl	[5M]	200	ml	Merck
PVP (K-30)		10	g	Sigma

First dissolve CTAB in ddH₂O (heating can speed up the reaction) and then all other chemicals. After cooling down to RT adjust pH to 8.

App. 7.9. SSTE buffer for RNA extraction

SDS	[10%]	0.5	ml	Roth
Tris-HCl (pH 8.0)	[1M]	0.1	ml	Sigma
EDTA	[0.5M]	20	µl	Sigma
NaCl	[5M]	2	ml	Merck
DEPC-water	[0.1%]	7.38	ml	Sigma

Adjust pH to 8.

App. 7.10. 10x MOPS running buffer for RNA gel electrophoresis

MOPS	[1M]	50	ml	Sigma
Na acetate	[1M]	12.5	ml	Merck
EDTA	[0.5M]	5	ml	Sigma
ddH ₂ O		up to 250	ml	

Adjust pH to 7.

App. 7.11. RNA loading dye (2x)

Formamid	[1M]	660	ml	Sigma
MOPS buffer	[10x] (App. 10)	100	ml	
Formaldehyd*	[0.5M]	80	ml	Merck
Bromphenol blue	[10%]	10	μl	Roth
EtBr**	[10mg/ ml]	10	μl	Roth
ddH ₂ O		140	ml	

* Under laminar air flow. ** Wear nitrile gloves.

App. 7.12. Lists of primers used

Use*	Name	Sequence (5'→3')	Tm°C
1	AthTIL_exp_LP	GTTATCTCTGGATTATGAGC	53.2
1	AthTIL_exp-RP	CCGAAGAGAGATTTGAACC	54.5
2	AthUnk_exp_LP	CAAGACTGGTGGTAATGTTG	55.3
2	AthUnk_exp_RP	GTAGAGTTGCTGGTGGAAATT	55.3
3	PeTIL-V-LP	CATTCTTGCCCATCATTCT	55.3
3	PeTIL-V-RP	ATAGTATCCAGAGATATTTCT	52.8
4	Unknown-IX-LP	AGGCAGTGCTTCAAGAGGAA	57.3
4	Unknown-IX-RP	GCGCTACACGCTGACTGATA	59.4
5	ExActin-5	CGTACAACCTGGTATTGTGCT	55.3
5	ExActin-3	ATCAAAGCATCAGTGAGATCA	54.0
6	PeTIL-II-RP	CGCGGATCCATACTGCTCTATGTTGTGCATGTG	70.7
6	PeTIL-II-LP	CGCGGATCCAAAAAGCAAGGCGATAAAACC	68.1
6	PeTIL-III-RP	CGCGGATCCTGCTCTATGTTGTGCATGTG	69.5
6&8	PeTIL-III-LP	CGCGGATCCAAAGCGAAAAAGCAAGGCGA	69.5
7	TrUnk-I-LP	CGCGGATCCCTGGGTTGGGTTTGAAAGAA	69.5
7	TrUnk-I-RP	CGCGGATCCGTAATAGAGGCCCTGCAT	72.3
8	PeuTIL-pQE-RP	CGCGGATCCCTTTCTAGAATAGATTTGATC	66.8
9	Unk-FUS-pQE-LP	CGCGGATCCTGGGTTGGGTTTGAAAGAAG	69.5
9	Unk-pQE-RP	CGCAGATCTCTAACAGGTCATACCCTGCCAC	70.8
10	PeuLIP_RNAi_LP	CGCGGATCCTCGAGAAATGGAAGTG	66.3
10	PeuLIP_RNAi_RP	CGCGAATCCATGGGTCAGTCTGTG	66.3
11	LBa1	TGGTTCACGTAGTGGGCCATCG	64.0
11	LBb1	GCGTGGACCGCTTGCTGCAACT	65.8
11	AtTIL136775_LP	TTGGCTTTGATTTCATTTCTC	54.0
11	AtTIL136775_RP	TCATTTTTGGGATCAATTTCCG	52.0
11	Unk-LP	CATCGTACCAGGTGAGTCTTTG	60.3
11	Unk-RP	TGAAACACGAAATTGAAAAACAAC	54.2
12	AbiFor	ACGACGTTGTAACGACGCGCCAG	64.4
12	AbiRev	TTCACACAGGAAACAGCTATGACC	61.0
13	35S-LP	GCACAATCCCACTATCCTTC	57.3
13	35S-RP	GCCTGCAGGTCACTGGATTT	59.4
14	BigTDNA-5	GCCAGTGAATTCCCGATCTA	57.3
14	BigTDNA-3	TCAAGTCGGTGACGGTGATA	57.3

* Primers usage descriptions are as follow:

- | | |
|---|---|
| 1- Transcript level AthTIL | 8- Inserting PeuTIL fragment in pQE60 |
| 2- Transcript level AthUnk | 9- Inserting PeuUnk fragment in pQE60 |
| 3- Transcript level PeuTIL and PcaTIL | 10- Inserting PeuTIL fragment in pCK.GUSs/as.Intron2 (RNAi) |
| 4- Transcript level PeuUnk and PcaUnk | 11- Homozygosity test in SALK lines |
| 5- Transcript level Actin in <i>Populus sp.</i> | 12- Sequencing of pGEM-T insertions |
| 6- Amplification of PeuTIL, PcaTIL and PtrTIL | 13- 35S promoter pPCV702 |
| 7- Amplification of PeuUnk and PcaUnk | 14- Detecting TDNA in SALK lines |

App. 7.13. SOC medium (for *Ecoli* transformation)

Bacto tryptone	20 g	Becton, Dickinson
Yeast extract	5 g	Becton, Dickinson
NaCl	0.6 g	Merck
KCl	0.2 g	Merck
MgCl ₂ / MgSO ₄ [1M]*	10 ml	Merck
Glucose [0.5]**	40 ml	Merck
ddH ₂ O	Up to 1 liter	

* Autoclave separately and add after autoclaving medium when its temperature reaches to 50°C. ** Filtrate and add after autoclaving medium when its temperature reaches to 50°C.

App. 7.14. YEB medium for *Agrobacterium* transformation

Beef extract	5 g	Difco
Yeast extract	1 g	Becton, Dickinson
Bacto peptone	5 g	Becton, Dickinson
Sucrose	5 g	Duchefa
biochemie		
Bacto agar*	15 g	Becton, Dickinson
MgSO ₄ [1M]**	2 ml	Merck
ddH ₂ O	Up to 1 liter	
Rifampicin [100mg/ml DMF]***	1 ml	
Gentamycin [10mg/ml]***	1 ml	
Carbenicillin [100mg/ml]***	1 ml	

* When agar plates are needed. ** Autoclave separately and add after autoclaving medium when its temperature reaches to 50°C. *** Don't use after electroporation of competent cells. For YEB agar plates, add after autoclaving medium when its temperature reaches to 50°C. For liquid culture, add at the same time of overnight culturing.

App. 7.15. LB medium for *Ecoli* cultures

Bacto tryptone	10 g	Becton, Dickinson
Yeast extract	5 g	Becton, Dickinson
NaCl	10 g	Merck
Bacto agar*	15 g	Becton, Dickinson
ddH ₂ O	Up to 1 liter	
Ampicillin [100 mg/ ml]**	1 ml	

* When agar plates are needed. ** For LB agar plates, add after autoclaving medium when its temperature reaches to 50°C. For liquid culture, add at the same time of overnight culturing.

App. 7.16. Indicator agar plates for bleu white screening (for 200 ml medium)

Bacto tryptone	2	g	Becton, Dickinson
Yeast extract	1	g	Becton, Dickinson
NaCl	0.2	g	Merck
MgSO ₄ · 7H ₂ O [1M]	0.5	ml	Merck
Bacto agar	3	g	Becton, Dickinson
ddH ₂ O	up to 200	ml	
Ampicillin [100 mg/ ml]*	1	ml	
X-Gal [2% in DMF]*	1	ml	
JPTG*	0.05	g	

* Add after autoclaving medium when its temperature reaches to 50°C.

App. 7.17. TBE buffer (10x)

Ultra Tris	108	g	Roth
Boric acid	55	g	Roth
EDTA	7.46	g	Sigma
ddH ₂ O	up to 1	liter	

Adjust pH to 8 – 8.3.

App. 7.18. DNA loading dye (10x)

Glycerol	[99%]	575	µl	Roth
SDS	[20%]	50	µl	Roth
EDTA	[1M]	200	µl	Sigma
TBE	[10x] (App. 17)	100	µl	
Bromphenol blue	[10%]	10	µl	Roth
ddH ₂ O		65	µl	

App. 7.19. λ Pst DNA ladder (0.2 µg λPst/µl)

λ-DNA	[0.3 mg DNA/ml]	416.5	µl	Fermentas
10x buffer O	[10x]	50	µl	Fermentas
PstI	[10u/µl]	12.5	µl	Fermentas
ddH ₂ O		21	µl	

Note: Incubate at 37°C over night. Add 62.5µl DNA loading dye (10x) and 62.5µl ddH₂O.

App. 7.20. Extraction buffer for DNA extraction from *Arabidopsis*

Tris/HCl pH 7.5	3.15	g	Roth
NaCl	1.46	g	Merck
EDTA	1.04	g	Sigma
SDS	0.5	g	Roth
ddH ₂ O	up to 100	ml	

App. 7.21. 10x TE buffer for DNA extraction from *Arabidopsis*

Tris/HCl pH 7.5	1.576	g	Roth
EDTA	0.416	g	Sigma
ddH ₂ O	up to 100	ml	

App. 7.22. SOB medium for preparation of *E. coli* electrocompetent cells

Trypton	20	g	Becton, Dickinson
Yeast extract	5	g	Becton, Dickinson
NaCl	0.6	g	Merck
KCl	0.2	g	Merck
Bacto agar*	15	g	Becton, Dickinson
MgCl ₂ / MgSO ₄ ** [1M]	10	ml	Merck
ddH ₂ O	up to 1	L	
Tetracycline*** [100mg/ml]	1	ml	

* When agar plates are needed. ** Autoclave separately and add after autoclaving medium when its temperature reaches to 50°C. *** For SOB agar plates, add after autoclaving medium when its temperature reaches to 50°C. For liquid culture, add at the same time of overnight culturing if is needed.

App. 7.23. GTE buffer for plasmid extraction (Mini-Prep)

Glucose	0.99	g	Merck
Tris	0.30	g	Sigma
EDTA	0.38	g	Sigma
ddH ₂ O	up to 100	ml	
Lysozyme*	0.2	g	

Note: Adjust pH to 8.0. * Just for Mini-Prep Agro.

App. 7.24. SDS / NaOH solution for plasmid extraction (Mini-Prep)

SDS [20% w/v]	0.5*	(0.45)**	ml	Roth
NaOH [1M]	2.0*	(1.80)**	ml	Merck
ddH ₂ O	7.5*	(6.76)**	ml	

Note: Prepare fresh before use. * For 50 Mini-Prep *E. coli* preparations ** For 30 Mini-Prep Agro preparations.

App. 7.25. TE buffer for solving DNA pellets

Tris HCl [1 M]	1	ml	Roth
EDTA pH 8.0 [0.5 M]	200	μl	Sigma
ddH ₂ O	up to 100	ml	

Note: Adjust pH to 8.0.

App. 7.26. Potassium acetate (5M) for plasmid extraction (Mini-Prep).

Acetic acid	[1 M]	29.5	ml	
KOH *				Merck
ddH ₂ O		up to	100	ml

* Add KOH pellets up to pH adjust to 4.8 and reach the volume to 100 ml using ddH₂O.

App. 7.27. Amino acid abbreviations

1-letter	3-letter	description
A	Ala	Alanine
R	Arg	Arginine
N	Asn	Asparagine
D	Asp	Aspartic acid
C	Cys	Cysteine
Q	Gln	Glutamine
E	Glu	Glutamic acid
G	Gly	Glycine
H	His	Histidine
I	Ile	Isoleucine
L	Leu	Leucine
K	Lys	Lysine
M	Met	Methionine
F	Phe	Phenylalanine
P	Pro	Proline
S	Ser	Serine
T	Thr	Threonine
W	Trp	Tryptophan
Y	Tyr	Tyrosine
V	Val	Valine
B	Asx	Aspartic acid or Asparagine
Z	Glx	Glutamine or Glutamic acid
X	Xaa	Any amino acid

App. 7.28. Mean and standard deviation of maximum electrolyte conductivity (mS cm^{-1}) per ml tissue water content diluted in 25 ml ddH₂O.

	Control	25 mM	100 mM	200 mM
Root	0.94 ± 0.06	1.04 ± 0.09	1.34 ± 0.15	1.11 ± 0.36
Xylem	0.98 ± 0.20	0.74 ± 0.07	0.98 ± 0.19	1.32 ± 0.20
Bark	1.22 ± 0.08	1.17 ± 0.06	1.35 ± 0.09	2.11 ± 0.32
Stem	1.09 ± 0.06	1.10 ± 0.04	1.25 ± 0.05	1.64 ± 0.26
Shoot apex	1.34 ± 0.03	1.49 ± 0.14	1.65 ± 0.09	1.80 ± 0.55
Leaf	1.66 ± 0.11	1.88 ± 0.08	2.38 ± 0.29	2.61 ± 0.38

App. 7.29. Publication. In the following paper, I have investigated the effect of gradual water deficit on vessel and fiber lumen area and fiber cell wall thickness variations and its reversibility after reirrigation. Changes in xylem anatomy of *P. euphratica* under salinity have been investigated by Junghans *et al.*, 2006. As salinity limit available water to the plant due to osmotic stress, pure water deficit in *P. euphratica* was investigated in following papre. All together it can be concluded that lumen area of vessels and fibers decrease and fiber cell wall increase under both salt and drought stress but *P. euphratica* is much sensible to droght that to salt stress.

Gradual Soil Water Depletion Results in Reversible Changes of Gene Expression, Protein Profiles, Ecophysiology, and Growth Performance in *Populus euphratica*, a Poplar Growing in Arid Regions^{1[W][OA]}

Marie-Béatrice Bogeat-Triboulot^{2*}, Mikael Brosché², Jenny Renaut², Laurent Jouve², Didier Le Thiec, Payam Fayyaz, Basia Vinocur, Erwin Witters, Kris Laukens, Thomas Teichmann, Arie Altman, Jean-François Hausman, Andrea Polle, Jaakko Kangasjärvi, and Erwin Dreyer

Institut National de la Recherche Agronomique Nancy, Unité Mixte de Recherche 1137 Institut National de la Recherche Agronomique-Université Henri Poincaré Ecologie et Ecophysologie Forestières, Institut Fédératif de Recherche 110 Génomique, Ecophysologie et Ecologie Fonctionnelle, F-54280 Champenoux, France (M.-B.B.-T., D.L.T., E.D.); Plant Biology, Department of Biological and Environmental Sciences, University of Helsinki, FIN-00014 Helsinki, Finland (M.B., J.K.); Centre de Recherche Public-Gabriel Lippmann, Cellule de Recherche en Environnement et Biotechnologies, L-4422 Belvaux, Grand-Duché de Luxembourg (J.R., L.J., J.-F.H.); Institut für Forstbotanik, Georg-August-Universität Göttingen, 37077 Goettingen, Germany (P.F., T.T., A.P.); Robert H. Smith Institute of Plant, Sciences and Genetics in Agriculture, Hebrew University of Jerusalem, Faculty of Agricultural, Food and Environmental Quality Sciences, Rehovot 76100, Israel (B.V., A.A.); and Laboratory of Plant Biochemistry, Department of Biology (E.W., K.L.), and Center for Proteome Analysis and Mass Spectrometry (E.W., K.L.), University of Antwerp, B-2020 Antwerp, Belgium

The responses of *Populus euphratica* Oliv. plants to soil water deficit were assessed by analyzing gene expression, protein profiles, and several plant performance criteria to understand the acclimation of plants to soil water deficit. Young, vegetatively propagated plants originating from an arid, saline field site were submitted to a gradually increasing water deficit for 4 weeks in a greenhouse and were allowed to recover for 10 d after full reirrigation. Time-dependent changes and intensity of the perturbations induced in shoot and root growth, xylem anatomy, gas exchange, and water status were recorded. The expression profiles of approximately 6,340 genes and of proteins and metabolites (pigments, soluble carbohydrates, and oxidative compounds) were also recorded in mature leaves and in roots (gene expression only) at four stress levels and after recovery. Drought successively induced shoot growth cessation, stomatal closure, moderate increases in oxidative stress-related compounds, loss of CO₂ assimilation, and root growth reduction. These effects were almost fully reversible, indicating that acclimation was dominant over injury. The physiological responses were paralleled by fully reversible transcriptional changes, including only 1.5% of the genes on the array. Protein profiles displayed greater changes than transcript levels. Among the identified proteins for which expressed sequence tags were present on the array, no correlation was found between transcript and protein abundance. Acclimation to water deficit involves the regulation of different networks of genes in roots and shoots. Such diverse requirements for protecting and maintaining the function of different plant organs may render plant engineering or breeding toward improved drought tolerance more complex than previously anticipated.

¹ This work was supported by the Commission of the European Union (contract ESTABLISH, no. QLK5-CT-2000-01377, coordinator A.P., University of Göttingen, Germany, within the Quality of Life and Management of Living Resources Programme) and by the German Science Foundation to the Poplar Research Group.

² These authors contributed equally to the paper.

* Corresponding author; e-mail triboulo@nancy.inra.fr; fax 33-383-39-40-69.

The author responsible for distribution of materials integral to the findings presented in this article in accordance with the policy described in the Instructions for Authors (www.plantphysiol.org) is: Marie-Béatrice Bogeat-Triboulot (triboulo@nancy.inra.fr).

^[W] The online version of this article contains Web-only data.

^[OA] Open Access articles can be viewed online without a subscription.

www.plantphysiol.org/cgi/doi/10.1104/pp.106.088708

Drought is one of the most important constraints limiting the growth of plants and ecosystem productivity around the world (Passioura, 1996; Aussenac, 2000). Plant responses to water deficit are complex and encompass many aspects, including stress sensing and signaling, changes in growth and biomass allocation patterns, water status homeostasis, decreased stomatal conductance and CO₂ assimilation, osmoregulation, and detoxification processes (Passioura, 1996; Chaves et al., 2003). The impacts of water shortage on plant physiology are numerous and can be assessed at different spatial scales, ranging from the canopy to molecular processes. Approaches at finer scales are expected to improve the understanding of the processes recorded at larger scales. For instance, the biophysics of drought-induced

reduction of cell expansion (Boyer et al., 1985; Cosgrove, 1987) and, at the molecular scale, identification of key genes involved in drought-induced cell wall stiffening (Cosgrove, 2000; Sharp et al., 2004), will contribute to the understanding of the loss of productivity recorded at the organism and ecosystem scales. Moreover, they may help to select genotypes with an improved ability to cope with drought in the future (Vinocur and Altman, 2005; Polle et al., 2006).

Several recent studies have dealt with molecular responses to water shortage (Kreps et al., 2002; Salekdeh et al., 2002; Seki et al., 2002; Xiong and Zhu, 2002; Bray, 2004; Kawaguchi et al., 2004; Vera-Estrella et al., 2004; Hajheidari et al., 2005). However, our knowledge of drought responses in plants is still fragmentary, because previous studies have focused mainly on short-term responses to acute stress rather than on long-term acclimation processes to moderate and gradually increasing water deficits. While short-term studies provide useful information about water deficit sensing and signaling pathways, long-term studies may shed light on genes and/or proteins involved in long-term responses to water deficit and in potential acclimation to low water availability.

In the case of soil water deficit, as opposed to many other abiotic constraints, the time course of water depletion is of central importance, as it may be an effective response modulator in addition to the intensity of the deficit. Indeed, slowly developing soil water depletion usually has physiological consequences that are different from rapid tissue dehydration and possibly implicates different gene networks (Chaves et al., 2003). Up to now, gene expression has been analyzed in plant tissues after exposure to one level of water deficit and/or to short-term dehydration (Kreps et al., 2002; Ozturk et al., 2002; Seki et al., 2002). Furthermore, the impact of water deficit at the proteome level remains relatively unknown and has been restricted to a single level of stress intensity (Salekdeh et al., 2002; Hajheidari et al., 2005; Blödner et al., 2007; Plomion et al., 2006). Gradual soil water depletion is the most common situation for drought in the field and in natural ecosystems. At the whole plant scale, the sequence of events during gradual soil water depletion is well characterized. It usually begins with shoot growth cessation, followed by decreased stomatal conductance, leading in turn to a reduced net CO₂ assimilation rate, impaired photosynthesis, solute accumulation in cells, root growth cessation, and finally, when water availability is very low, induction of leaf senescence and of plant decline (for review, see Passioura, 1996). The changes in transcript and protein profiles underlying the gradual steps of such acclimation processes have received little attention to date.

The genus *Populus* is an obvious choice for analyzing the responses and acclimation processes occurring during soil water depletion in a tree species, due to the numerous genomic tools that have become available during the last few years (Tuskan et al., 2004). Poplars are known to be drought sensitive (Tschaplinski et al.,

1994; Dreyer et al., 2004), so their natural distribution area is mainly restricted to riparian zones (Bruehlheide et al., 2003; Rood et al., 2003). However, some diversity occurs among species and clones with respect to water use efficiency and drought tolerance (Tschaplinski et al., 1994, 1998; Brignolas et al., 2000; Monclus et al., 2006). *Populus euphratica* Oliv. differs considerably from other species of the genus. It grows in semiarid areas and has a strong tolerance to salinity (Sharma et al., 1999; Chen et al., 2003; Gries et al., 2003). Laboratory studies showed that it is able to cope with osmotic stress imposed by NaCl and mannitol (Watanabe et al., 2000; Gu et al., 2004). However, its xylem vessels are among the most vulnerable to drought-induced cavitation (Hukin et al., 2005), suggesting that *P. euphratica* is not intrinsically tolerant to soil water deficit. It is believed that *P. euphratica* is a phreatophyte, able to access deep water, and that its growth rate depends on the depth of the water table (Gries et al., 2003). In an earlier study, we sequenced around 14,000 expressed sequence tags (ESTs) representing genes involved in abiotic stress responses from several normalized and subtracted cDNA libraries produced from control, stress-exposed, and desert-grown *P. euphratica* trees (Brosché et al., 2005). On this basis, a microarray with a unigene set of 6,340 ESTs enriched in stress-related genes was constructed (Brosché et al., 2005) and used in this study to characterize transcriptional responses to gradual soil water depletion. The changes in gene expression were determined at defined stages of water deficit, together with proteomic and physiological alterations and selected stress-related metabolites, to provide a comprehensive analysis of drought acclimation and recovery in Poplar.

RESULTS

Growth, Water Relations, and Gas Exchange in Relation to Water Availability

Young clonal plants of *P. euphratica* were exposed to gradually increasing soil water depletion for about 4 weeks and were fully reirrigated afterward. The soil water content was monitored continuously and was stable through the addition of controlled amounts of water for 3 d prior to sampling (Supplemental Fig. S1). Harvests H1, H2, H3, and H4 were respectively conducted at 35%, 24%, 13%, and 8% relative extractable soil water (soil-REW; Supplemental Fig. S1A; Table I). Harvest H5 was conducted 10 d after full reirrigation.

Decline of stem diameter increment was the first detected effect of soil water depletion (Fig. 1A). It started as soon as soil-REW dropped below 60%, while stem elongation declined at later stages (Fig. 2A; Supplemental Fig. S2). Anatomical analyses of the xylem adjacent to cambium showed that vessel and fiber lumen cross-sectional areas were reduced (Fig. 3, A and B). The decrease in lumen cross-sectional area was accompanied by an increase in vessel density and a

Table 1. Summary of key dates during the soil water depletion experiment

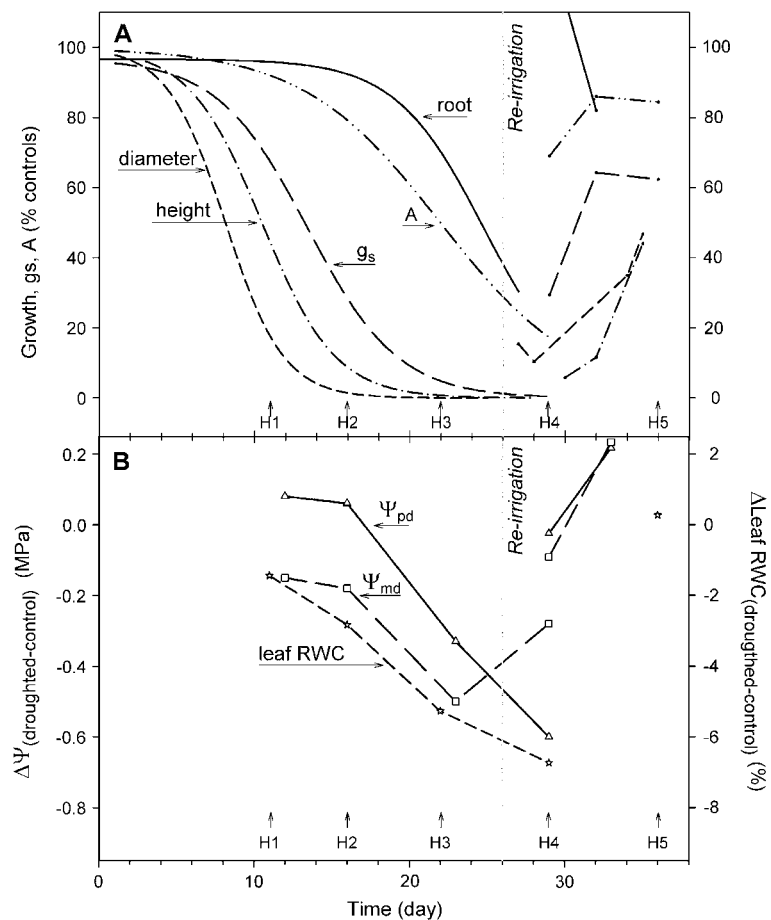
Day	Time Point/Harvest	Stress Level of Harvested Plants
1	Start	
11	Harvest H1	Control and 35% Soil-REW (10% SWC)
16	Harvest H2	Control and 24% Soil-REW (7.5% SWC)
22	Harvest H3	Control and 13% Soil-REW (5% SWC)
26, 29, and 32	Harvest H4	Control and 8% Soil-REW (4% SWC)
26	Rewatering of plants of batch H5	
36	Harvest H5	Control and reirrigated plants (100% soil-REW)

small decrease in fiber density (vessels per fiber per millimeter; data not shown). Reirrigation resulted in the resumption of diameter growth, with an almost full return to predeficit vessel and fiber diameters. This demonstrated that the effect of soil water deficit on cambial activity was reversible. Parallel to reductions in cell lumen size, a significant increase in the thickness of fiber cell walls was recorded (Fig. 3C).

Stem elongation was reduced when soil-REW dropped below 50%, whereas fine root growth was maintained until soil-REW fell below 20% (Fig. 2A; Supplemental Fig. S2). Stomatal conductance to water

vapor (g_s) decreased when soil-REW fell below 40%, before relative leaf water content (RWC) began to decrease (Figs. 1 and 2; Supplemental Fig. S3). Net CO_2 assimilation rate (A) was maintained close to the control level until soil-REW fell below 25%, i.e. long after the onset of stomatal closure. The time lag between the decrease of net CO_2 assimilation rate and that of stomatal conductance demonstrated that *P. euphratica* leaves operated at low instant water use efficiency under conditions of optimal water availability and that water deficit-induced stomatal closure increased it substantially. Reirrigation resulted in a recovery of

Figure 1. Level of physiological functions in drought-stressed *P. euphratica* (relative to controls) as a function of time. A, Growth (diameter, height, and fine roots), net CO_2 assimilation rate (A), and g_s were expressed as a percentage of controls. Sigmoidal curves were adjusted to the data ($y = 100/[1 + \exp\{- (x - x_0)/b\}]$), and correlation coefficients r^2 were 0.90, 0.89, 0.38, 0.78, and 0.95, respectively. B, Ψ_{pd} , Ψ_{md} , and RWC were expressed as the difference between drought stressed and controls. Arrows indicate the five harvest dates (H1–H5). Drought-stressed plants were under controlled irrigation until day 29, while the batch of drought-stressed, reirrigated plants were under controlled irrigation until day 26 and then fully reirrigated.



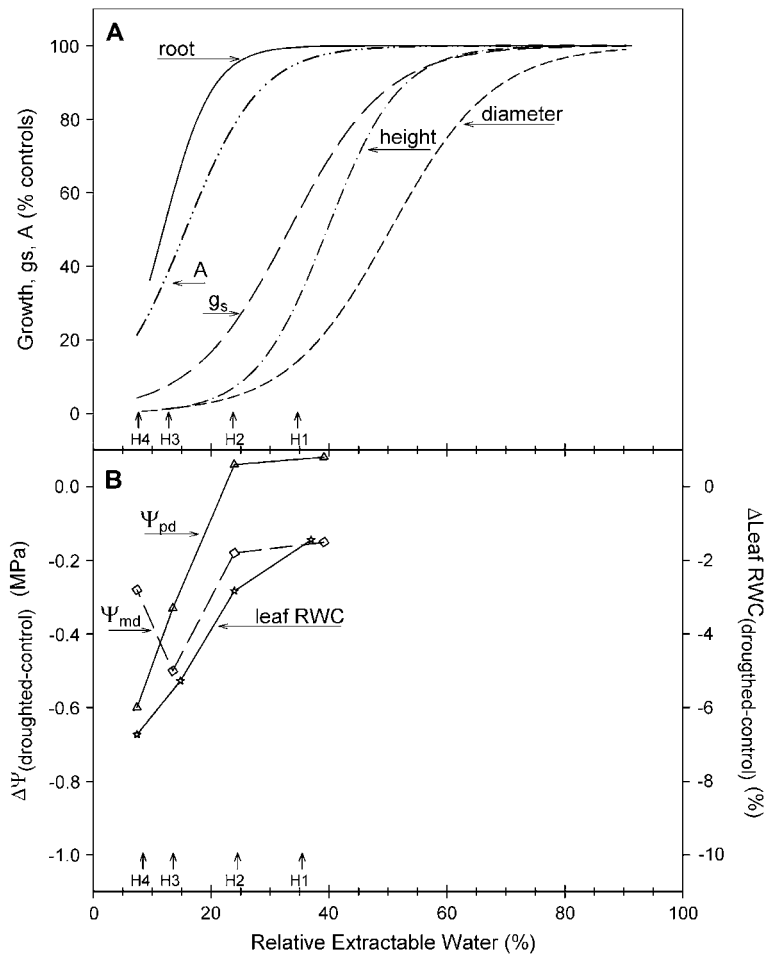


Figure 2. Level of physiological functions in drought-stressed *P. euphratica* (relative to controls) as a function of soil-REW. A, Growth (diameter, height, and fine roots), net CO₂ assimilation rate (A), and g_s were expressed as percent of controls. Sigmoidal curves were adjusted to the data ($y = 100/[1 + \exp\{-(x - x_0)/b\}]$), and correlation coefficients r^2 were 0.90, 0.91, 0.38, 0.80, and 0.94, respectively. B, Ψ_{pd} , Ψ_{md} , and RWC were expressed as the difference between drought stressed and controls. Arrows indicate the soil-REW reached at the first four harvest dates (H1–H4).

these activities at levels varying between 60% and 90% of the control levels (Fig. 1).

Predawn leaf water potential (Ψ_{pd}) was a poor index of the changes in water availability, because it was the latest to be affected out of all the recorded parameters (Fig. 1B). Ψ_{pd} of controls was -0.35 MPa, and it decreased only when soil-REW fell below 20% (Fig. 2B). In contrast, midday leaf water potential (Ψ_{md}) was reduced earlier, when soil-REW was still 40% (Figs. 1B and 2B). After a decrease related to soil water depletion (until soil-REW was 15%), Ψ_{md} recovered partially although soil-REW decreased further, and this was due to transpiration cessation induced by almost complete stomatal closure. RWC of controls was 96%. It decreased by less than 2% when soil-REW was reduced to 40% and by only 8% at the peak stress level (Figs. 1B and 2B).

Characterization of Water Stress Levels

These responses to soil water depletion are indices of the intensity of stress undergone by the plants when harvested for metabolic and molecular analyses (Table

I). At harvest H1, plants were submitted to a moderate level of stress resulting in reduced shoot growth (diameter and elongation) and stomatal conductance and in only slightly reduced RWC and Ψ_{md} . The maintenance of root growth led to an increase in the root-to-shoot ratio, a well-known response to mild water deficit, contributing to the maintenance of plant water status through improved/stabilized water uptake capacity at constant or decreasing transpiration. At harvest H2, the plants displayed reduced stomatal conductance and larger intrinsic water use efficiency due to the maintenance of large net CO₂ assimilation rates. Root growth was still active, while shoot growth stopped almost completely. At H3, plants were stressed; Ψ_{pd} , leaf RWC, CO₂ assimilation, and root growth showed significant decline. At H4, plants suffered very severe stress (shoot growth and transpiration stopped completely; photosynthesis, leaf RWC, and root growth decreased strongly), and this even led to senescence symptoms such as yellowing and shedding of older leaves.

Stressed *P. euphratica* plants were able to recover functionality after 10 d of reirrigation (Fig. 1; Supplemental

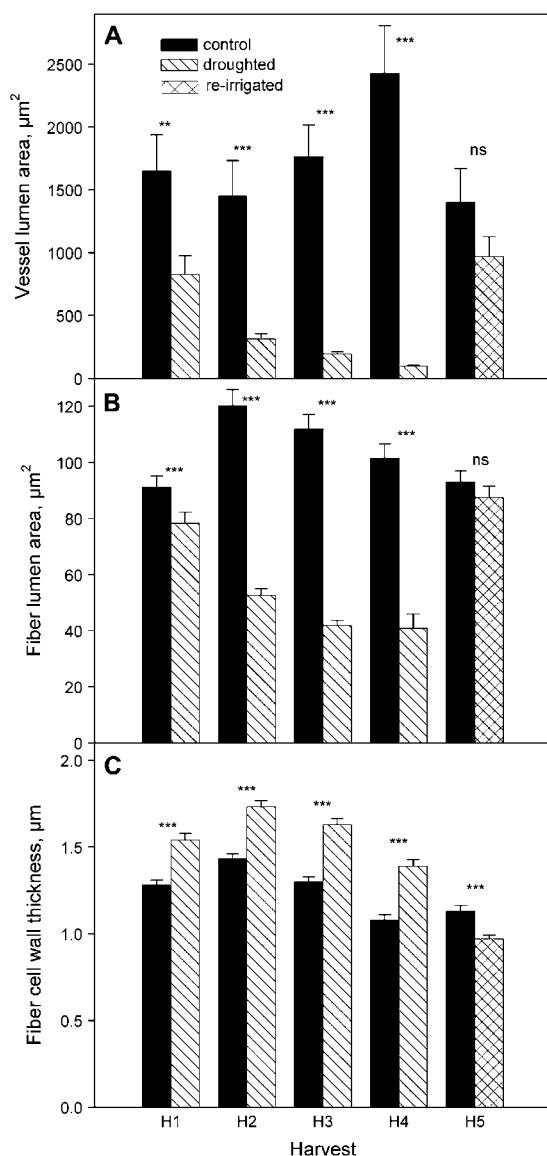


Figure 3. Lumen area of xylem vessels (A) and fibers (B) and fiber cell wall thickness (C) as recorded in stems of *P. euphratica* during water deficit at the five harvest dates. H1 to H4 correspond to four harvest points with increasing soil water depletion and H5 to the harvest after 10 d of reirrigation. Data were recorded in the youngest 100-µm xylem tissue (close to cambium) on two to four plants per harvest and treatment. Mean \pm SE; vessels, $n = 9$ to 95; fibers, $n = 22$ to 369; cell walls, $n = 12$ to 60. *, **, and ***, Difference was significant with $P < 0.05$, $P < 0.01$, and $P < 0.001$, respectively; ns, No significant difference.

Figs. S2 and S3). Stem growth, root growth, stomatal conductance, net CO₂ assimilation, and Ψ (Ψ_p and Ψ_{md} values), respectively, returned to 60%, 80%, 60%, 80%, and 100% of the controls. Growth would probably have recovered completely a few days later, as can be extrapolated from the slope of the growth curves (Fig. 1). Stomatal conductance and photosynthesis reached a plateau 6 d after reirrigation, which may reflect a durable

acclimation induced by the drought episode (improved instant water use efficiency).

Metabolites

The effects of water deficit were also recorded at the metabolite level in leaves. Chlorophyll and carotenoid contents per leaf area were not affected by soil water depletion in mature nonsenescent leaves (harvested from the upper part of the plant; data not shown), but the chlorophyll *a*-to-chlorophyll *b* ratio was significantly increased (Fig. 4). This effect was fully reversed after reirrigation.

Reactive oxygen species (ROS), which occur under stress (Noctor and Foyer, 1998; Mittler, 2002), lead to the oxidation of unsaturated fatty acids in membranes yielding lipid hydroperoxides (LOOH; Taylor et al., 2004). LOOH and malondialdehyde (MDA), a breakdown product resulting from lipid peroxidation, were used as indices for the occurrence of oxidative stress. No direct correlation was found between water deficit level and LOOH or MDA. While MDA concentrations increased at moderate (H1 [$P = 0.06$] to H3) and not high (H4) stress levels, LOOH concentrations increased at H2 and also after reirrigation (Fig. 4). Because the observed increases in these products of oxidative stress were moderate, we concluded that severe membrane injury did not occur.

To analyze the relationship between detoxification pathways and their products, the ratios of MDA and LOOH from stressed relative to nonstressed plants were plotted against the relative transcript abundance of aldehyde dehydrogenase (AIDH), an enzyme involved in the detoxification of products of lipid peroxide metabolism (Bartels and Souer, 2003; Fig. 5). Increases in AIDH transcript abundance under stress initially correlated with increasing concentrations of MDA. This suggests that the moderate induction of AIDH was insufficient to maintain cellular homeostasis of MDA. However, MDA returned to control levels when AIDH transcript abundance was almost 10-fold higher than that of the controls, indicating successful detoxification. It is noteworthy that the relative enrichment of MDA was accompanied by decreases in LOOH (Fig. 5).

Carbohydrate profiling showed that inositol, salicin, Glc, Fru, Suc, and Gal were major osmotic compounds present in the leaves (Supplemental Figs. S4 and S5). Taken altogether, they generated a carbohydrate-induced osmotic pressure of 0.35 MPa in the leaves of the controls (Fig. 6) and their relative contributions were 39%, 38%, 8%, 7%, 7%, and 1%, respectively (data not shown). This was probably a minor fraction of the total osmotic pressure, expected to be around 1.5 MPa in such leaves (Gebre et al., 1998), other potential contributors being mineral ions, amino acids, polyamines, and polyols. Water deficit significantly increased the concentration of these carbohydrates. They generated an osmotic pressure above 0.53 MPa ($P < 0.001$) with only small changes in the relative contribution of the

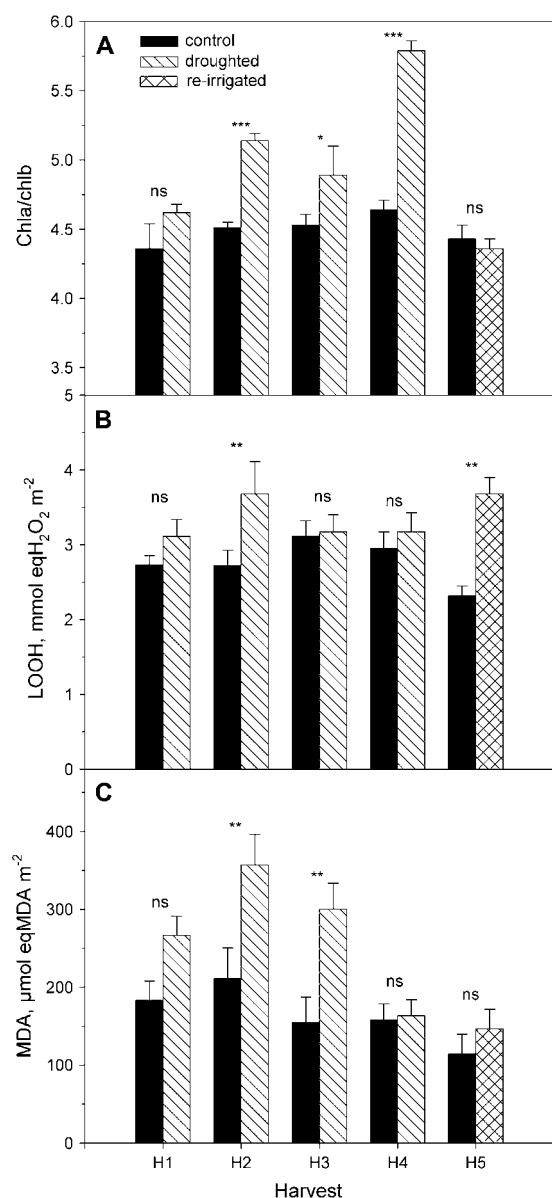


Figure 4. Chlorophyll *a*-to-chlorophyll *b* ratio (A), LOOH (B), and MDA (C) content in *P. euphratica* leaves expressed on a surface area basis at the five harvest dates. H1 to H4 correspond to four harvest dates with increasing soil water depletion and H5 to the harvest after 10 d of reirrigation. *, **, and ***, Difference was significant with $P < 0.05$, $P < 0.01$, and $P < 0.001$, respectively. ns, No significant difference.

different solutes (44%, 32%, 7%, 8%, 6%, and 3%, respectively). Increased carbohydrate content was an early response to water deficit and did not change with increasing soil water depletion. Reirrigation did not result in a return to the control value despite a slight decrease (Fig. 6). Sorbitol, mannitol, trehalose, and stachyose made a negligible contribution to osmotic pressure and were not affected or decreased slightly during water deficit (except for sorbitol and stachyose

that increased transiently at H2; Supplemental Figs. S4 and S5). Galactose and raffinose showed significant increases during water deficit despite a negligible contribution to osmotic potential (Supplemental Fig. S5). Sorbitol, mannitol, and salicin (a phenolic glucoside) remained almost completely unaffected by water deficit but increased sharply following reirrigation (Supplemental Figs. S4 and S5). There was no evidence that leaves were depleted in soluble carbohydrates, even at H4 when the net CO₂ assimilation rate had fallen to 20% of the control level (Fig. 1).

Transcriptional Response to Water Deficit

Leaf and root samples were subjected to gene expression profiling using a *P. euphratica* microarray containing 6,340 different genes (Brosché et al., 2005). Less than 1.5% of the genes on the array displayed significant changes in transcript levels at a 2-fold cutoff, 70 genes in leaves and 40 genes in roots (Fig. 7; Supplemental Tables S1 and S2). In leaves, the number of genes with changed transcript levels increased with the severity of the stress, and one-half of them were specific to harvest H4 at peak stress intensity. The expression profile in roots was very different from that of leaves. Changes occurred earlier, at lower stress intensity, and predominantly consisted of decreased transcript abundances. In both leaves and roots, most genes displaying altered expression during water deficit returned to the control levels after the plants were reirrigated and allowed to recover.

The water deficit-regulated genes were subjected to a cluster analysis to identify patterns of regulation among them (Fig. 7). In leaves, cluster A (eight genes) displayed early increases in transcript levels and a gradual increase in expression level with stress intensity (Supplemental Table S2). Among them were 1,4- α -glucan branching enzyme, thioredoxin H, alcohol dehydrogenase, and cold-regulated LTCOR12. Asn synthetase was not clustered in A but had a similar trend, with a very strong increase at H4. Cluster B (16 genes) showed increased transcript levels at harvests 3 and 4 and included cyclic nucleotide and calmodulin-regulated ion channel, putative pheophorbide *a* oxygenase, and a homeodomain transcription factor. Cluster C (22 genes) showed increased transcript levels only at the most severe stress level H4 and included many genes with a function in protein and sugar metabolism: Cys protease(s), trypsin inhibitors, Xyl isomerase, and Suc synthase. Genes with decreased transcript abundance fell into two clusters: D (five genes) displayed lowered transcript levels at harvests 2 to 4 and included a Pro-rich cell wall protein and an aquaporin; E (14 genes) showed a large decrease in transcript levels at harvest 4; the majority of these genes were related to photosynthesis.

Cluster analysis of transcript levels in roots identified five major clusters (Fig. 7). Cluster F (seven genes) displayed early (H1) decreased transcript abundance and included a Leu-rich repeat protein. Genes with the

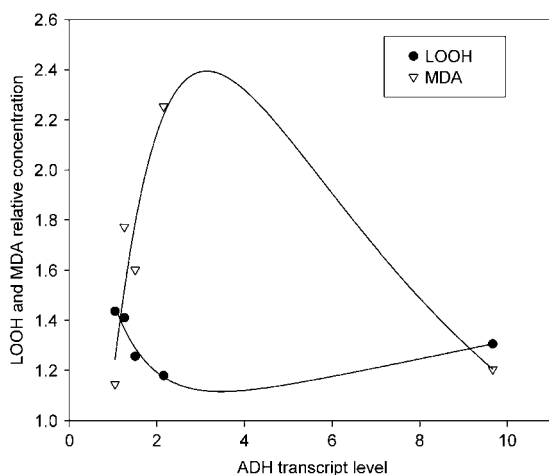


Figure 5. Correlation between relative concentrations (drought stressed versus controls) of LOOH, MDA, and ADH transcript levels in leaves of *P. euphratica*. Log normal peak and exponential decay regression curves were fitted to LOOH and MDA, respectively.

lowest transcript level at the most severe stress intensity fell into cluster G (16 genes) and included three aquaporins (two plasma membrane intrinsic proteins [PIPs] and one tonoplast intrinsic protein [TIP]), Suc synthase, and, more strangely, genes identified as responsive to abiotic stress such PR10 protein, dehydration-responsive protein RD22, and glutathione S-transferase. Cluster H grouped genes with lowered transcript abundance, specifically at H2, and three of the four genes had a chaperone function, namely two heat shock proteins (HSPs) and a DNA K-type molecular chaperone. Cluster I (six genes) had increased transcript abundance, showed the highest expression level at H4 and included storage protein(s). Genes with early increased transcript levels in roots were clustered in J (seven genes), and most of them had a putative role in biotic or abiotic stress: cold-regulated LTCOR12 and drought-inducible short-chain alcohol dehydrogenase and metallothionein 2a.

Only one gene (cold-regulated LTCOR12) displayed increased, and another one (metallothionein type 2b) reduced, transcript levels in both tissues. Intriguingly, other members of the metallothionein family displayed opposite expression patterns with increased transcript levels in roots (metallothionein type 2a and 3a). Furthermore, Suc synthase increased in leaves but decreased in roots, suggesting the translocation of carbon from leaves to roots.

To validate the array results, quantitative real-time reverse transcription (RT)-PCR (qPCR) was conducted on three genes selected on the basis of different transcript level increases: no (ribosomal protein L17), moderate (calmodulin-regulated ion channel), and large (Cys protease). The RNA samples used in the DNA microarray analysis were used as templates in qPCR (Table II). For the first two genes, the expression

measured with qPCR agreed with the microarray results. Cys protease displayed a significantly higher relative expression in the qPCR analysis, but the overall response pattern was similar to that found with the microarrays. This difference probably reflects the higher dynamic range of qPCR compared to array analysis (Czechowski et al., 2004).

Protein Abundance

The abundance of individual proteins was measured in leaves by two-dimensional gels combined with fluorescent labeling (Supplemental Fig. S6). Changes in intensity were detected for 375 spots, but, in contrast to the leaf transcriptome, where the number of regulated genes increased with stress intensity, no such trend was detected for proteins (Fig. 8). Furthermore, a higher number of proteins showed changed abundance at the first harvest than at later ones. After reirrigation, the number of proteins with changed abundance increased again slightly. Among the 100 proteins tested, 39 could be identified by mass spectrometry, either by peptide mass fingerprinting (PMF) or by matrix-assisted laser-desorption ionization (MALDI)-tandem mass spectrometry (MS-MS) analysis (Supplemental Table S3). Among proteins whose abundance was higher in stressed plants, we found proteins related to energy and carbon metabolism (ATP synthase β -subunit, ATPase α -subunit; Rubisco activase, oxygen-evolving complexes involved in photosynthesis) and proteins involved in glycolysis, such as glyceraldehyde-3-P dehydrogenase and phosphoglycerate kinase. Their relative abundance (as compared to the controls) was higher at moderate stress levels and after reirrigation than at peak stress intensity. Unexpectedly, most of the proteins with decreased abundance were HSPs and

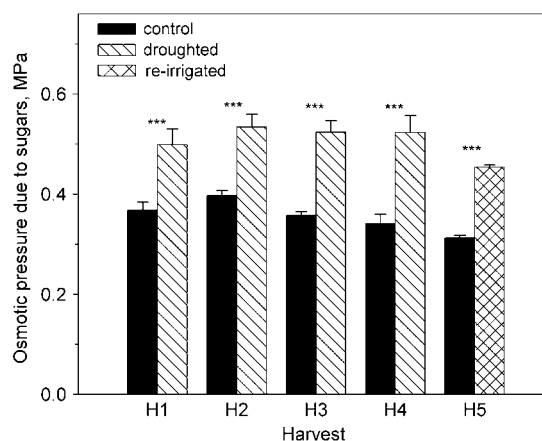


Figure 6. Full turgor osmotic pressure generated in *P. euphratica* leaves by soluble carbohydrates (megaPascal) as computed from concentrations at the five harvest dates. H1 to H4 correspond to four harvest points with increasing soil water depletion and H5 to the harvest after 10 d of reirrigation. ***, Difference was significant with $P < 0.001$.

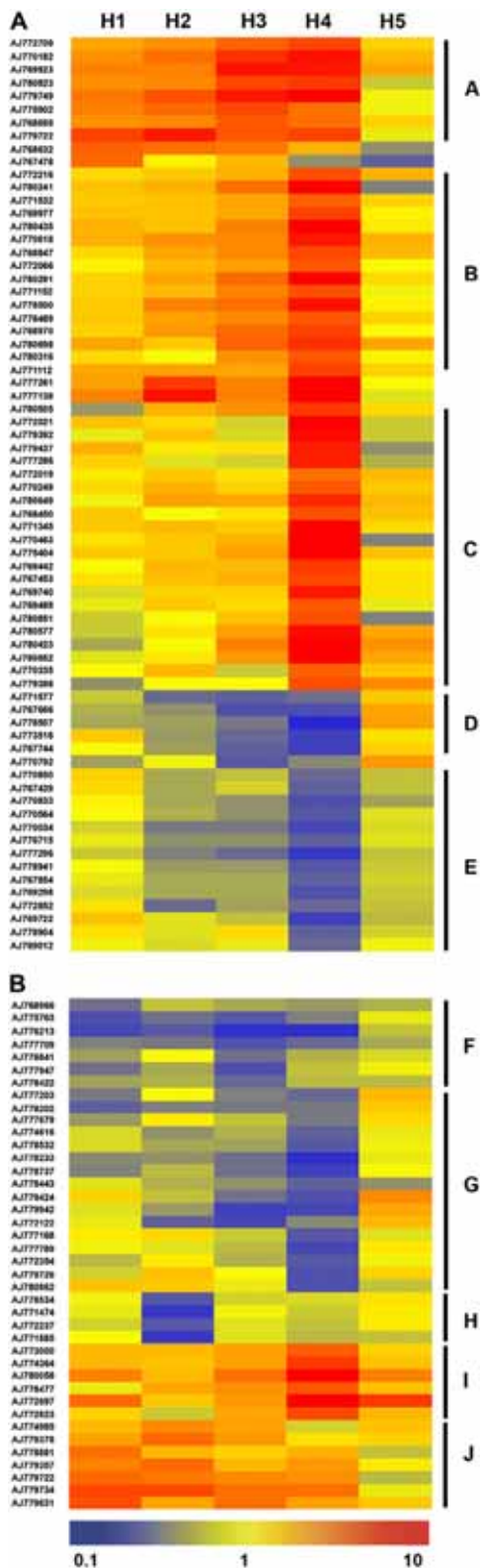


Figure 7. Differentially expressed transcripts in leaves (A) and roots (B) of *P. euphratica* during water deficit at the five harvest dates (minimum

chaperones known to be involved in stress response and defense mechanisms. Their relative abundance was more or less independent of stress intensity except for the chaperones, whose abundance was close to the control level at H2.

Stable protein-1 (SP1) was extracted from separate samples and its abundance was measured independently. SP1 is a homoooligomeric protein with exceptional stability under a variety of harsh conditions, such as boiling, proteolysis, and denaturation by strong detergents and high salt concentrations (Wang et al., 2002). Similarly to chaperonins and HSP, the abundance of SP1 was decreased by water deficit (Fig. 9) and the difference between the controls and water-stressed plants was highest when stress was still moderate (H2) and decreased at peak stress intensity (H4).

Relationship between Gene Expression and Protein Abundance

For eight of the 39 proteins identified, we found a corresponding EST on the microarray. These EST-protein pairs were Rubisco activase, chloroplast glyceraldehyde-3-P dehydrogenase A, carbonate dehydratase, chloroplast phosphoglycerate kinase, cytosolic phosphoglycerate kinase, 60-kD chaperonin β -subunit, HSP 70, and cell division cycle 48. Within each pair, there was no correlation between the transcript and the protein abundance ratios (Table III). Globally, for these eight genes, the transcript ratios were close to 1 (with two exceptions), independently of harvest date, while the protein abundance ratio significantly differed from 1. Similarly, the transcript level of *sp1* did not vary despite the recorded changes in abundance of the protein SP1 (data not shown).

DISCUSSION

Transcriptome Analysis

This is the first comprehensive study, to our knowledge, encompassing a detailed characterization of whole plant performance, ecophysiology, and molecular responses to a gradually increasing water deficit and recovery, taking into account the time course and the intensity of the stress imposed on the plants. *P. euphratica*, a relatively drought-sensitive poplar species (Hukin et al., 2005), was used, and the whole response spectrum of acclimation from mild to severe water deficit was covered.

Transcriptional profiling showed that less than 1.5% of the genes on the stress-enriched EST microarray (Brosché et al., 2005) were responsive to water deficit. This is in contrast to the 30% to 35% genes that were

fold change of 2 and *P* value of 0.05). H1 to H4 correspond to four harvest dates with increasing soil water depletion and H5 to the harvest after 10 d of irrigation. The most important clusters of transcriptional changes (A–H) are indicated. See text for details.

Table II. Transcript abundance ratio of three genes in *P. euphratica* leaves measured by microarray and by qPCR at the five time points of the experiment (H1–H5)

For the qPCR, Ct values were normalized against a glucosidase α -subunit standard to get normalized Δ Ct values, which were used to calculate the fold change in expression between control and drought samples.

GenBank ID	Gene	Method	H1	H2	H3	H4	H5
AJ780423	Cys protease	Array data	0.7	1.0	2.3	13.1	1.9
		RT-PCR	4.3	31.9	266.9	600.5	7.3
AJ780698	Cyclic nucleotide and calmodulin-regulated ion channel	Array data	1.5	1.2	3.0	4.3	1.5
		RT-PCR	1.2	1.8	3.5	3.6	1.7
AJ777362	Ribosomal protein L17	Array data	1.1	1.1	1.0	0.9	1.2
		RT-PCR	1.0	1.4	0.8	1.0	1.0

reported to undergo changes at the same cutoff of 2 in response to different abiotic stresses in *Arabidopsis* (*Arabidopsis thaliana*; El Ouakfaoui and Miki, 2005). Nevertheless, in several other studies, a smaller fraction of genes (from 1%–10%) was regulated depending on the applied stress and on the plant organ (Kreps et al., 2002; Ozturk et al., 2002; Seki et al., 2002). In *Arabidopsis*, the number of regulated genes was higher shortly after stress onset (Kreps et al., 2002). Similarly, *P. euphratica* exposed to salt shock expressed a higher number of genes than after acclimation (Ottow et al., 2005). Because we focused on long-term and acclimation responses to drought in this study, genes involved in stress sensing or signaling were probably missed. Many genes identified in our study are probably involved in processes maintaining new steady states arising from decreased water availability. Several of these genes may play a role in acclimation to reduced water availability, as the intensity of the changes in transcript level increased with water deficit intensity.

Among the putative acclimation genes that showed an early response were Asn synthetase, cold-regulated LTCOR12, thioredoxin H, and alcohol dehydrogenase. Significantly increased transcript levels of a homeo-domain transcription factor and RING zinc finger protein were detected at a slightly higher stress level (H2); this indicated that acclimation to water deficit also involved reprogramming of transcriptional regulation. Some of the genes regulated at harvest H4 only, i.e. under severe stress, may be related to the induction of senescence, because older leaves were shed. The pronounced induction of Asn synthetase (20-fold at this time point) suggests a strong remobilization of nitrogen before leaf senescence. The concomitant strong induction of storage proteins in roots ($\times 23$ at H4) supports this suggestion. Thaumatin-like protein (osmotin), which showed increased transcript abundance at H4 in leaves, has been suggested to be induced by cell turgor loss (Bray et al., 2000). Callose synthase could be implicated in the blockage of vessels before leaf abscission. Finally, Cys protease, involved in protein catabolism and programmed cell death (Harrak et al., 2001), was also strongly induced at H4. However, changes in transcript level are not sufficient to indicate a role in water deficit acclimation, because translational and posttranslational regula-

tions largely affect the amount and activity of the corresponding proteins (Gygi et al., 1999; Kawaguchi et al., 2004).

A corresponding trend, i.e. increasing transcript levels with decreasing extractable soil water, was not found in roots. Over one-half of the regulated genes in roots were repressed, and there was no general relationship between the extent of change and soil water deficit. In both roots and leaves, reirrigation resulted in a recovery of transcripts to the control levels for most genes, showing that the observed transcriptional responses were fully reversible. For a few genes (1,4- α -glucan branching enzyme, Cys protease), significantly increased transcript levels persisted but with a lower ratio. This may be due to the inertia of the response or to a slow turnover of these mRNAs.

Proteome Analysis

In contrast to the transcriptional response in leaves, the number of proteins whose relative abundance was modified by water deficit showed no correlation with stress intensity. This could be due to the fact that, contrary to the ESTs present on the microarray that

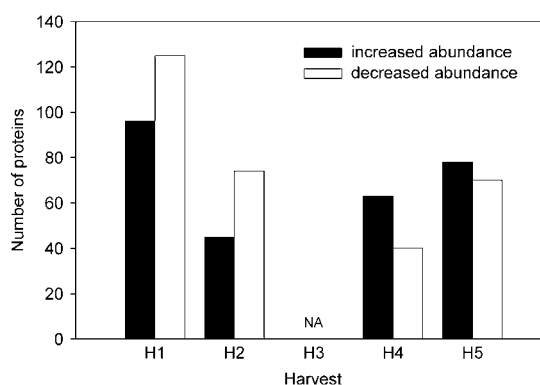


Figure 8. Number of proteins showing an increased or decreased abundance in *P. euphratica* leaves during water deficit at four harvest time dates. H1, H2, and H4 correspond to three harvests with increasing soil water depletion and H5 to the harvest after 10 d of reirrigation. NA, Not analyzed.

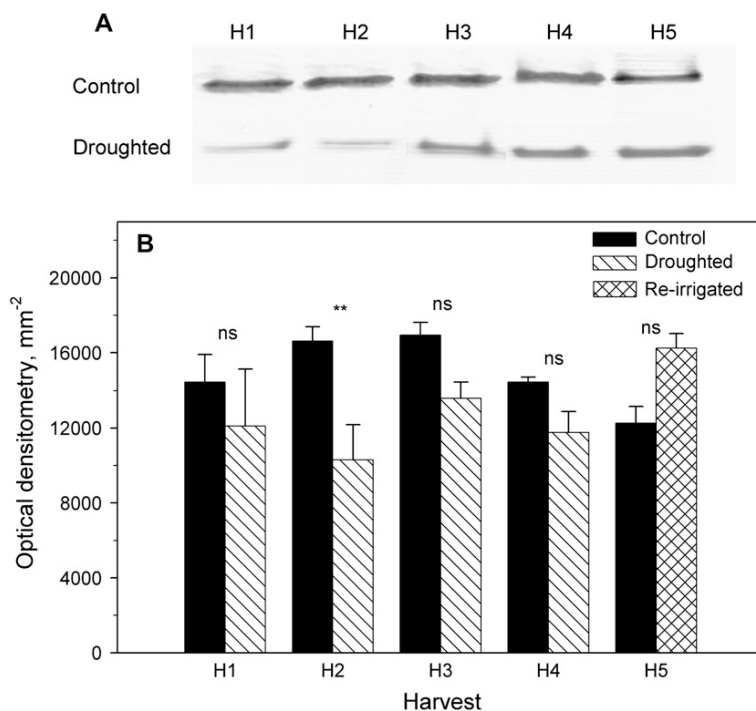


Figure 9. Abundance of SP1 proteins in *P. euphratica* leaves analyzed by SDS-PAGE analysis with Coomassie Blue staining (A; one representative sample) and by optical densitometry (B) at five harvest dates. H1 to H4 correspond to the four harvest dates with increasing water depletion and H5 to the harvest after 10 d of reirrigation. Values are means \pm SE ($n = 2-4$). **, Significant difference at $P < 0.01$; ns, no significant difference.

belong to a stress-enriched collection, the proteins separated on the gel only cover soluble proteins in the pH range 4 to 7. Moreover, the analysis was also limited because proteins of low abundance were likely to be overlooked, and the results might be biased toward dominant housekeeping proteins. Among the few identified proteins for which ESTs were present on the array, no correlation between transcript level and protein abundance was found, but, as highlighted by Gygi et al. (1999), mRNAs identified by transcriptome analysis are not always translated, and, therefore, transcript and protein abundances are not necessarily linked. Recently, Kawaguchi et al. (2003, 2004) have shown that differential translational regulation makes a large contribution to the response to water deficit. Moreover, posttranslational modifications (e.g. phosphorylation, methylation, glycosylation) may further modify the apparent abundance of proteins by displacing them on the gel (Newton et al., 2004). The relative importance of changed transcription and of posttranscriptional regulation during stress responses in plants will be an important area for future studies.

Growth Reduction and Biomass Allocation in Relation to Molecular Physiology

The frequency of measurements in this study allowed the physiological perturbations induced by water deficit to be finely dissected. Growth was the most drought-sensitive process, as already described by Hsiao (1973). Stem radial growth was reduced before stem elongation, and the high sensitivity of

radial growth to drought is a well-known feature in adult trees (Breda and Granier, 1996). Growth results from cell division and cell expansion, and both processes are sensitive to water shortage (Lecoeur et al., 1995). It would be interesting to understand why secondary meristems are more sensitive to reduced water availability than primary meristems.

In the analysis of gene expression in young mature leaves, two ESTs corresponding to a Pro-rich cell wall protein showed early lowered transcript abundance with respect to the course of soil water depletion. Moreover, transcript abundance was negatively correlated to water deficit intensity, suggesting that leaf growth was also reduced. Interestingly, this gene showed significantly increased transcript abundance following reirrigation when shoot growth was resuming.

In contrast to leaf or stem growth, root growth was maintained until a low level of soil water content was reached. This change in growth allocation in favor of roots resulted in an increase of the root-to-shoot ratio, which alleviated to some extent the impairment of the plant water status through improved soil prospection at constant leaf area (Sperry et al., 2002). These water deficit-induced changes of growth allocation were accompanied by a large regulation of carbohydrate and nitrogen metabolisms, which are coregulated in higher plants (Ferrario-Mery et al., 1998). For instance, the increased transcript levels of Asn synthetase already present at mild stress levels may correspond to the shift of growth allocation from shoots to roots, because Asn is a major metabolite for nitrogen remobilization upon senescence (Dangl et al., 2000). Suc

Table III. Protein and gene transcript abundance ratios in *P. euphratica* leaves for eight genes at 4/5 dates corresponding to different water deficit intensities

H1 to H4 correspond to the four harvests with increasing water depletion and H5 to the harvest after 10 d of reirrigation. Protein AC, Protein accession number in Uniprot Database.

Protein AC	Name	Proteomics Data					Array Data					GenBank ID
		H1	H2	H3	H4	H5	H1	H2	H3	H4	H5	
Q9ATC1	Rubisco activase (fragment)	2.3	1.2		0.9	1.3	1.1	0.9	1.0	0.9	1.0	AJ780799
P12858	Glyceraldehyde-3-P dehydrogenase A, chloroplast (precursor)	2.8	1.7		1.3	2.1	1.2	0.9	1.0	1.0	0.9	AJ767436
Q41089	Carbonate dehydratase (EC 4.2.1.1) 1b	2.9	1.5		1.3	1.8	1.1	1.1	0.9	0.7	0.9	AJ767433
O82160	Chloroplast phosphoglycerate kinase	2.0	1.5		1.1	1.6	1.1	0.8	0.7	0.7	0.9	AJ769268
O82159	Cytosolic phosphoglycerate kinase 1	0.7	1.1		0.5	0.5	1.1	0.9	0.8	1.2	1.1	AJ775507
P08927	60-kD chaperonin β -subunit	0.7	0.9		0.7	0.5	1.1	1.0	1.0	1.0	1.0	AJ773373
Q9M4E6	HSP70	0.4	0.6		0.9	0.6	1.0	0.6	0.5	1.4	1.1	AJ772900
P54774	Cell division cycle 48	0.6	0.5		0.6	0.5	1.0	1.0	0.9	2.1	1.4	AJ775535

synthase was induced early in leaves and Suc concentration was increased by 25% under mild stress and by 50% under severe stress, whereas the transcript level of Suc synthase was consistently repressed in roots from the early stages of soil water depletion. The small contribution of Suc to the carbohydrate-induced osmotic potential (less than 0.03 MPa) suggests that Suc may play a role as a messenger (sugar sensing) or as a membrane/macromolecule stabilizer rather than an osmoprotectant.

Water Status in Relation to Metabolic and Transcriptional Profiles

P. euphratica is a phreatophyte species able to grow in desert areas because its roots access deep water tables (Gries et al., 2003). The occurrence of vessel embolism before stomatal closure (Hukin et al., 2005) confirmed that this species is not intrinsically drought tolerant. Thus, we expected that its capacity to acclimatize to water deficit would be limited. Although Ψ_{pd} was affected late in the time course of the experiment, Ψ_{md} and RWC were already significantly decreased at early stages of water deficit. Mild water deficit resulted in increased concentrations of soluble sugars and polyols, increasing the carbohydrate-induced osmotic pressure and thus potentially contributing to cell turgor maintenance. The osmotic adjustment capacity based on soluble carbohydrates was however, limited, because no further increases were observed, and, at maximum stress, the transcript level of thaumatin-like protein was increased; this has been suggested to be a response to turgor loss (Bray et al., 2000).

The role of aquaporins in the regulation of water relation during water deficit has been the subject of numerous studies but remains unclear (Javot and Maurel, 2002; Aharon et al., 2003; Luu and Maurel, 2005). A decreased transcript abundance of three water channel-encoding genes (two PIPs and one TIP) was recorded in roots but only at peak water deficit. A down-regulation of aquaporins by water shortage has

already been observed (Smart et al., 2001), but when all members of the PIP family of Arabidopsis were taken into account, some were up-regulated and others were markedly down-regulated by water shortage (Jang et al., 2004). The decrease of aquaporin transcripts was simultaneous to severe root growth decline. Another event occurring toward peak stress intensity was the decrease of Ψ_{pd} , indicating that leaf water status was no longer recovered during the night and that stress became severe. Thus, the decreased transcript level of aquaporins in roots could also be seen as enabling the construction of a barrier against water efflux from roots to dry soil due to reduced membrane water permeability (Smart et al., 2001).

Photosynthesis in Relation to Molecular Response

The maintenance of a high rate of net CO₂ assimilation until a relatively low extractable soil water content was reached, despite the recorded decline of stomatal conductance, allowed an increase in the instantaneous water use efficiency (A/g_s). Full or partial maintenance of photosynthesis at moderate stress levels, despite lower internal CO₂ concentrations, was accompanied by almost no transcriptional changes of photosynthesis-related genes before the most severe stress level was attained. However, it was accompanied by an increased abundance of photosynthesis-related proteins, such as oxygen-evolving complex 33-kD PSII, Rubisco activase, carbonate dehydratase (or carbonic anhydrase), chloroplast glyceraldehyde-3-P dehydrogenase, and phosphoglycerate kinase. Oxygen-evolving complex 33-kD PSII protein, an extrinsic subunit of PSII probably involved in the stabilization of the PS components (Murakami et al., 2005), was also affected under mild drought stress in spruce (*Picea abies*; Blödner et al., 2007). Rubisco activase, which regulates the activity of Rubisco in response to changes in light or temperature via ADP-to-ATP ratio and redox potential (Zhang and Portis, 1999), also accumulated in rice (*Oryza sativa*) under drought stress (Salekdeh et al., 2002). Carbonic anhydrases may be

candidates for the coregulation of mesophyll conductance and photosynthesis (Evans and von Caemmerer, 1996) and play an important role during drought and salinity stress (Flexas et al., 2004). Glyceraldehyde-3-P dehydrogenase and phosphoglycerate kinase are enzymes involved in the pentose phosphate cycle but could be impaired under drought stress (Flexas et al., 2004). This early occurrence of increased abundance of photosynthesis-related proteins during the stress treatment may have partly counterbalanced the decreased internal CO₂ concentration and contributed to the partial maintenance of photosynthesis during the first stages of water deficit. On the other hand, a putative pheophorbide a oxygenase displayed an increased transcript level (at H2). This observation is consistent with the observed increase of the chlorophyll *a*-to-chlorophyll *b* ratio, a known indication of chlorophyll catabolism when chlorophyll *b* is converted to chlorophyll *a* during senescence (Tanaka et al., 2003). At peak stress intensity, the repression of photosynthesis-related genes (Rubisco small subunit, PSI reaction center subunit VI and X) may be due to stress severity and could indicate the beginning of senescence.

Cell Homeostasis and Detoxification

The analyses of transcript, protein, and metabolite abundances showed that many enzymes or metabolites involved in cell homeostasis were regulated under soil water deficit. Among the identified regulated proteins, we found many HSPs and chaperonins, involved in protein repair and protection against denaturation, which are normally synthesized on abiotic stress exposure (Sung et al., 2001; Wang et al., 2004). For instance, a significantly higher content of chaperonin 60 (β -subunit) was found in a drought-resistant variety of sorghum, as compared with susceptible varieties, and was thought to have a positive impact on the stability of the photosynthetic components (Jagtap et al., 1998). In watermelon (*Citrullis vulgaris*), HSP70 accumulated in plants exposed to water deficit (Kawasaki et al., 2000). Surprisingly, the abundance of HSP and chaperonins were significantly decreased by water deficit in leaves of *P. euphratica*, especially at the first harvest. This may point to the inability of *P. euphratica* to activate protective processes against drought. Another reason for these contrasting results may be that our measurements were carried out after acclimation of the plant for several days to a new stress level, whereas earlier studies usually analyzed instantaneous stress responses. This idea is supported by the stress behavior of SP1, which probably has similar functions to HSP and chaperonins (Dgany et al., 2004). The *sp1* gene in *Populus tremula* plants was found to be up-regulated shortly after the application of different abiotic stresses, such as salt, cold, heat, and mannitol, but *sp1* was severely down-regulated after 24 h of exposure to mannitol (Wang et al., 2002). Similarly, the abundance of SP1 proteins was slightly reduced in water stress-acclimatized *P. euphratica* plants.

Raffinose accumulated in *P. euphratica* leaves in response to water deficit without significantly contributing to osmotic adjustment because of its low concentration. This oligosaccharide may increase drought tolerance due to its role in stabilization of membranes via interactions with phospholipid headgroups (Bentsink et al., 2000). We had no evidence of oxidative membrane degradation, and fatty acid biosynthesis appeared to be stimulated, as suggested by the elevated abundance of a putative macrolide-type polyketide synthase. Pro accumulated in leaves of *P. euphratica* in response to osmotic stress during earlier studies (Watanabe et al., 2000; Ottow et al., 2005). This is a common drought response, but, as for raffinose, the overall Pro concentrations were too low to affect cell osmotic pressure and were expected to have protective functions. It has also been suggested that compatible solutes may function as ROS scavengers (Ottow et al., 2005). The role of components such as sorbitol, mannitol, and salicin, which accumulated only after reirrigation, remains to be explained.

Metallothioneins belong to a small multigene family, of which different genes are constitutively expressed in poplar and respond differentially to environmental stimuli (Kohler et al., 2004). In addition to their role in detoxification of heavy metals, they probably contribute to cell homeostasis in response to diverse stresses (Cobbett and Goldsbrough, 2002). For instance, transcript levels of type 2 metallothionein increased in water-stressed watermelon; an increase of type 2 metallothionein was proposed to enhance scavenging of oxygen radicals (Akashi et al., 2004). In our experiment, type 2b metallothionein decreased both in leaves (late at H4) and in roots (earlier), but type 2a and 3a metallothioneins severely increased in roots only, confirming the diversity of the response of these genes.

It remains unclear how redox regulation was achieved during water deficit in our experiment. No significant changes were found in transcript or protein abundance for typical antioxidative systems such as superoxide dismutase, catalase, or other enzymes constituting typical ROS-scavenging pathways (Polle et al., 2006). Only thioredoxin transcript abundance was increased. In leaves of *P. euphratica*, typical ROS-detoxifying systems were activated during salt shock but not during long-term salinity stress, suggesting that they are required during acute stress scenarios (Ottow et al., 2005). ROS lead to the oxidation of unsaturated fatty acids in membranes, yielding LOOH (Taylor et al., 2004). These hydroperoxides are degraded nonenzymatically and cause the formation of carbonyl compounds, many of which are aldehydes (Noordermeer et al., 2000; Schneider et al., 2001). The moderate increases in MDA and LOOH were, therefore, indicating moderate oxidative stress. Moreover, MDA appeared to have been purged when transcript levels of AIDH were significantly increased. Indeed, enzymes such as alcohol dehydrogenase and AIDH have been shown to play vital roles in the detoxification

of products of lipid peroxide metabolism (Bartels and Souer, 2003). Increased transcript abundance of AIDH was also found in other plant species in response to water shortage (Ozturk et al., 2002; Bray, 2004), and its overexpression in transgenic *Arabidopsis* conferred higher stress tolerance (Sunkar et al., 2003).

This study provided some clues about the long-term acclimation process to soil water deficit. The reduction of shoot growth and changes of transcription levels in genes related to carbon and nitrogen metabolism were the earliest recorded responses. They occurred before other process involved in water balance maintenance, such as stomatal closure or the increase of instant water use efficiency. Most of these water deficit-induced changes were reversible, at the transcriptome as well as the whole plant level. Acclimation involved the regulation of only a small number of genes, and changes in transcription level increased with stress intensity. Different networks of genes were involved in roots and shoots. Such diverse requirements for protecting and maintaining the function of different plant organs may render plant engineering or breeding toward improved drought tolerance more complex than previously anticipated.

MATERIALS AND METHODS

Experimental Design

Plantlets of *Populus euphratica* Oliv. were multiplied by in vitro culture from tissues collected from a single mother tree originating from the desert in the Ein Avdat National Park, Israel (provided by A. Altman, Rehovot University, Israel). After ex vitro acclimation to greenhouse conditions for 6 weeks in Goettingen, plantlets were transferred to Institut National de la Recherche Agronomique Champenoux and acclimatized in a greenhouse made of fully transparent glass. After 2 weeks, they were transplanted into 7.5-L pots made from transparent Perspex tube (35 cm height, 15 cm in diameter) covered by black plastic film and filled with a peat-sand mixture (50:50, v/v). Full fertilization was provided using a slow release fertilizer (4 g L⁻¹ Nutricote 13:13:13 NPK and oligonutrients). The plants were grown there for 2 months (May and June). Ambient conditions in the greenhouse depended on the external weather conditions, but the temperature was maintained in the range 15°C to 27°C with a few uncontrolled peaks (34°C), and peak irradiance varied between 400 and 1,500 μmol m⁻² s⁻¹ (cloudy versus sunny days).

Before the experiment started, batches of plants (of homogeneous size) were constituted and designated to an identified purpose. A batch of 19 plants, referred to as nondestructive measurement (NDM) plants (seven controls and 12 water-deprived plants, of which one-half were reirrigated after 25 d of water deficit), was used to monitor growth and physiological parameters nondestructively during the whole experiment: height and diameter increment, leaf emission rate, root growth, leaf water potential, net CO₂ assimilation, and stomatal conductance. Five other batches (of five controls and five water-stressed plants each) were designated to be harvested at five successive dates corresponding to four increasing water deficit intensities and one recovery point. These plants were moved only for monitoring the water content of the substrate. Soil water depletion evolved similarly in all batches during the course of the experiment (Supplemental Fig. S1).

Controls were watered to field capacity twice per day. A moderate and slowly increasing water deficit was applied and controlled for 4 weeks. Soil volumetric water content (SWC) was measured once or twice per day, depending on the stress intensity, by weighing the pots with a time domain reflectometry probe (Trase, Soilmoisture Equipment). For each pot, watering was withheld until SWC reached the target level (which took several days), and thereafter, controlled amounts of water were added to maintain this target SWC (±1%) for 3 d before the harvest. The target soil water contents were 10%, 7.5%, 5%, and 3%. Taking into account that the field capacity and the

permanent wilting point of this substrate were close to 25% and 2% SWC, respectively, values of soil-REW were calculated as: soil-REW = (SWC - 2)/(25 - 2) × 100.

Harvest

Five control and five stressed plants were harvested at four different levels of water deficit (H1-H4; 35%, 24%, 13%, and 8% soil-REW, respectively) and after recovery (H5; 10 d at field capacity). Mature leaves and young roots were collected and frozen immediately in liquid nitrogen for transcriptome (leaves and roots) and proteome and metabolite (leaves only) analyses. A summary of the key dates of the experiment is given in Table I.

Growth Monitoring

Shoot height was recorded three to seven times per week on NDM plants. Changes in diameter of the base of the stem were continuously recorded on three controls and five water-stressed plants every 30 s with linear variable displacement transducer sensors. Root growth was monitored on the NDM plants by recording the increment of the fine root length on transparent plastic film stuck to the transparent Perspex pot twice per week. Root growth rate was calculated as the total length increment divided by the number of recorded roots and the time between two successive measurements.

Gas Exchange

g_s and net CO₂ assimilation rate were measured at 12 AM Universal Time, every other day on leaf 15 (a fully expanded young leaf) of all plants of the NDM batch with a portable gas exchange chamber Licor 6200 (LI-COR).

RWC and Leaf Water Potential

RWC of fully expanded nonsenescent leaves was calculated as RWC = (FW - DW)/(FTW - DW) × 100, where FW, DW, and FTW are fresh, dry, and full turgor weight, respectively. FW was measured immediately after the leaf was detached from the plant, FTW after the leaf was incubated in the dark at 4°C for 24 h with the petiole plunged in distilled water, and dry weight after the leaf was dried at 65°C for 48 h. Leaf water potential was measured on similar mature, nonsenescent leaves with a Scholander pressure bomb.

Xylem Anatomy

Measurements of the xylem anatomy were carried out on two to four plants per treatment and per harvest point. Stem segments were fixed in 2% formaldehyde, 5% acetic acid, 63% ethanol (modified after Sanderson, 1994), dehydrated in an ethanol/isopropanol series (modified after Gerlach, 1977) and embedded in Rotiplast with Roti-Histol (Roth) as the intermedium according to the manufacturer's instructions. Then, 30-μm sections were cut with a sliding microtome (Reichert-Jung) and mounted on gelatin-coated slides. The paraffin was removed with xylene, sections were stained for 15 min with Toluidine Blue (0.05% [w/v] in 0.1 M sodium acetate, pH 5.8; Merck) and examined under a microscope (Axioskop, Zeiss). Photographs were taken at 400× magnification with a digital camera (Nikon CoolPix 4500). All cells in a defined area (approximately 100 × 200 μm) containing the first fully expanded xylem cells adjacent to the cambial zone were considered. The lumen areas were measured for vessels and fibers using the image processing software analySIS (Soft Imaging System). Cell wall thickness was estimated as one-half the distance between the lumina of adjacent cells.

Microarray Analysis

Three biological replicates were used from each of the harvests with the exception of the controls of harvest 5 (only two). Each of the biological replicates contained mature nonsenescent leaves (or roots) from one or two trees. To avoid bias in the microarray evaluation as a consequence of dye-related differences in labeling efficiency and/or differences in recording fluorescence signals, dye labeling for each paired sample was reversed in two subsequent individual hybridizations. Thus, a total of six hybridizations per harvest were obtained (four hybridizations for harvest 5). The complete protocols for probe labeling and hybridization and raw data files are available from the ArrayExpress database (www.ebi.ac.uk/arrayexpress/) under the

accessions of E-MEXP-276. The production of the *P. euphratica* microarray is described in detail in Brosché et al. (2005).

Images were analyzed with GenePix-Pro 5.1 (Axon Instruments). Visually bad spots or areas on the array and low intensity spots were excluded. Low intensity spots were identified as spots where fewer than 55% of the pixels displayed an intensity above the background + 1 SD in either channel. The data from GenePix-Pro 5.1 was imported into GeneSpring 7.2 (Silicon Genetics) and normalized using the Lowess method. The background subtracted median intensities were used for calculations. Genes were selected using two criteria: (1) the gene transcript level ratio (water-stressed plants/controls) should be consistently higher than 2 or lower than 0.5 in at least one of the five harvests; and (2) the gene transcript level ratio should be significantly different from 1.0, determined using the Student's *t* test in GeneSpring. Gene trees (clustering) were drawn employing the unweighted pair-group method using arithmetic averages with pairwise distances calculated by standard correlation in GeneSpring 7.2.

qPCR

The microarray results were compared with qPCR. RT was performed with 5 µg of DNase I-treated total RNA with SuperScript III according to the manufacturer's instructions (Invitrogen). The RT reaction was diluted to a final volume of 100 µL, and 1 µL was used as a template for the PCR using qPCR Mastermix Plus for SYBR Green I (Eurogentec). PCR was performed in duplicate using ABI Prism 7000 default cycling conditions (Applied Biosystems). The following primer pairs were used for PCR: Cys protease, 5'-AAGTGGGTATATGCGGATGCA, 5'-ATCCATGGCAACACCACAGA; cyclic nucleotide and calmodulin-regulated ion channel, 5'-CGTGTGTGCCA-CAGGACTTT, 5'-TGCACGTGTCGCTTATTGAGA; glucosidase II α -subunit, 5'-CTCTCATTGAGCCGCAAAT, 5'-CCCCCTTCAAGCATAAAGG; ribosomal protein L17, 5'-GCAACATGGGTACAAAACGAGTT, 5'-CGTTTCA-GACTCTCTCTTGAAG. The raw threshold cycle (Ct) values were normalized against glucosidase II α -subunit (shown to have a constant expression in all experiments performed on the *P. euphratica* DNA microarray) to obtain normalized Δ Ct values that were then used to calculate the difference in expression levels between water-stressed and control samples.

Protein Analysis

For each harvest, three (two for harvest 5) controls were pooled into one control sample, and three drought-stressed plants were pooled into one drought sample. Proteins were extracted from 300-mg leaf samples, as described previously (Renaut et al., 2004). Dried samples were resuspended in a labeling buffer (7 M urea, 2 M thiourea, 4% CHAPS, 30 mM Tris) and incubated for 1 h at room temperature. Prior to the quantification, the pH of the solution was adjusted to 8.5. The concentration of proteins contained in the resuspended solution was then determined using a quantification kit (2D Quant kit, Amersham Biosciences).

Protein extracts and an internal standard (prepared with a pool of one-sixth of controls and stressed plants of harvests H1, H2, and H4) were labeled prior to electrophoresis with CyDyes. Three gels (corresponding to harvests H1, H2, and H4), each carrying the internal standard (Cy2), controls (Cy3), and water-stressed plants (Cy5) of the corresponding harvest, were run simultaneously. A fourth gel, carrying an internal standard (Cy2; prepared with one-half of the controls and one-half of the stressed plants of harvest H5), controls (Cy5), and drought-stressed plants (Cy3) of harvest H5, was run afterward.

A 1-nmol µL⁻¹ stock solution of each dye was diluted 2:3 with anhydrous dimethyl formamide just prior to the labeling reaction. A total of 50 µg of each protein extract was mixed with 1.2 µL of Cy2, Cy3, or Cy5 (400 pmol µL⁻¹), vortexed, and incubated on ice for 30 min in the dark, as described previously by Skynner et al. (2002). The reactions were quenched by the addition of 1.2 µL of 10 mM Lys, vortexed, and incubated on ice for 10 min in the dark. An equal volume of 2× lysis buffer (7 M urea, 2 M thiourea, 4% [w/v] CHAPS, 2% dithiothreitol [DTT], and 2% [v/v] pH 4–7 immobilized pH gradient [IPG] buffer) was added. The samples were vortexed and incubated on ice for a further 15 min in the dark. Then the pooled Cy2-labeled internal standard was combined with the Cy3-labeled extracts and Cy5-labeled extracts of each batch, as described previously.

The volume of the combined labeled samples was adjusted to 450 µL with the 2× lysis buffer to dilute the samples and to avoid precipitation in the sample cup. A total of 150 µL of pooled sample (i.e. 150 µg of proteins) was loaded onto each gel and separated by electrophoresis, as indicated below.

Immobiline DryStrips (GE Healthcare, pH 4–7, 24 cm) were rehydrated overnight with rehydration buffer (7 M urea, 2 M thiourea, 1% CHAPS, 0.4% DTT, 0.5% [v/v] IPG buffers, 0.002% [v/v] bromophenol blue).

Isoelectric focusing (IEF) was carried out on an Ettan IPGphor Manifold (Amersham Biosciences) with the following settings: 100 V for 2 h, 300 V for 3 h, 1,000 V for 6 h, a gradient step up to 8,000 V during 3 h, and a constant step at 8,000 V for 4 h at 20°C with a maximum current setting of 50 µA per strip in an IPGphor IEF unit (Amersham Biosciences). After the IEF, the IPG strips were equilibrated for 15 min in equilibration buffer (50 mM Tris, pH 8.8, 6 M urea, 30% [v/v] glycerol, 2% [w/v] SDS) supplemented with 1% (w/v) DTT. A second equilibration step of 15 min with the same equilibration buffer, now containing 2.5% (w/v) iodoacetamide was carried out afterward. The IPG strips were then sealed with 0.5% agarose in SDS running buffer at the top of the gel slabs (280 × 210 × 1 mm) polymerized from 12.5% (w/v) acrylamide and 0.1% *N,N'*-methylenebisacrylamide. The gels were cast between low fluorescent glass plates, one treated with bind-silane. The SDS-PAGE step was performed at 15°C for 18 h in an Ettan Dalt II tank (Amersham Biosciences) using a total voltage-current energy limit of 13 W.

Cy2-, Cy3-, and Cy5-labeled protein images were produced by excitation of the gels at 488, 532, and 633 nm, respectively, and emission at 520, 590, and 680 nm, respectively, using a Typhoon Variable Mode Imager 9400 (Amersham Biosciences). Images were analyzed using the Decyder v5.02.02 software (Amersham Biosciences). The software provided automated spot detection (Differential In-gel Analysis), matching, and radiometric quantification between the images using the Biological Variation Analysis (BVA) software (GE Healthcare). Matching of gels was facilitated by the presence of the internal standard in each gel.

Only statistically significant results were considered (Student's *t* test, *P* < 0.05), and differentially expressed proteins with a ratio of at least 2 observed in one condition were selected using BVA.

Selected spots were located on a gel, and a picking list was generated with BVA. Spots of interest were excised from gels using the Ettan Spot Picker from the Ettan Spot Handling Workstation (Amersham Biosciences). Spots were then digested *in situ* with Trypsin Gold (mass spectrometry grade, Promega) using the Ettan Digester robot (Amersham Biosciences) from the same workstation, according to the manufacturer's protocols. Automated spotting of the samples was carried out with the spotter of the Ettan Spot Handling Workstation (Amersham Biosciences). Peptides dissolved in 50% acetonitrile containing 0.5% trifluoroacetic acid were spotted onto MALDI-time of flight (TOF) disposable target plates (Applied Biosystems) prior to the precoat deposit of 0.3 µL of α -cyano-4-hydroxycinnamic acid (10 mg mL⁻¹, Sigma Aldrich). Both PMF and peptide sequence analyses were carried out using MALDI-TOF/MS and MALDI-TOF/MS spectra (4700 Proteomics Analyzer, Applied Biosystems). Spectral information (PMF and combined PMF and peptide sequence information) was submitted to a local search engine (Mascot V2.0, Matrix Science) and queried against the latest updates of Swiss-Prot, nrNCBI, and TrEMBL databases. The query parameters allowed for a single miscleavage, a variable oxidation state of Met, and a 50-ppm mass window resolution. For the two latter databases, taxonomic restrictions were set to *Viridiplantae*. Proteins were considered as positively identified when probability criteria exceeding 99.9% were met using the MOWSE based identification score (Perkins et al., 1999).

Comparison of EST and Protein Data

ESTs were translated in all six reading frames. For each protein identification corresponding to an EST, a multiple sequence alignment between the peptide sequence of the protein ortholog and the translated EST sequences was performed using the algorithm provided by the ClustalW WWW Service at the European Bioinformatics Institute (<http://www.ebi.ac.uk/clustalw/>). The translated sequence frame showing the highest score was selected for matching mass spectral data.

SP1 Protein Abundance

For each harvest, proteins were extracted from 300 mg of leaves in three or four controls and water-stressed plants chosen from the five replicates. Leaf tissue was homogenized with a chilled mortar and pestle in an extraction buffer (100 mM Tris-HCl, pH 8.5, 0.10% DTT) containing 20% of polyvinylpyrrolidone per gram plant tissue. Total soluble protein samples were digested with Proteinase-K (1:4) for 1 h at 37°C. Protein samples were then boiled (100°C) for 5 min, kept on ice for another 5 min, and centrifuged for 10 min at 10,000g. The supernatant fraction was precipitated by mixing it with 4 volumes of precooled acetone and kept overnight at -20°C, then centrifuged

for 10 min at 10,000g. The pellet was resuspended in diluted SDS-PAGE sample application buffer (50%, v/v). Before loading, the samples were heated at 100°C for 5 min.

Proteins were separated by SDS-PAGE in which the lower gel contained 15% polyacrylamide and the stacking gel contained 4% polyacrylamide. Each lane was loaded with 50 µg total protein, or, in the case of boiling-stable proteins, with the equivalent of 200 µg total protein, in addition to low M_r standards (kit no. SDS-7, Sigma) and run at 200 V for 45 min (on minigel). Gels were stained with Coomassie Blue stain solution (Sigma). Densitometry was measured by TINA 2.20 g Software.

Metabolite Analyses

Analyses were carried out on mature leaves of each individual plant of the five harvests (H1–H5). Concentration initially obtained in mole per gram fresh weight were converted into mole per square meter using the fresh weight-to-surface area ratio measured on another leaf sample of the same plant to avoid interference with leaf water content. For carbohydrates, concentrations were converted into mole per liter using the water content ($[FW - DW]/FW$) measured on another leaf sample and then into an estimate of carbohydrate-generated osmotic pressure at full turgor according to Van t'Hoff's law ($\Pi = RT \sum c_s$, where Π is the osmotic pressure and c_s the molarity of the osmotica at full turgor).

LOOH

LOOH concentration was measured according to DeLong et al. (2002). Plant material was ground in 80:20 ethanol:methanol (v/v) containing 0.01% (w/v) butylated hydroxytoluene (BHT). After centrifugation, the supernatant was recovered (50 µL) and added to 1 mL of a solution of 250 µM ferrous ammonium sulfate hexahydrate, 100 µM xylenol orange, and 4 mM BHT dissolved in 90% (v/v) methanol and 10% (v/v) 250 mM H₂SO₄ for 10 min at room temperature. Sample absorbance was measured at 560 nm. A standard curve was obtained using hydrogen peroxide, and the LOOH values were expressed as the hydrogen peroxide equivalent. Nonspecific turbidity was subtracted from the 560-nm signal by using the measurements at 560 nm of totally reduced samples by a prior reaction with triphenylphosphin (DeLong et al., 2002).

MDA

A modified thiobarbituric acid reactive substance assay was used as an alternative assessment of lipid oxidation (Hodges et al., 1999). Plant material was ground in 80:20 ethanol:methanol (v/v) containing 0.01% (w/v) BHT. After centrifugation, the supernatant was recovered (200 µL) and added to 1 mL of a solution of 20% (w/v) TCA and 0.01% (w/v) BHT containing 0.65% (w/v) thiobarbituric acid for 25 min at 95°C. After centrifugation, sample absorbance was measured at 532 nm. Blank measurements were performed using reagent solution without thiobarbituric acid. Nonspecific turbidity was subtracted from the 532-nm signal by using the measurements at 600 and 440 nm (Hodges et al., 1999). The results were expressed as MDA equivalent.

Pigments

Pigments were extracted from frozen leaf discs by grinding in a mortar with 2 mL acetone water (90:10; v/v) and centrifuged at 10,000g for 10 min at 4°C. The supernatant was recovered and filtered on 0.2-µm filters. Pigments were then analyzed by HPLC as described by Wright et al. (1991). HPLC separation using Photo Diode Array detection was performed on a Dionex chromatograph (Dionex) consisting of a Gina 50 autosampler, a P580 gradient pump, and a UVD340S detector. A Zorbax Bonus-RP 4.6- × 250-mm column (Agilent Technologies) was used for the pigment separation.

Carbohydrates

Soluble carbohydrate contents were determined according to Guignard et al. (2005). Samples were ground in liquid nitrogen and extracted with 80% ethanol for 1 h with gentle shaking. After centrifugation at 10,000g and 4°C for 10 min, the supernatant was dried by vacuum centrifugation at 40°C. Samples were resuspended in water prior to analysis. Ion chromatography with Pulsed Amperometric Detection analyses were carried out on a Dionex DX-500 chromatograph (Dionex) consisting of a Spark Midas autosampler, a GP-40 gradient pump, and an ED-40 electrochemical detector. Two different sets of

column and precolumn were used for carbohydrate separation. A first set, combining a CarboPac PA10 4 × 50 mm and CarboPac PA10 4 × 250 mm (Dionex) was used for the separation of common mono-, di-, and polysaccharides, while the second set combined a CarboPac MA1 4 × 50 mm and CarboPac MA1 4 × 250 mm (Dionex) and was used for the separation of sugar alcohols and trehalose.

Statistics

For the anatomy, parametric two-way ANOVA could not be used, because homoscedasticity tests failed. The differences between the controls of the five harvests were tested with a parametric one-way ANOVA for vessel lumen area and with the Kruskal-Wallis test (ANOVA on ranks) for fiber lumen area and fiber cell wall thickness. The difference between the control and water-stressed plants at each harvest was tested either with the Student's *t* test or the Mann-Whitney rank sum test.

For metabolites, osmotic pressure, and SP1, differences between treatments were tested with parametric two-way ANOVA, and, when significant, multiple comparison tests were made using Tukey's test.

Sequence data from this article can be found in the ArrayExpress database (www.ebi.ac.uk/arrayexpress/) under accession number E-MEXP-276.

Supplemental Data

The following materials are available in the online version of this article.

Supplemental Figure S1. Time course of SWC recorded for potted *P. euphratica* individuals during the experiment.

Supplemental Figure S2. Time course of stem diameter growth rate (A), shoot elongation rate (B), and root elongation rate (C) of *P. euphratica* during the experiment.

Supplemental Figure S3. Time course of net CO₂ assimilation rate (A) and stomatal conductance (B) of *P. euphratica* during the experiment.

Supplemental Figure S4. Inositol (A), salicin (B), sorbitol (C), mannitol (D), and trehalose (E) contents of *P. euphratica* leaves at five dates corresponding to different water deficit intensities.

Supplemental Figure S5. Gal (A), Suc (B), Glc (C), Fru (D), raffinose (E), and stachyose (F) contents of *P. euphratica* leaves at five dates corresponding to different water deficit intensities.

Supplemental Figure S6. Differential in-gel electrophoresis image.

Supplemental Table S1. Transcript abundance ratio (water-stressed to control) of 70 genes in *P. euphratica* leaves at five dates corresponding to different water deficit intensities.

Supplemental Table S2. Transcript abundance ratio (water-stressed to control) of 40 genes in *P. euphratica* roots at five dates corresponding to different water deficit intensities.

Supplemental Table S3. Relative abundance of 39 proteins (water-stressed to control) in *P. euphratica* leaves at four dates corresponding to different water deficit intensities.

ACKNOWLEDGMENTS

The authors thank David Hukin, Dany Afif, Anna Shvaleva, François Willm, Bernard Clerc, and Airi Lamminmäki for their support and help during the experimental work. The contribution of two anonymous referees is gratefully acknowledged.

Received September 9, 2006; accepted November 21, 2006; published December 8, 2006.

LITERATURE CITED

Aharon R, Shahak Y, Wininger S, Bendov R, Kapulnik Y, Galili G (2003) Overexpression of a plasma membrane aquaporin in transgenic tobacco improves plant vigor under favorable growth conditions but not under drought or salt stress. *Plant Cell* 15: 439–447

- Akashi K, Nishimura N, Ishida Y, Yokota A** (2004) Potent hydroxyl radical-scavenging activity of drought-induced type-2 metallothionein in wild watermelon. *Biochem Biophys Res Commun* **323**: 72–78
- Aussenac G** (2000) Interactions between forest stands and microclimate: ecophysiological aspects and consequences for silviculture. *Ann Sci* **57**: 287–301
- Bartels D, Souer E** (2003) Molecular responses of higher plants to dehydration. In H Hirt, K Shinozaki, eds, *Topics in Current Genetics: Plant Response to Abiotic Stress*, Vol 4. Springer Verlag, Heidelberg, pp 9–38
- Bentsink L, Alonso-Blanco C, Vreugdenhil D, Tesnier K, Groot SPC, Koornneef M** (2000) Genetic analysis of seed-soluble oligosaccharides in relation to seed storability of *Arabidopsis*. *Plant Physiol* **124**: 1595–1604
- Blödner C, Majcherczyk A, Kües U, Polle A** (2007) Mild drought stress affects the proteome of spruce needles. *Tree Physiol* (in press)
- Boyer JS, Cavalieri AJ, Schulze ED** (1985) Control of the rate of cell enlargement: excision, wall relaxation, and growth-induced water potentials. *Planta* **163**: 527–543
- Bray EA** (2004) Genes commonly regulated by water-deficit stress in *Arabidopsis thaliana*. *J Exp Bot* **55**: 2331–2341
- Bray EA, Bailey-Serres J, Weretilnyk E** (2000) Responses to abiotic stresses. In B Buchanan, W Gruissem, R Jones, eds, *Biochemistry and Molecular Biology of Plants*. American Society of Plant Physiologists, Rockville, MD, pp 1158–1203
- Breda N, Granier A** (1996) Intra- and interannual variations of transpiration, leaf area index and radial growth of a sessile oak stand (*Quercus petraea*). *Ann Sci For* **53**: 521–536
- Brignolas F, Thierry C, Guerrier G, Boudouresque E** (2000) Compared water deficit response of two *Populus x euramericana* clones, Luisa Avanzo and Dorskamp. *Ann Sci* **57**: 261–266
- Brosché M, Vinocur B, Alatalo ER, Lamminmaki A, Teichmann T, Ottow EA, Djilianov D, Afif D, Bogeat-Triboulot MB, Altman A, et al** (2005) Gene expression and metabolite profiling of *Populus euphratica* growing in the Negev desert. *Genome Biol* **6**: R101
- Bruelheide H, Jandt U, Gries D, Thomas FM, Foetzki A, Buerkert A, Gang W, Zhang XM, Runge M** (2003) Vegetation changes in a river oasis on the southern rim of the Taklamakan Desert in China between 1956 and 2000. *Phytocoenologia* **33**: 801–818
- Chaves MM, Maroco JP, Pereira JS** (2003) Understanding plant responses to drought: from genes to the whole plant. *Funct Plant Biol* **30**: 239–264
- Chen SL, Li JK, Wang SS, Fritz E, Huttermann A, Altman A** (2003) Effects of NaCl on shoot growth, transpiration, ion compartmentation, and transport in regenerated plants of *Populus euphratica* and *Populus tomentosa*. *Can J For Res* **33**: 967–975
- Cobbett C, Goldsbrough P** (2002) Phytochelatins and metallothioneins: roles in heavy metal detoxification and homeostasis. *Annu Rev Plant Biol* **53**: 159–182
- Cosgrove D** (1987) Wall relaxation and the driving forces for cell expansive growth. *Plant Physiol* **84**: 561–564
- Cosgrove DJ** (2000) New genes and new biological roles for expansins. *Curr Opin Plant Biol* **3**: 73–78
- Czechowski T, Bari RP, Stitt M, Scheible WR, Udvardi MK** (2004) Real-time RT-PCR profiling of over 1400 *Arabidopsis* transcription factors: unprecedented sensitivity reveals novel root- and shoot-specific genes. *Plant J* **38**: 366–379
- Dangl JL, Dietrich RA, Thomas H** (2000) Senescence and programmed cell death. In B Buchanan, W Gruissem, R Jones, eds, *Biochemistry and Molecular Biology of Plants*. American Society of Plant Physiologists, Rockville, MD, pp 1044–1100
- DeLong JM, Prange RK, Hodges DM, Forney CF, Bishop MC, Quilliam M** (2002) Using a modified ferrous oxidation-xylene orange (FOX) assay for detection of lipid hydroperoxides in plant tissue. *J Agric Food Chem* **50**: 248–254
- Dgany O, Gonzalez A, Sofer O, Wang WX, Zolotnitsky G, Wolf A, Shoham Y, Altman A, Wolf SG, Shoseyov O, et al** (2004) The structural basis of the thermostability of SP1, a novel plant (*Populus tremula*) boiling stable protein. *J Biol Chem* **279**: 51516–51523
- Dreyer E, Bogeat-Triboulot MB, Le Thiec D, Guehl JM, Brignolas F, Villar M, Bastien C, Martin F, Kohler A** (2004) Drought tolerance of poplars: can we expect to improve it? *Biofutur* **247**: 54–58
- El Ouakfaoui S, Miki B** (2005) The stability of the *Arabidopsis* transcriptome in transgenic plants expressing the marker genes nptII and uidA. *Plant J* **41**: 791–800
- Evans JR, von Caemmerer S** (1996) Carbon dioxide diffusion inside leaves. *Plant Physiol* **110**: 339–346
- Ferrario-Mery S, Valadier MH, Foyer CH** (1998) Overexpression of nitrate reductase in tobacco delays drought-induced decreases in nitrate reductase activity and mRNA. *Plant Physiol* **117**: 293–302
- Flexas J, Bota J, Loreto F, Cornic G, Sharkey TD** (2004) Diffusive and metabolic limitations to photosynthesis under drought and salinity in C-3 plants. *Plant Biol* **6**: 269–279
- Gebre GM, Tschaplinski TJ, Tuskan GA, Todd DE** (1998) Clonal and seasonal differences in leaf osmotic potential and organic solutes of five hybrid poplar clones grown under field conditions. *Tree Physiol* **18**: 645–652
- Gerlach D** (1977) *Botanische Mikrotechnik*. Georg Thieme Verlag, Stuttgart, Germany
- Gries D, Zeng F, Foetzki A, Arndt SK, Bruelheide H, Thomas FM, Zhang X, Runge M** (2003) Growth and water relations of *Tamarix ramosissima* and *Populus euphratica* on Taklamakan desert dunes in relation to depth to a permanent water table. *Plant Cell Environ* **26**: 725–736
- Gu RS, Liu QL, Pei D, Jiang XN** (2004) Understanding saline and osmotic tolerance of *Populus euphratica* suspended cells. *Plant Cell Tissue Organ Cult* **78**: 261–265
- Guignard C, Jouve L, Bogeat-Triboulot MB, Dreyer E, Hausman JF, Hoffmann L** (2005) Analysis of carbohydrates in plants by high performance anion-exchange chromatography coupled with electrospray mass spectrometry. *J Chromatogr* **1085**: 137–142
- Gygi SP, Rochon Y, Franza BR, Aebersold R** (1999) Correlation between protein and mRNA abundance in yeast. *Mol Cell Biol* **19**: 1720–1730
- Hajheidari M, Abdollahian-Noghabi M, Askari H, Heidari M, Sadeghian SY, Ober ES, Salekdeh GH** (2005) Proteomic analysis of sugar beet leaves under drought stress. *Proteomics* **5**: 950–960
- Harrak H, Azelmat S, Baker EN, Tabaeizadeh Z** (2001) Isolation and characterization of a gene encoding a drought-induced cysteine protease in tomato (*Lycopersicon esculentum*). *Genome* **44**: 368–374
- Hodges DM, DeLong JM, Forney CF, Prange RK** (1999) Improving the thiobarbituric acid-reactive-substances assay for estimating lipid peroxidation in plant tissues containing anthocyanin and other interfering compounds. *Planta* **207**: 604–611
- Hsiao TC** (1973) Plant responses to water stress. *Annu Rev Plant Physiol* **24**: 519–570
- Hukin D, Cochard H, Dreyer E, Le Thiec D, Bogeat-Triboulot MA** (2005) Cavitation vulnerability in roots and shoots: does *Populus euphratica* Oliv., a poplar from arid areas of Central Asia, differ from other poplar species? *J Exp Bot* **56**: 2003–2010
- Jagtap V, Bhargava S, Streb P, Feierabend J** (1998) Comparative effect of water, heat and light stresses on photosynthetic reactions in *Sorghum bicolor* (L.) Moench. *J Exp Bot* **49**: 1715–1721
- Jang JY, Kim DG, Kim YO, Kim JS, Kang HS** (2004) An expression analysis of a gene family encoding plasma membrane aquaporins in response to abiotic stresses in *Arabidopsis thaliana*. *Plant Mol Biol* **54**: 713–725
- Javot H, Maurel C** (2002) The role of aquaporins in root water uptake. *Ann Bot (Lond)* **90**: 301–313
- Kawaguchi R, Girke T, Bray EA, Bailey-Serres J** (2004) Differential mRNA translation contributes to gene regulation under non-stress and dehydration stress conditions in *Arabidopsis thaliana*. *Plant J* **38**: 823–839
- Kawaguchi R, Williams AJ, Bray EA, Bailey-Serres J** (2003) Water-deficit-induced translational control in *Nicotiana tabacum*. *Plant Cell Environ* **26**: 221–229
- Kawasaki S, Miyake C, Kohchi T, Fujii S, Uchida M, Yokota A** (2000) Responses of wild watermelon to drought stress: accumulation of an ArgE homologue and citrulline in leaves during water deficits. *Plant Cell Physiol* **41**: 864–873
- Kohler A, Blaudez D, Chalot M, Martin F** (2004) Cloning and expression of multiple metallothioneins from hybrid poplar. *New Phytol* **164**: 83–93
- Kreps JA, Wu YJ, Chang HS, Zhu T, Wang X, Harper JF** (2002) Transcriptome changes for *Arabidopsis* in response to salt, osmotic, and cold stress. *Plant Physiol* **130**: 2129–2141
- Lecoeur J, Wery J, Turc O, Tardieu F** (1995) Expansion of pea leaves subjected to short water-deficit: cell number and cell-size are sensitive to stress at different periods of leaf development. *J Exp Bot* **46**: 1093–1101
- Luu DT, Maurel C** (2005) Aquaporins in a challenging environment: molecular gears for adjusting plant water status. *Plant Cell Environ* **28**: 85–96
- Mittler R** (2002) Oxidative stress, antioxidants and stress tolerance. *Trends Plant Sci* **7**: 405–410

- Monclus R, Dreyer E, Villar M, Delmotte FM, Delay D, Petit JM, Barbaroux C, Thiec D, Brechet C, Brignolas F (2006) Impact of drought on productivity and water use efficiency in 29 genotypes of *Populus deltoides* x *Populus nigra*. New Phytol 169: 765–777
- Murakami R, Ifuku K, Takabayashi A, Shikanai T, Endo T, Sato F (2005) Functional dissection of two *Arabidopsis* PsbO proteins. FEBS J 272: 2165–2175
- Newton RP, Brenton AG, Smith CJ, Dudley E (2004) Plant proteome analysis by mass spectrometry: principles, problems, pitfalls and recent developments. Phytochemistry 65: 1449–1485
- Noctor G, Foyer CH (1998) Simultaneous measurement of foliar glutathione, gamma-glutamylcysteine, and amino acids by high-performance liquid chromatography: comparison with two other assay methods for glutathione. Anal Biochem 264: 98–110
- Noordermeer MA, Feussner I, Kolbe A, Veldink GA, Vliegenthart JFG (2000) Oxygenation of (3Z)-alkenals to 4-hydroxy-(2E)-alkenals in plant extracts: a nonenzymatic process. Biochem Biophys Res Commun 277: 112–116
- Ottow EA, Brinker M, Teichmann T, Fritz E, Kaiser W, Brosche M, Kangasjarvi J, Jiang XN, Polle A (2005) *Populus euphratica* displays apoplastic sodium accumulation, osmotic adjustment by decreases in calcium and soluble carbohydrates, and develops leaf succulence under salt stress. Plant Physiol 139: 1762–1772
- Ozturk ZN, Talame V, Deyholos M, Michalowski CB, Galbraith DW, Gokukirmizi N, Tuberosa R, Bohnert HJ (2002) Monitoring large-scale changes in transcript abundance in drought- and salt-stressed barley. Plant Mol Biol 48: 551–573
- Passioura JB (1996) Drought and drought tolerance. Plant Growth Regul 20: 79–83
- Perkins DN, Pappin DJC, Creasy DM, Cottrell JS (1999) Probability-based protein identification by searching sequence databases using mass spectrometry data. Electrophoresis 20: 3551–3567
- Plomion C, Lalanne C, Claverol S, Meddour H, Kohler A, Bogeat-Triboulot MB, Barre A, Le Provost G, Dumazet H, Jacob D, et al (2006) Mapping the proteome of poplar and application to the discovery of drought-stress responsive proteins. Proteomics 6: 6509–6527
- Polle A, Altman A, Jiang XN (2006) Towards genetic engineering for drought tolerance in trees. In M Fladung, D Ewald, eds, Tree Transgenesis: Recent Developments. Springer Verlag, Berlin, pp 275–297
- Renaut J, Lutts S, Hoffmann L, Hausman JF (2004) Responses of poplar to chilling temperatures: proteomic and physiological aspects. Plant Biol 6: 81–90
- Rood SB, Braatne JH, Hughes FMR (2003) Ecophysiology of riparian cottonwoods: stream flow dependency, water relations and restoration. Tree Physiol 23: 1113–1124
- Salekdeh GH, Siopongco J, Wade LJ, Ghareyazie B, Bennett J (2002) Proteomic analysis of rice leaves during drought stress and recovery. Proteomics 2: 1131–1145
- Sanderson JB (1994) Biological Microtechnique. Microscopy Handbooks 28, Royal Microscopical Society. Bios Scientific Publishers, Oxford
- Schneider C, Tallman KA, Porter NA, Brash AR (2001) Two distinct pathways of formation of 4-hydroxynonenal: mechanisms of nonenzymatic transformation of the 9- and 13-hydroperoxides of linoleic acid to 4-hydroxyalkenals. J Biol Chem 276: 20831–20838
- Seki M, Narusaka M, Ishida J, Nanjo T, Fujita M, Oono Y, Kamiya A, Nakajima M, Enju A, Sakurai T, et al (2002) Monitoring the expression profiles of 7000 *Arabidopsis* genes under drought, cold and high-salinity stresses using a full-length cDNA microarray. Plant J 31: 279–292
- Sharma A, Dwivedi BN, Singh B, Kumar K (1999) Introduction of *Populus euphratica* in Indian semi-arid trans Gangetic plains. Ann For 7: 1–8
- Sharp RE, Poroyko V, Hejlek LG, Spollen WG, Springer GK, Bohnert HJ, Nguyen HT (2004) Root growth maintenance during water deficits: physiology to functional genomics. J Exp Bot 55: 2343–2351
- Skynner HA, Rosahl TW, Knowles MR, Salim K, Reid L, Cothliff R, McAllister G, Guest PC (2002) Alterations of stress related proteins in genetically altered mice revealed by two-dimensional differential in-gel electrophoresis analysis. Proteomics 2: 1018–1025
- Smart LB, Moskal WA, Cameron KD, Bennett AB (2001) MIP genes are down-regulated under drought stress in *Nicotiana glauca*. Plant Cell Physiol 42: 686–693
- Sperry JS, Hacke UG, Oren R, Comstock JP (2002) Water deficits and hydraulic limits to leaf water supply. Plant Cell Environ 25: 251–263
- Sung DY, Vierling E, Guy CL (2001) Comprehensive expression profile analysis of the *Arabidopsis* hsp70 gene family. Plant Physiol 126: 789–800
- Sunkar R, Bartels D, Kirch HH (2003) Overexpression of a stress-inducible aldehyde dehydrogenase gene from *Arabidopsis thaliana* in transgenic plants improves stress tolerance. Plant J 35: 452–464
- Tanaka R, Hirashima M, Satoh S, Tanaka A (2003) The *Arabidopsis*-accelerated cell death gene ACD1 is involved in oxygenation of pheophorbide a: inhibition of the pheophorbide a oxygenase activity does not lead to the “Stay-Green” phenotype in *Arabidopsis*. Plant Cell Physiol 44: 1266–1274
- Taylor NL, Day DA, Millar AH (2004) Targets of stress-induced oxidative damage in plant mitochondria and their impact on cell carbon/nitrogen metabolism. J Exp Bot 55: 1–10
- Tschaplinski TJ, Tuskan GA, Gebre GM, Todd DE (1998) Drought resistance of two hybrid *Populus* clones grown in a large-scale plantation. Tree Physiol 18: 653–658
- Tschaplinski TJ, Tuskan GA, Gunderson CA (1994) Water-stress tolerance of black and eastern cottonwood clones and four hybrid progeny. 1. Growth, water relations, and gas exchange. Can J For Res 24: 364–371
- Tuskan GA, DiFazio SP, Teichmann T (2004) Poplar genomics is getting popular: the impact of the poplar genome project on tree research. Plant Biol 6: 2–4
- Vera-Estrella R, Barkla BJ, Bohnert HJ, Pantoja O (2004) Novel regulation of aquaporins during osmotic stress. Plant Physiol 135: 2318–2329
- Vinocur B, Altman A (2005) Recent advances in engineering plant tolerance to abiotic stress: achievements and limitations. Curr Opin Biotechnol 16: 123–132
- Wang W, Pelah D, Alergand T, Shoseyov O, Altman A (2002) Characterization of SP1, a stress-responsive, boiling-soluble, homo-oligomeric protein from aspen. Plant Physiol 130: 865–875
- Wang W, Vinocur B, Shoseyov O, Altman A (2004) Role of plant heat-shock proteins and molecular chaperones in the abiotic stress response. Trends Plant Sci 9: 244–252
- Watanabe S, Kojima K, Ide Y, Sasaki S (2000) Effects of saline and osmotic stress on proline and sugar accumulation in *Populus euphratica* in vitro. Plant Cell Tissue Organ Cult 63: 199–206
- Wright SW, Jeffrey SW, Mantoura RFC, Llewellyn CA, Bjornland T, Repeta D, Welschmeyer N (1991) Improved HPLC method for the analysis of chlorophylls and carotenoids from marine-phytoplankton. Mar Ecol Prog Ser 77: 183–196
- Xiong L, Zhu JK (2002) Molecular and genetic aspects of plant responses to osmotic stress. Plant Cell Environ 25: 131–139
- Zhang N, Portis ARJ (1999) Mechanism of light regulation of Rubisco: a specific role for the larger Rubisco activase isoform involving reductive activation by thioredoxin-f. Proc Natl Acad Sci USA 96: 9438–9443

Acknowledgment

At the end of this work I would like to express my deep gratitude to the people who helped me during this study. First of all I would like to thank my supervisor Prof. Dr. Polle for the topic of this work, the support and her kind advice. Also, I would like to thank Prof. Dr. Finkeldey for evaluating my thesis and Prof. Dr. Beese for agreeing to be my third referee.

I further thank Dr. Thomas Teichmann who was a big help for me every time I had a new question in the course of my work, and Dr. Urs Fischer who helped me with the *in silico* analysis. From Dr. Heyser I learned many things about wood anatomy. I had a very nice working relationship with Christine Kettner and Sabine Elend in the laboratory. I would also like to thank Thomas Klein for helping me with the quantitative real-time PCR and RNA extraction. I would like to say thanks to Gisbert Langer-Kettner, Karin Lange and Marianne Smiatacz for their friendly help and advice, and to my colleagues Peter Hawighorst, Dennis Janz and Frauke Kleemann for helping me with critical discussions. I favourably remember Dr. Eric Ottow and Dr. Monika Brinker for their good advices and Bernd Kopka for helping me to solve all arising computer problems.

Especially, I would like to express my deep and sincere gratitude to my wife Banafshe for her patience during the hard days and to my daughter Armita for being there at the right time.

This study has been done with financial support of the DFG project “Poplar Research Group Germany”, TP 06 characterization of salt tolerance in Poplar (PO 362/12-3).

Curriculum vitae

Born August 6, 1976 in Lahijan (Iran)
Nationality Iranian
Marital status Married

Education- School

1982-1987 Primary school, Lahijan (Iran)
1987-1990 Guidance school, Lahijan (Iran)
1990-1994 High school, Lahijan (Iran)

Education- University

1995-1999 BSc, Forestry, Guilan University (Iran)

1999-2002

Master thesis

Survival, freshness and height growth of beech (*Fagus orientalis* Lipsky) seedlings and saplings in different gap sizes.

Institute of Forestry, Faculty of Natural Science, University of Mazandaran (Iran)

(Major advisor: Dr. Seyyed-Fazl-Allah Emadian)

2002-2004

Lecturer assistant in Mazandaran University (Advanced statistic, Survey, Aerial photos interpretation, Forest exploitation, Remote sensing)

2004-2008

Ph.D. thesis

Effects of salt stress on ecophysiological and molecular characteristics of *Populus euphratica* Oliv., *Populus x canescens* (Aiton) Sm. and *Arabidopsis thaliana* L.

Institute of Forest Botany, Division of Tree Physiology, University of Goettingen (Germany)

(Major advisor: Prof. Dr. A. Polle)

Publications

- 2005 Tabari M, **Fayyaz P**, Espahbodi K, Staelens J, Nachtergale L. Response of oriental beech (*Fagus orientalis* Lipsky) seedlings to canopy gap size. *Forestry* 78:443–450
- 2007 Bogeat-Triboulot MB, Brosche M, Renaut J, Jouve L, Thiec D, **Fayyaz P**, Vinocur B, Witters E, Laukens K, Teichmann T, Altman A, Hausman JF, Polle A, Kangasjärvi J and Dreyer E (2007) Gradual soil water depletion results in reversible changes of gene expression, protein profiles, ecophysiology, and growth performance in *Populus euphratica*, a poplar growing in arid regions. *Plant Physiology* 143: 876–892

Posters

- 2004 Ottow EA, **Fayyaz P**, Teichmann T, Fritz E, Brosché M, Kangasjärvi J, Dibrov P, Polle A. 12th NPS on Functional Genomics of Environmental Adaptation in *Populus* (10.-13. October 2004), Gatlinburg, USA
‘Primary characterization of the putative Na⁺/H⁺ antiporter PeNhaD1 and its role in salt resistance’
- 2004 Ottow EA, **Fayyaz P**, Teichmann T, Brosché M, Kangasjärvi J, Polle A, Botanikertagung, Branchweig (05.-10. September 2004), Germany
‘Functional analysis of the putative Na⁺/H⁺ antiporter PeNhaD1’

Oral presentations

- 2007 PhD seminar of 'Wood Biology and Technology' program. Effects of salt stress on ecophysiological characteristics of *Populus euphratica* Oliv., *Populus x canescens* and *Arabidopsis thaliana*
- 2006 PhD seminar of 'Wood Biology and Technology' program. Response of oriental beech (*Fagus orientalis* Lipsky) seedlings to canopy gaps
- 2006 PhD seminar of 'Wood Biology and Technology' program. Anatomical investigation of stem cross sections in *Populus canescens* under salt and nitrogen treatments
- 2004 PhD seminar of 'Wood Biology and Technology' program. Membrane - structure and function

Languages Farsi, English, German

